REFERENCE ONLY

UNIVERSITY OF LONDON THESIS

Degree MD Year 2005 Name of Author MAMSOEN, A.

New approaches to gene therapy and prognostic markers in melanoma.

MD Thesis

Alex Ramsden

2004

ProQuest LLC
789 East Eisenhower Parkway
P.O. Box 1346
Ann Arbor, MI 48106-1346

New approaches to gene therapy and prognostic markers in melanoma.

Alex Ramsden.

The *c-myc* proto-oncogene plays a key role in cell proliferation, malignant transformation and apoptosis. Previous work at RAFT demonstrated that *c-myc* expression levels are an accurate prognostic marker in melanoma.

Ribozymes are catalytic RNA molecules that cleave specific mRNA sequences to prevent gene expression. A ribozyme was constructed targeting the *c-myc* translation initiation site. A375M melanoma cells were transfected using liposomes and growth was assessed using a MTS growth assay. *c-myc* expression was measured with immuno-staining and flow-cytometry. Ribozyme treatment of A375M melanoma cells reduced *c-myc* expression when compared to non-specific controls ($p<0.001$). Ribozyme treatment also significantly reduced growth of A375M cells *in-vitro* compared to untreated controls ($p<0.001$). Ribozymes were investigated in combination with interferon and cis-platinum.

A prospective investigation of *c-myc* expression in 117 melanomas was undertaken using immunostaining and flow cytometric analysis. Clinico-pathological details were also studied. Analysis revealed that high *c-myc* expression was associated with a worse prognosis ($p=0.043$). Multivariate analysis demonstrated *c-myc* as an independent prognostic marker when measured against other routine parameters including Breslow thickness.

To facilitate rapid screening for molecular alterations in melanoma, a tissue micro-array was created using historical paraffin embedded specimens. 126 tumours were included in the array block representing all stages of disease progression. Analysis was performed on a variety of genes associated with *c-myc* examining prognostic significance. High expression of p27 and p53 were significantly associated with improved survival ($p<0.05$). Cyclins A, E and D1 correlated with disease progression ($p<0.05$).

Conclusions. Ribozymes can effectively block *c-myc* gene expression *in vitro* and may have a role in the treatment of melanoma. Flow cytometric analysis of c-myc expression provides a new important independent prognostic marker for melanoma. Tissue array technology is a simple and powerful tool in the search for new prognostic markers in melanoma.

Acknowledgements

There have been many wonderful people involved in this thesis that have helped me complete the work presented. I am deeply thankful for all their generosity, patience, kindness and advice. Without them none of the work would have been possible, as they have guided me through the complexities of science. I have also made many friendships and enjoyed my time completing this thesis.

I am extremely grateful to Professor George Wilson who not only provided me with this project and guided me through to the end. All the staff at the Gray Cancer Institute were incredibly helpful, especially Francis Daley, Chris Martindale, Mick Woodcock, Sheena Balroop, Kay Wilson and Sara Bourne. Simon Scott and Brian Marples inspired my scientific thought and experiments with ribozymes and have become good friends. My colleague, Philip Lim, provided immense support, humour and advice throughout my two years at the Gray Cancer Institute whilst he also completed a MD thesis.

The RAFT Institute of Plastic Surgery provided huge support and encouragement throughout the completion of this thesis. In particular, I am very grateful to Professor Sanders for his involvement and to Addie Grobbelaar for his superb support and advice before, during and after this thesis. Thanks also to Hilary Bailey and Stephanie Easton whose help and enthusiasm make RAFT a wonderful place to work.

Finally, many thanks to Claire and all my family for their patience and sympathy during the long times I was unable to spend time with them whilst I completed this work.

Contents

Figures

Tables

Abbreviations

AJCC	**American Joint Committee on Cancer**
BCG	**Bacillus Calmette-Guérin**
CDK	**Cyclin Dependent Kinase**
cDNA	**Complementary Deoxyribonucleic Acid**
CMV	**Cytomegalovirus**
CGW	**Computer Generated Windows**
DMSO	**Dimethyl Sulphoxide**
DNA	**Deoxyribonucleic Acid**
DTIC	**Dacarbazine**
ECACC	**European Catalogue of Animal Cell Culture**
EDTA	**Ethylene Diamine Tetraacetic Acid**
EGFP	**Enhanced Green Fluorescent Protein**
ELISA	**Enzyme-Linked Immunosorbent Assay**
ELNB	**Elective Lymph Node Dissection**
EMEM	**Eagles Minimal Essential Medium**
FACScan	**Fluorescence Activated Cell Sorter**
FCM	**Flowcytometric**
FDA	**Food and Drug Administration**
FISH	**Fluorescent In-Situ Hybridisation**
FITC	**Fluorescein Isothiocyanate**
GAPDH	**Glyceraldehyde-3-Phosphate Dehydrogenase**
GFP	**Green Fluorescent Protein**
HIV	**Human Immuno-deficiency Virus**
HSVtk	**Herpes Simplex Virus Thymidine Kinase**
kDa	**Kilo Dalton**
LB	**Luria-Bertani**
LDH	**Lactate Dehydrogenase**
MHC	**Major Histocompatibility Complex**
MOPS	**4-Morpholinepropanesulfonic acid**

mRNA	**Messenger Ribonucleic Acid**
MTS	**3-(4,5-dimethylthiazol-2-yl)-5-(3-carboxymethoxyphenyl)-2-(4-sulphophenyl)-2H-tetrazolium**
MTT	**3-[4,5-dimethylthiazol-2-yl]-2,5-diphenyl tetrazolium bromide**
NGS	**Normal Goat Serum**
ODN	**Oligodeoxynucleotides**
PBS	**Phosphate Buffered Saline**
PCR	**Polymerase Chain Reaction**
PMS	**Phenazine Methosulfate**
RAFT	**Restoration of Appearance and Function Trust**
RT-PCR	**Reverse Transcriptase Polymerase Chain Reaction**
RNA	**Ribonucleic Acid**
SEER	**The Surveillance, Epidemiology and End Results Program of the National Cancer Institute, USA**
SLNB	**Sentinel Lymph Node Biopsy**
T25	**Flask with 25cm^2 area**
T75	**Flask with 75cm^2 area**
TMA	**Tissue Microarray**
TNFα	**Tumour Necrosis Factor**
TNM	**Tumour Node Metastasis**
UICC	**International Union Against Cancer**
UVA	**Ultraviolet A**
UVB	**Ultraviolet B**
WHO	**World Health Organization**

Chapter 1

Introduction

Section 1 Cutaneous Melanoma

1.1.1 History

Cutaneous melanoma results from malignant transformation of melanocytes in the skin. Melanocytes are dendritic pigment cells derived from embryonic neural crest tissue. They are found in epithelial structures including the epidermis, eye, small and large bowel, oropharynx, oesophagus, gall bladder, anus, vagina and have also been found in the capsules of lymph nodes (Woodruff 1976). The majority of melanomas are cutaneous but it can arise in any of the above body sites where melanocytes are present. Melanoma cells have marked chromosome abnormalities, are capable of aggressive local invasion into adjacent tissues and also have the ability to metastasise at an early stage.

The incidence of cutaneous melanoma has increased rapidly during the last 50 years, indeed faster than any other solid tumour (Koh 1991). With the increasing incidence, mortality from the disease has also risen with 1,640 deaths from melanoma in England and Wales each year (Cancer Research Campaign 1997) and 7,400 in the US with 51,000 new cases being diagnosed in 2001 (American Cancer Society. 2001). The life-time risk of a white male born, in the United States of America, being afflicted with melanoma according to the Surveillance, Epidemiology and End Results Program (SEER 2001) of the National Cancer Institute, is now 1 in 72. It affects all ages with a relatively high rate in young adults when compared to other cancers. Melanoma comprises 10% of all skin cancers but 80% of skin cancer deaths.

Effective treatment for melanoma has unfortunately not increased at the same dramatic rate as incidence. Once visceral dissemination has occurred, the prognosis is poor with only 5% of patients surviving for 5 years and a median survival of 6 months. Metastatic

disease is resistant to surgery, chemotherapy and radiotherapy, which are the mainstays of cancer treatment. There is a clear need for novel treatment strategies to improve survival in metastatic melanoma. Recently, understanding of the molecular biology and immunology of melanoma has advanced significantly, leading to the prospect of innovative new therapies. The most developed of these novel treatments are interferon-α-2b, selective lymph node dissection and tumour vaccines, all of which are currently undergoing clinical trials. None however, have yet to demonstrate consistent improvements in outcome and currently remain controversial.

With increasing knowledge of nucleic acid structure and function it has become a realistic possibility to manipulate the actions of these molecules in the treatment of disease. 'Gene Therapy' can be defined as 'The genetic modification of body cells of an individual patient, directed to alleviating disease in that patient' (Gene Therapy Advisory Group 1997). There are two main types of cancer gene therapy, destructive and corrective. Destructive gene therapy aims to destroy the tumour in its entirety, whereas the corrective approach attempts to repair the genetic changes that have lead to a malignant phenotype. In this way therapy will stop the cancer developing further whilst leaving it vulnerable to other therapeutic interventions. The main targets for corrective gene therapy are oncogenes that confer the malignant potential to the cell. There are many potential cell cycle targets for corrective gene therapy (Fussenegger and Bailey 1998).

Work performed at RAFT by previous surgical research fellows has identified *c-myc* oncogene expression to be an independent prognostic marker in cutaneous melanoma. It is more accurate than Breslow thickness for primary disease and nodal positivity in secondary disease (Grover, Ross et al. 1997). It is also related to prognosis in head and neck melanoma (Chana, Grover et al. 2001), acral lentiginous (Grover, Chana et al. 1999) and melanoma of the scalp (Chana, Grover et al. 1998). These investigations have highlighted both the prognostic importance of *c-myc* expression but also it's role in pathogenesis of the disease. Biological markers, such as *c-myc* are important as they can be targeted by gene therapy techniques. Previous work performed at RAFT has

demonstrated that antisense oligonucleotides can inhibit growth of melanoma cells *in-vitro* and *in-vivo* by down regulation of *c-myc* (Chana 1998).

The aim of this thesis is to present investigation of the significance of the proto-oncogene *c-myc* as a potential target for ribozyme mediated corrective gene therapy. We also aimed to investigate other biological markers in melanoma that could be future targets for gene therapy.

1.1.2 Epidemiology

Between 1940 and 1990 all countries that have maintained epidemiological studies have demonstrated a steady rise in incidence of melanoma. In the UK, accurate records are available for Scotland (MacKie, Hunter et al. 1992). During the 1980's incidence rose for both males and females, but more rapidly for males. Since 1990, the rate of increase in incidence has slowed and for females under 65 years the rate appears to be steady (MacKie, Hole et al. 1997). World standardised rates are 6.0 per 100,000 per year in males and 8.5 per 100,000 per year in females. Australia has the highest rates in the world. In both Queensland and New South Wales the incidence doubled between 1980 and 1987 (MacLennan, Green et al. 1992) (Burton, Coates et al. 1993). Australia has the highest reported incidence with figures in 1990 standing at 39.2 cases per 100,000 per year. The incidence in Scotland, however, was 7.8 per 100,000 per year for males and 12.3 per 100,000 per year in females in 1994 and is a better representation of UK figures (MacKie, Hole et al. 1997). Less than 0.3% of melanomas occur in children under 15, but thereafter incidence increases steadily with age. Incidence rates for blacks are a fraction of the rates of whites in the same geographical area. Based on selected cancer registry data (SEER 2001) the lifetime risk of being diagnosed with a melanoma for a white male is 1.60% compared to 0.13% for a black male. In the United States incidence rates increase from North to South suggesting a geographical basis for the causation of melanoma.

1.1.3 Causation

The risk of melanoma depends on both a constitutional predisposition and subsequent exposure to risk factors. Genotypic and phenotypic characteristics that predispose to melanoma are skin colour (less skin colour correlates with increased risk), skin reaction to strong sunlight (more reaction correlated with increased risk), large numbers of pre-existing naevi, freckling and a family history of melanoma (Evans, Kopf et al. 1988). The rare congenital condition, xeroderma pigmentosa, that is characterised by deficient repair of ultra violet B (UVB) damaged DNA, is associated with development of melanoma at a young age (Halpern and Altman 1999) (Kraemer, Lee et al. 1987). This reveals that UVB is involved in the formation of melanoma and UVB in sunlight can be considered the most important environmental risk factor. Ultra violet light can be divided into two distinct clinically important groups. UVB radiation has a wavelength of 290-320nm and UVA 320-400nm. UVB is thought to be the most carcinogenic terrestrial radiation (Cole, Forbes et al. 1986).

Several countries exhibit a latitudinal gradient of incidence of melanoma such as the United States of America. Melanoma becomes increasingly prevalent moving from Northern states towards the Equator. The same is true in Australia, where Victoria has a lower rate than Queensland. Since UV exposure is greater at the Equator this can be seen as evidence linking UV dose with melanoma. Severe sunburn, especially in childhood, is known to increase the risk of melanoma. Migration studies have demonstrated that moving to a sunnier region in childhood increases the risk more than moving as an adult (Koh 1991) suggesting that sun exposure at an early age is more important than exposure as an adult. This evidence supports the theory that sunlight is a causative factor.

However, the risk of melanoma is higher for indoor workers than outdoor and is more common in higher socio-economic groups than lower who traditionally would be exposed to less UV radiation (Lee and Strickland 1980; Cooke, Skegg et al. 1984). Interestingly melanoma is more common on areas of the body that receive a lower level of light exposure than highly exposed areas. This evidence is difficult to reconcile with sunlight

being a causative factor as there is higher incidence in groups that seem to have a lower total dose of UV. However, this apparent inconsistency has been attributed to infrequent but short exposures to high doses UV radiation, could be more harmful than a prolonged low level exposure (Elwood and Jopson 1997). This is unlike the relationship between UV exposure and risk for non-melanoma skin cancers where total cumulative dose seems to be most important.

Exposure in early life appears to be the most important risk but there is hazard associated with sun exposure as an adult (Westerdahl, Olsson et al. 1994). Tanning lamps are thought to be a risk given the high UV dose they emit. However the evidence remains controversial (Swerdlow and Weinstock 1998). Sunscreen use has long been recommended for prevention of melanoma but there is evidence for this in only two studies (Holly, Aston et al. 1995; Rodenas, Delgado-Rodriguez et al. 1996). However two recent studies have reported a significantly increased risk of melanoma with the use of sunscreens. Westerdahl et al found a risk of 1.8 for those who almost always used suntan creams in Sweden (Westerdahl, Olsson et al. 1995). Autier et al also reported an increased risk particularly in those with a poor ability to tan (Autier, Dore et al. 1995). Setlow and Woodhead have suggested that the use of sunscreens allow longer exposure to the sun by preventing sunburn (Setlow and Woodhead 1994). If the sun cream doesn't protect against UVA and UVB, this leads to increased exposure and therefore can increase risk. The evidence remains controversial with some clinicians recommending suntan creams and some not.

1.1.4 Mortality

In the last 10 years there is evidence to suggest that mortality from melanoma has fallen slightly in some population groups despite the rapid increases in incidence. The fall in mortality is only recent and death rates had previously been increasing but not as rapidly as incidence. Overall the 5-year survival for melanoma is good compared to other solid cancers and has recently been increasing, but it will still kill 7,400 Americans and around 1600 British citizens this year. Survival rates are highly dependent on the stage of

disease at diagnosis. In 2001 it is estimated that the 5-year survival for local disease is 96%. This represents a very high level for a malignant solid tumour. Regional disease has a 59% 5-year survival and for widespread metastatic disease the figure is only 13%. As 84% of melanomas are picked up at a relatively early localized stage, the total overall 5-year survival of the disease is 88% (American Cancer Society. 2001). Melanoma associated mortality has increased from the 1940's to 1990's, in most parts of the world. The increases in mortality have not been at the same rate as incidence. This is probably attributable to the effects of public and professional education, resulting in diagnosis at an earlier, and therefore improved, prognostic stage.

Survival has been most closely linked to thickness of the primary tumour in mm from the skin surface, the so-called 'Breslow thickness' (Breslow 1970). Patients with the thinnest tumours (<0.76mm) have a greater than 95% 10-year survival, while the thickest group, (>4mm) have a less than 50% 10-year survival. Other important variables include site of primary tumour, sex, ulceration and Clark's level of invasion.

1.1.5 Treatment of Primary Disease

William Norris described the first case of melanoma recorded in English literature in 1820 (Norris 1820) and the first surgical treatment of the disease 37 years later (Norris 1857). By 1885, surgical excision was recommended with wide margins (Coats 1885). William Handley, presenting two historic Hunterian lectures in 1907, advocated wide local excision of the primary lesion, regional lymph node dissection and amputation in selected cases (Handley 1907). These recommendations formed the basis of treatment for the next fifty years. Although margins, depth and volume of subcutaneous fat excision are still debated, surgical excision is the treatment of choice for primary melanoma. Handley suggested that margins should be 2.5cm from the border of the tumour and should extend down to the deep fascia. The argument for wider excision margins is the removal of occult foci of melanoma cells that could lead to local recurrence. Morphologically bizarre melanocytes have been reported up to 5cm from the primary tumour, suggesting that recurrence will inevitably occur in a minority of cases

with less than 5cm excision margins (Wong 1970). The aim of surgical treatment is to remove all melanoma cells from the surrounding tissue and achieve local control of the disease. Current practice is to vary the excision margin depending on the thickness of the tumour. If the tumour was less than 0.76mm thick, excision margin has no effect on local recurrence (Breslow and Macht 1977). However this was not based on prospective randomized controlled trials.

In an attempt to address the problem of thicker lesions, the WHO melanoma programme compared 1cm and 3cm excision margins for lesions of under 2mm (Veronesi and Cascinelli 1991). After a mean follow up of 90 months, 612 patients were assessed. 305 patients received a 1cm margin and 307 patients a 3cm margin. Disease free and overall survival was similar in both groups. However of the 4 cases of local recurrence all were from the 1cm margin group between 1-2mm thickness. This represents 3.3% of all the tumours in this thickness group. The Intergroup Melanoma Surgery Trial randomized 486 patients with intermediate thickness lesions (1.0-4.0mm) on the trunk or extremities to either 2 or 4cm margins (Balch, Urist et al. 1993). An update of this trial (Karakousis, Balch et al. 1996) with average follow up of 91 months revealed a greater recurrence in the 4cm margin group. Recurrence increased with tumour thickness and the presence of ulceration but was not significantly affected by choice of resection margins. Further investigations are in process comparing 1 and 3cm resection margins in tumours of greater than 2mm in depth by the Melanoma Study Group and the British Association of Plastic Surgeons. Excision margins using the AJCC/UICC classification system based on the above trials would support the excision margins below (McCarthy 1998).

Classification	Stage	Thickness	Margins
1	PTis	Melanoma in situ	5mm
2	PT1, pT2	Melanoma 0 to 1.5mm	1cm
3	PT3	Melanoma >1.5 to 4.0mm	1cm (min) to 2cm (max)
4	PT4	Melanoma > 4.0mm	2cm (min) to 3cm (max)

Table 1.1 Thickness of primary melanoma and recommended excision margins.

Primary closure should be used for resected tumour wounds if possible. With the trend towards smaller excision margins more wounds can be closed primarily. The skin graft rate for lesion excised with a 4cm margin is 47% compared to 11% in those with a 2cm margin (Balch, Urist et al. 1993). Smaller margins also reduce the cosmetic defect and in-patient stay. This is especially important in cosmetically sensitive areas such as the face. Melanomas on digits usually require amputation of the digit to achieve clearance.

1.1.6 Lymph Node Biopsy

Following excision of the primary tumour, patients with a thick tumour have a high risk of regional or metastatic recurrence. The 5-year survival for tumours greater than 4mm thick is 47% (Koh 1991). There has been much controversy as to whether further surgical intervention at the time of primary excision is warranted before recurrence occurs. Elective lymph node dissection (ELND) was proposed to remove regional lymph node basins for histology at the time of primary surgery. Firstly, this could provide important prognostic information about lymph node status. Secondly, it would remove micrometastatic deposits if present in the regional lymph node basin and therefore may confer a survival benefit. However, there is significant morbidity associated with ELND so the technique had to be shown to improve survival. However, several randomised prospective studies did not show any significant overall survival advantage (Veronesi, Adamus et al. 1977; Veronesi, Adamus et al. 1982; Cascinelli and Belli 1993; Balch, Soong et al. 1996). Two patient subgroups in the Intergroup study did show a survival benefit, patients over 60 years old and those with tumours between 1-2mm (Balch, Soong et al. 1996). Given this evidence, ELND is not routine clinical practice. A reason for the failure of ELND is that only 25% of patients have micrometastatic disease to the time of surgery and 75% of patients undergo an unnecessary procedure with significant morbidity that cannot benefit them. Protagonists of ELND argue that the benefit to the 25% of patients with occult lymph node disease is diluted by the 75% with node negative disease. In an attempt to select patients who would benefit from ELND, Cochran and Morton (Cochran, Wen et al. 1992; Morton, Wen et al. 1992) devised a method of intra-operative lymphatic mapping and removal of the sentinel node for histological analysis.

Sentinel lymph node biopsy (SLNB) is a procedure with low morbidity that can accurately detect micrometastatic deposits in regional lymph node basins. This has important prognostic implications and could direct people towards adjuvant therapy at time of presentation (Gershenwald, Thompson et al. 1999). If micrometastses are present, the patient could be selected for radical lymph node dissection during the same operation as the SLNB (Cascinelli, Belli et al. 2000). SLNB remains controversial and is currently under investigation by the WHO Melanoma Program but ultimately it will only benefit a small group of patients, ie those with occult lymph node micrometastasis at time of presentation.

1.1.7 Treatment of Metastatic Disease

Since the original descriptions of melanoma, 200 hundred years ago, the prognosis of patients with metastatic disease has not improved. Whilst progress has been made in prognostic markers and surgical techniques, advances in the treatment of metastatic disease are rare. Treatment depends on many factors including: age of patient, site and number of metastatic deposits and the personal preferences of the patient. Treatment is directed at palliation of symptoms and not elimination of the disease. Unfortunately there is no evidence that treatment of metastatic melanoma has any positive effect on overall survival (Ahmann, Creagan et al. 1989).

The prognosis for metastatic disease varies depending on the area of metastatic growth. Certain sites of the body have better overall survival with skin, non-regional lymph nodes and lung being associated with an improved median survival of 12-15 months (Barth, Wanek et al. 1995). This is contrasted with a median survival of only 3-4 months when metastases are present in bone, brain or liver. Overall the survival for all patients with a single metastasis is 7 months compared to 2 months if the patient has 3 or more metastatic deposits (Ahmann, Creagan et al. 1989; Barth, Wanek et al. 1995).

Single chemotherapeutic agents have shown treatment activity but no single agent has shown response rates greater than 25%. Dacarbazine (DTIC) remains the only

chemotherapeutic agent approved by the Food and Drug Administration (FDA). DTIC has demonstrated a response rate of 10-20%, which persists for an average of 3-6 months (Lee, Betticher et al. 1995). DTIC is well tolerated and has relatively few side effects for a chemotherapeutic agent. Temozolomide is an analogue of DTIC, demonstrating excellent central nervous system penetration and therefore can be used for brain metastasis (Bleehen, Newlands et al. 1995). Due to the relatively poor response rates for single agents, various drug combinations have been evaluated. Large, multicentre randomised trials suggest that combination regimens are not superior to DTIC alone. A four-drug combination of bleomycin, vincristine, CCNU and DTIC (BOLD) was first used 25 years ago but follow-up studies failed to demonstrate the early impressive response rates (Atkins 1997). Cisplatinum, Vinblastine and DTIC (CVD) has produced response rates of 24-45% (Legha, Ring et al. 1989) and this regimen is currently being compared to DTIC in a randomised clinical trial. The Dartmouth regimen (Cisplatinum, Carmustine, DTIC and Tamoxifen) was initially reported to have a response rate of 55% but there were low sample numbers and high numbers of side effects with one patient dying of respiratory failure (Del Prete, Maurer et al. 1984). Again, larger follow-up studies failed to reproduce the high response rates for this regimen (McClay, Mastrangelo et al. 1987; Margolin, Liu et al. 1998).

There has been significant interest in the development of biological therapies, such as interferon, in combination with chemotherapy, referred to as 'biochemotherapy'. These regimens may not have high overall response rates but some evidence suggests any response may be durable with 5-10% of patients having long-term survival (Legha 1997). The rationale is that there may be synergistic effect between the chemotherapy and immunotherapy. In addition, these two modalities have different mechanisms of action, non-overlapping toxicity and do not produce cross-resistance (Green and Schuchter 1998). Results of chemotherapy in addition to interferon have proved disappointing. Phase II trials have found no benefit of interferon with cisplatin, vinca alkaloids or nitroureas (Bleehen, Newlands et al. 1995). Early work suggested promising results with interferon and DTIC but a recent ECOG randomised phase III trial demonstrated no

increase in response rate or survival (Falkson, Ibrahim et al. 1996). Other biochemotherapy trials have generally elicited poor results.

Treatment of metastatic disease presents a huge challenge. No progress has been made in the last hundred years in patient survival. The goal at this stage is purely palliation and so therapy must be tailored to the each patient's individual needs. Standard therapy for this stage of disease remains elusive.

1.1.8 Adjuvant Therapy

Adjuvant therapy aims to complement surgery in the management of melanoma by treating any occult residual disease remaining after surgery. Post surgical adjuvant therapy is needed for patients who are free of macroscopic disease but at high risk of relapse because of micrometastatic deposits being present at the time of surgery. Occult micrometastases cause the high rate of recurrence in thick primary melanomas, as these deposits are currently impossible to discover. The resection would remove the primary tumour but the patient would quickly relapse due to the remaining undetected disease. Adjuvant therapy aims to 'mop up' any small deposits of disease, that are difficult to detect but thought likely to exsist. There has been intense research into the field of adjuvant therapy given the high rate of relapse seen in thick melanomas with regional spread. Clinical trials have been ongoing but with no clear success. The current candidates for a novel therapy are; interferons, specific immunotherapy (viral oncolysates, gangliosides, polyvalent vaccines, whole cell vaccines) and non specific immunotherapy (BCG, levamisole, transfer factor, chemotherapy, isolated limb perfusion, radiation therapy, hormonal therapy and retinoid therapy).

Interferon-alpha 2b is a pleiotropic cytokine with direct and indirect inflammatory response modulating activities including antiproliferative activity, enhancement of the immune elimination of melanoma by induction of expression of tumour-associated antigens as well as Major Histocompatability Complex (MHC) class I cell surface antigens. Interferons have been widely studied in the adjuvant setting for stage II and III

melanoma and have been shown to increase overall and disease free survival (Kirkwood, Strawderman et al. 1996), (Grob, Dreno et al. 1998; Kirkwood, Ibrahim et al. 2000) (Kirkwood, Ibrahim et al. 2001). There is also contrasting evidence, suggesting that it may not make a significant benefit (Cascinelli, Bufalino et al. 1994; Creagan, Dalton et al. 1995; Pehamberger, Soyer et al. 1998; Cascinelli, Belli et al. 2001). Many of the trials have been underpowered with a variety of dosing regimens and mixed patient populations. Meta-analysis has demonstrated an overall increase in relapse-free survival but no significant increase in overall survival (Eggermont 2001). Given the significant side effects of high dose interferon, longer but smaller dosing regimens are being investigated in the large US-intergroup trial and the EORTC 18871 trial. Interferon is licensed for use as adjuvant therapy in melanoma but it's role remains controversial.

Immunotherapy aims to stimulate the reticuloendothelial system to induce a host response to the tumour. Spontaneous regression is a recognized feature of some melanomas and this is thought to be due to antibodies directed against the tumour (Sumner 1953; Morton, Malmgren et al. 1968; King, Spooner et al. 2001). Several specific immunotherapy approaches have been investigated but none have demonstrated a clear survival benefit in randomised prospective controlled trials (Demierre and Koh 1997). In 1970 Bacillus Calmette-Guérin (BCG) was reported to invoke regression of the tumour when injected directly into melanoma nodules (Morton, Eilber et al. 1970) and subsequently many studies have been performed to investigate this effect. A trial conducted by the World Health Organization, reported in 1982, showed no difference between groups treated with BCG alone, dacarbazine alone, and BCG combined with dacarbazine. Retrospective analysis revealed that for AJCC stage III patients who had previously been BCG skin test negative there was a significant increase in survival (Veronesi, Adamus et al. 1982). But the trial had failed to enrol sufficient patients in this group. The initially promising results achieved with systemic BCG have not been repeated in several large, well-conducted trials and therefore BCG currently has no role in the treatment of melanoma.

Section 2 Prognostic Factors

1.2.1 Clinical

The role of prognostic markers in melanoma is two fold. Firstly to provide the clinician and also the patient with reliable information on the likely course of the disease. This will allow an open and frank discussion on the treatment options available to the patient, to allow them to make rational decisions concerning their management. The second role is to help in the design and analysis of clinical trials that evaluate new treatments against the natural course of the disease. In 1992 the American Joint Cancer Committee on Cancer (AJCC) Melanoma Committee published a Tumour, Node, Metastases (TNM) staging system which has recently been updated (Balch, Buzaid et al. 2001). The AJCC Melanoma Database consists of 17,600 patients and provided the prognostic information for the staging classification. This system is based on classification of the tumour thickness and ulceration (T category), number of metastatic lymph nodes (N category), site of distant metastases and presence of elevated serum lactate dehydrogenase (M category). Melanoma can then be conveniently divided into 4 stages, localized disease without regional lymph node involvement is defined as stages I and II, depending on tumour thickness and presence of ulceration. Regional lymph node involvement and/or in-transit metastasis is defined as stage III, and systemic metastasis as stage IV. The staging system permits calculation of survival rates for each stage of the disease, which are practical and convenient to use (Ketcham, Moffat et al. 1992)

Melanoma TNM Classification

T Classification	**Thickness**	**Ulceration status**
T1	< 1.0mm	A: without ulceration
		B: with ulceration
T2	1.01 -2.0mm	A: without ulceration
		B: with ulceration
T3	2.01 – 4.0mm	A: without ulceration
		B: with ulceration
T4	> 4mm	A: without ulceration
		B: with ulceration
N Classification	**No. of Metastatic Nodes**	**Nodal Metastatic Mass**
N1	1 node	A: micrometastasis
		B: macrometastasis
N2	2 – 3 nodes	A: micrometastasis
		B: macrometastasis
N3	> 4 nodes or intransit nodes	
M Classification	**Site**	**Serum LDH***
M1	Distant skin, subcutaneous or nodal mets	Normal
M2	Lung metastatasis	Normal
M3	All other visceral mets	Normal
	Any distant mets	Elevated

*Lactate Dehydrogenase

Table 1.2 AJCC TNM Classification of Melanoma

Stage	Tumour	Nodes	Metastasis
0	Tis (In-situ)	0	0
IA	T1a	0	0
IB	T1b/T2a	0	0
IIA	T2b/T3a	0	0
IIB	T3b/T4a	0	0
IIC	T4b	0	0
III	Any T	N1-3	0
IV	Any T	Any N	Any M

Table 1.3 The AJCC 2001 Staging classification

The most important prognostic factor identified in stage I and II primary melanoma is tumour thickness. In 1953, Allen and Spitz first suggested that thicker primary tumours carried a worse prognosis and this was echoed by Peterson (Allen and Spitz 1953; Peterson 1962). In 1969 Clark classified melanoma on the basis of microscopic dermal invasion depending on the tissue level invaded by the tumour (Clark, From et al. 1969). By 1970 Breslow had introduced a simplified prognostic classification by measuring the vertical height in mm of the maximum tumour invasion from the skin surface (Breslow 1970). The 'Breslow thickness' has been demonstrated to be prognostically significant in several later studies and is more accurate than Clark's level of invasion in thicker melanomas (Van Der Esch, Cascinelli et al. 1981; Koh 1991; Balch, Soong et al. 2001). Clark's level of invasion is important in thin melanomas (<.76mm) (Balch, Murad et al. 1978) (Buttner, Garbe et al. 1995).

Tumour thickness (mm)	Five year survival (%)
<0.75	96
0.75-1.49	87
1.5-2.49	75
2.5-4.0	66
>4.0	47

Table 1.4 The relationship between Breslow thickness and five-year survival for primary melanoma

Other prognostic indicators are also important. Ulceration is the next most powerful independent variable in primary melanoma and seems to be associated with a more aggressive biological behaviour of the tumour, even when controlling for other risk factors such as tumour thickness. It is estimated that the relative risk to the patient for an ulcerating tumour is twice that of a non-ulcerating tumour. Other statistically significant risk factors are patient age, sex, site of tumour and level of invasion. Increasing age is known to be associated with a worse prognosis (Austin, Cruse et al. 1994). Patient sex is a factor with male patients having a worse prognosis than females for similar lesions. Melanoma that arise in the trunk, head and neck, have a significantly worse prognosis than those on the limbs (Balch, Soong et al. 1992). Lesions on the hands and feet also have a worse prognosis than lesions elsewhere on the limbs (Day, Sober et al. 1981; Day, Sober et al. 1981). Wells et al, failed to demonstrate the correlation between location of melanoma on the hands and feet and a poorer prognosis if Breslow thickness is taken into account (p=0.54) (Wells, Reintgen et al. 1992). Several anatomical groupings have been used to predict outcome. Day suggested that tumours in the upper Back, upper Arm, Neck and Scalp, (BANS area) have a worse prognosis but several subsequent studies have failed to reproduce these findings (Day, Mihm et al. 1982). In contrast to BANS, Garbe et al, suggested another group of body areas that had high risk, Thorax, upper Arm, Neck and Scalp (TANS) based on multivariate analysis of 5093 patients (Garbe,

Buttner et al. 1995). The lower trunk, thigh, lower leg, foot, lower arms, hands, and face were identified as intermediate sites. There is clear overlap between these two groupings.

New prognostic indicators are relevant in stage III disease. Three variables are known to be prognostic; the number of metastatic nodes, the tumour burden at the time of staging (macroscopic vs microscopic) and the presence or absence of ulceration in the primary lesion (Balch, Soong et al. 2001). Site of the tumour and age of the patient are also significant risk factors but not as statistically powerful.

Metastatic spread beyond the regional lymph node basin is associated with a very poor prognosis. However there are differences in survival between visceral and non-visceral sites (skin, subcutaneous lymph nodes) in stage IV disease with visceral sites having a worse prognosis.

Established prognostic features of Melanoma for each stage

I	II	III	IV
Thickness	Thickness	No of metastatic nodes	Visceral v's non visceral
Ulceration	Ulceration	Tumour burden	Visceral v's lung
Age	Age	Ulceration	Serum LDH level
Site	Site	Intralymphatic sites	
Clark's Level	Clark's Level	Site	
Sex	Sex	Age	
		Sex	

Table 1.5 Established prognostic features of melanoma for each stage

Traditionally Breslow thickness is regarded as the most accurate prognostic indicator in stage I and II primary melanoma and this has been backed up by numerous well organized studies. However it is not perfect and it may fail to predict outcome in a significant number of thin and intermediate melanomas (Slingluff, Vollmer et al. 1988; Andersson, Dahlstrom et al. 1996). There is an ongoing search for increasingly accurate

prognostic indices. Models using several different parameters in combination, such as mitotic rate, tumour infiltrating lymphocytes, tumour thickness, anatomic site of the primary tumour, sex, and histologic regression, have been used with reported success (Clark, Elder et al. 1989; Halpern and Schuchter 1997).

1.2.2 Biological

Whilst Breslow thickness remains the gold standard prognostic factor used in melanoma today it fails to predict outcome in a significant minority of patients. Many patients with thick lesions are cured and some patients with superficial spreading melanomas die from metastasis. Clearly there is a need to identify other markers that provide more accurate prognostic information. A number of factors have recently been shown to have independent prognostic significance. Interestingly most are related to the four histopathological signs of poor prognosis suggested by Clark. (ie, mitotic rate, tumour thickness, histological regression and the presence of tumour infiltrating lymphocytes). Tumour thickness and mitotic rate indicate abnormal cellular proliferation reflecting altered cell cycle protein expression. Tumour thickness is dependent on invasion into surrounding tissues and is controlled by adhesion molecules, enzymes and angiogenic factors. Tumour regression and lymphocyte infiltration is related to immuno-regulatory molecules that determine the host immune response. These processes have been investigated in the search for increasingly accurate prognostic markers and a number are presented below.

1.2.3 Cell surface molecules

Adhesion molecules are essential for migration and attachment of melanoma cells in the extra-cellular matrix and several have been shown to affect prognosis. CD44 is a family of membrane glycoproteins that has a diverse range of functions related to homing and motility. Certain isoforms of the protein have been associated with tumour progression and the ability to metastasize in both melanoma and gastric carcinoma (Dietrich, Tanczos et al. 1997; Xin, Grace et al. 2001). However, Schaider et al reported that serum CD44 levels measured by ELISA were not prognostic in melanoma (Schaider, Rech-

Weichselbraun et al. 1997) indicating that expression of different isoform s is important for prognosis. Integrins are heterodimeric transmembrane proteins that play a diverse role in cell adhesion. Integrin αvβ3 acts as a receptor for vitronectin and over expression may to lead increased production of matrix metalloproteinase 2, breaking down the extracellular matrix and increasing invasive potential of the tumour. αvβ3 has been shown to be closely correlated to tumour thickness, local recurrence and reduced survival (Hieken, Farolan et al. 1996; Natali, Hamby et al. 1997). The melanoma cell adhesion molecule (Mel-CAM) is an integral membrane glycoprotein whose expression is correlated to tumour thickness and metastatic competence and may play a role in vascular invasion (Shih, Speicher et al. 1997). Angiogenesis is considered essential for tumour progression and it has been shown that the degree of tumour vascularity provides prognostic information. Several other cell surface molecules: CD31, Very Late Antigen 4 (VLA-4), Human endothelial leukocyte-adhesion molecule 1(ELAM-1) and CD62, are associated with increased angiogenicity and also a worse prognosis (Schadendorf, Heidel et al. 1995; Vlaykova, Muhonen et al. 1997).

Cell surface molecules are also involved in the host immune response and can be the target for immunotherapies directed at specific proteins. Tumour infiltrating T cells recognize several proteins including MART-1, tyrosinase, tyrosinase related protein 2 (TRP-2), gp75 and gp100. Expression of such protein targets may decrease with tumour progression and reduce the effectiveness of immunotherapy (Marincola, Hijazi et al. 1996). Transforming growth factor-β (TGF-β) is expressed at higher levels in deeply invasive and metastatic lesions. High serum levels are associated with disseminated disease. Targeted reduction in TGF-β inhibits both the tumour growth and metastatic potential in immunodeficient mice (Wojtowicz-Praga 1997). Transporters associated with antigen processing, Transporter associated with Antigen Processing (TAP 1) are involved in host recognition of tumours. Kamarashev et al demonstrated that TAP 1 expression on primary melanomas was a significant prognostic marker with TAP 1 down regulation correlating with development of metastasis (Kamarashev, Ferrone et al. 2001). This provides another addition to the battery of assays that attempt to evaluate melanoma patients' prognosis.

1.2.4 Abnormal gene expression

Dysregulated proliferation is an early event in the formation of a melanoma and is triggered by the loss of normal cell cycle controls in melanocytes leading to either sustained proliferation or a reduction in apoptosis. The wide range of biological behaviour demonstrated by melanomas, such as early metastasis from thin lesions or short recurrence times, reflects variety in gene expression (Polsky and Cordon-Cardo 2003). Using cDNA array methodology and knowledge of the recently completed human genome project, genes will be identified that are associated with subsets of behaviour. Many studies have focused on abnormal cell cycle or apoptosis pathways that are controlled by oncogene expression. A multitude of proteins have been implicated in tumour behaviour and therefore prognosis (Table 1.6).

p16 is a small 16kDa protein that plays a critical role in cell cycle control by inhibition of CDK-4 and CDK-6 and thereby stopping the passage of the cell into G_1. Studies have demonstrated that p16 expression is lost in advanced stages of melanoma (Reed, Loganzo et al. 1995) and in primary thick nodular melanomas expression is associated with recurrent disease (Straume and Akslen 1997). Abnormal expression of another tumour suppressor gene, p53, is found in many tumours including melanoma. Abnormalities of p53 involve over expression of a wild type protein or the accumulation of a non-functional mutant form. Over expression is significantly associated with a worse prognosis (Vogt, Zipperer et al. 1997). Another tumour suppressor gene, p21, acts as an inhibitor of cyclin-dependant kinases and so prevents transition from G_1 to S phase of the cell cycle. Cell stress, that activates p53, results in direct transcriptional up-regulation of p21. Studies investigating p21 expression in melanoma have revealed that high levels are found in malignant cell lines and even in cells undergoing mitosis (Trotter, Tang et al. 1997). This suggests that an inactive aberrant form of p21 is being produced and additional studies are required to assess the functional status of the p21 protein.

Gene function	High expression	Reduced expression
Cell-cycle modulators	p53	CDKN2A/B
		Apaf-1
		p19/ARF
		p21/WAF-1
		p27Kip1
		RB-1
Growth factors	bFGF	Endothelin-3
	VEGF	SCF
	TGF-β	
	EGF	
	PDGF	
	MGSA/GRO	
	NGF	
	IGF-1	
DNA repair		XRCC3
		MLH1
		MSH2
		PMS1
Receptor tyrosine kinases	EGFR	cKit1
Nulcear proteins and transcription factors	c-myc	AP2
	E2F	
Cell adhesion molecules	N-cadherin	Integrin VLA-4
	MCAM/MUC-18	E-cadherin
	CD44	
	Integrin VLA-1,2,6	
Metalloprotease	MMP-2	
Anti-apoptotic factors	bcl-2	nm23

Table 1.6 Genes with altered expression in melanoma.

A variety of human malignancies demonstrate the prognostic value of the Ki-67 protein. This antigen is expressed throughout the cell cycle but not in G_0 and so can be used as a marker of cell proliferation. Vogt demonstrated in thick nodular melanoma patients, low Ki-67 correlated with a lower risk of recurrence (Vogt, Zipperer et al. 1997). Increased expression correlates with p53 over expression and with disease progression (Gelsleichter, Gown et al. 1995). The oncogene bcl-2 specifically inhibits apoptosis and over expression leads to increased tumour growth. Flow cytometric studies have revealed that over expression of bcl-2 leads to a significantly shorter survival and bcl-2 is an independent prognostic marker in cutaneous melanoma (Grover and Wilson 1996).

1.2.5 Tissue Micro-arrays

For over a century, preservation of tissue in formalin, followed by embedding in paraffin for sectioning and microscopic examination, has been the standard technique for histopathological analysis. In 1998 Kononen described a method for examining multiple histological specimens simultaneously by arraying them on a single paraffin block (Kononen, Bubendorf et al. 1998). The technique involves taking representative needle cores from pre-existing paraffin blocks and re-embedding them on a master block. Several hundred specimens can be represented in the master block and analysed by a variety of techniques such as immunohistochemistry or fluorescent in-situ hybridisation (FISH). A tissue microarray, in contrast to traditional techniques, facilitates the analysis of hundreds of specimens, simultaneously under identical conditions. Traditional staining would involve laborious and time-consuming examination of individual specimens using large amounts of antibody or DNA probes.

Gene amplification is a common feature of many cancers and may confer both prognostic and therapeutic information. Determination of gene expression in the hundreds of tumours required for statistical analysis, using traditional techniques is tedious and time consuming. Tissue array technology may allow high throughput and rapid screening of gene abnormalities in a wide variety of tissue specimens.

The greatest potential disadvantage of this technique is the small amount of tumour analysed. Each 0.6mm disc of tissue consists of $1.4x10^6$ cubic microns which equates to roughly 0.3% of the amount of tissue currently considered "representative" ie a traditional histopathogical slide (Camp, Charette et al. 2000). A major obstacle is that the samples used in the tissue array may not be representative of the tumour as a whole and so lead to erroneous results. Hoos et al addressed this problem by comparing full tissue specimens with a tissue array using multiple cores from each sample (Hoos 2001). Concordance between 3 cores per specimen in a tissue array and a traditional slide was 96, 98 and 91% for Ki-67, p53 and pRB respectively. The correlation between clinical outcome and phenotype was not found to be significantly different between the two methods. Camp et al compared whole slides with staining in a varying number of microarray cores (2-10 cores) and found that 2 cores were comparable with whole slides in greater than 95% of cases (Camp, Charette et al. 2000). This important study also demonstrated that archival specimens could retain their protein antigenicity for at least 60 years. Tissue array technology therefore has the potential for large-scale retrospective studies using archival formalin-fixed, paraffin-embedded tissues.

A study of gene amplification in prostate cancer using FISH demonstrated that the myc gene is increasingly expressed during cancer progression. Primary lesions had no myc overexpression compared to local recurrence and metastatic disease which showed 4.3 and 10.6% expression respectively. By combining multiple sections from different stages of the disease, in the same microarray, Bubendorf et al was able clearly to show the development of abnormal gene expression (Bubendorf, Kononen et al. 1999). Large-scale genomic screening techniques, such as cDNA microarrays, could potentially be combined with tissue microarrays. cDNA analysis of gliomas (to identify a selection of abnormally expressed genes) followed by tissue microarray immunohistochemistry combined with survival data, demonstrated that strong expression of insulin-like growth factor binding protein 2 (IGFBP2) was significantly associated with a poor prognosis (Sallinen, Sallinen et al. 2000).

1.2.6 Serum markers

The biological markers discussed so far, are present either on the cell surface or intracellularly but markers may also be released in to the tissue fluid. Knowledge of new and easily performed assays on blood serum has resulted in a widespread search for new tumour markers that can be detected in blood samples. This has the advantage of permitting monitoring of disease status cheaply and with low morbidity. However many of the tumour markers investigated lack the sensitivity or specificity to be clinically useful.

Lactate dehydrogenase levels have been shown to be elevated in several neoplastic disorders and are thought to reflect tumour burden and increased cell turnover. Serum LDH levels are an independent prognostic marker for patients with stage IV disease and have recently been included in the AJCC classification of melanoma (Buer, Probst et al. 1997) (Balch, Buzaid et al. 2001). Seventeen types of a 21kDA protein called S100 have been described in the human and are found to be expressed in a wide range of tissues. The β subunit has been positively correlated with the potential invasiveness of melanoma and also with the stage of the disease (Hauschild, Michaelsen et al. 1999; Jackel, Deichmann et al. 1999). Hauschild has also shown that serum S100 levels predict response to chemotherapy with high levels suggesting a poor response (Hauschild, Engel et al. 1999).

Reverse transcriptase-polymerase chain reaction (RT-PCR) is a very sensitive tool for the detection of tissue specific mRNA in blood samples. Since mRNA is only transcribed in viable cells and rapidly degraded in serum, the technique can assess the level of circulating tumour cells. This technique can detect one malignant cell in 10^7 normal cells (Johnson, Burchill et al. 1995). Clearly specific mRNA targets for Reverse Transcriptase Polymerase Chain Reaction (RT-PCR) must be tumour specific and not expressed in normal haematopoietic tissues. There are no such targets currently known and so sequences only expressed in melanocytes are used which indicate tissue, as oppose to, tumour specificity. Tyrosinase mRNA is the most widely used marker in the detection of circulating melanoma cells. Melanocytes are not normally found in the circulation and

tyrosinase expression is conserved in many melanomas. Other melanocyte specific markers such as gp 100, Melan-A and MART-1 have been described (Adema, de Boer et al. 1994; Coulie, Brichard et al. 1994; Kawakami, Eliyahu et al. 1994). However, expression of these proteins is lost in a high percentage of melanomas and so reduces sensitivity of the test. The melanoma-asociated antigens (MAA) family may prove to be more useful. RT-PCR assays may provide a method for detection of occult neoplastic cells and predict disease recurrence but large prospective trials are currently needed to assess the prognostic value of this technique.

Section 3 *c-myc*

1.3.1 *c-myc*

The *c-myc* proto-oncogene has emerged as one of the key regulators of mammalian cell proliferation, differentiation and apoptosis. Indeed it is the fascinatingly diverse array of biological activities that makes the *c-myc* proto-oncogene so intriguing. The proto-oncogene is expressed in a wide range of normal adult and embryonic tissue. It has also been found to be over-expressed in several tumour types and indeed is prognostic in many (Field, Spandidos et al. 1989). *c-myc* is a member of a small multigene family of proto-oncogenes including N-myc, v-myc, L-myc, s-myc and B-myc. Whereas N-myc and L-myc are expressed mainly in embryonic tissue *c-myc* is expressed throughout the life-time of the individual (Mugrauer, Alt et al. 1988; Mugrauer and Ekblom 1991). *c-myc* is located on chromosome 8(q24) and encodes two proteins of between 62 and 64kDa molecular weight (Hann and Eisenman 1984). They are shortlived nuclear phosphoproteins probably acting as site-specific transcription factors. Although *c-myc* can immortalize cultured fibroblasts (Minks, Di Vinci et al. 1992) it is unable to transform normal cells completely and falls into a complementation group of genes that interact with other oncogenes and reflect the multi-step pathogenesis of cancer (Land, Parada et al. 1983; Land, Chen et al. 1986).

1.3.2 *c-myc* and malignant transformation

Myc genes were first discovered in an avian retrovirus named MC29 as a transforming gene and were subsequently found in four more viruses (Meichle, Philipp et al. 1992). These viruses had the ability to transform a wide selection of tissues especially in the chicken. Homologues were then discovered in a wide range of cells including humans and found to be involved in tumourigenesis. Ig/myc translocations in Burkitt's lymphoma drive *c-myc* expression, producing supra-normal quantities of protein, contributing to the genesis of a B cell neoplasia (Burns 1989). However many tumours have no chromosomal alterations at the myc encoding region and still demonstrate a higher than normal expression of *c-myc*, presumably caused by upstream deregulation of *c-myc* effector genes (Field and Spandidos 1990). In a classic experiment, Land demonstrated that neither ras nor deregulated myc could indivdually transform primary rat embryo fibroblasts but had to co-operate to achieve transformation (Land, Parada et al. 1983). ras-mediated growth inhibition is inactivated by *c-myc* and reciprocally, ras is able to inhibit myc-mediated apoptosis (Evan and Littlewood 1998). Further evidence shows that Ig-myc or MMTV-myc transgenic mice develop clonal tumours after long latency periods, suggesting that additional genetic changes must occur before transformation (Stewart, Pattengale et al. 1984; Sinn, Muller et al. 1987). These observations suggest that immortalization of primary cell lines is a complex phenomenon in which normal safeguard of apoptotic pathways are inactivated, allowing immortalized cells to emerge from a crisis period of massive cell death.

1.3.3 Molecular function of *c-myc*

The exact molecular function of *c-myc* remains unknown but it appears to act as a multimeric DNA binding protein involved in regulation of specific genes. *c-myc* encodes a helix-loop-helix/leucine zipper domain (HLH/LZ) that mediates sequence specific DNA binding and recognizes E-box (Enhancer-box) elements with a central CACGTG sequence (Blackwell 1990, Prendegast 1991). Myc dimers only bind with very low affinity *in vivo* and are not detectable in cell extracts (Dang 1991). Instead, myc

heterodimers with another HLH/LZ protein, termed Max, and this seems to be crucial for all the biological function of myc (Amati, Littlewood et al. 1993). In contrast to myc, Max is a stable protein and expressed at relatively constant levels even in quiescent cells in which myc is not being expressed. Also Max homodimers alone appear to cause passive repression of transcription (Kato, Lee et al. 1992). Another protein in the HLH/LZ family of transcription factors, known as Mad, associate with Max to form heterodimeric Mad/Max complexes in direct competition with myc. The Mad/Max heterodimer is an active repressor of transcription and often accumulates in differentiating cells (Hurlin, Queva et al. 1995). Mad/Max proteins therefore strongly antagonize the transforming abilities of myc (Cerni, Bousset et al. 1995). The relative balance of myc and Mad therefore has a key role in the control of growth and differentiation of cells by regulation of transcriptional activity.

Specific DNA binding for the myc/Max dimer allows transcriptional activation of specific genes. These target genes that ecode proteins required for cell proliferation (eg ornithine decarboxylase and prothymosin-α) or direct components of the cell cycle machinery (cdc25A). Myc is also thought to act as a transcriptional repressor of several genes such as *c-myc* itself (Penn, Brooks et al. 1990), cyclin D1 (Marhin, Hei et al. 1996) and several cell surface proteins (which may be important in immune surveillance). However the myriad of biological effects influenced by *c-myc* suggests that at least some of the critical gene targets have not been identified.

Ectopic expression of myc also induces cell death via apoptotic pathways in a number of cell lines. Evan demonstrated in Rat-1 fibroblasts that apoptotic cell death was dependant on *c-myc* expression (Evan, Wyllie et al. 1992) due to p53 mediated apoptosis (Hermeking and Eick 1994). This is thought to be due to a different group of target genes from those involved in cell proliferation but operates through similar transcriptional mechanisms (Evan, Wyllie et al. 1992). Putative targets are ornithine decarboxylase (inhibition of which blocks myc induced apoptosis), p53 and cdc25A (Packham and Cleveland 1994) (Hermeking and Eick 1994; Galaktionov, Chen et al. 1996). Telomerase, H-ferritin and IRP2 have recently been discovered to be direct targets of *c-*

myc and may be involved in apoptosis (Fuhrmann, Rosenberger et al. 1999). Is *c-myc* mediated apoptosis just a catastrophic consequence of unregulated ectopic expression or a normal physiological event? Despite two decades of intense research and discussion this apparently contradictory role of *c-myc* is still an enigmatic subject.

1.3.4 *c-myc* and tumour prognosis

The relationship between *c-myc* expression and prognosis has been investigated for a wide variety of human tumours. High *c-myc* expression has been associated with a poor prognosis in a number of different tumours including breast, colorectal, cervical, small cell lung cancers, endometrial, head and neck squamous cell, adrenocortical and gastric carcinomas (Field, Spandidos et al. 1989; Borst, Baker et al. 1990; Noguchi, Hirohashi et al. 1990; Ranzani, Pellegata et al. 1990; Riou, Bourhis et al. 1990; Heerdt, Molinas et al. 1991; Pavelic, Steele et al. 1991; Liu, Voutilainen et al. 1997). This suggests that loss of the normal tight regulation of *c-myc* may represent a frequent step in the tumourgenesis in a wide variety of cancers.

Section 4 Gene therapy

1.4.1 Gene therapy

Melanoma is a suitable disease for gene therapy. Melanomas and their metastases are often accessible, either in the skin or in regional lymph nodes. Advanced disease often has a fatal outcome and there are currently no effective therapies available. Patients with a high risk of disease progression can be identified at an early stage through accurate prognostic indicators. Gene therapy offers both adjuvant therapy at the time of diagnosis to prevent recurrence and in disseminated melanoma to control disease progression.

1.4.2 Destructive gene therapy

The majority of gene therapy strategies are based on increasing immune response towards melanoma cells. Melanoma appears to be inherently immunogenic with most lesions possessing some form of T-cell infiltrate and a small but definite incidence of complete regression of disseminated disease. Melanomas are detected by the immune system via antigen presentation by MHC class I and II molecules on the cell surface. MHC molecules activate T-helper cells and other antigen presenting cells which release a cascade of co-stimulatory molecules that lead to T-cell and natural killer cell mediated cell lysis. However most melanomas develop an immune escape either by down-regulation of MHC molecules or reduced expression of co-stimulatory molecules. Therefore the immunology strategy must over-come the immune escape mechanisms of the tumour cells, either by restoring the ability of cells to present antigens or the activity of the tumour-specific T cells. Vaccination with genetically modified melanoma cells can stimulate cell-mediated immunity but it is difficult to distinguish between cytokine effects and the transfection procedure. Genetic modification of melanoma cells to produce cytokines results in significant anti-tumour effects by sensitizing the immune system (Cao, Chen et al. 1996).

Drug sensitization gene therapy in melanoma has mainly focused on direct intra-tumoural delivery of the herpes simplex virus thymidine kinase (HSVtk) gene in combination with subsequent administration of the prodrug gancyclovir. The HSVtk, which is not present in normal mammalian cells, activates the gancyclovir by phosphorylation. The gancyclovir is then incorporated into DNA and kills dividing cells. This system has the advantage of a significant bystander effect.

1.4.3 Corrective gene therapy

Corrective gene therapy attempts to reverse the transformed phenotype by introducing genes that either correct or block the genetic damage that has occurred. There are several important limitations to corrective gene therapy in melanoma. Melanoma seems to be

genetically heterogeneous with multiple genetic abnormalities and therefore many genes may have to be targeted. Corrective genes need effective delivery to every neoplastic stem cell if they are to be curative. Currently no vector system has either the efficiency or specificity required. The role envisaged for corrective gene therapy is in combination with other current or novel treatment strategies eg interferon. There are two approaches used in this thesis: antisense and ribozymes.

1.4.4 Antisense

Antisense oligonucleotides are single-stranded DNA oligonucleotides that modify gene expression at the translation stage. They are normally between 10-25 bases long and specifically created to hybridise to corresponding RNA via Watson-Crick binding. Once the antisense is bound to the target, it is recognized as an abnormal duplex by endogenous RNase H and is rapidly degraded. Another proposed mechanism is abortion of translation by preventing the ribosome complex reading through the DNA:RNA duplex region.

RNA transcripts fold to form a secondary structure by intramolecular base-pairing and so areas of the molecule may not be accessible for hybridization. Targets must therefore be carefully considered. The translation/initiation sequence is an excellent area as this must already be accessible to intracellular enzymes and therefore also to antisense.

Antisense was first used to inhibit gene expression in 1977 in a cell free system (Paterson, Roberts et al. 1977) and the following year in chicken fibroblasts (Zamecnik and Stephenson 1978). The subsequent ten years produced little progress mainly because of difficulty in synthesis of oligonucleotides and the lack of specific sequences known in the human genome. In 1983, naturally occurring antisense RNAs were discovered and their role in gene expression was elucidated (Simons and Kleckner 1983). This encouraged the idea that oligonucleotides could be used in manipulation of gene expression in mammalian cells. A wide range of targets have since been *analysed in-vitro* and *in-vivo*.

Target	Cell type analysed	Biological endpoints
BCL2	B-cell-lymphoma, melanoma	Apoptosis
MDM2	Multiple tumours	p53 activation
BCLXL	Lung tumours	Apoptosis
RAS	Endothelial cells, bladder cancer	CAM expression, proliferation
BCR-ABL	Primary progenitor bone marrow cells	Adhesion, proliferation
Telomerase	Prostate cell lines	Cell death
c-myc	Leukaemia cell lines	Proliferation, apoptosis
c-myb	Leukaemia cell lines	Proliferation

Table 1.7 Antisense targets tested in vitro and in animals.

Antisense leads a new class of selective protein systhesis inhibitors based on the Watson-Crick hybridisation. With the rapidly growing pool of genes identified and sequenced by the human genome project there is an ever expanding list of target genes that can be investigated and treated using antisense technology. Clinical trials using antisense to treat cancer have been ongoing for several years and include melanoma. In 1998, the US Food and Drug Administration (FDA) approved the first-ever antisense drug for the treatment of cytomegalovirus-induced retinitis in patients suffering from AIDS. Antisense was delivered by local intravitreal injection, was not detected systemically and effectively inhibited cytomegalovirus-induced retinitis (de Smet, Meenken et al. 1999). Clinical trials have investigated antisense directed at protein kinase C, RAF kinase, HRAS, protein kinase A and DNA methyltransferase. The Department of Dermatology in Vienna led by Jansen have investigated BCL2 antisense in combination with dacarbazine in patients with advanced melanoma (Jansen, Wacheck et al. 2000). The target sequence 5'-TCTCCCAGCGTGCGCCAT-3' codes for the first six codons of BCL2 mRNA. Using a within-patient dose-escalation protocol, antisense was given intravenously or subcutanously to 14 patients. Side-effects were well tolerated with only mild haematological consequences such as lymphopaenia being common, transient

elevation in liver enzymes and fever. There were no dose-limiting side-effects. Immunoblot measurement of BCL2 expression demonstrated a 40% reduction in the melanomas compared to baseline. The reduced BCL2 expression was associated with a high level of apoptosis. Six of the 14 patients showed a response (one complete, two partial and 3 minor). This is the first antisense trial to demonstrate a down regulation of the target protein expression and the US FDA recently approved a phase III multi-centre trial (GENTA-GM301).

1.4.5 Ribozymes

In 1981, Cech et al described an RNA molecule that had a catalytic activity by hydrolysing phosphodiester bonds in the absence of protein (Cech, Zaug et al. 1981). These catalytic species were subsequently named ribozymes and permitted the development of molecules that can specifically suppress gene expression. Ribozymes are single stranded RNA molecules that fold into complex 3-dimensional structures. These naturally occurring molecules play a role in RNA processing. Ribozymes have an intrinsic antisense action and bind to RNA sequences via the Watson-Crick mechanism. Ribozymes mediate catalytic cleavage of mRNA molecules and so are theoretically more efficient at down regulation of gene expression. They are not bound by the one to one stoichiometric relationship that hold for antisense. The target is an NUH (N: any ribonucleotide, U: uracil, H: adenine, cytosine or uracil) sequence flanked by a known and accessible hybridisation zone. Once the mRNA is cleaved it becomes vulnerable to RNAse H and clearly cannot be transcribed by a ribosome into a full length and active protein. A number of artificial ribozymes have now been created based on a conserved catalytic core structure flanked by two variable sequence side arms. It is the side arms that bind to the target and confer the specificity of ribozymes. The catalytic core cannot form conventional Watson-Crick base pairs and so folds into a more complex structure which mediates catalysis. Ribozymes are metalloenzymes and require a divalent metal ion, such as Mg^{2+}, to cleave the RNA.

Custom designed ribozymes have great potential as both therapeutic agents and powerful tools in the investigation of gene expression.

Chapter 2

Materials and Methods

2.1 Cell lines and culture conditions

2.1.1 Cell culture medium

All melanoma cell lines were grown in cell culture medium, which was freshly prepared every two weeks and stored at 4^0C. The cell lines were grown as monolayer cultures in Modified Eagle's Mininmal Essential Medium (EMEM, Gibco, UK) which had been supplemented with:

10% fetal calf serum L-Glutamine (2mM)
Non-essential amino acids (Sigma, UK)
Penicillin 200μg/ml
Streptomycin 0.1mg/ml
Sodium Pyruvate 1mM
Sodium Bicarbonate 7.5%

2.1.2 Cell lines

Established melanoma cell lines were obtained from the European Catalogue of Animal Cell Culture (ECACC 2001) and included the A375m.

A375M

Human amelanotic melanoma derived from a 54-year old patient with metastatic melanoma. Cultures produce a confluent monolayer with a doubling time of 29 hours. ECACC Ref No: 88113005 (Giard, Aaronson et al. 1973).

2.1.3 Storage of cell lines in liquid nitrogen

Cells were stored frozen in liquid nitrogen. 1ml of cells was frozen at a concentration of 2 x 10^6 cells /ml in 2ml cryovials in a mixture of EMEM supplemented medium and 10% dimethylsulphoxide (DMSO). The vials were frozen slowly overnight to avoid excess physical damage, by being placed above liquid nitrogen and then stored in liquid nitrogen until required.

2.1.4 Recovery of cell lines from liquid nitrogen

Frozen aliquots of cells were removed from liquid nitrogen and thawed rapidly in a 37^0C water bath. The cells were then immediately added to a T-75 flask with 15ml of EMEM supplemented medium and allowed to attach to the flask for at least twelve hours. The T-75 flask is a sterile plastic tissue culture flask with an area of 75cm^2. The medium was then replaced with 15 ml of fresh medium to remove DMSO derived from the frozen aliquot.

2.1.5 Maintenance of human melanoma cell lines

Monolayer tumour cells were kept in T-75 tissue culture flasks in 15ml of EMEM supplemented medium in a 37^0C incubator, equilibrated with 5% CO_2 in air. Cells were trypsinized twice a week and re-seeded at a ratio of 1:3 – 1:6.

2.1.6 Mycoplasma testing

All cell lines were tested for mycoplasma contamination before use and at six month intervals thereafter. To test for mycoplasma, cells were sub-cultured into flasks containing antibiotic-free medium in which they were maintained for 3 days prior to testing. They were then removed from the growth surface using EDTA/trypsin and approximately 2×10^2 cells were inoculated onto a covered slide ('Flaskette' chamber

slide 177453 Nunc) with 5 ml of EMEM and placed in an incubator for 72 hours. The medium was then poured off and washed twice with PBS to remove non-specific DNA and dead cells. The cell layer was fixed in 70% industrial methanol for 30 minutes and left to air dry. Following fixation the slide was again washed twice in PBS. The cells were then stained with a 0.5 μmml^{-1} solution of Hoechst stain (Benzimidazole 33258 at 0.5 μgml^{-1}) which was left in contact for 15-20 minutes in subdued lighting. The stain was washed off with double-distilled water and the preparation was then inspected using a Nikon UFX–II microscope under UV illumination. The preparation was carefully inspected for bright cytoplasmic staining puncticular dots which represents Mycoplasma contamination. If mycoplasma was detected, the cells are discarded and cells from an earlier passage cultured. No passages of cells were found to be positive for Mycoplasma.

2.2.1 Flow Cytometry

Flow cytometry is a method of making rapid measurements on particles or cells. Several parameters based on light scatter and fluorescence can be measured as cells flow in a single stream past a single sensing point. An important feature is that each cell can be individually measured. Populations of cells can also be purified depending on cell characteristics for functional studies. The FACScan system is an automated cell analyser developed for both research and clinical applications. It is used to analyse cell populations based on the principles of flow cytometry in which cells and cell sub-populations are recognised by their light scattering and reflecting properties when they are illuminated by laser light. Unstained cell populations can be recognised depending on cell size (forward scatter of laser light) and granularity (side scatter). Side scatter is produced by diffraction of laser light caused by cellular structures such as the nucleus or mitochondria. Cellular stains, which produce characteristic fluorescence, can also be used to differentiate sub-populations.

The FACScan was used in this project to assess c-myc oncoprotein levels in melanoma cell lines. Following staining of the cells with antibodies targeting the c-myc protein, the level of c-myc expression was measured based on the degree of fluorescence emitted

from the secondary antibody. Green fluorescent protein (GFP) expression in melanoma cells lines was also evaluated using this technique.

The FACScan consists of a bench top sensor module coupled with a computer module which controls both acquisition and analysis of data. The cells to be analysed are enclosed in a pressurised saline solution. The fluidic system within the flow cytometer delivers particles from a random three-dimensional suspension singly to a specific measuring point to within an accuracy of +/- 1 micron. This is achieved by hydrodynamic focusing using the principle of turbulent boundary flow. The moving column of cells and fluid passes through a flow cell where they are illuminated and generate up to 5 signal pulses simultaneously. Intense illumination is required as the cells are small and have a high velocity. They are irradiated by a 15mW, 488nm air-cooled argon-ion laser. The scattered and fluorescent light generated is collected by photodectors that convert the photon pulses into electrical signals. Dichroic mirrors spectrally filter emitted light, separating and deflecting shorter wavelengths whilst transmitting longer wavelengths. Longer wavelengths are detected on two light scatter channels (front and side). These shorter wavelengths are further separated by other mirrors into the path of one of three photomultiplier detectors, FL1, FL2 and FL3, following which the electrical signals are amplified, digitised, processed and stored on computer for further analysis. The data was displayed either as a frequency histogram or a dual-parameter correlated plot, often known as a dot plot.

At 530nm the FL1 detector is optimised for FITC and GFP detection (green fluorescence) whilst the FL3 detector absorbs wavelengths in excess of 650nm, suitable for detection of red light emitted by propidium iodide. The FL2 channel detects intermediate wavelengths (585nm), emitted by phycoerythrin in the red/orange band used in the dual staining experiments. Dual parameter collection of data on FL1 and FL2 allows bivariate dot plots to be formulated, recording expression of GFP on the FL1 channel against c-myc expression using streptavidin phycoerythrin conjugate on the FL2 channel.

2.2.2 C-myc antibodies

The c-myc protein was identified using a rabbit polyclonal antibody raised against myc oncoproteins (Cambridge Research Biochemicals Ltd.). Both N-myc and L-myc are highly tissue specific (Garte 1993) and the oncoprotein products of these genes have not been described in melanoma. Furthermore, no evidence of either the mRNA or protein product of N-myc or L-myc was found in a study of 21 different melanoma cell lines of varying metastatic capability. Consequently, it was assumed that neither of these genes would be expressed in benign or malignant melanocytes and that the polyclonal myc antibody would only label the c-myc oncoprotein. Immunohistochemical detection of c-myc oncoprotein using the c-myc monoclonal antibody, 6E10, has been described in several papers (Jack, Kerr et al. 1986; Watson, Stewart et al. 1986; Sikora, Chan et al. 1987). However, the experience of previous RAFT fellows suggested that for c-myc estimation in paraffin embedded tissue samples the polyclonal antibody was superior (Ross and Wilson 1998). This was also the finding of other workers (Lincoln and Bauer 1989). The monoclonal antibody, 6E10, was found to be slightly more specific than the polyclonal antibody in the estimation of c-myc oncoprotein in whole cells (Ross and Wilson 1998) and was therefore used for measurement in the experiments involving c-myc manipulation *in-vitro*.

Rabbit polyclonal antibody to myc oncoproteins (Cambridge Research Biochemical Ltd) is raised against a synthetic oligopeptide, Ala-Pro-Ser-Glu-Asp-Ile-Ttp-Lys-Lys-Phe-Glu-Leu-Cys, which is common to c-, L- and N-myc and between several species. The IgG is isolated directly from rabbit sera and affinity purified prior to stabilisation and lyophilisation.

6E10 (Cambridge Research Biochemical Ltd) is a mouse monoclonal antibody raised against a synthetic peptide sequence, which recognises an epitope between residues 171 and 188 on the human c-myc oncoprotein (Evan, Lewis et al. 1985). The immunoglobulin was obtained from a cell culture supernatant.

2.2.3 Fixation of cell lines

The melanoma cell lines investigated in this thesis were fixed prior to immunostaining and FACS analysis. Cells were first trypsinized from T75 culture flasks and then fixed.

1 A T75 was drained of medium.

2 The flask was washed in 15mls of PBS and drained.

3 The flask was incubated at 37^0C with 5mls of 10% trypsin EDTA for 1 minute.

3 15mls of EMEM was added to neutralize the trypsin.

4 The solution of cells was transferred to a 25ml universal container.

5 The solution was centrifuged at 1000rpm (118G) for 5 minutes to pellet the cells. The supernatant was decanted leaving only a pellet of cells.

6 The cells were resuspended in 5mls of PBS by vortexing and separated by pippetting.

7 At this stage the cells were counted using a modified Fuchs-Rosenthal haemocytometer.

8 The correct volume of cellular solution containing the required number of cells was placed in another universal container and mixed with 5mls of PBS. Usually 250,000 cells were included for each stain used.

9 The solution was centrifuged at 1000rpm (118G) for 5 minutes to pellet the cells.

10 The cells were mixed with 5mls of ice cold 70% ethanol whilst vortexing to fix the cells.

G forces were calculated using the following equation.

$$R.C.F = 0.0000118 \times r \times N^2$$

Where RCF = relative centrifugal force, r = radius, N = rotating speed (rev per minute).

2.2.4 Staining of c-myc oncoprotein expression in cell lines

1. 250,000 fixed melanoma cells were aliquoted into conical bottomed test tubes.
2. The same number of cells were added to the control tube.
3. The cells were washed with 5ml of PBS and centrifuged at 2000rpm (472G) for 5 minutes.
4. The cellular pellet of the test sample was resuspended in 100µl of PBS containing rabbit anti-human c-myc polyclonal antibody (Sigma) at a dilution of 1:25 and also containing 0.5% normal goat serum (NGS) and 0.5% detergent (Tween 20). The cells were incubated for one hour at room temperature. The control sample was incubated in the absence of the myc antibody, but with a non-specific mouse IgG class specific antibody (Sigma Ltd, UK).
5. A further wash with 5mls PBS was performed as above to remove the primary antibody.
6. The secondary antibody (rabbit anti-mouse IgG conjugated to fluorescein isothiocyanate - Sigma Immunochemicals, UK) was added at a dilution of 1:50 in PBS containing 0.5% NGS and 0.5% Tween 20 and the cells incubated for 45 minutes at room temperature.
7. The secondary antibody was removed by washing with PBS as above.
8. The mixture was re-suspended in 1ml of PBS containing 1mg/ml of Ribonuclease A (Sigma Immunochemicals, UK). DNA staining was performed by the addition of 20µl of propidium iodide at a concentration of 1mg/ml (Sigma Immunochemicals, UK).
9. The stained samples were analysed on a FACScan flow cytometer (Becton Dickinson, San Jose CA).

Data was analysed on at least 20,000 events (cells) for each sample. The fluorescence ratio was calculated by dividing the mean FITC fluorescence of the sample (i.e. with primary antibody) by that of the corresponding control (i.e. without primary antibody) for each specimen.

2.2.5 Data Analysis and measurement of oncoprotein

The data was analysed using a computer acquisition/analysis programme, Lysys II (Becton Dickinson, San Jose CA). Events were quantified by the imposition of computer generated windows (CGW) to define specific regions on the histogram or two-dimensional dot plot. A dotplot or cytogram is a two dimensional plot of one parameter against another. CGWs allow definition of specific populations of nuclei or cells and required phases of the cell cycle. Polygons can be set around populations to omit extraneous interference from debris, or from populations of cells whose data is not required. These regions are retained and superimposed on the control sample, to allow comparison of the number of nuclei and fluorescence in identical regions.

2.2.6 Calculation of oncoprotein levels

Using Lysys II software, oncoprotein positivity was calculated from comparison of the number of events within regions applied to the dot plots of both the control and test sample (Figure 2.1). Figure 2.1 shows forward and side scatter in Plot A. Initially, a region (Region 1) was set using FL3-Width and FL3-Area to define doublet discrimination, exclude debris and cell aggregates (Figure 2.1B). Region 1 was used to gate the dotplots of DNA versus FITC (Figure 2.1 C and D). Secondly, a region was gated around the control dot plot to demarcate and differentiate labelled from unlabelled nuclei (Figure 2.1 Plot C). The same dotplot was used for the FITC labelled sample to determine the number of myc postive cells (Figure 2.1 Plot D). However the secondary antibody (FITC) adheres non-specifically to a small proportion of nuclei and cellular debris, estimated to be less than 2% of the whole population of labelled material. To exclude this fluorescence, a region is set around those 2% of nuclei exhibiting the highest fluorescence values. Using computer analysis this same region was superimposed on the antibody-labelled dot plot of the same specimen and subtraction of the event count of the antibody sample from the control gives the overall number of nuclei showing specific labelling due to oncoprotein expression. This is represented as a percentage of all nuclei,

to give the % positivity. Further regions can be set around populations of nuclei that lie within different phases of the cell-cycle, to allow analysis of oncoprotein expression within each phase. The mean fluorescence of the FITC labelled-nuclei gives an estimate of the relative amount of protein contained within each cell cycle phase and this can be represented numerically as a ratio of mean green fluorescence of positive cells compared to control (unlabelled) cells. Figure 2.1 shows a specimen with a myc positivity of 68% (Note this is an aneuploid tumour).

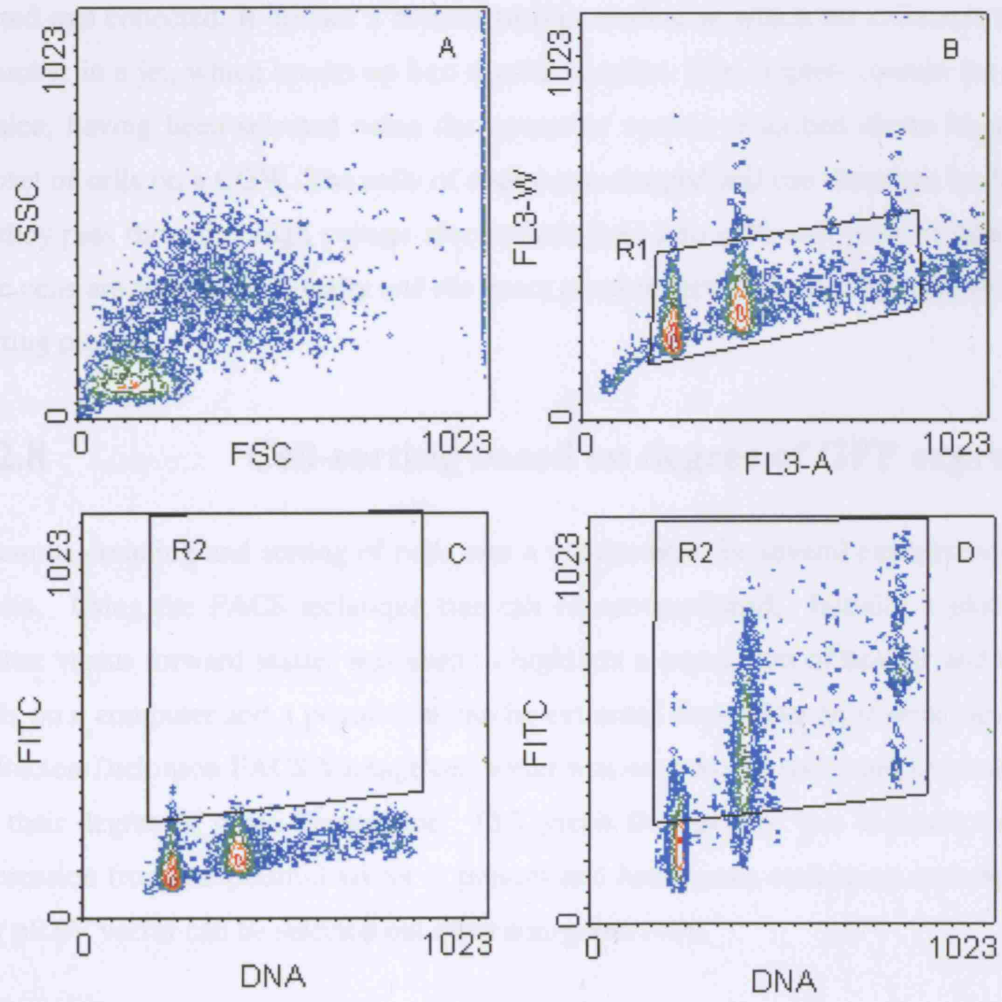

Figure 2.1 FACS dotplot.

2.2.7 Fluorescence Activated Cell Sorting

The Fluorescence Activated Cell Scan (FACScan) is an automated cell analyser attached to a computer. Cell analysis is based on the principles of flow cytometry. In the experiments described here a Becton-Dickinson FACScan was used for flow cytometry studies.

The Cell Sorter (CS) is a flow cytometer with an additional sort facility. In addition to the recognition of cell populations based on optical parameters, the cell sorter enables sub-populations of cells to be selected and individual cells from the selected population to be sorted and collected. It utilises a droplet sorting method in which the cells exit the flow chamber in a jet, which breaks up into regular droplets. The droplets contain the cells of choice, having been selected using the computer system described above by gating a subset of cells on a CGW. The cells of choice are charged and can therefore be deflected as they pass through a high voltage electrostatic field into a 96-well plate or falcon tube. The cells are sorted individually and the exact number sorted can be displayed during the sorting process.

2.2.8 Cell-sorting based on degree of GFP expression

Accurate counting and sorting of cells was a requirement for several experiments in this thesis. Using the FACS technique this can be accomplished. Initially a plot of side scatter versus forward scatter was used to highlight a population of healthy and uniform cells on a computer and a population can be extracted depending on several parameters. A Becton-Dickinson FACS Vantage cell sorter was used to sort and count live cells based on their degree of green-fluoresence. Cell green fluorescence is a indicator that GFP expression from the plasmid vector is present and hence cells containing and expressing our pREV vector can be selected out from non-green cells.

A sterile cell suspension was introduced into the flow stream and each event seen by the computer was analysed using forward and side scatter. From this resulting cytogram dot

plot, cell doublets, debris and single cells may be visualised as distinct regions. The cells required are then isolated from the unwanted material by creating a computer generated polygonal area around the population required. Cells expressing green would have FL1 values of fluorescence greater than 10^2 (this figure is arbitary). However, FL1 values from 10^1 to 10^4 indicating a wide variation of GFP expression within cells depending on the cell line or clone used. The settings used were a flow rate of 200 events/second, drop-delay frequency of 10.0–12.0, an oscillation frequency of 20-24kHz, FL1 voltage of 400–500mV voltage and log amplification. A 3-drop envelope was used to maximise the accuracy of sorting. The count mode was set to 'normal-c', the sheath pressure at 11psi and the sample differential at ≥ 1psi. These parameters are variable and may be altered to control both the speed of sorting and the accuracy. Sorting is a compromise between speed and accuracy and depends on the numbers of target cells to be sorted and the time available. Many different factors affect the sorting process eg multiplicity, amount of debris, cell density etc, and therefore settings are variable within or between each sorting experiment. FACS has 1024 channels on a linear scale (or a 4-decade log scale) such that 10^2 means channel 100 out of a possible 10,000. Hence, FL1 values are relative as they depend on the voltage set on the photomultiplier. It means that a cell found at a similar channel number may have a quite different level of GFP unless the voltage is kept the same for all samples.

The whole system is not sterile and there is a risk of infection of the cell solution after sorting. Contamination occurs from air borne particles between the sorter and 96 well plate and therefore antibiotic-containing medium must be used. The longer the sort takes the greater the risk of infection of the plates from any contaminating micro-organisms. As the cells were sorted, they were simultaneously counted and the count was displayed on the vantage console. An exact pre-determined number of cells could therefore be sorted into each well of a 96-well plate. Clones can be selected by plating 1 cell per well. The MTS assay growth assay (see 2.5.7) would take a larger number of cells depending on cell line.

2.2.9 Paraffin embedded melanomas

Dewaxing of nuclei was performed using the following protocol. Four 35μm sections were cut from each paraffin-embedded block, applied to Sellotape and then onto a plain glass slide. Slides were stored at 4°C until re-hydrated. Attempts were made to limit analysis to tumour or naevus cells by excising the appropriate area from each slide, with reference to a haematoxylin and eosin stained serial section. Samples were dewaxed in conical glass tubes, using 5ml of xylene (BDH) for 10 min and the process repeated. Specimens were then rehydrated through successivly increased hydrated alcohols, commencing with 100% ethanol (Hayman), 90%, 70% and finally 50% solutions. In each case the sample was kept in 5ml of the alcohol for 10 min, prior to centrifugation at 1000rpm (118G) for 5 min. Samples could be stored in plastic universal containers with 50% ethanol indefinitely at 4°C.

2.2.10 Preparation of nuclei

Pepsin enucleation was achieved using a concentration of 4mg/ml in 0.1M hydrochloric acid incubated for a period of 45 minutes at 37°C. Previous work had showed that pepsin enucleation does not excessively damage nuclear c-myc. The mixture was filtered through a 35μm nylon mesh in a Swinnex holder. Nuclear concentration was estimated using a haemocytometer (Weber) and adjusted to achieve a concentration of 10^6 nuclei/mm^3. The suspension was then aliquoted into two samples and washed twice in phosphate buffered saline (PBS), (centrifuged at 2000rpm (472G), for 5 min between washes).

One pair of samples was allocated for the c-myc analysis: sample and a control. In the case of test samples (as opposed to control samples), each nuclear pellet was incubated with the pan-myc (Cambridge Research Biochemicals) antibody for 1hr at room temperature. Antibody was diluted 1:25 in 100μl of a solution of PBS containing 0.5% normal goat serum (NGS) and 0.5% of a detergent, Tween 20 (Polyoxyethylenesorbitan monolaurate, Sigma). Control tubes were incubated with a solution of rabbit immunoglobulin fraction (Sigma) added at the concentration as the pan myc antibody and

diluted 1:25 in a solution of PBS containing 0.5% NGS and 0.5% Tween 20. The suspension was then washed in PBS and incubated with a secondary antibody, goat anti-rabbit IgG-FITC conjugate (Sigma). This was added at a dilution of 1:50 in 100µl of the PBS/NGS/Tween 20 staining solution for 30 minutes at room temperature.

The mixture was then washed in PBS and re-suspended in a 1ml solution of PBS containing 1mg/ml ribonuclease (Sigma), prior to addition of 20µl of propidium iodide (Sigma). Ribonuclease was used to minimise labelling of extrachromosomal oligonucleotides and RNA, which would otherwise interfere with measurement of DNA content. Flow cytometric analysis was usually performed on the day of processing and always carried out within 24 hours to minimise antigen leakage and other potential artefacts.

2.3 Green Fluorescent Protein

Green Fluorescent Protein (GFP) is a naturally occuring, spontaneously fluorescent protein found in coelenterates, such as the pacific jellyfish, Aequoria Victoria (Chalfie, Tu et al. 1994). Its role is to transduce, by energy transfer, the blue chemiluminescence of the protein aequorin into green fluorescent light. GFP can be used as a protein tag by fusion to a wide variety of proteins, many of which have been shown to retain their function. When expressed in mammalian cells GFP fluorescence is distributed throughout the cytoplasm and nucleus. It therefore has a wide range of applications as a measure of protein-protein interactions and as a reporter of gene expression.

GFP is a cylindrical protein, composed of 238 amino acids. Its absorbance/excitation peak is at 395nm, with a minor peak at 475nm. The emission peak is at 509nm. However, wild type GFP is sub-optimal for many applications due to its low fluorescence intensity when excited by blue light (488 nm), a significant lag in the development of fluorescence after protein synthesis, and poor expression in many higher eukaryotes. To improve upon these qualities, a mutant of GFP with a significantly larger extinction coefficient for excitation at 488nm has been combined with a re-engineered GFP gene sequence containing codons preferentially found in highly expressed human proteins

(Yang, Cheng et al. 1996). The combination of improved fluorescence intensity and higher expression levels yield an enhanced GFP (EGFP) which provides greater sensitivity in most systems. EGFP can be detected at much lower concentrations than GFP, 100nM as compared with 1μM for GFP. This is equivalent to 10 000 molecules per cell. The excitation peak for EGFP is 488nm and the emission peak is 509nm.

For the experiments performed in this thesis, EGFP was therefore used (Clontech).

2.4 Oligonucleotides

All oligonucleotides used were synthesised by Genosys Biotecnnologies Ltd. (Cambridge), with a phosphorothioate backbone to aid stability *in-vitro*.

2.4.1 *c-myc* antisense and '4G' quartet control sequences

The *c-myc* antisense sequence was a 15-mer oligodeoxynucleotide (ODN) complementary to the translation-initiation codon of exon 2 of the *c-myc* gene. The '4G' quartet control was also a 15-mer ODN. This was not complementary to the *c-myc* gene sequence but contained 4 guanosine residues that are known to produce non-specific effects on cell growth in some experiments (Stein 2001). This was therefore the most important control sequence to use. Neither sense nor nonsense ODNs had previously been shown to affect the growth of the A375m cell line *in-vitro* (Chana 1998) and were therefore not used in these experiments. The sequences of the *c-myc* antisense and the '4G' control are shown in Table 2.1.

Phosphorothioate Oligonucleotide	**Sequence**
c-myc antisense	5'-AACGTTGAGGGGCAT-3'
'4G' Quartet Control	5'-AAGCATACGGGGTGT-3'

Table 2.1 *c-myc* antisense and '4G' quartet ODN control sequences

2.4.2 Preparation and storage of oligonucleotides

Oligonucleotides were purified by high-pressure liquid chromatography (Genosys Biotechnologies Ltd). The products were supplied lyophilised and were then dissolved at a concentration of 0.5nM/µl in sterile Buffer TE. Prepared aliquots containing 500µl of dissolved oligonucleotide were stored at -20^{0}C in Eppendorf tubes until required.

2.5.1 Targeting the *c-myc* gene using a ribozyme

A ribozyme targeting gene was designed according to standard principles to target the translation-initiation codon of exon 2 of the *c-myc* mRNA. This is close to the area successfully targeted by the previous RAFT fellow, using antisense oligodeoxynucleotides. The efficacy of this *c-myc* antisense ODN has been demonstrated in melanoma by Jagdeep Chana (MD thesis 1998) and by Citro and Leonetti both *in-vitro* and *in-vivo* (Leonetti, D'Agnano et al. 1996; Citro, D'Agnano et al. 1998). The cleavage site at base pair 231-232 on exon two of the *c-myc* mRNA has previously been cleaved successfully *in-vitro* (Cheng, Luo et al. 2000). It targets a specific GUC sequence in the RNA molecule known to be the most efficient cleavage sequence. Adopting this as a suitable site for ribozyme mediated cleavage of the RNA molecule, a ribozyme was designed based on current protocols. The ribozyme consists of 3 areas. Stem 1 and 3 are designed to be complementary to the *c-myc* mRNA molecule whilst stem 2 is a constant region. Both stem 1 and 3 are variable and complementary to the RNA either side of the cleavage site. Stem 1 consists of a base sequence 3' AUG CAA CGC C 5'. Stem 2 consists of a base sequence 3' GU GGG AAG AGG 5'. The side arms are 10 and 11 bases long respectively and this length allows specificity of action whilst not making the ribozyme excessively large. Stem 2 is a constant structure for all hammerhead ribozymes following elucidation of the catalytic core (Haseloff and Gerlach 1988). Stem 2 consists of a base sequence 3' AAA GCA GGA GUG CCU GAG UAG UCU 5'. Therefore the base sequence for the entire ribozyme structure was as follows, 3' AUG CAA CGC CAA AGC AGG AGU GCC UGA GUA GUC UGU GGG AAG AGG 5'. This is a total of 45 bases and folds to form a complex 3 dimensional molecule.

The double stranded mammalian expression vector pREV, previously constructed by Spencer Collis at the Paterson Institute of Cancer Research in Manchester, was selected as a vector to express the ribozyme targeting *c-myc* (Collis, Tighe et al. 2001). This plasmid had been constructed from a mammalian expression vector pCGFP. This vector contains the GFP expression gene in combination with a human cytomegalovirus (CMV) immediate-early enhancer/promoter region resulting in high expression of GFP. In addition a further CMV immediate-early enhancer/promoter region, multiple cloning site, neomycin phosphotransferase gene and SV40 poly(A) regions were extracted from a commercial available plasmid, pCI-neo (Promega) using *Bam*HI/*Bgl*II restriction sites. These elements were then ligated into the *Bam*HI site in the pCGFP. The human CMV immediate-early enhancer/promoter region promotes constitutive expression of cloned DNA inserts. The neomycin phosphotransferase gene is a selectable marker for mammalian cells and therefore the plasmid can be used for transient expression or for stable expression by selection of transfected cells with the antibiotic G418. The pREV plasmid is 7550 base pairs. A ribozyme-cloning restriction site is present in the plasmid between M*lu*I and X*ba*I. This site is driven by a CMV enhancer/promoter with a SV40 late polyadenylation site at the 3' end, to promote ribozyme expression. The plasmid also contains genes encoding ampicillin resistance whose expression is again promoted by a SV40 promoter. This plasmid is known to express functional ribozymes (Collis, Tighe et al. 2001) and was used as the vector for the anti *c-myc* ribozyme. A scheme for ribozyme production can be seen in Figure 2.2.

Target sequence selected near translation/initiation site

↓

2 side arms designed to hybridise to target either side of catalytic core

↓

Oligonucleotide sequences created with Mlu and Xba overhanging ends

↓

Oligonucleotides annealed

pREV plasmid linearized at Mlu and Xba restriction sites

↓

Ligation with oligonucleotides

↓

Transformation of E coli with circular plasmid

↓

Clones transformed with plasmid selected by Ampicillin in agar

↓

(Screening of clones for ribozyme using PCR)

↓

E coli clones grown over night and DNA extracted

↓

(DNA sequenced using LiCor squencer across ribozyme site)

↓

Large scale production of plasmid vector, extraction

and purification using maxi-prep protocol

Figure 2.2 Flow chart of production of ribozyme

2.5.2 Ribozyme synthesis and insertion into pREV

2.5.2.1 Annealing of oligonucelotides

Two complementary oligonucleotides were obtained from MWG Biotech. A 49-mer oligonucleotide, *c-myc* Ribo 3.1, and its complementary partner, *c-myc* Ribo 3.2 were dissolved in sterile double distilled water at 50pmol/µl. The two oligodeoxynucleotides were added in equal but varying amounts to an Eppendorf tube. 1µl, 2.5µl and 0.2µl of 50pmol/µl solution was added to water to make up a total of 5µl. Control solution was created by adding double the amount of oligonucleotide but of only one oligonucleotide. This ensured no annealing would take place and could thus be used as a control at the ligation stage (see below). The solutions were heated to 55^0C for 5 minutes and then allowed to slowly cool to room temperature using a programmable heating block (Biometra). Annealing of the oligonucleotides occurred with a 4-base overhang at each end so that a double-stranded base sequence resulted with two single-stranded ends. The single-stranded terminae are compatible to the *Xba*I and *Mlu*I cloning sites in the vector.

2.5.2.2 Preparation of the Vector

The pREV circular vector was linearized by digestion using a MluI resriction enzyme (MBI Fermentas). 1.2µl pREV1 vector (1.68mg/ml) was added to 14.8µl H_2O, 2µl R buffer, 2µl MluI to make a total volume of 20µl. The solution was incubated at 37^0C for 40 hours on a programmable heating block (Biometra). This produced a linear pREV plasmid with 2 MluI terminal ends. The solution then had to be cleaned before further digestion could take place. This was performed using a QIAquick Nucleotide Removal Kit (QIAGEN) that includes the various buffers used. The protocol is as follows:

1 Add 200µl Buffer PN to 20µl pREV + MluI digest and place in a spin column. This allows binding of the digest mixture to the column resin.

2 Spin for 1 minute at 6000rpm (1699G) and discard the supernatant. The digest remains on the column resin but the restriction enzyme is removed.

3 Add 750µl Buffer PE to the column.

4 Spin for 1 minute at 6000rpm (1699G) and discard the supernatant. This step is performed to wash the final salts off the DNA fragments

5 Spin for 1 minute at 13500rpm (8600G) and discard any follow through. The digest is cleaned of all alcohol and dried.

6 Add 34µl Buffer EB to the column to elute pREV-MluI and place in a clean centrifuge tube. Buffer EB removes the DNA digest from the resin allowing it to pass into the clean tube.

7 Spin for 1 minute at 13500rpm (8600G).

The linearized plasmid is next digested using the XbaI restriction enzyme (MBI Fermentas) using a similar protocol to the digestion with MluI. 34µl pREV-MluI is added to 4µl Buffer Y and 2µl XbaI to make a total of 40µl. Again this solution was incubated at 37 ^{0} C for 4 hours. The resulting digest requires a clean up to remove the restriction enzymes and unwanted nucleotides. The pREV plasmid now has an MluI and XbaI 'sticky ends'. The clean up was performed using a QIAquick Nucleotide Removal Kit (QIAGEN) that includes the buffers used.

8 Add 200µl Buffer PN to 20µl pREV-MluI + XbaI digest and place in a spin column. This allows binding of the digest mixture to the column resin.

9 Spin for 1 minute at 6000rpm (1699G) and discard the supernatant.

10 Add 750µl Buffer PE to the column.

11 Spin for 1 minute at 6000rpm (1699G) and discard the supernatant.

12 Spin for 1 minute at 13500rpm (8600G) and discard any supernatant.

13 Add 50µl Buffer EB to the column to elute pREV-MluI-XbaI and place in a clean centrifuge tube.

14 Spin for 1 minute at 13500rpm (8600G).

15 Determine the concentration and purity of pREV-MluI-XbaI by spectrophotometry (Eppendorf).

NB MluI and XbaI were at a concentration of 8-12u/µl.

2.5.2.3 Ligation reaction

The pREV plasmid is now linearised and has two incompatible ends, (MluI and XbaI) that ensures unidirectional cloning during ligation. The previously annealed oligodeoxynucletides encoding the ribozyme gene have overhanging ends complementary to the overhanging ends on the linearised plasmid. By mixing the two solutions with a suitable DNA ligase, the oligodeoxynucleotides will insert between the two 'sticky ends' of the plasmid. This process will reform the linear plasmid back into a circlar plasmid with the ribozyme encoding gene inserted in the correct orientation and position. The ligation reaction was initiated by adding 5µl of annealed oligodeoxynucleotides to 1.5µl of H_2O, 1µl of 10x reaction buffer, 1.5µl of pREV-MluI-XbaI and 1µl of T4 DNA ligase (Fermentas) to a total volume of 10µl. The solution was incubated at 22^0C for 24 hours on a programmable heating block.

2.5.2.4 Transformation of E. coli bacteria

1. TOP10 One Shot (Invitrogen) E coli chemically competent bacteria were slowly thawed on ice from –70° C storage in Eppendorf tubes for 10 minutes.
2. 2.5µl of each ligation mixture was placed in a cold Eppendorf tube. It is important that the mixture and cells are kept cold to avoid damage to the fragile membranes. Cells should not be mixed by pipetting. 25µl of E.Coli were added and the solution was incubated on ice for 30 minutes. This stage allows the plasmid to stick to the bacterial cell walls.
3. The bacteria were then heat-shocked at 42°C for 20 seconds to allow transformation to occur and then immediately put back on ice for 2 minutes. The heat shock disrupts the cell membrane allowing transformation of the cell with plasmid DNA.
4. The bacterial suspensions were then added to 250µl of SOC (rich culture medium).
5. Shake at 225 rpm for 1 hour at 37°C to allow expression of the plasmid containing the gene for ampicillin resistance and recovery of integrity of the cell membrane.
6. After 1 hour, 100µl of each bacterial suspension were plated out onto ampicillin

(50μg/ml) containing Luria-Bertani (LB) agar plates and incubated overnight at 37°C. The ampicillin will select out E. Coli that contain the plasmid and are therefore resistant to ampicillin. The control ligation mixture should still be linear as the incompatible ends should be unable to ligate. This leads to inefficient uptake and expression of the ampicillin resistance and hence death of the E.coli.

2.5.2.5 Selection of clones

1 Following overnight incubation of the transformed E. Coli, the number of colonies on each plate was counted. A plate was picked containing a large number of discrete colonies when compared to its negative control. A small amount of bacterial material from each colony to be screened was removed. The material was screened for the presence of a correctly sized DNA plasmid vector encoding the ribozyme mini gene using polymerase chain reaction (PCR). CMV and SV40 primers were used to amplify across the ribozyme insert region. A small amount of bacterial material from each colony to be screened was removed using a sterile loop and streaked onto a numbered agar and ampicillin plate. At this stage a positive control (consisting of a previously made complete pREV plasmid of similar size) and a negative control (consisting of the origin pREV plasmid without any ligated gene) were also streaked out.

2 The colonies were incubated at 37^0C for 4 hours.

3 A small amount of material from the colonies was added to 100μl of H_2O in a 0.5ml tube.

4 Each tube was heated to 95^0C for 3 minutes using a programmable thermostat. Cells were lysed and DNA released into solution.

5 10μl of the ligated plasmid solution was added to 1μl of SV40 primer, 1μl of CMV (SP) primer and 38μl of Readyload (containing dTP, cTP, aTP, tTP, magnesium, Taq polymerase and buffer).

6 The PCR solution was placed in a programmable thermostat block and run on the following program.

a. 94^0C for 2 minutes for the initial denaturing of the DNA.
b. 94^0C for 1 minutes to denature.
c. 50^0C for 1 minute to anneal primers to plasmid.
d. 72^0C for 1 minute to extend primers and polymerisation.
e. Steps b to d were repeated 40 times.
f. 72^0C for 5 minute for the final extension.
g. 24^0C for 4 hours.

7 Steps 6b to 6e were repeated 40 times.

8 The product of PCR is specific and present in high concentration and ready to be visualized on an ethidium bromide stained agarose gel.

9 Following PCR, 10µl of each PCR mixture was run on a 1.5% agarose electrophoresis gel at 100 volts for 45 minutes to establish the size of the amplified fragments. A 100 base DNA ladder marker was used as a measurement of band sizes. The positive control was a pREV plasmid with a similar sized gene incorporated. The negative control was pREV plasmid with no ligated insert.

10 The gel was recorded using a Polaroid photograph in ultra violet light.

The gel was prepared from a 1.5% agarose gel containing 3g of agarose dissolved in 200ml of Buffer TAE and 100µl of ethidium bromide (10mg/ml).

At this stage the clones having appropriately sized bands on the running gel were selected for further analysis before a final clone was selected. A small amount of high purity DNA was obtained by using a QIAprep Spin Miniprep Kit (QIAGEN) which is supplied with buffers. The protocol is as follows:

1 Inoculate 5mls of Luria-Bertani (LB) medium with small number of cells from a numbered colony on an agar plate.

2 Incubate overnight at 37^0C (total 16 hours) and shake the solution at 225rpm.

3 Spin solution at 6000rpm (1699G) for 5 minutes and remove the supernatant.

4 Re-suspend the cells in 250µl of cold Buffer P1 containing an RNAse at a concentration of 100µg/ml to remove any traces of RNA, which might interfere with DNA sequencing.

5 Add 250µl Buffer P2 and invert gently 6 times. Buffer P2 contains sodium hydroxide and SDS detergent to lyse the bacteria and release the DNA. The genomic DNA is fragile and must be handled gently to prevent shearing of the DNA.

6 Add 350µl Buffer N3 and invert gently 6 times to neutralise the solution and to precipitate the DNA.

7 Spin at 13500rpm (8600G) for 10 minutes.

8 Place the supernatant containing the plasmid DNA and cytosol components into a QIAprep spin column by pipetting. The pellet containing large DNA molecules and cell membrane fragments is discarded. The QIAprep spin column is placed in a 1.5ml Eppendorf tube.

9 Spin at 13500rpm (8600G) for 1 minute and discard the supernatant.

10 Add 500µl of Buffer PB to wash the column.

11 Spin at 13500rpm (8600G) for 1 minute and discard the supernatant.

12 Add 750µl Buffer PE to wash the column. Buffer PE contains ethanol, which removes small fragments of cell membrane from the column.

13 Spin at 13500rpm (8600G) for 1 minute and discard the supernatant.

14 Spin at 13500rpm (8600G) for 1 minute.

15 Place the column in a clean 1.5ml Eppendorf tube.

16 Add 50µl of Buffer EB and let the mixture stand for 1 minute.

17 To elute the plasmid DNA spin at 13500rpm (8600G) for 1 minute.

The plasmid DNA, dissolved in 50µl of Buffer EB was quantified for concentration and purity using spectrophotometry. 5µl of the plasmid DNA solution was mixed with 95µl of H_2O and placed in a transparent plastic disposable cuvette for UV-light measurements using a Biophotometer (Eppendorf). This device passes UV light with a wavelength of 260nm and 280nm through the sample. Absorbance of the UV radiation by the solution of DNA is measured. The concentration of the DNA is related to the optical density at 260nm of the solution. The purity is estimated by the ratio of optical density at 260nm and 290nm. The concentration and purity of the DNA sample is important for the

sequencing of the plasmid DNA. The sample must have a sufficient purity and concentration for the DNA sequence to be correctly sampled.

2.5.3 Storage of E. Coli

For long term storage of the E. coli that were shown to be expressing the plasmid vector, the cells were frozen. 700µl of LB medium containing E. coli from the Step 1 of the miniprep protocol was mixed with 300µl of 50% glycerol. The solution was immediately cooled to minus 60^0C and stored in a freezer. Glycerol stocks of E. coli ensure that future mini or maxipreps could be performed immediately without performing ligation reactions on the plasmid vector.

2.5.4 DNA sequencing of the plasmid vector.

In order to ensure that the ribozyme encoding oligonucleotides had been inserted in the correct orientation, number and with the original base sequence, the plasmid was sequenced across the MluI and XbaI resriction sites. DNA sequences requires a small quantity of highly pure DNA and appropriate primers to analyse the DNA base sequence. Using the PolyL2 primer the plasmid vector was sequenced across the area containing the ribozyme minigene. This identified whether the ribozyme and reverse ribozyme had been inserted into the plasmid in the correct orientation and position. There was only one copy present. Theoretically 3 copies could be ligated into the plasmid with the middle copy reversed as this would allow correct orientation of the overhanging MluI and XbaI ends.

The plasmid vector was sequenced on a Li-Cor DNA sequencer (Li-Cor Biotechnology, USA) by Sarah Bourne.

2.5.5 Large-scale production of plasmid vector and extraction and purification using the maxi-prep protocol

Following confirmation of the correct DNA sequence of the plasmid, the DH5α e.coli bacteria producing the plasmid were grown up at a larger scale. This yielded large quantities of the plasmid DNA to enable testing of its efficacy in-vitro. The DNA was extracted and purified from the cultures using the QIAFilter maxi-prep protocol (QIAGEN).

1 A starter culture of bacteria was initially produced by innoculating 5ml of LB culture medium containing ampicillin (50μg/ml) with the E. coli from a correctly sequenced clone in a universal and incubating it at 37°C for 8 hours with vigorous shaking (250rpm). The bacteria were either taken directly from a selective plate or from the frozen glycerol stocks.

2 0.5ml of the starter culture was then added to 100ml LB medium (Sigma) with ampicillin (50μg/ml) in a flask and incubating overnight at 37°C with vigorous shaking (250rpm).

3 The bacterial suspension was then centrifuged at 6000rpm (1699G) for 15 minutes at 4°C to obtain a pellet containing approximately 100mg of bacteria.

4 The supernatant was removed and the bacterial pellet resuspended in 10ml of buffer P1 (containing 50mM of Tris-Cl, 10mM EDTA and 100μg/ml of RNAase A).

5 10ml of buffer P2 (containing 200mM of sodium hydroxide and 1% SDS) was then added to lyse the cells and the tube inverted 4-6 times to mix and incubated at room temperature for a maximum of 5 minutes.

6 10ml of cold buffer P3 (containing 3.0mM potassium acetate) was then added to neutralise the pH and the tube again mixed by inverting it 4-6 times. This was followed by the appearance of a white precipitate containing genomic DNA, proteins, cell debris.

7 The solution was then poured into the barrel of a Maxi QIAfilter and incubated for 10 minutes at room temperature to allow the precipitate to float to the top and form a layer on top of the solution.

8 10ml of equilibration buffer QBT (containing 750mM sodium chloride, 50mM 4-Morpholinepropanesulfonic acid (MOPS) at pH 7.0 and 15% isopropanol) was added to the QIA cartridge to reduce surface tension. The cap was then removed from the base of the QIAfilter and the plunger inserted into the filter. Gentle pressure was applied to the plunger to filter the lysate through the QIA filter cartridge and into the QIA cartridge.

9 Approximately 25ml of lysate was recovered after filtration. The lysate was then allowed to enter the resin within the QIA cartridge by gravity.

10 The cartridge was subsequently washed twice with 30ml of buffer QC (containing 1.0M sodium chloride, 50mM MOPS at pH 7.0 and 15% isopropanol) to remove contaminants, particularly carbohydrates.

11 The plasmid DNA was eluted from the filter by the addition of 15ml of buffer QF (containing 1.25M sodium chloride, 50mM Tris-Cl at pH 8.5 and 15% isopropanolol) to the filter and the eluate collected in a clean 30ml tube.

12 The DNA was precipitated by the addition of 10.5ml of isopropanol at room temperature and the mixture immediately centrifuged at 1000rpm (47G) for 30 minutes at $4^{O}C$.

13 The supernatant was decanted and the DNA pellet washed by the addition of 5ml of 70% ethanol at room temperature and centrifugation at 9500rpm (4260G) for 10 minutes.

14 The pellet was air-dried for 5-10 minutes and redissolved in 1ml of buffer (10mM Tris-Cl at pH 8.5).

15 The quantity and purity of the DNA was measured using a spectrophotometer in the same way as described in the miniprep protocol.

16 The DNA plasmid vector was then stored in a labelled Eppendorf tube at minus $20^{0}C$ in a freezer.

The plasmid vectors were named pREVc-myc3Ribo denoting the ribozyme, pREVc-mycRev denoting the reverse control ribozyme.

2.5.6 Transfection of melanoma cells

Transfection is the transfer of DNA into cells and is essential for the expression of pREVc-myc3Ribo and pREVc-mycRev plasmid vectors. Cationic lipids have been used extensively to enhance cellular uptake of DNA and RNA. Cationic lipids interact with the negatively charged phosphate groups on DNA to form lipid-DNA complexes. When introduced to cells they are thought to either fuse with the cell membrane or be taken up by endocytosis. A variety of transfection agents were tested to find the optimum transfection strategy. Lipofectamine (Gibco), Escort (Sigma), ExGen 500 (Fermentas) and Transfast (Promega) were all tested. Different cell lines require significantly different transfection conditions to produce optimum uptake of DNA constructs. It is necessary to test several transfection agents in a variety of conditions to optimise the transfection process. Factors that need to be investigated are the type of transfection agent and formulation, culture medium during the uptake period, duration of application and ratio of transfection agent to DNA. Using a 6 well plate format cells were incubated for varying periods of time with different transfection agents. The ratio of DNA to transfection agent and the total amount of transfection agent used were also investigated. Following incubation of the lipid-plasmid complex, cells were washed and reincubated for 24 hours in EMEM medium. Flow cytometry was then used to determine the percentage of cells expressing GFP. After several investigations ExGen 500 was selected as the most cost effective, efficient and practical of the group tested. Typical transfection protocols for each of the agents used is seen below.

Transfection protocol for Lipofectamine.

1. Mix 10µg DNA with 90µl serum free medium. Mix 10µl Lipofectamine Transfection Reagent and 90µl warm Serum Free Medium (SFM) for each well to be transfected then add the two solutions together.
2. Mix gently and leave at room for 15-20 minutes.
3. Remove the medium from the cells and wash with SFM.
4. Add the DNA mixture to two of the 6-well plates, the other is the control plate.

5. Swirl the plate gently and add 1ml warm 5% FCS.
6. Repeat for each of the different plates.
7. Incubate for 4 hrs.
8. Remove the DNA mixture and add 2ml of EMEM.

Transfection protocol for Escort.

1. Mix 10µg DNA with 15µl Escort Transfection Reagent and 230µl warm Serum Free Medium (SFM) for each well to be transfected.
2. Mix gently and leave at room temperature for 15-20 minutes.
3. Remove the medium from the cells and wash with SFM.
4. Add the DNA mixture to one of the 6-well plates, the other is the control plate.
5. Swirl the plate gently and add 1ml warm 5% FCS RPMI.
6. Incubate for 4 hrs.
7. Remove the DNA mixture and add 2ml EMEM.

Transfection protocol of ExGen 500.

1. Mix 125µl 0.15% NaCl with 5µg DNA for each well to be transfected.
2. Mix 17µl ExGen 500 with 100µl 0.15%NaCl, Vortex and spin briefly.
3. Add 2 to 1.
4. Incubate for 10 minutes at room temperature.
5. Add DNA to well.
6. Gently swirl by slow hand rotation.
7. Add 1ml of 55 FCS RPMI 2-3 hours.
8. Remove 5% FCS.
9. Add 2ml of EMEM.

Transfection protocol for Polyfect.

1. Dilute 1.5µg DNA in 100µg of Serum Free Medium (SFM). Vortex and spin briefly
2. Add 15µl Polyfect and vortex.
3. Incubate for 10 minutes at room temperature.

4. Remove medium from cells, wash in PBS and add 1.5ml complete medium to each well.
5. Add 0.6ml EMEM to reaction tubes, pipette-mix twice then immediately add to wells. Gently swirl dish.

2.5.7 Assessment of the effect of *c-myc* ribozyme on the growth of the A375M melanoma cell line

The effect of transfection with the pREVmyc3ribo plasmid on the growth of the A375M cell line was compared with the growth rates of A375M cells transfected with the pREVmyc3Rev, pREVmyc3AS or untransfected A375M cells treated with either antisense or nonsense oligonucleotides or normal A375M cells to act as controls. Antisense treated A375M cells acted as positive controls.

1. A375M cells in a T75 were split into 5 T25 flasks. These were then incubated for 24 hours.
2. At 50% confluence in T25 flasks the flasks were transfected with the groups above.
3. Each flask was drained of EMEM medium, washed with 2mls of serum free medium and then drained again.
4. 125µl of 0.15% NaCl was added to 20µg of plasmid DNA for each of the plasmids used in 3 separate Eppendorf tubes and vortexed briefly.
5. 100µl of 0.15% NaCl was added to 50µl of ExGen 500 in 3 different separate 1.5ml Eppendorf tubes and vortexed briefly.
6. The NaCl and ExGen 500 solution was the added to the NaCl and DNA Eppendorf and immediately vortexed.
7. Each Eppendorf was incubated at room temperature for 10 minutes.
8. Each T25 then had one DNA-ExGen 500 solution added and immediately hand swirled to ensure even distribution of the lipid-DNA complex.
9. 2mls of medium containing 0.5% fetal calf serum was added to each T25 and the flasks incubated at 37^0C for 3 hours. This allowed the lipid-DNA complexes time to come into contact with the cells.
10. 5mls of EMEM medium was added for 24 hours.

11. Each T25 was drained, washed with 5mls of PBS and 2mls of trypsin EDTA was added for 1 minute.
12. Following confirmation that the cell layer had been suspended, 10mls of EMEM medium was added to neutralize the trypsin.
13. The cell suspension was placed in a 15ml conical bottomed centrifuge tube (Greiner) and centrifuged at 1000rpm (118G) for 5 minutes.
14. The supernatant was removed and discarded.
15. The cellular pellet was vortexed and resuspended in 1ml of EMEM.
16. Each sample was then sorted using the FACS Vantage cell sorter into 96 well plates (TPP). 1000 cells were plated into each well. Each well contained 100µl of EMEM.

The plates were then incubated for five days to allow adequate cell growth for any differences in growth rate to be detectable using the MTS assay (Promega) in the last three days. Cell number in each well was measured indirectly by measuring the degree of conversion of MTS (Owen's reagent) into a coloured, water-solule formazan that absorbs light at 490nm. MTS is 3-(4,5-dimethylthiazol-2-yl)-5-(3-carboxymethoxyphenyl)-2-(4-sulfophenyl)-2H-tetrazolium:

1. 250mg of MTS reagent 1 was dissolved in 125ml PBS and filter-sterilised. For each plate, 10ml of this mixture was added to 900µl PBS and 100µl PMS (MTS reagent 2).
2. After two days incubation of the 96-well plates, 40µl of this mixture was added to each well and the plates incubated for four hours. The colour change was then measured using a luminometer (Berthold BL536) linked to a personal computer and the data collated using Microsoft Excel.
3. Growth measurements were repeated on the next two days.

2.5.8 Fixation of A375M melanoma cells for dual staining of *c-myc* and GFP.

Paraformaldehyde/methanol fixation following growth of A375M melanoma cells in T75 flasks.

1. Trypsinize cells in a T75.
2. Add 5mls PBS.
3. Spin at 1000rpm (118G) for 5 minutes.
4. Wash in 5mls of PBS
5. Spin at 1000rpm (118G) for 5 minutes.
6. Add 1ml of 1% paraformaldehyde solution (1gm of paraformaldehyde in 100ml PBS: warm PBS to near boiling and stir in the paraformaldehyde. Store at 4°C in foil-wrapped bottle) and incubate for 15 minutes at room temperature.
7. Spin at 1000rpm (118G) for 5minutes.
8. Wash in 5mls of PBS.
9. Resuspend in 200µl of PBS.
10. Add 3.5mls of 100% methanol and incubate for 10mins at –20°C.
11. Dilute to 70% with 1.5mls distilled water and store at 4°C.

c-myc staining protocol following paraformaldehyde/methanol fixation.

1. Aliquot $1x10^6$ cells into four 10ml tubes
2. Add 5ml PBS and spin at 2000rpm (472G) for 5mins
3. Resuspend pellet in 200µl of PBS containing 0.5% normal goat serum (NGS), 0.5% Tween-20 and either 25µg of c-myc polyclonal antibody or isotypic control (Rabbit Immunoglobulin). Incubate for 1hour at room temperature.
4. Add 5ml PBS and spin at 1500rpm (265G) for 5mins.
5. Resuspend pellet in 200µl of PBS containing 0.5% normal goat serum (NGS), 0.5% Tween-20 and 4µl swine anti-rabbit biotinylated antibody. Incubate for 30-60 mins at room temperature.

6. Add 5ml PBS and spin at 1500rpm (265G) for 5mins.
7. Re-suspend pellet in 200µl of PBS containing 0.5% normal goat serum (NGS), 0.5% Tween-20 and 10µl streptavidin phycoerythrin antibody. Incubate for 30-60 mins at room temperature. Add 5mls PBS, spin at 1500rpm for 5mins.
8. Re-suspend in 1ml PBS.
9. Analyse on FACScan.

2.5.9 Antibodies information.

Rabbit Immunoglobulin Fraction (Solid-Phase Absorbed)(DAKO No. X936)

10µl Rabbit IgG in 150µl PNT then 25µl of this in 1000µl PNT.

Swine Serum (Normal) (DAKO No. X0901)

Biotinylated Swine Anti-Rabbit Immunoglobulins (DAKO No. E0353)

R-phycoerythrin-conjugated Streptavidin (DAKO No. R0438)

Rabbit Polyclonal Antibody to myc (SIGMA GENOSYS No. OA-11-802A)

2.6 Assessment of the effect of the pREVc-mycribo3 ribozyme on *c-myc* oncogene expression in A375M melanoma cells

1. $9x10^6$ A375m melanoma cells were seeded into each of three T150 flasks. The flasks were incubated overnight in a humidified, 5% CO_2 incubator at 37°C to allow them to attach.
2. The following day the cells were checked for the presence of infection, an even cell distribution in the flask. One flask was designated as the control flask and received no treatment. The cells in the second flask were designated for transfection with the pREVmyc3.1 ribozyme and those in the third flask to receive the pREV plasmid control sequence.
3. The transfection mixtures containing either the ribozyme or plasmid control were prepared in the following manner. 260µl of DNA solution containing 130µg of DNA mixed with 390µl of ExGen500 (Fermentas) reagent. 4.2ml of serum-free medium

was then added at 37°C. The contents were mixed and left to stand for 45 minutes at room temperature to allow DNA-lipofectamine complexes to form.

4. After 45 minutes the medium was removed from the A375m cells in the T150 flasks and the cells washed with 20ml of serum-free medium. The transfection mixtures were then added to the A375m cells and 5ml of medium containing 5% FCS added.
5. The flasks were then placed back in the incubators (level to ensure even coverage of the cells with the DNA) for 5 hours to allow transfection to occur.
6. After 5 hours the DNA was removed from the flasks and the cells washed with 20ml of PBS. 50ml of culture medium containing 10% FCS was added to each flask and the cultures incubated for a further 48 hours.
7. After 48 hours the cells were harvested from each flask in the normal manner by trypsinisation and centrifugation at 1000rpm (118G) for 5 minutes and resuspended in 3ml of 10% medium.
8. The cell suspension from each flask was then sorted as described in section 2.3.4. Cells were sorted from both the pREVmyc3.1 and pREV flasks by the assessment of their green fluorescence into GFP positive and negative populations. The cell suspension from the control flask was also passed through the cell sorter to control for the effect of the sorting process.
9. At least $5x10^5$ cells were sorted for each group except for the control cells, where at least 1 million were sorted, $5x10^5$ for each of the positive and negative controls.
10. The sorted cell suspensions were then transferred into conical tubes and centrifuged at 1500 rpm for 5 minutes to form a cellular pellet. The cells were then resuspended in 1ml of ice cold 70% ethanol to fix them whilst being agitated on a vortex machine.
11. Each cell suspension was then counted using a haemocytometer and 5 $x10^5$ cells from each suspension transferred into conical tubes for staining of c-myc protein.
12. 5 $x10^5$ cells from the control group were transferred into each of two conical tubes, one to act as the positive control and one to act as the negative control.
13. The cells were then washed once with 1ml of PBS and centrifuged at 2000rpm (472G) for 5 minutes.
14. The mouse anti-human c-myc primary antibody 6E10 (Genosys Cambridge) was then added and incubated for 1 hour.

15. The cells were washed again as previously, the secondary antibody (goat anti-mouse-FITC) added and they were incubated for 45 minutes.
16. After a further wash in PBS, as above, the cells were resuspended in 1ml of PBS containing Ribonuclease A and propidium iodide. The c-myc oncoprotein level was assessed by FACS analysis.

A full description of the methods used for the staining of c-myc protein described in steps 11-16 is present in 2.2.4.

Chapter 3

Design of a ribozyme targeting *c-myc*

3.1.1 Introduction

Corrective gene therapy using antisense oligodeoxynucleotides can specifically down regulate gene expression in humans (Jansen, Wacheck et al. 2000). This strategy has the potential for a wide range of diseases, including cancer. However this approach has several weaknesses. Firstly, antisense oligonucleotides have an intrinsic one to one stoichiometric relationship with the target mRNA. This means that one molecule of antisense can only block one mRNA strand before both are degraded. To overcome this problem large amounts of antisense are needed to provide an effective block of gene function. The rapid degradation of antisense results in only a short term down regulation of specific genes from a single administration of antisense. To provide a long-term block of gene function a continuous supply of antisense must be provided to the tumour.

Dogma maintains that proteins are responsible for the complex enzymatic reactions within cells. However, it was discovered in 1981 that RNA molecules, previously thought to be passive carriers of genetic information, can execute complex functions similar to proteins (Cech, Zaug et al. 1981). The reactions include cleavage (of either themselves or other RNA molecules), ligation or *trans*-splicing. They are capable of catalytic function in the absence of proteins. These catalytic RNA molecules have been rapidly categorised and their structure and function elucidated. Their structure is easily manipulated allowing different target RNA sequences to be selected. Custom-designed RNA molecules have the potential to become both powerful investigative tools for molecular biologists and also therapeutic agents in the clinical setting. Catalytic nucleic acids are known as ribozymes.

Ribozymes have the potential to be a more efficient system for specific down regulation of gene function than antisense. Ribozymes are a naturally occurring form of RNA that has the ability to catalytically cleave RNA in a sequence specific manner. Short sequences of RNA undergo primary folding into tertiary structure, that allows both the binding of Mg^{2+} and sequence specific target binding that enable ribozymes to bind to and cleave in either intra or inter molecular basis.

In nature, ribozymes catalyze sequence-specific RNA processing. Their specificity is determined by the hybridization of the ribozyme to the target RNA via Watson-Crick base pairing. This ensures the correct orientation of the catalytic site and subsequent cleavage of target RNA. The reaction products then dissociate, allowing the ribozyme to find another target site.

Ribozymes were discovered in the ciliated protozoan *Tetrahymena thermophilia* when it was noted that RNA processing involved an RNA intron. The 413 nucleotide group I intron in pre-rRNA was found to undergo self-cleavage (Cech, Zaug et al. 1981) (Kruger, Grabowski et al. 1982) (Zaug, Been et al. 1986). This intron appeared to self-splice in the absence of protein resulting in ligation of exons and excision of the intron. The reaction is based on trans-esterification. This is not, by definition, an enzymic reaction because it is intra-molecular in nature.

Further evidence that RNA may have complex functions was demonstrated using ribonuclease P. This ubiquitous endoribonuclease processes tRNA by cleaving the 5' end of precursor tRNA. This molecule consists of two components, a 20kD polypeptide and a 375 base RNA strand. It was shown in E. Coli and B. Subtilis that the RNA molecule could independently catalyze cleavage without the protein *in vitro*. The protein molecule increased activity but was not itself needed for the reaction (Guerrier-Takada, Gardiner et al. 1983).

The particular folding pattern of the ribozyme exposes an active site, in a similar fashion to a proteinaceous enzyme. Cleavage can occur for both *cis* and *trans* (Symons 1992).

Being relatively small molecules (30-50 nucleic acids), ribozymes were then redesigned to target new and specific sites on RNA molecules using the Watson-Crick model (Haseloff and Gerlach 1988).

3.1.2 Structure

There are six types of ribozyme motifs: hairpin, hammerhead, group I intron, ribonuclease P, mitochondrial and hepatitis delta virus. Due to their relatively small size, simplicity, and ease of manipulation, hammerhead and hairpin ribozymes have received most attention. They both originate from plant viroid and virusoids. Both are potentially useful in both the experimental and clinical environments.

Hairpin ribozymes have four helical domains and five loops (Hampel and Tritz 1989) and therefore have a more complicated structure than the hammerhead motif. The hairpin ribozyme group is thought to have good potential for clinical applications (Hampel 1998).

The hammerhead ribozyme (so called due to its two dimensional structure) can direct site specific cleavage. Uhlenbeck described cleavage of target RNA by a 19 nucleotide chemically synthesised ribozyme (Uhlenbeck 1987). The motif consists of three regions (helices I, II, III) with two being single-stranded and one being a highly conserved area (Forster and Symons 1987). Following extensive mutagenesis a structure was proposed that contained the catalytic site only (Haseloff and Gerlach 1988) with variable side arms that conferred specificity. Haselhoff and Gerlach rearranged the base sequence in the variable side arms (helices I and III) allowing different areas of the mRNA coding for chloramphenicol acetyl transferase to be cleaved *in-vitro*. The arm regions are complementary to the single stranded mRNA and so confer specificity. Applying recent developments in chemical synthesis of RNA, new molecules can be designed as inhibitors of specific gene expression by selecting specific sequences in the target gene. The target cleavage site on the mRNA can be any three nucleotide NUH sequence where H = A, C, or U (IUB system) and N is any nucleotide. The complementary arms align the catalytic core region to the cleavage sequence. The hammerhead ribozyme has the

greatest range of potential target sequences allowing flexibility in choice of target. The GUC site has been shown to have the highest rate of cleavage (Ruffner and Uhlenbeck 1990) but this is dependent on the composition of the helices I and III. Cleavage efficiency is in the order of GUC>GUA>GUU with little effect on a GUG target (Perriman, Delves et al. 1992), (Zoumadakis and Tabler 1995).

3.2.1 Designing a ribozyme

Once the base sequence for the substrate mRNA molecule has been obtained, the first task is to locate GUC sites. Cleavage efficiency is maximal at this sequence (see above). The next step is to find which of the GUC sites is in the most accessible position on the molecule. Messenger RNA is known to adopt secondary structure through a process of folding and complementation, producing loop structures and single-strand regions. This is partly due to RNA binding proteins (Nagai 1994) in combination with intra-molecular energy levels. The complex folding structure of the mRNA dictates that some GUC cleavage sites will be less accessible to a ribozyme eg if involved in loop areas. Computer folding programs, eg MFOLD (Zuker 1989), that attempt to predict the structure of these large and complex molecules are inaccurate, produce several different structures with similar energy profiles and may not take account of RNA binding proteins found *in vivo*. Since the biophysical properties of *in vivo* mRNA have yet to be determined, prediction of folding will be prone to error (Yu 1998). Due to these problems, attempts have been made to predict accessible sites experimentally. Using oligodeoxynucleotide binding as a marker, subsequent cleavage by RNase H and analysis of the fragments produced in conjunction with folding programs, has been shown to aid identification of binding sites (Scherr, Rossi et al. 2000). Another approach has been the combinatorial technique in which a library of ribozymes with randomly generated arm sequences is built and then screened on the mRNA target molecule. Cleavage sites are detected by RACE (rapid amplification of cDNA ends). NUH sequences within the translation and initiation regions, polyadenylation signal and intron splice sites should be considered as good targets. These best-guess regions need to be accessible to normal protein factors and one would therefore expect them to be also accessible to ribozymes.

Despite these attempts identification of cleavage sites for ribozymes remains largely a 'trial and error' process.

Following identification of a suitable target GUC sequence a ribozyme specific to this site must be designed. Creation of the complementary binding arms of the ribozyme has been shown to affect the binding and efficiency of cleavage. Length and base composition of the hybridisation arms is crucial in the dynamics of the ribozyme (Fedor and Uhlenbeck 1990), (Herschlag, 1991). In basic terms, the longer the binding arms the greater the specificity, but the lower the turn-over and the greater potential for interference by secondary folding of the target. Arm lengths from 5 to 50 nucleotides have been described in the literature. The T_m (temperature at which the two complementary strands dissociate) of the binding arms should be below the physiological temperature if they are to bind in culture and *in vivo*. If a very stable configuration occurs following cleavage then the rate of dissociation is decreased. This then potentially limits the turnover activity of the ribozyme. Producing binding arms with low GC and high AU content may reduce this possibility, as this will produce weaker binding energy (Herschlag 1991). Therefore the ribozyme/substrate complex needs to be stable enough to allow cleavage to occur but also allow the cleavage products to dissociate rapidly. By reducing the binding arm length from 20 to 12 nucleotides, a 10-fold increase in cleavage rates have been reported, targeting HIV-1 RNA (Goodchild and Kohli 1991). Making the lengths of the two arms asymmetrical may also increase turnover (Hendry and McCall 1996). Having stem I shorter than stem II increases rate of cleavage but currently the mechanisms involved have not been elucidated. Specificity is also determined by arm length. Very short arms have low specifity as do very long arms as the hammerhead will bind with comparable strength to targets with a few mismatched pairs (Herschlag 1991). The optimal length of arms is in the region of 6-8 nucleotides (Amarzguioui and Prydz 1998). Clearly a balance must be achieved between the above factors and each individual ribozyme will have its own ideal length of binding arms. Optimization of arm length should be determined by experimentation.

Ribozymes are normally synthesised by transcription within target cells and therefore consist of RNA. If ribozymes are synthesised chemically then greater variation in structure is permitted. Either RNA binding protein or DNA can be incorporated into the structure. Addition of p7 nucleocapsid protein of HIV-1 can increase substrate binding and dissociation by 10-20 fold (Tsuchihashi, Khosla et al. 1993). This is thought to be due to unfolding activity of the protein. The specific binding of glyceraldehyde-3-phosphate dehydrogenase (GAPDH) enhanced a ribozyme directed against tumour necrosis factor alpha (TNFα) (Sioud and Jespersen 1996).

Attempts to make the design of ribozymes more simple are limited by the extremely complex intra- and inter-molecular events that all these large RNA molecules undergo *in vivo*. Therefore all ribozymes still have a significant element of 'suck it and see' about their design!

3.2.2 Ribozyme mechanism

The first step of this process involves the ribozyme complexing with the substrate in the correct orientation. The binding arms engage the single stranded mRNA and form two double helix duplexes. The ribozyme-substrate complex is thus created. The cleavage domain of the ribozyme can now position a divalent cation (Mg^{2+}) next to the cleavage site. The phosphodiesterase bond is cleaved resulting in a 5'-product with a 2',3'-cyclic phosphate terminus and a 3' product with a 5'-hydroxyl terminus. The ribozyme stabilises the transition state complex allowing the reaction to be significantly enhanced. The presence of Mg^{2+} is essential for cleavage to take place. The products then dissociate and the ribozyme is free to complex with more substrate (McKay 1996; Scott and Klug 1996) and can be seen in Figure 3.1.

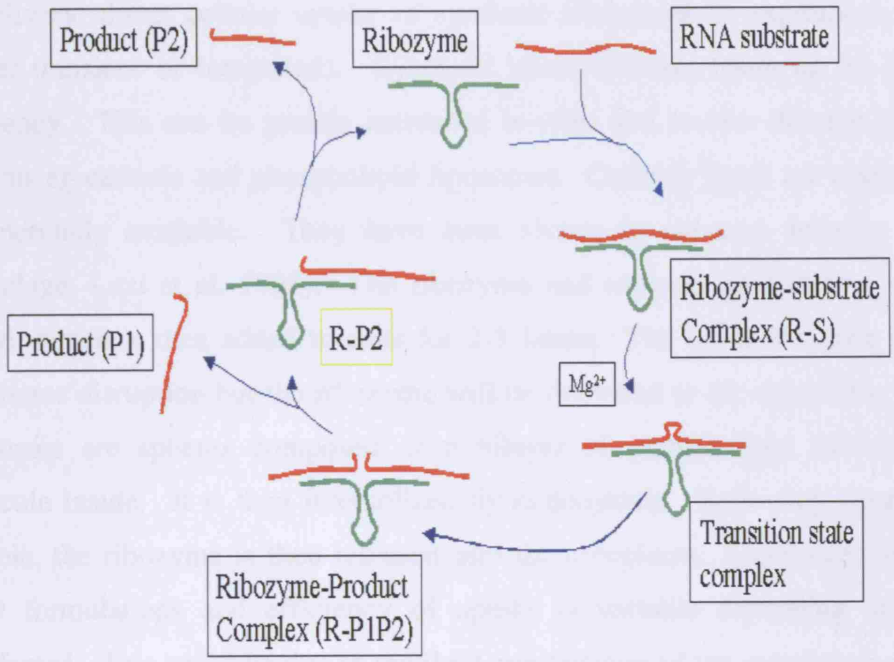

Figure 3.1 Catalytic Mechanism of Hammerhead Ribozyme

3.2.3 Ribozyme Stability

Hammerhead ribozymes are inherently unstable in biological fluids. They are susceptible to degradation by RNases. Several approaches have increased stability but with a reduction in cleavage rate. Modifications of the 2'-OH group by replacement with other groups, eg amino, fluoro, have increased stability (Jarvis, Wincott et al. 1996; Usman, Beigelman et al. 1996). In addition, by exchanging the linking phosphates with phosphorothionates resistance is conferred to endonuclease attack (Ruffner and Uhlenbeck 1990). Intact ribozymes have been detected in extra-cellular fluid, after a period of 2 hours following subcutaneous administration in mice (Sandberg, Bouhana et al. 1999). Analysis of *in-vitro* cell cultures has shown that majority of degradation occurs within the intracellular fluid and not in the extra-cellular medium. Ribozymes have been detected in plasma and urine specimens 24 hours following i.v. injection of rats (Desjardins, Sproat et al. 1996)

3.3 Delivery

The greatest hurdle facing gene therapy is delivery. Ribozymes have two potential routes of delivery: direct cellular uptake of synthetic ribozymes or expression from a vector (either transient or integrated). Synthetic ribozymes are taken up by cells with low efficiency. This can be greatly increased *in-vitro* and *in-vivo* through use of delivery systems eg cationic and phospholipid liposomes. Cationic lipids are easy to use and are commercially available. They have been shown to enhance delivery of ribozymes (Bramlage, Luzi et al. 1998). The ribozyme and cationic lipid form a complex when mixed, which is then added to cells for 2-3 hours. The lipids are toxic to cells due to membrane disruption but the ribozyme will be delivered to the cytoplasm. Phospholipid liposomes are spheres composed of a bilayer of phospholipid that traps the RNA molecule inside. It is then internalized by endocytosis. Following degradation of the vacuole, the ribozyme is then released into the cytoplasm. Liposomes are available in many formulations and efficiency of uptake is variable depending on the cell line transfected. This could be due to the lipid composition of the membrane or the enzymes present within the cell. However liposomes require testing for both toxicity and efficient uptake for each cell line to be used.

Production of the ribozyme from an expression vector has several advantages over synthetic ribozyme delivery. It is dependent on the use of a non-replicating virus (eg retroviruses or adenoviruses) that has been shown to be non-pathogenic in patients. Retroviruses are efficient, produce an integrated vector with long term expression of the ribozyme and have broad cell tropism. However this can lead to specificity problems and retroviral titres are not sufficient for efficient *in-vivo* gene delivery. They are also rapidly degraded by complement (Takeuchi 1994). Adenoviruses are efficient, can be produced in large titres, can infect non-dividing cells and carry up to 8kb of DNA. Expression is only transient because the viral genome is extrachromosomal. Adenoviral vectors were first used in treatment of cystic fibrosis (Zabner, Couture et al. 1993) and have been used in several clinical trials since. They also produce a significant immune response, which has potential benefits in cancer therapy. Adeno-associated virus and Herpes simplex virus are also being investigated and have potential applications.

The field of gene therapy is continuing to improve and gene delivery techniques will hopefully overcome the current problems and allow greater efficacy of this mode of treatment.

3.4 *In-vitro* applications

The majority of *in-vitro* applications of ribozymes have been reported in two areas; HIV-1 and cancer. HIV-1 has received much attention, as there are few effective treatment strategies. Work has tried to protect lymphocytes from infection or replication of the virus. Stable and freshly isolated lymphocytes have been induced to produce an anti-HIV ribozyme, resulting in a resistance to challenge with viral clones compared to non-transduced control cells that were fully permissive to HIV-1 infection (Leavitt, Yu et al. 1994). The expression of the ribozyme had no effect on proliferation of cells. Inhibition was specific, as the ribozyme had no effect when HIV-2 was the infective agent; HIV-2 does not posses the target sequence. Peripheral blood monocytes isolated from HIV-1 patients have demonstrated 1000-fold inhibition of HIV-1 replication following transduction of an anti-HIV-1 ribozyme (Bauer, Valdez et al. 1997). Homann observed inhibition of HIV-1 replication using a ribozyme that was 4-7 fold stronger than antisense targeting the same sequence (Homann, Tzortzakaki et al. 1993). HIV-1 replication dropped to 4.3% of controls.

The application of ribozymes in cancer is numerous, and there are many potential gene targets. Haselhoff first suggested that synthetic ribozymes could be used as both tools for molecular biology and gene therapy. Subsequently, ribozymes have been targeted against many oncogenes in an attempt to attenuate protein expression. The *ras* oncogene is associated with increased tumourgenicity. The wild-type gene has a mutational hot spot on codon 12. H-ras becomes activated if a GGC sequence mutates to GUC. This rather fortunate event provides an ideal ribozyme target site. Targeting of this sequence by ribozymes has reduced growth rates in cultured bladder carcinoma EJ cells and reduced tumourigenicity (Irie, Anderegg et al. 1999). Adenoviral-mediated down regulation of H-ras using a ribozyme resulted in significant inhibition of growth. Indeed,

at 5 days no viable cells were seen *in-vitro*. Heterotopic transplantation of control EJ and ribozyme expressing cells into nude mice, resulted in complete reversal of tumourgenicity in the ribozyme group (Feng, Cabrera et al. 1995). Reduced tumourgenicity has been shown over a period of several months and correlated with a two-fold increase in survival rates in EJ cells (Kashani-Sabet, Funato et al. 1992). Ribozymes have been directed against the nuclear proto-oncogenes *c-fos* and *c-myc* and have also achieved a reduction in cell proliferation but not to the same degree as anti-*ras* ribozymes. FEM melanoma cells have been used to demonstrate that an increase in doubling time was associated with diminished DNA synthesis and reduced mRNA expression (Ohta, Kijima et al. 1996). They used ribozymes directed against H-*ras, c-fos* and *c-myc*. Reductions in growth were greatest in the H-*ras* group followed by *c-fos* and *c-myc* respectively. Recent work targeting bcl-2 using an adenovirus vector to deliver a ribozyme, reduced cell growth in three oral cancer cell lines. This is thought to be due to increased apoptosis following a decease in bcl-2 expression (Gibson, Pellenz et al. 2000).

These studies indicate that ribozymes are showing significant potential in *in-vitro* experiments in both the fields of HIV and cancer.

3.5 *In-vivo* applications

Ribozymes are specific agents that target mRNAs of genes controlling both cellular and viral diseases. They have potential to be therapeutic compounds in a wide range of diseases. Having demonstrated a significant potential *in-vitro* this must now be carried through into the *in-vivo* setting. Encouraged by the *in-vitro* success several groups are taking ribozymes into the clinical setting.

3.6.1 Target and structure of the *c-myc* ribozyme

A series of hammerhead ribozymes targeting the *c-myc* mRNA was designed according to the system outlined above. The ribozymes were synthesized using two

complementary, single stranded oligodeoxynucleotides whose sequence coded for ribozyme sequence. The sequence contained the central catalytic core flanked by two antisense sequences, complementary to a selected area of the human c-myc transcript. The two complementary oligonucleotides were synthesised (Figure 3.2) and hybridised to give *Xba*1 and *Mlu*1 compatible overhangs and then inserted in to a pREV mammalian DNA plasmid. The plasmid, pREV, previously constructed at the Paterson Institute of Cancer Research in Manchester by Spencer Collis, was used as the expression vector.

This system has previously been shown to express active hammerhead ribozymes that could down regulate gene function in cells (Collis, Tighe et al. 2001). The structure of the plasmid is shown in Figure 3.3. The plasmid is based on the mammalian expression vector pCGFP. The cytomegalovirus immediate early gene promoter/enhancer, multiple cloning site and the SV40 poly(A) sections from the plasmid vector pCI (Promega) were extracted using a *Bam*HI/*Bgl*II digestion and ligated into a unique *Bam*HI site of pCGFP. Analyses using restriction endonuclease digestion and PCR were performed to confirm the orientation of the insert.

C-myc mRNA 5' UAC GUU GCG **GUC** ACA CCC UUC UCC 3'

Ribozme 3 3' AUG CAA CGC CA UGU GGG AAG AGG 5'

A C
A U
G A G
C G G A
A-U U
Stem II G-C
G-C
A G
G U

c-mycribo3.1

5' CGCG GGAGAAGGGTG TCTGATGAGTCCGTGAGGACGAAA CCGCAA CGTA 3'

c-mycribo3.2

5' CTAG TACGTTGCGG TTTCGTCCTCACGGACTCATCAGA CACCCTTCTCC 3'

c-mycribo2.1

5' CGCG CTCTGCTTGC TGATGAGTCCGTGAGGACGAAA CTCTGCTTGC 3'

c-mycribo2.2

5' CTAG CATCCTGTCCG TTTCGTCCTCACGGACTCATCAG CAAGCAGAG 3'

c-mycribo1.1

5' CGCG GAAGCT CTGATGCCGTGAGGACGAAA CGTTGAGG 3'

c-mycribo1.2

5' CTAG CCTCAACG TTTCGTCCTCACGGCATCAG AGCTTC 3'

CGCG = Mlu

CTAG = Xba

Figure 3.2 Ribozyme sequences

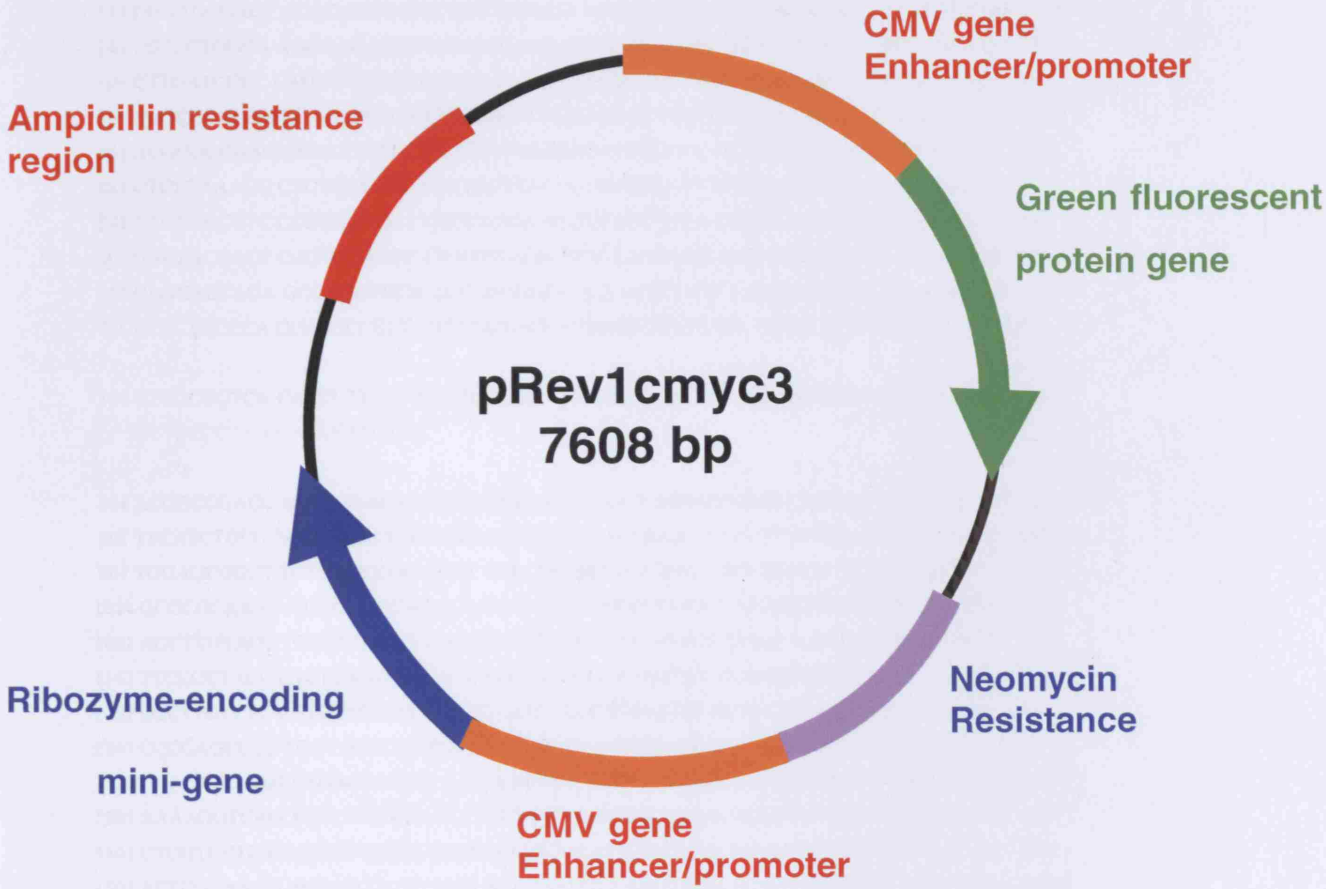

Figure 3.3 Structure of pREV plasmid

1 CTGCTCGCGG CCGCCACCGC CGGGCCCCGG CCGTCCCTGG CTCCCCTCCT GCCTCGAGAA 60
61 GGGCAGGGCT TCTCAGAGGC TTGGCGGGAA AAAAGAACGG AGGGAGGGAT CGCGCTGAGT 120
121 ATAAAAGCCG GTTTTCGGGG CTTTATCTAA CTCGCTGTAG TAATTCCAGC GAGAGGCAGA 180
181 GGGAGCGAGC GGGCGGCCGG CTAGGGTGGA AGAGCCGGGC GAGCAGAGCT GCGCTGCGGG 240
241 CGTCCTGGGA AGGGAGATCC GGAGCGAATA GGGGGCTTCG CCTCTGGCCC AGCCCTCCCG 300
301 CTTGATCCCC CAGGCCAGCG GTCCGCAACC CTTGCCGCAT CCACGAAACT TTGCCCATAG 360
361 CAGCGGGCGG GCACTTTGCA CTGGAACTTA CAACACCCGA GCAAGGACGC GACTCTCCCG 420
421 ACGCGGGGAG GCTATTCTGC CCATTTGGGG ACACTTCCCC GCCGCTGCCA GGACCCGCTT 480
481 CTCTGAAAGG CTCTCCTTGC AGCTGCTTAG ACGCTGGATT TTTTTCGGGT AGTGGAAAAC 540
541 CAGCAGCCTC CCGCGACGAT GCCCCTCAAC GTTAGCTTCA CCAACAGGAA CTATGACCTC 600
601 GACTACGACT CGGTGCAGCC GTATTTCTAC TGCGACGAGG AGGAGAACTT CTACCAGCAG 660
661 CAGCAGCAGA GCGAGCTGCA GCCCCCGGCG CCCAGCGAGG ATATCTGGAA GAAATTCGAG 720
721 CTGCTGCCCA CCCCGCCCCT GTCCCCTAGC CGCCGCTCCG GGCTCTGCTC GCCCTCCTAC 780
TAC
781 GTTGCGGTCA CACCCTTCTC CCTTCGGGGA GACAACGACG GCGGTGGCGG GAGCTTCTCC 840
GTTGCGGTCA CACCCTTCTC C

841 ACGGCCGACC AGCTGGAGAT GGTGACCGAG CTGCTGGGAG GAGACATGGT GAACCAGAGT 900
901 TTCATCTGCG ACCCGGACGA CGAGACCTTC ATCAAAAACA TCATCATCCA GGACTGTATG 960
961 TGGAGCGGCT TCTCGGCCGC CGCCAAGCTC GTCTCAGAGA AGCTGGCCTC CTACCAGGCT 1020
1021 GCGCGCAAAG ACAGCGGCAG CCCGAACCCC GCCCGCGGCC ACAGCGTCTG CTCCACCTCC 1080
1081 AGCTTGTACC TGCAGGATCT GAGCGCCGCC GCCTCAGAGT GCATCGACCC CTCGGTGGTC 1140
1141 TTCCCCTACC CTCTCAACGA CAGCAGCTCG CCCAAGTCCT GCGCCTCGCA AGACTCCAGC 1200
1201 GCCTTCTCTC CGTCCTCGGA TTCTCTGCTC TCCTCGACGG AGTCCTCCCC GCAGGGCAGC 1260
1261 CCCGAGCCCC TGGTGCTCCA TGAGGAGACA CCGCCCACCA CCAGCAGCGA CTCTGAGGAG 1320
1321 GAACAAGAAG ATGAGGAAGA AATCGATGTT GTTTCTGTGG AAAAGAGGCA GGCTCCTGGC 1380
1381 AAAAGGTCAG AGTCTGGATC ACCTTCTGCT GGAGGCCACA GCAAACCTCC TCACAGCCCA 1440
1441 CTGGTCCTCA AGAGGTGCCA CGTCTCCACA CATCAGCACA ACTACGCAGC GCCTCCCTCC 1500
1501 ACTCGGAAGG ACTATCCTGC TGCCAAGAGG GTCAAGTTGG ACAGTGTCAG AGTCCTGAGA 1560
1561 CAGATCAGCA ACAACCGAAA ATGCACCAGC CCCAGGTCCT CGGACACCGA GGAGAATGTC 1620
1621 AAGAGGCGAA CACACAACGT CTTGGAGCGC CAGAGGAGGA ACGAGCTAAA ACGGAGCTTT 1680
1681 TTTGCCCTGC GTGACCAGAT CCCGGAGTTG GAAAACAATG AAAAGGCCCC CAAGGTAGTT 1740
1741 ATCCTTAAAA AAGCCACAGC ATACATCCTG TCCGTCCAAG CAGAGGAGCA AAAGCTCATT 1800
1801 TCTGAAGAGG ACTTGTTGCG GAAACGACGA GAACAGTTGA AACACAAACT TGAACAGCTA 1860
1861 CGGAACTCTT GTGCGTAAGG AAAAGTAAGG AAAACGATTC CTTCTAACAG AAATGTCCTG 1920
1921 AGCAATCACC TATGAACTTG TTTCAAATGC ATGATCAAAT GCAACCTCAC AACCTTGGCT 1980
1981 GAGTCTTGAG ACTGAAAGAT TTAGCCATAA TGTAAACTGC CTCAAATTGG ACTTTGGGCA 2040
2041 TAAAAGAACT TTTTTATGCT TACCATCTTT TTTTTTTCTT TAACAGATTT GTATTTAAGA 2100
2101 ATTGTTTTTA AAAAATTTTA A 2121

Figure 3.4 Nucleotide sequence for the c-myc proto-oncogene and ribozyme binding site within the gene sequence.

3.6.2 Ribozyme targets

As a first stage in the development of a *c-myc* ribozyme, a target sequence was selected based on previous RAFT Research Fellows' experience with antisense oligonucleotides. The translation-initiation codon of exon 2 of *c-myc* mRNA had successfully been targeted using 15-mer oligodeoxynucleotide sequences at 296-311 base pairs (Chana 1998). The first ribozyme produced targeting this sequence had a –GUU- cleavage site and was known to be accessible for binding with complementary antisense oligodeoxynucleotide molecules. However the –GUC- sequence is known to be the most efficient triplet target for ribozyme cleavage and not the –GUU- sequence. Despite accessibility of the target site, cleavage may be relatively slow because of inefficient ribozyme mediated cleavage. The triplet –GUU- sequence was sited at base pairs 303-305 of the *c-myc* mRNA. A sequence of 5'-GAAGCU-3' was complementary to the base sequence on the 3' side of the –GUU- triplet and formed stem 1. A 5'- CGTTGAGG -3' sequence was complementary to the base sequence on the 5' side of the –GUU- triplet and formed stem 2.

A different nucleotide sequence on the *c-myc* mRNA may have the potential for more efficient cleavage by a ribozyme and therefore be targeted, containing a –GUC- sequence, to maximise cleavage efficiency. Ohta et al demonstrated successful ribozymes targeting the *ras*, *fos* and *c-myc* oncogenes in melanoma cell lines transfected with the ras oncogene (Ohta, Kijima et al. 1996). They concluded that is was the anti-ras ribozyme that down regulated cell growth the most but this is not unexpected as the ribozyme was investigated in a ras over-expressing cell line. If the anti-*c-myc* ribozyme was tested in a *c-myc* over-expressing cell line, such as the A375M, a significant down regulation may have been seen. We therefore decided to design and produce a second ribozyme that targeted a similar sequence. A –GUC- triplet was located at 1234-1237 nucleotides on the *c-myc* mRNA. Stem 1 was constructed to be complementary to the substrate mRNA and consisted of the sequence 5'-CUCUGCUUG-3'. Stem 2 consisted of the sequence 5'-GGACAGGAUG-3'.

A third ribozyme was designed to target a separate area on the *c-myc* mRNA and cleave at a GUC site (nucleotides 231-3). The efficacy of this site has been demonstrated in heptatoma cells by Cheng (Cheng, Luo et al. 2000). Using a similar hammerhead ribozyme a significant down regulation of *c-myc* expression was demonstrated which also produced a reduction in cell growth measured using an MTT assay (3-4,5-dimethylthiazol-2-yl-2,5-diphenyl tetrazolium bromide). Stem 1 of the ribozyme was constructed using the sequence 5' – ACCGCAACGUA- 3' and stem 2 using 5' - GGAGAAGGGUGU- 3'. The annealed oligonucleotides were ligated into the pREV plasmid between *Xba*1 and *Mlu*1 restriction sites.

A non-functional ribozyme was designed to act as a negative control for each of the active versions. By synthesis of two complementary oligonucleotides with the identical sequence of the ribozyme but with the Mlu1 and Xba1 overhanging ends at the opposite end of the oligonucleotides, the RNA polymerase would read from the opposite end and the molecule would fold abnormally. Since 3D structure is key to the cleavage mechanism of the ribozyme then this would effectively be a non-functional molecule.

3.7.1 Results

The sequence and orientation of ribozyme coding inserts was checked using endonuclease digestion followed by PCR of the region, to confirm correct placement of the ribozyme cassette.

Analysis of all three of the ribozyme plasmids confirmed that each of the riboyzme coding inserts had been correctly ligated in the expected orientation without duplication. Figure 3.4 demonstrates the sequence for ribozyme 3. Figure 3.5 shows the entire region of the pREV plasmid that has been sequenced.

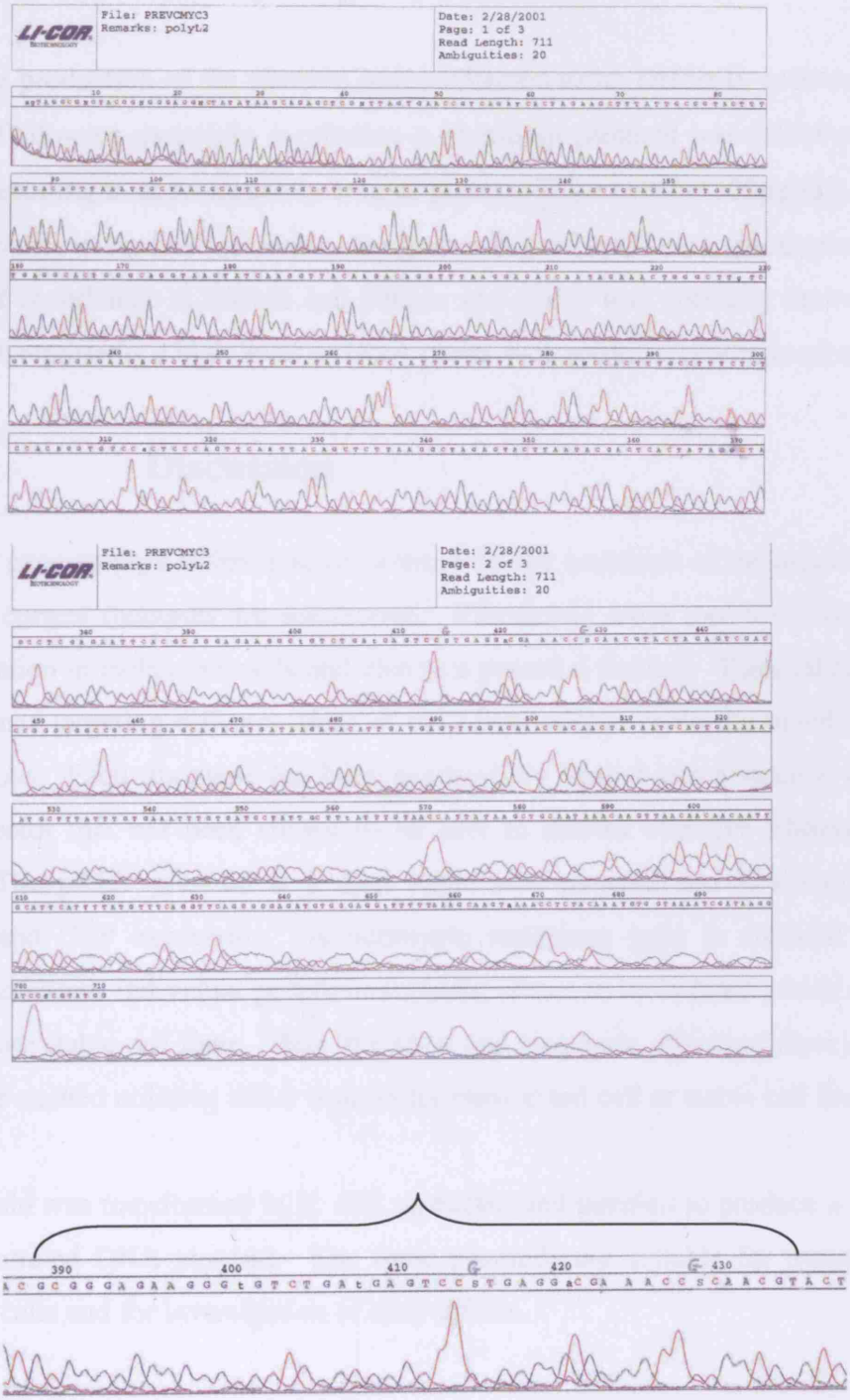

Figure 3.5 Sequence of pREV ribozyme3 across 710 bases including the correct ribozyme sequence.

3.7.2 Ribozyme production

Large scale production of the plasmid was performed using DH5α E. coli to express the plasmid. Following overnight incubation a Maxiprep protocol was followed to extract the DNA resulting in approximately 1mg of plasmid DNA (1000-1500μg/ml). The DNA is of high purity using this technique. Analysis was performed on a spectrophotometer by the ratio of absorbance at 260nm and 280nm and purity was normally between 1.7 and 1.85, which represents a high level of DNA purity with minimal contamination.

3.8 Discussion

Corrective gene therapy offers a novel strategy in the treatment of metastatic melanoma for which current therapies are ineffective. Ribozymes are a tool for investigation of gene regulation in melanoma cells and also as a potential therapy. Three ribozmyes have been designed targeting different areas of the *c-myc* mRNA molecule based on previous investigations. Each ribozyme has been successfully ligated into a suitable mammalian plasmid vector that has been shown to be able to deliver effective ribozymes in cell models. The pREV plasmid is a dual expression plasmid and is suitable for both ribozyme and GFP expression. A neomycin resistance gene is encoded within the plasmid and allows individual geneticin-resistant clones to be isolated which can then be used to create stable cell lines. Thus, the short and long-term effects of ribozymes within cells can be studied utilizing either transiently transfected cell or stable cell lines

Each plasmid was transformed in E. coli, extracted and purified to produce a highly pure and concentrated DNA plasmid. The three plasmids are suitable for transfection into melanoma cells and for investigation of their effects.

Chapter 4

Investigation of ribozymes targeting the *c-myc* proto-oncogene in transiently transfected A375M melanoma cells.

4.1 Introduction

Gene therapy involves transfection of cells with nucleic acids aiming to modify cell function for therapeutic gain. Transfection is a process by which nucleic acids gain access to the cytoplasm of cells. A potential gene therapy must be able to enter a high percentage of target cells and in sufficient quantities to achieve a therapeutic goal. It must also be capable of sustaining an effect for an appropriate time period to allow the therapy to work. There are several approaches to transfection of cells in gene therapy, but all encounter resistance to accept novel DNA by the host cell. Human cells have developed techniques preventing absorption of foreign DNA to prevent hijacking of the cell by pathogens such as viruses and plasmids. The cell membrane forms the main barrier to large DNA molecules gaining entry to the cell. Uptake of DNA from the surrounding tissue fluid does occur spontaneously but is extremely inefficient especially for large DNA molecules. Small oligonucleotides can be absorbed into cells via this approach but large molecules, such as the pREV plasmid, need more sophisticated techniques that are provided by either liposomal or viral delivery. Following absorption of DNA into the cell cytoplasm, it enters the nucleus of the cell where transcriptional enzymes initiate gene expression. The human cell can effectively be 'hijacked' by foreign DNA to produce specific therapeutic gene products. Transfection of cells using a plasmid vector encoding a specific gene or genes, has been shown to be an effective technique for intracellular production of gene products including ribozymes. The greater the amount of transfected DNA within cells, leads to a correspondingly larger quantity of

plasmid DNA within the nucleus of the cells. The number of copies of a gene in the nucleus will directly affect levels of transcription of RNA taking place. The more copies of the plasmid within the nucleus, the greater the amount of gene product that the cell will manufacture. The number of cells transfected and the quantity of DNA absorbed is therefore crucial to gene therapy strategies.

4.2.1 Investigation of transfection strategies

Delivery of DNA plasmid constructs into cells is obviously vital to gene therapy. Experiments were performed to transfect A375M cells using the pREV plasmid and assess efficiency using several liposomal techniques. Lipofectamine (Gibco), Escort (Gibco), ExGen 500 (MBI Fermantas) and Polyfect (Qiagen) were tested in a variety of conditions to try and determine the most reliable strategy. A375M cells were cultured in 6-well plates before exposure to transfection agents. Each transfection agent required slightly different protocols depending on the recommendations of the manufacturer. Following 24 hours incubation post transfection, allowing time for GFP expression to occur, the percentage of green fluorescent cells was assessed using a cell sorting FACS machine (Becton Dickinson). Transfection was accepted to have taken place if the cells had green fluorescence. Cells were gated using forward and side scatter to include only single cells and to exclude doublets and cell debris. Histograms of the number of cells versus green fluorescence measured in FL1 were generated. The percentage transfection rate of A375M cells could then be compared for each of the four transfection agents assessed. These methods are described in more detail in the section 2.5.6.

Liposomal transfection agents act by forming lipid bi-layer spheres around DNA molecules when mixed. A solution of tranfection agent/DNA spheres is then placed on the target cells. The lipid spheres settle onto the cells by gravity and amalgamate with the lipid bi-layer of the cell membrane, releasing its DNA contents into the cell. The concentration of liposome, ratio of DNA to lipid and the length of time in contact with the cells are all important variables in the success of a technique. Unfortunately, liposomal compounds are known to be highly cell line dependent and optimum

transfection conditions vary. Each tranfection agent has to be assessed directly with individual cell lines before transfection efficiency can be predicted in that cell line.

4.2.2 Results

Figure 4.1 shows examples of the histograms obtained from transfection of A375M cells with the pREV ribozyme plasmid. Cells were initally gated using forward and side scatter channels (FL1 and FL2) to only include cells within a healthy population. Cells within this population were screened for expression of green fluourensce. The transfection rates with both Escort and Polyfect were poor with 4.45% and 2.15% transfection rates respectively. Lipofectamine demonstrated a 9.96% transfection rate. The highest transfection rate achieved was by ExGen 500 with 15.0% of cells producing significant fluorescence (Figure 4.2). The untransfected control cells had no detectable green fluorescence. All 4 transfection agents caused a number of cells in the monolayer to die and so reduce efficiency of the overall transfection. Subjectively, ExGen 500 caused the least cell death on microscopic examination of the culture flasks. ExGen 500 was therefore used as the transfection agent of choice in the following series of experiments.

4.3.1 Establishment of optimal transfection conditions for A375M cells using ExGen 500

The analysis of the effect of the active ribozyme on *c-myc* expression in A375M cells requires a large number of transfected cells for immunocytochemical staining. Antibody staining and FACs analysis requires large numbers of cells to provide accurate information of the sample of cells. The more cells that are measured provide greater accuracy and we chose $1x10^5$ cells to be assessed as sufficient. Therefore large number of cells are needed to be successfully transfected and to express genes contained in the plasmid vector. If only a small percentage of cells take up the plasmid then very large numbers of cells need to be exposed to the tranfection agents. Clearly this is both expensive, laborious and time consuming. Transfection strategy in the A375M using ExGen 500 was therefore optimised by investigating the effect of varying concentrations

of both the plasmid DNA and ExGen 500. Transfected cells were then assessed by GFP expression .

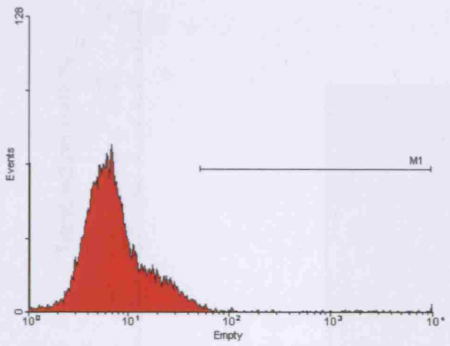

Polyfect

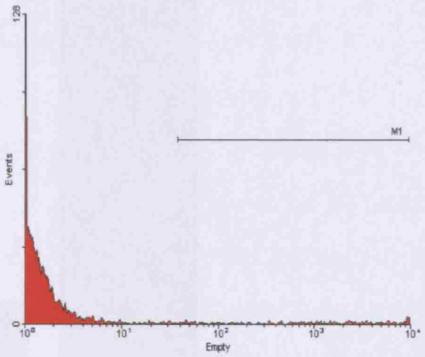

Escort

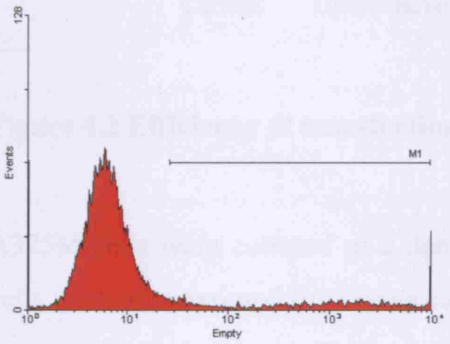

Lipofectamine

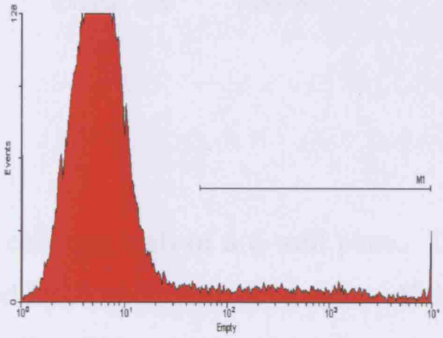

Exgen 500

Figure 4.1 Establishment of optimum transfection agent. Flow cytometric analysis of cell cultures following transfection for GFP. The x axis is FL1 and y the number of events.

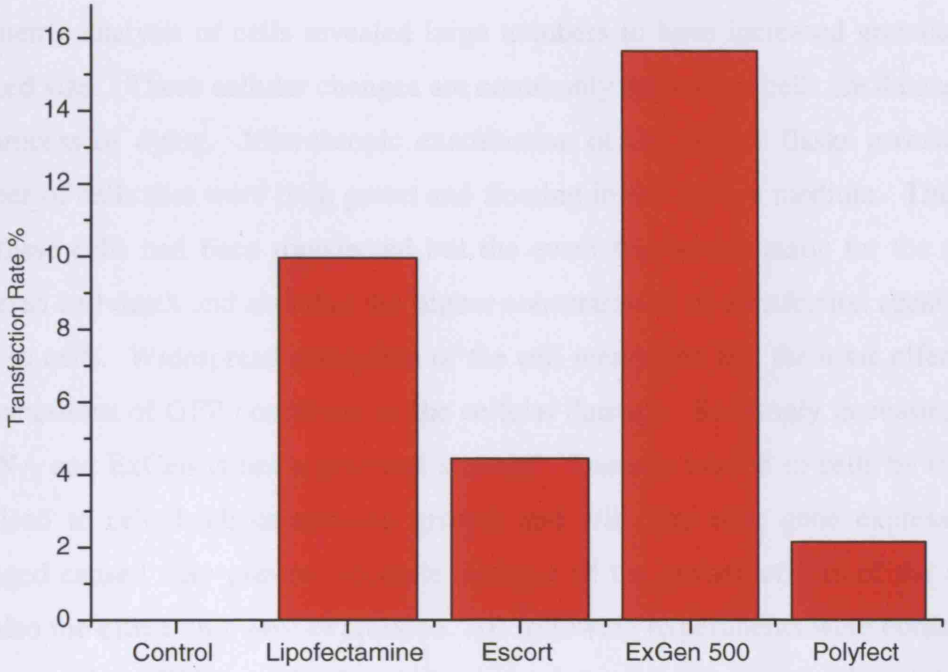

Figure 4.2 Efficiency of transfection agents

A375M cells were cultured to a density of $5x10^5$ cells per well of a 6-well plate. The cells were then exposed to varying ratios of plasmid DNA and transfection agent. Either 5µg or 10µg of plasmid DNA was used. The ExGen 500 was placed on the cells at volumes of 12.5µl, 16µl and 25µl per well. Following transfection, cells were left for 24 hours to allow time to express the green fluorescent protein and recover from the stress of the transfection process. At 24 hours cells were assessed for green fluorescence and the percentage of green cells was calculated using a flow cytometer.

4.3.2 Results

The ratio of DNA to ExGen 500 is an important factor in transfection of cells. 5µg of DNA in combination with 16µl of ExGen 500 produced the highest transfection rates of 19.23% whilst 10µg of DNA with 25µl of ExGen 500 resulted in 12.09% transfection.

Interestingly, doubling the volume of DNA and ExGen 500 from 5µg DNA and 12.5µl ExGen 500 to 10µg and 25µl respectively whilst maintaining the same ratio of DNA to ExGen produced approximately twice the rate of transfection. However the flow cytometric analysis of cells revealed large numbers to have increased granularity and a reduced size. These cellular changes are commonly seen when cells are damaged and in the process of dying. Microscopic examination of the culture flasks revealed a large number of cells that were both green and floating in the culture medium. This suggests that these cells had been transfected but the event was so traumatic for the cell that it triggered cell death and also that the higher concentration of transfection agent was more toxic to cells. Widespread disruption of the cell membrane and the toxic effects of high concentrations of GFP contribute to the cellular damage. So simply increasing the dose of DNA and ExGen is not a practical strategy. Damage caused to cells by transfection will lead to cell death or reduced growth and will also alter gene expression. The damaged caused may prevent accurate analysis of the growth effects of the ribozymes and also the effect on *c-myc* expression. All following experiments were conducted with the same ratio of DNA and ExGen with appropriate scaling up for the size of tissue flask. Transfection is therefore a compromise between maximising the amount of DNA within cells whilst minimising the toxic damage to the cell membranes caused by the tranfection process. These results are represented in Figure 4.3.

4.4.1 Assessment of the effect of *c-myc* ribozymes on the growth of A375M melanoma cells

It is known that antisense oligonucleotides directed against *c-myc* can down regulate *c-myc* expression in A375M melanoma cells and this has also been shown to reduce growth of cells *in-vitro* (Leonetti, D'Agnano et al. 1996). Ribozyme mediated down regulation of *c-myc* proto-oncogene expression may produce a similar effect to antisense. The effects on growth of A375M melanoma cell lines transfected with ribozyme 2 or ribozyme 3 were compared with the growth rates of A375M cells transfected with a reverse in-active ribozyme or untreated cells to act as negative controls. Growth was also assessed in A375M cells that were treated with antisense oligonucleotides targeting the *c-myc* proto-oncogene that are known to down regulate growth of cells (Chana 1998).

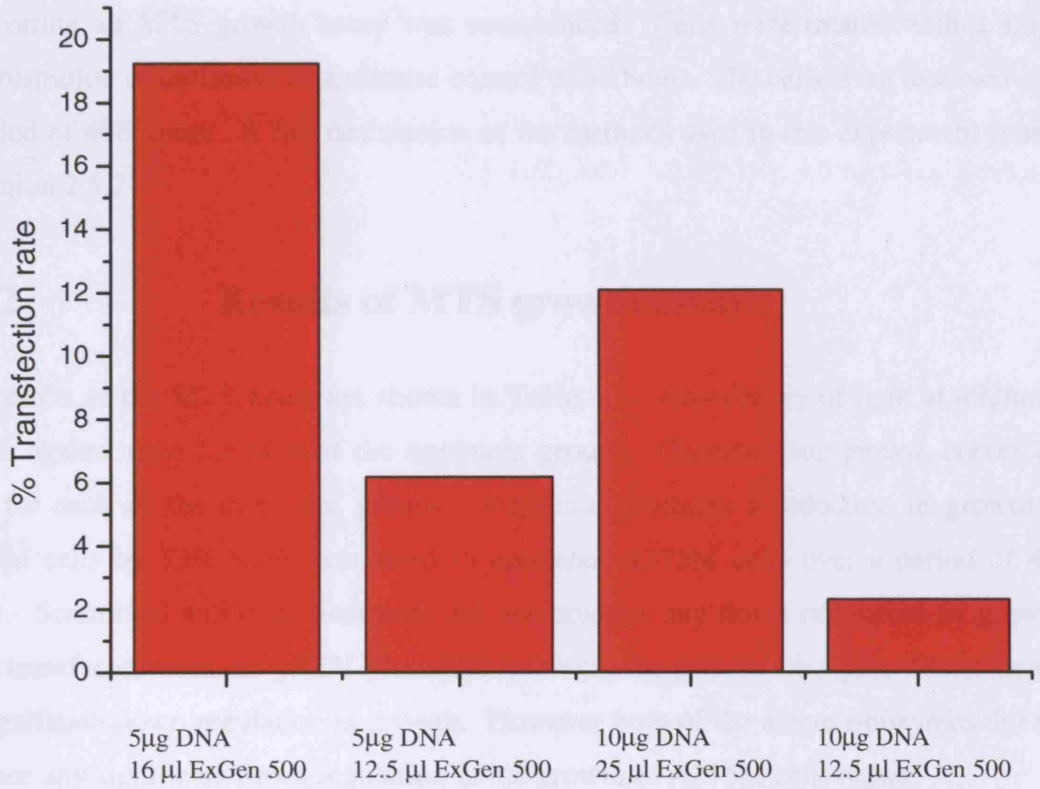

Figure 4.3 Establishment of ExGen 500 Optimum Transfection Conditions

A375M cells were treated with non-sense oligonucleotides to act as a negative control for the active antisense treatment.

A375M cells were cultured in T75 flasks and four flasks were transfected with one of the active or control ribozymes. The remaining flasks received no treatment at this stage. After a period of 24 hours to allow for expression of the plasmid the cells were sorted using a cell sorter into 96 well plates. Sorting was based on green fluorescence of the cells. Green cells were taken as expressing the ribozyme and cells without green fluorescence were thought not to be expressing the ribozyme. Cells were sorted in the

transfected populations based on a FL1 green fluorescence above 10^2. The untreated populations were then sorted based on FL1 green fluorescence below 10^1. All populations of cells were sorted into 10 wells of a 96 well plate at a concentration of 500 cells per well. Following incubation for 24 hours to allow the cells to recover from the cell sorting an MTS growth assay was commenced. Cells were treated with a single administration of antisense or antisense control at 48 hours. The cells were assessed over a period of 408 hours. A full description of the methods used in this experiment is seen in section 2.5.7

4.4.2 Results of MTS growth assay

The results of the MTS assay are shown in Table 4.1. Absorbancy of light at 492nm is shown against time for each of the treatment groups. Characteristic growth curves are seen for each of the treatment groups. Antisense produces a reduction in growth of A375M cells by 13% when compared to untreated A375M cells over a period of 408 hours. Scrambled antisense treatment did not produce any down regulation of growth. Cells transfected with the pREV plasmid expressing the reverse ribozyme demonstrated no significant down regulation in growth. However both of the active ribozymes did not produce any significant down regulation in the growth of A375M cells either.

Treatment group	Absorbance at 492nm at 408hrs	Standard error of the mean
Normal	3.00487	0.01414
Antisense	2.6705	0.01563
Antisense control	2.95646	0.01367
Ribozyme 3	2.91121	0.01545
Ribozyme 2	2.95092	0.02096
Reverse Ribozyme	2.92444	0.01453

Table 4.1 Results of MTS assay

Figure 4.4 demonstrates the normalized value for growth compared to the control in 4 of the treatment groups and highlights the reduction in growth. Figure 4.5 shows the change in absorbance over time for each group in the experiment. There was a reduction in growth in both of the transfected populations compared to normal untreated cells. There is no significant difference between the growth rates of the ribozyme 2 and the ribozyme control. Antisense reduces growth when compared to the other treatment groups. Normal cells grow at the fastest rate.

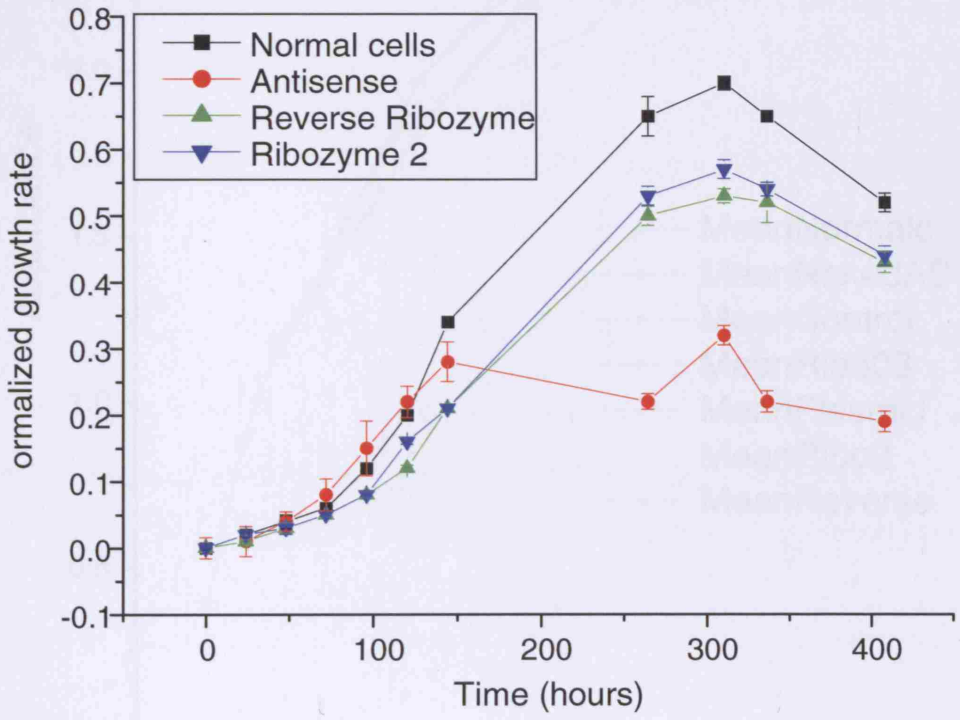

Figure 4.4 Normalized value of growth in the four treatment groups.

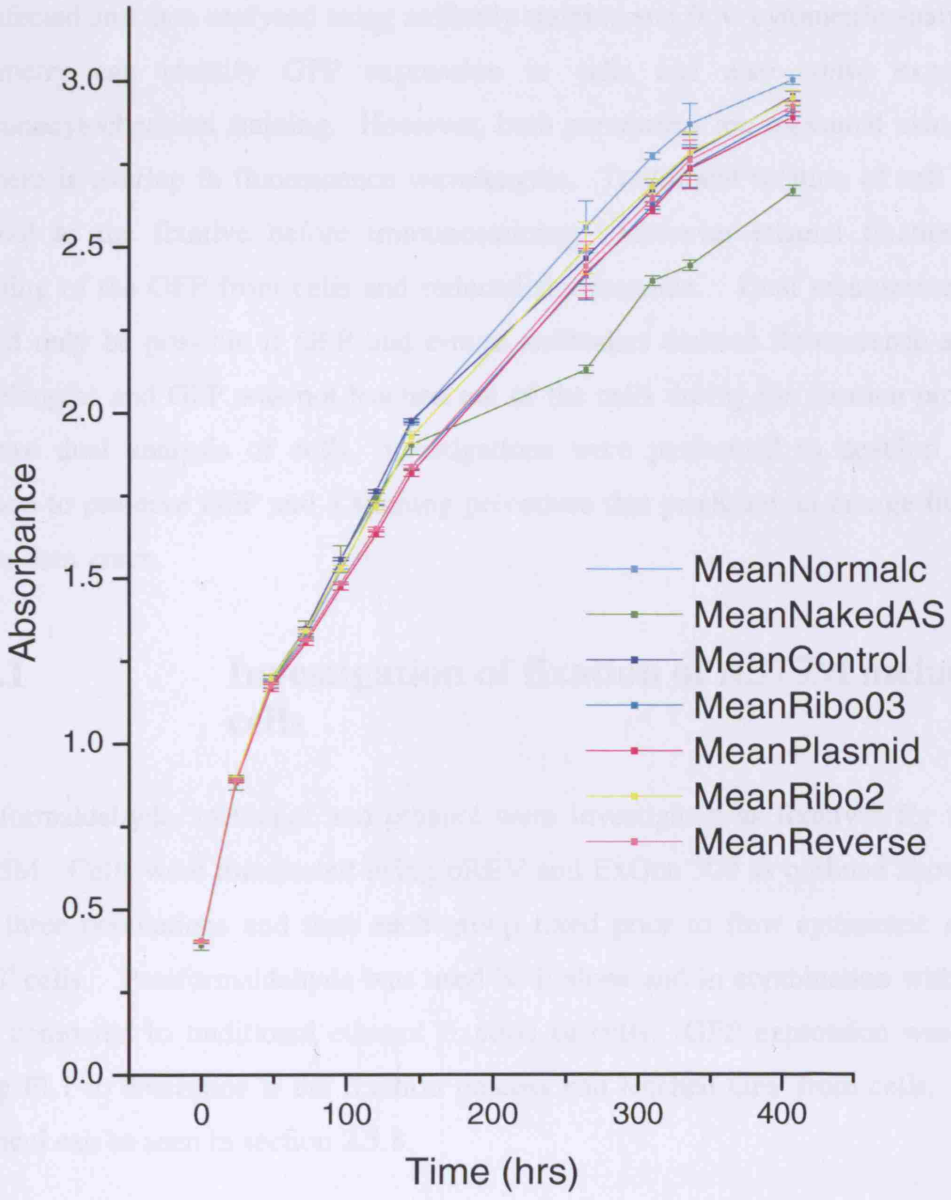

Figure 4.5 Graph to show absorbance over time for each group

4.4.3 Expression of *c-myc* in transiently transfected A375M cells.

Investigation of the effect of a ribozyme targeting *c-myc* mRNA required cells to be transfected and then analysed using antibody staining and flow cytometric analysis. Flow cytometry can identify GFP expression in cells and also *c-myc* expression by immunocytochemical staining. However, both parameters are measured using FL1 and so there is overlap in fluorescence wavelengths. Traditional fixation of cell lines used ethanol as the fixative before immunostaining. However ethanol fixation leads to leaching of the GFP from cells and reduced fluorescence. Dual measurement of cells would only be possible if GFP and c-myc antibodies emitted fluorescence at different wavelengths and GFP was not leached out of the cells during the fixation process. To achieve dual analysis of cells, investigations were performed to develop a fixation method to preserve GFP and a staining procedure that produced an orange fluorescence rather than green.

4.5.1 Investigation of fixation of A375M melanoma cells

Paraformaldehyde, methanol and ethanol were investigated as fixatives for transfected A375M. Cells were transfected using pREV and ExGen 500 as outlined above, divided into three populations and then each group fixed prior to flow cytometric analysis of $2x10^4$ cells. Paraformaldehyde was used both alone and in combination with methanol then compared to traditional ethanol fixation of cells. GFP expression was measured using FL1 to determine if the fixation process had leached GFP from cells. The exact protocol can be seen in section 2.5.8.

4.5.2 Results

The fluorescence ratios were calculated between GFP expressing cells and untransfected cells for each of the fixation protocols. Ethanol had a fluorescence ratio of 1.15

demonstrating that there was very little GFP left within cells. Paraformaldehyde alone had a fluorescence ratio of 3.3 and paraformaldehyde in combination with methanol fixation had a ratio of 5. These results comfirm that ethanol fixation reduces green fluorescence within cells and that paraformaldehyde in combination with methanol fixation preserves GFP signal. These are the results of a single experiment. The results are graphically represented in Figure 4.6

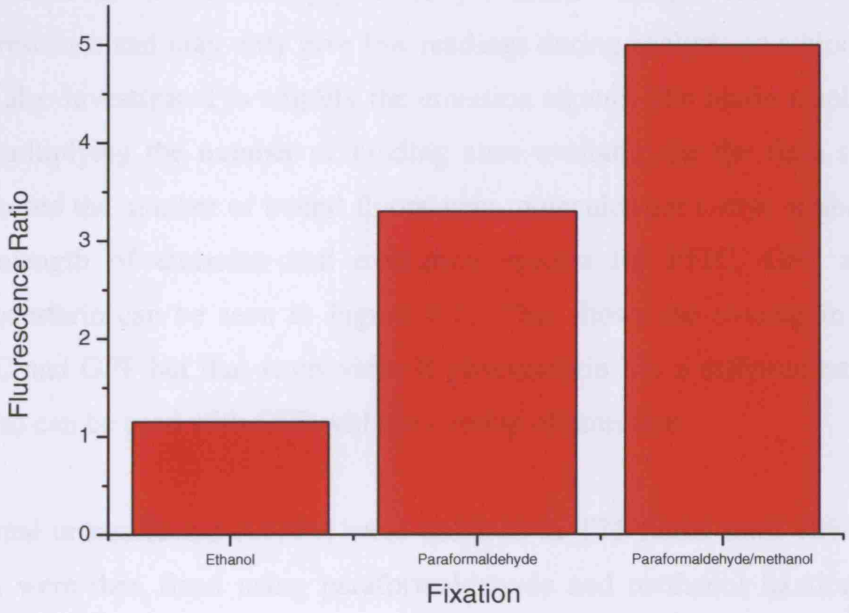

Figure 4.6 GFP fluorescence ratios by fixation method

4.6.1 Investigation of immunostaining for c-myc in A375M melanoma cells

Flow cytometric analysis of cells involves illumination of cells using a laser and measurement of the scattered light. There are several channels on a modern flow cytometry machine that can measure individual parameters at the same time. GFP is

detected in FL1 as green light with a maximum emission at 508nm. However, the normal staining protocol for c-myc at RAFT uses monoclonal antibody in combination with fluoroscein isothiocyanate conjugate (FITC). The secondary antibody, FITC, also produces a green fluorescence that is maximal at 520nm wavelength. There would be clear overlap between the two green signals (produced by GFP and FITC) and no meaningful readings could be taken. To solve this problem assessment of staining using different secondary antibodies was undertaken using different emission spectra to avoid overlap with GFP. The same monoclonal antibody was used in combination with an R-phycoerythrin-conjugated streptavidin secondary antibody that has an orange fluorescent spectrum with a maximum emission at 578nm (R-phycoerythrin-conjugated streptavidin is refered in the text simply as streptavidin). Streptavidin has a relatively weak fluorescence and may only give low readings during analysis so a biotinylated secondary was also investigated to amplify the emission signal. The biotin amplification is a result of multiplying the number of binding sites available for the final streptavidin and so increased the number of bound fluorescent molecules per c-myc antibody. The different wavelength of emission and excitation spectra for FITC, GFP and strepavidin-R-phycoerthrin can be seen in Figure 4.7. This shows the overlap in emission between FITC and GFP but that strepavidin-R-phycoerthrin has a different emission wavelength and so can be used with GFP without overlap of emission.

Normal untransfected A375M were cultured in T75 flasks until 70% confluent. $1x10^6$ cells were then fixed using paraformaldehyde and methanol fixation and stained with either c-myc monoclonal antibody or a non-specific control. Cells were stained with either FITC, streptavidin alone or streptavidin in combination with biotin. Analysis was then performed using the FL2 channel on the flow cytometry machine.

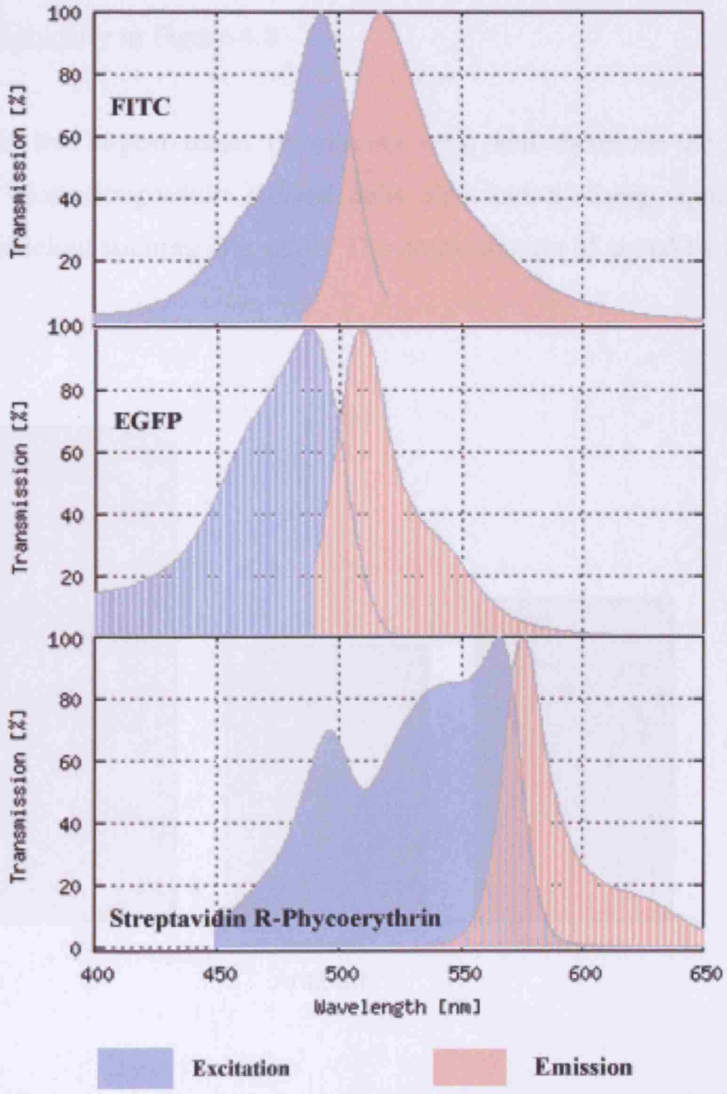

Figure 4.7 Emission and excitation spectra for chromaphores used.

4.6.2 Results

Fluorescence ratios were calculated between the non specific control and the c-myc monoclonal antibody average FL2 readings. FITC had a ratio of 8.6 compared to 4.8 for the streptavidin and 5.6 for the biotin and streptavidin group. These results are represented graphically in Figure 4.8

FITC produced the largest mean fluorescent ratio and therefore the strongest signal. However, the biotin/strepavidin stained cells also had a strong signal that would be sufficient for efficient staining of c-myc. The amplification of signal by biotin was 17%.

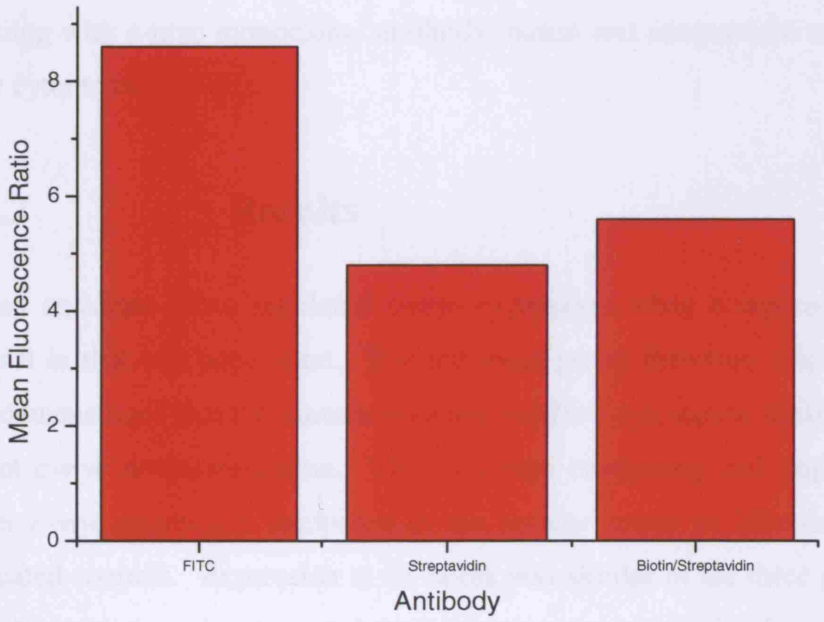

Figure 4.8 Antibody staining versus Mean Fluorescent Ratio in A375M cells

4.7.1 Simultaneous dual analysis of A375M cells for GFP and *c-myc* expression levels

Green fluorescent protein can be taken as a marker of expression from the plasmid within cells and hence the ribozyme. The aim of dual analysis of A375M cells using flow cytometry is to obtain simultaneous analysis of both GFP expression and *c-myc* expression within individual cells. If the ribozyme is active and cleaving *c-myc* mRNA, then down-regulation of c-myc protein expression would result. Investigation of the quantity of GFP expression may find an inverse correlation with *c-myc* with increasing down regulation of expression when GFP is high.

A375M cells were cultured in T25 flasks. Flasks were transfected with ribozyme 3, reverse ribozyme or were treated with one dose of antisense, antisense control or left untreated. One flask from each group was then fixed using paraformaldehyde and methanol fixation at 24, 48 and 72 hours post transfection or antisense application. Staining with c-myc monoclonal antibody, biotin and streptavidin was then followed by flow cytometric analysis.

4.7.2 Results

Naked antisense down regulated *c-myc* expression when compared with the antisense control in that cell population. The antisense group therefore acted as positive control and demonstrated that the immunostaining and flow cytometric analysis could adequately detect *c-myc* down regulation. The ribozyme expressing cell population initially had lower *c-myc* expression compared to the reverse group at 24hours but more than the untreated controls. Expression at 48 hours was similar in the three groups. At 72 hours all cell populations demonstrated their lowest *c-myc* expression levels. Normal untreated cells had the lowest *c-myc* expression at 24 hours but relatively high at 48 hours (Figure 4.9). The results of the untreated cells are difficult to explain and one would not expect such variation in this group. Rapid growth of A375M cells in the untreated flasks resulted in populations becoming 90% confluent at the end of the experiment. Confluent

monolayers of cells reduce their rate of growth by contact inhibition and so *c-myc* may be down regulated by normal cellular mechanisms. However this does not adequately explain the initial low level of expression shown by the untreated controls.

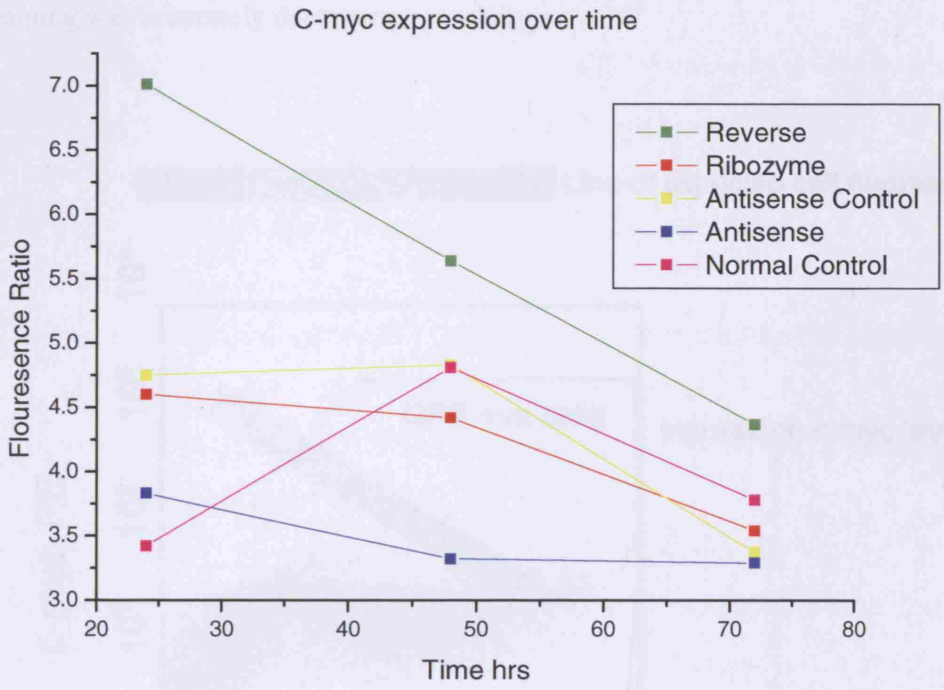

Figure 4.9 Expression of *c-myc* in transiently transfected A375M cells

Down regulation of c-myc would be expected to the greatest extent in the cells with the highest expression of the ribozyme. These cells would have a high level of GFP corresponding to the high level of ribozyme expression. We aimed to dual stain for both GFP and Streptavidin using two separate channels on the flow cytometer. If down regulation of c-myc by the ribozyme was present, the expected result would have been a inverse relationship between GFP and Streptavidin fluoresence ie low GFP associated

with high c-myc and high GFP with low c-myc. Flow cytometry analysis of the cell cultures did not demonstrate this correlation. A sample cytogram showing GFP against R-phycoerythrin-conjugated streptavidin (representing c-myc) shows no inverse correlation (Figure 4.10). This cytogram reveals that the c-myc level in cells was constant despite increases in GFP expression. The green bar represents the position of the cells in the cytogram if c-myc was down regulated by ribozyme action and the system of staining was accurately dectecting any change.

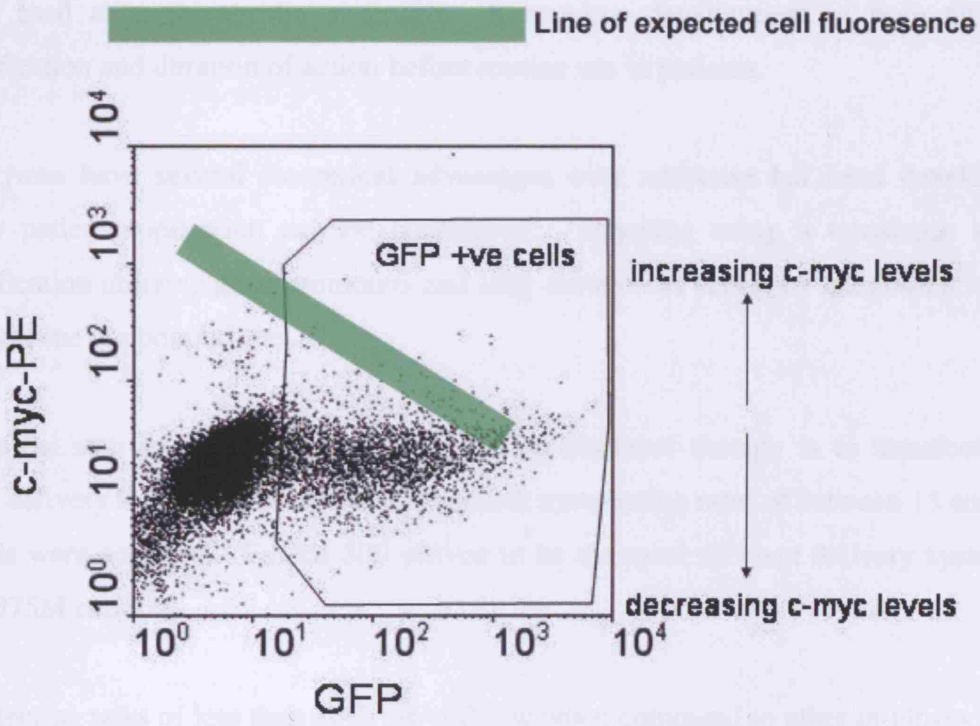

Figure 4.10 Cytogram showing GFP against Phycoerythrin fluorescence.

4.8 Discussion

Corrective gene therapy offers a new approach to the treatment of metastatic melanoma. Targeting the *c-myc* proto-oncogene is a rational strategy in the investigation of novel therapies. *c-myc* is known to be a prognostic marker in cutaneous melanoma and over expression of *c-myc* is correlated with a poor prognosis. It is also a key regulator of cell cycle mechanisms and helps to control many cellular pathways.

Antisense oligonucleotides targeting *c-myc* and bcl-2 have been shown to down regulate gene expression in melanoma. However antisense has a number of disadvantages if it is to be used as a therapeutic approach. It requires development of both targeting, amplification and duration of action before routine use in patients.

Ribozymes have several theoretical advantages over antisense but need development before patient application can be considered. Targeting using a tyrosinase switch, amplification utilizing gene promoters and long duration of action by integration into the host genome are possibilities.

The initial step in development of a ribozyme-mediated therapy is to transfect cells. Using delivery liposomal techniques, consistent transfection rates of between 15 and 20% of cells were achieved. ExGen 500 proved to be the most efficient delivery system for the A375M cell line.

Transfection rates of less than 20% are still low when compared to other *in-vitro* systems and increase the difficulty of extracting useful results from transiently transfected cell populations. Delivery of gene therapy is a major hurdle that must be overcome. New delivery systems are being developed constantly with the main focus on liposomal and viral techniques. This thesis presents data on 4 such liposomal products but subsequently several new products have been developed. The low transfection rate and toxicity of the transfecting agents mean that large numbers of cells need to be used or selected for

experiments. It is a concern that if *in-vitro* transfection is difficult then moving to *in-vivo* work will be a great challenge for delivery of the gene therapy product.

Successful transfection of the A375M cell line with the pREV plasmid encoding ribozyme 2 and ribozyme 3 allowed cell sorting and investigation of cell growth using an MTS assay. The ribozymes had no significant effect on the growth rate of cells over a period of 408 hours. The reverse control ribozymes also had no effect on growth. However, antisense oligonucleotides had a significant down regulation on growth of cells and this means that the positive control for the system was working. Control antisense had no significant effect on growth. A single application of antisense at 48 hours had a long and sustained effect on the growth of cells. However the antisense may have a longer period than 24 hours because following down regulation of *c-myc* it takes time for changes in transcription and gene expression to occur.

The effect of the ribozyme on growth is poor for both ribozyme 1 and 2. Transfection and gene expression by the pREV plasmid is taking place as evidenced by the green fluorescence of cells. There are a number of potential reasons to explain the failure to reduce growth in A375M melanoma cell lines. Firstly, gene expression is transient in transfected cells and may not be stable. The plasmid may become phosphorylated in the nucleus leading to reduced ribozyme expression. Secondly, there may be only small amounts of plasmid DNA in the cell and this may be sufficient to express enough GFP but not to produce an effective quantity of ribozyme. Therefore, the ribozyme may not be able to reduce *c-myc* enough to have any effect on growth. Another potential explanation is that the ribozyme is not targeting and cleaving the mRNA in a targeted and efficient manner. The target sequences are known to be suitable for ribozyme cleavage as the ribozyme 2 and 3 cleavage sequences have been successfully targeted in different cell lines (Ohta, Kijima et al. 1996; Cheng, Luo et al. 2000). The expression plasmid and cloning sites have also been demonstrated to be an effective delivery vehicle for ribozymes (Collis, Tighe et al. 2001).

Simultaneous dual analysis of *c-myc* and GFP has been shown to successfully evaluate two parameters concomitantly. Ribozyme 1 and 2 produced no significant reduction in *c-myc* expression and neither did ribozyme 3. Antisense, acting as a positive control, did reduce *c-myc* expression at 48 hours. The results from the dual staining experiments are difficult to interpret. This is probably due to disruption of the cell membrane by the transfection agent causing greater permeability to the antibody probes. This will tend to artificially increase the amount of c-myc staining compared to both the negative and positive controls and so any down regulation of c-myc protein expression will not be seen. Over the experiment time period the cells rapidly formed a confluent monolayer in a T25. This would result in contact inhibition and a reduced growth that may reduce *c-myc* expression. Hence why the sample demonstrated the lowest *c-myc* expression at 72 hours.

Transiently transfected cells are difficult to work with because of some of the problems outlined above. Most of the published work on ribozymes involves stably transfected cells. These are cells that are transfected with a plasmid vector that contains a gene encoding resistance to a certain toxic drug. The population of transfected cells is then exposed to the drug and only the cells expressing the resistant gene will survive. Populations of stably transfected cells can therefore be selected that are known to be actively expressing genes from the plasmid. Using this method, cells that all express the genes required can be grown and do not have to be transfected shortly prior to analysis. Experiments with stably transfected cells will be detailed in the next chapter.

Chapter 5

Investigation of ribozymes in a stably transfected A375M cell line.

5.1 Introduction

Metastatic melanoma is resistant to conventional forms of treatment such as surgery, chemotherapy and radiotherapy. Many chemotherapeutic drugs have been used to treat advanced disease but few have shown significant benefit in large-scale trials. Response rates of individual drugs are low and this has prompted investigation of combination chemotherapy regimens such as the Dartmouth regimen (Cis-platinum, Carmustine, DTIC and Tamoxifen) (Margolin, Liu et al. 1998). However, the low efficacy of current chemotherapeutic drugs has lead to investigation of novel treatment strategies including corrective gene therapy. Several groups have reported promising investigations in the treatment of melanoma using gene therapy, both *in-vitro* and *in-vivo* (Leonetti, D'Agnano et al. 1996; Jansen, Wacheck et al. 2000). Previous work performed at RAFT has demonstrated that over expression of the *c-myc* oncogene plays a key role in the development of melanoma. Inhibition of melanoma cell growth was shown, both *in-vitro* and *in-vivo*, to be correlated with a reduction of *c-myc* oncogene expression following administration of *c-myc* antisense (Chana 1998; Chana, Grover et al. 2002).

In clinical practice, corrective gene therapy in melanoma will probably be used in combination with other treatment modalities such as conventional chemotherapy. A dual approach has several potential benefits for the patient. Firstly, additive anti-proliferative effects may be observed. Secondly, abnormal oncogene expression is thought to be linked to the development of drug resistance in a wide variety of tumours and targeting those genes associated with resistance using corrective gene therapy may also combat

tumour chemo-resistance. Realistically, corrective gene therapy will have a role in augmenting other treatment strategies rather than as a single stand alone therapy.

The only licensed adjuvant treatment for use in melanoma patients is interferon. The ECOG 1684 trial demonstrated that patients with stage III melanoma treated with high dose interferon, had an increase in relapse free survival from 1 to 1.7 years and an overall survival from 2.8 to 3.8 years (Kirkwood, Strawderman et al. 1996). However this improvement in prognosis has not been seen in subsequent studies (Creagan, Dalton et al. 1995; Pehamberger, Soyer et al. 1998; Cascinelli, Belli et al. 2001). Interferon is both toxic and expensive and its use remains controversial as an adjuvant therapy. Administration of interferon results in down-regulation of *c-myc* expression and up-regulation of p21/WAF leading to G1/S phase delay and a subsequent inhibition of proliferation (Dron, Modjtahedi et al. 1986; Subramaniam, Cruz et al. 1998). Combined interferon and ribozyme therapy of melanoma may produce additive effects mediated through a synergistic reduction in *c-myc* expression. Melanomas that express high levels of *c-myc* oncogene have the worst prognosis (Grover, Ross et al. 1997; Grover, Chana et al. 1999). These patients also have the most to gain from a successful therapeutic intervention and so a combined approach using both corrective gene therapy and interferon may be beneficial. *C-myc* over expression is also associated with resistance to cis-platinum (Sklar and Prochownik 1991; Walker, White et al. 1996) and therefore any reduction in *c-myc* expression by the tumour may help to overcome cis-platinum resistance. These associations have fuelled interest in corrective gene therapy.

Studies targeting different genes have been performed on transiently transfected cell lines and have demonstrated significant reduction in gene expression (Zhang, Wang et al. 2001; Tekur and Ho 2002). However this is not the case in myc expression. Ohta et al described the first reported ribozyme targeting *c-myc* and demonstrated successful downregulation of mRNA expression using stably transfected melanoma cell lines that had been selected by G418 resistance and that were known to express ribozymes (Ohta, Kijima et al. 1996). Further ribozyme investigations by Cheng, targeting a different area of *c-myc* mRNA, were also performed in selected stable cell clones (Cheng, Luo et al.

2000). Ribozyme mediated suppression of v-myc was performed using stable cell lines selected in G418 (Dolnikov, King et al. 1996). There are no reported successful transient ribozyme assays targeting myc.

The *c-myc* ribozyme presented in this thesis had no significant effect on *c-myc* expression in transiently transfected cells as described in Chapter 4. A possible explanation may be that the levels of *c-myc*, in overexpressing cell lines, may be too high for the amount of ribozyme produced during a transient transfection. *C-myc* has a short half-life, which is approximately 20-30 minutes (Gregory and Hann 2000). Therefore high levels of *c-myc* mRNA are present in the cell and turnover is high. For any gene therapy to have a significant effect on *c-myc* expression it must be present in sufficient concentration to destroy or inhibit the large quantities of *c-myc* mRNA present. Therefore, G418-resistant cell lines, that have been selected to guarantee plasmid expression, may be a more suitable experimental system for studying the effects of myc targeting ribozymes and is investigated in the following series of experiments.

5.2.1 Selection of stable ribozyme expressing A375M clones

Transfection of A375M melanoma cells using liposomal delivery for the pREV plasmid was disappointing with only 20% of cells expressing the plasmid. The low transfection rates present several potential problems.

a) Accurate detection of change in *c-myc* expression in the transfected cells would be obscured by the population of cells as a whole.
b) Transfections are time consuming and expensive.

Stable transfections were achieved using the G418/neomycin strategy. G418 is an aminoglycoside antibiotic that inhibits protein synthesis and leads to cell death of mammalian cells. Neomycin phosphotransferase is an enzyme that degrades G418 and therefore protects any cell that produces this protein. The pREV plasmid construct

contains a neomycin phosphotransferase gene so that successfully transfected cells will produce this enzyme and therefore be resistant to G418, while non-transfected cells will be killed. After a period of time a population of cells that are expressing the plasmid are gradually selected. This is easily confirmed by examining the culture under UV light for GFP. G418 kills any non transfected cells (because they don't produce the protective enzyme) and these cells float in the culture medium leaving the transfected cells adherent to the flask. The method is described in more detail below.

5.2.2 Method for selection of stably transfected cells.

1 A375M melanoma cells were transfected in a T75 flask using a standard technique as describe in section 2.5.6. The plasmids used were pRevmycRibo3 and pRevmycRev3.

2 The cells were then left for 48 hours to recover from the stress of the transfection process.

3 Following this period the normal culture medium was changed to one containing G418 (10μg/ml). This concentration is used in all G418 containing medium unless otherwise stated. The cells were then allowed to grow for 48 hours before the medium was changed again.

4 Following UV examination of the cultures to confirm that cells were fluorescent with GFP, individual cultures were picked off under direct vision using a sterile probe.

5 Each culture was then mixed in 2mls of G418 medium in each well of a 6 well plate.

6 These cells were then allowed to grow for 48 hours before the medium was changed again and incubated for a further 48 hours.

7 The G418 medium was then drained and the cells washed in 5ml of PBS. 1ml of trypsin was then used to remove the cells from the plate. The suspension was resuspended in 5ml of G418 medium.

8 The cell suspension was sorted into 96-well plates using the FACS Vantage cell sorter. The sorting of cells was based on green fluorescence. One cell

was sorted into each well of the 96-well plate that contained 100µl of G418 medium. The cells were then incubated for 5 days.

9 Following five days incubation the 96-well plate was examined and wells with colonies present were marked. For each plasmid 20 wells were selected.

10 Each well had the medium drained and then washed with 200µl of PBS.

11 Cells were then incubated with 100µl of trypsin for 90 seconds to remove the cells from the plate. Each colony was then transferred to a well in a 24-well plate containing 1ml of G418 medium.

12 Following 5 days of incubation each well was drained of medium, washed in 1ml of PBS and then typsinized with 0.5ml of trypsin for 90 seconds. The cells were then placed in a T25 flask and incubated with 5ml of G418 medium for 5 days.

13 Once the cells had grown into a 70% confluent layer the A375M cells were washed with 5mls PBS and treated with 2mls of trypsin for 90 seconds. The cell suspension was mixed with 5ml of medium, centrifuged at 1000rpm (118G) for 5 minutes and resuspended in medium containing 10% DMSO. Aliquots of cells were frozen in liquid nitrogen with $1x10^6$ cells per ml.

Each plasmid was therefore expressed in 10 clonogenic populations with each one growing from a single cell. Every cell within the cloned population is known to be expressing the plasmid as there is a continual selection pressure resulting from the presence of G418 in the medium (Figure 5.1).

A population of non-transfected cells was produced using similar methods except normal medium was used at all stages. Each of the 10 non-transfected clonogenic populations was grown from one cell. These cells were grown so they could be used as untransfected control groups.

Using the above methods, 10 cloned populations were selected and grown for each of the treatment groups. These consisted of an active ribozyme, a reverse inactive ribozyme, an antisense sequence and a non transfected population.

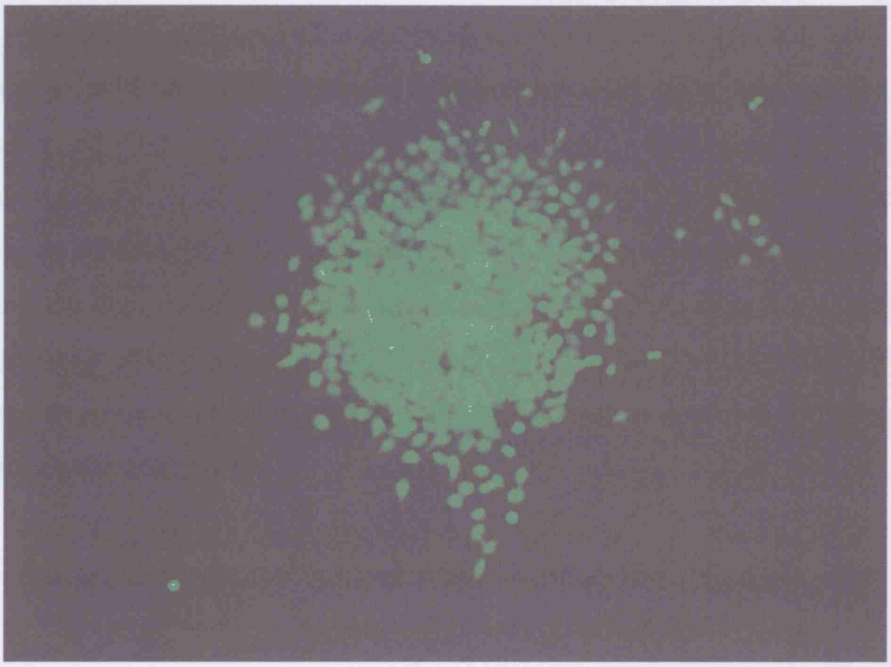

Figure 5.1 A colony of stably transfected cells demonstrating GFP production under UV light .

5.2.3 Investigation of GFP levels using flow cytometry in ribozyme transfected A375M cell lines.

Flow cytometric analysis of GFP in 30 different cell clones revealed that all of the clones transfected with the pREV plasmid expressed GFP to a high degree compared to untransfected clone (Figure 5.2). Clones transfected with the reverse ribozyme plasmid had an average GFP of 949 with a range of 96 to 2590. Ribozyme transfected clones had a range of 39 to 2100 with an average of 784. These results demonstrate that all of the clones were expressing GFP and therefore had functional copies of the plasmid. There is a wide range of expression levels for each of the groups. Untransfected clones had an average expression of GFP of 1.1 and clearly had no green fluorescence. These are arbitary fluoresence units.

This experiment confirmed that the plasmid transfected cell lines were all expressing GFP and therefore had at least one copy of the plasmid vector correctly working within cells. They should therefore also be expressing the ribozyme component of the vector.

5.3 Investigation of *c-myc* expression using flow cytometry in ribozyme transfected A375M cell lines.

It has been previously demonstrated that antisense oligonucleotides, targeting *c-myc*, can effectively down regulate protein expression (Chana 1998). Treatment of non-transfected clonogenic populations of A375M cells with antisense (and appropriate controls) would therefore act as a positive control for the stably transfected ribozyme-producing cells to demonstrate reduced expression of c-myc using FCM analysis and immunostaining.

In addition a non-functioning ribozyme was designed and constructed to act as another negative control. This ribozyme was composed of exactly the same sequence as the active ribozyme but the two flanking sequences (stem 1 & 3) were reversed. This

ensured that this reverse ribozyme could not hybridise to the *c-myc* target sequence and therefore have no effect on *c-myc* expression

Each of the non-transfected clonogenic populations would remain untreated with either with antisense or ribozyme, to act as a negative control. By using these controls the ability of the experiment to accurately recognise protein down-regulation could be assessed and any effects on cells of transfection with the pREV plasmid could also be quantified.

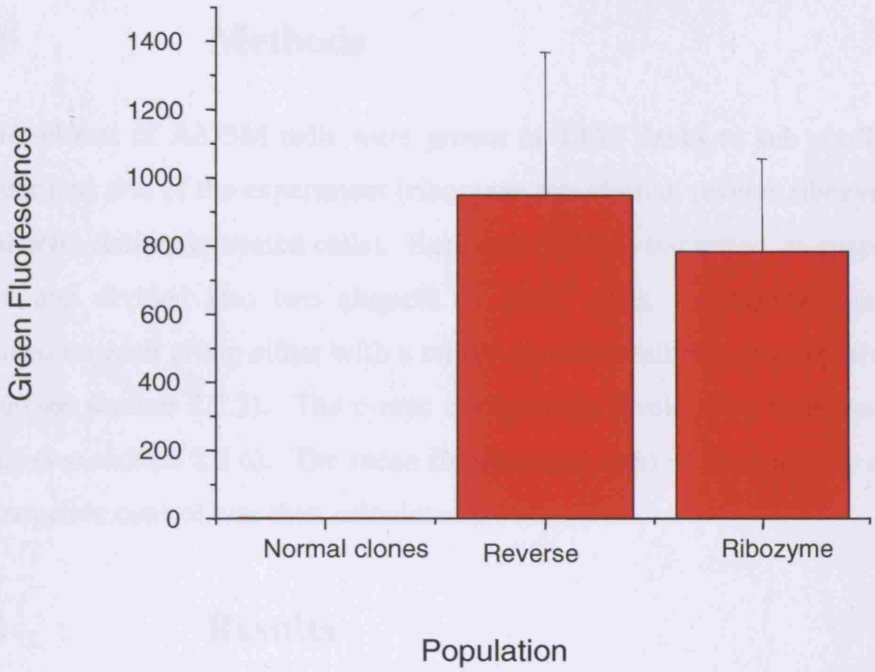

Figure 5.2 Graph to show GFP expression detected using flow cytometric analysis in the three clonogenic groups.

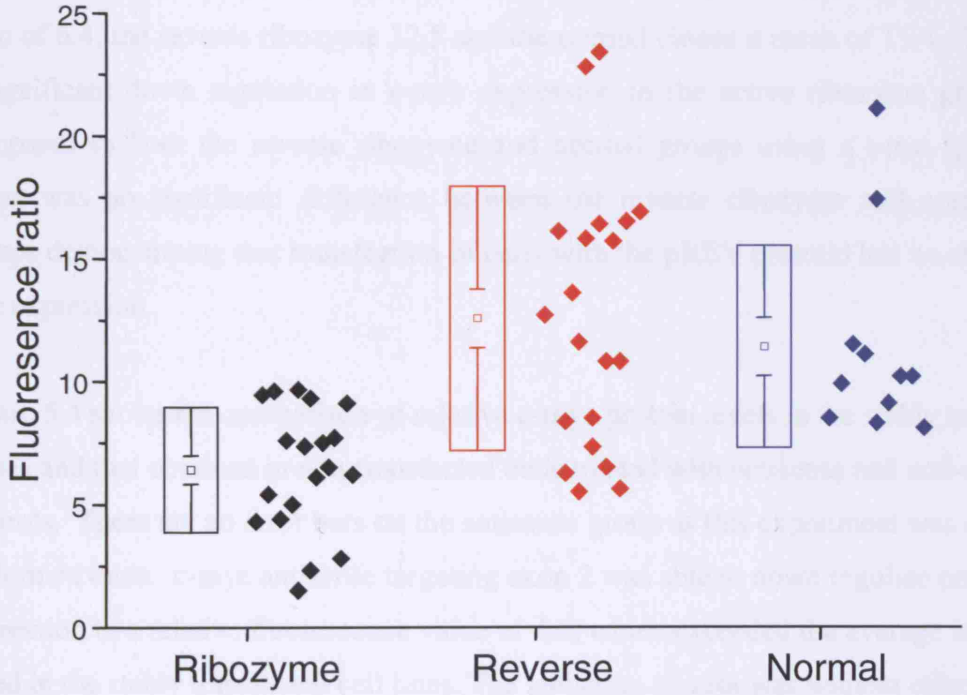

Figure 5.3 Expression of *c-myc* in clonogenic populations of A375M cells. The graph shows the individual fluorescent ratios for each clone to the right of a box plot whose centre is the mean, arms the standard error of the mean and the outer box the standard deviation.

5.3.1 Methods

Ten sub-clones of A375M cells were grown in T150 flasks to sub confluent levels for each required arm of the experiment (ribozyme transfected, reverse ribozyme transfected, normal cells, antisense treated cells). Each cell line was harvested, re-suspended, fixed in ethanol and divided into two aliquots of $1x10^6$ cells. Antibody staining was then performed on each group either with a c-myc specific antibody or a negative non-specific control (see section 2.2.2). The c-myc oncoprotein levels were then assessed by FCM analysis (see section 2.2.6). The mean fluorescence ratio of the antibody stained relative to the negative control was then calculated.

5.3.2 Results

The ratio of c-myc fluorescence of each clone compared to negative controls for each of the cell lines is displayed in Figure 5.3. The active ribozyme had a mean fluorescence ratio of 6.4; the reverse ribozyme 12.5 and the normal clones a mean of 11.4. There was a significant down regulation in *c-myc* expression in the active ribozyme group when compared to both the reverse ribozyme and normal groups using a t-test ($p<0.0001$). There was no significant difference between the reverse ribozyme and normal clone groups demonstrating that transfection of cells with the pREV plasmid has no effect on *c-myc* expression.

Figure 5.4 shows the comparison of relative c-myc protein levels in the stably transfected clones and that obtained in non-transfected cells treated with antisense and non-sense controls. There are no error bars on the antisense group as this experiment was only performed once. c-myc antisense targeting exon 2 was able to down regulate protein expression to a relative fluorescence value of 4.5, which exceeded the average inhibition noted in the stably transfected cell lines. The antisense control was without effect.

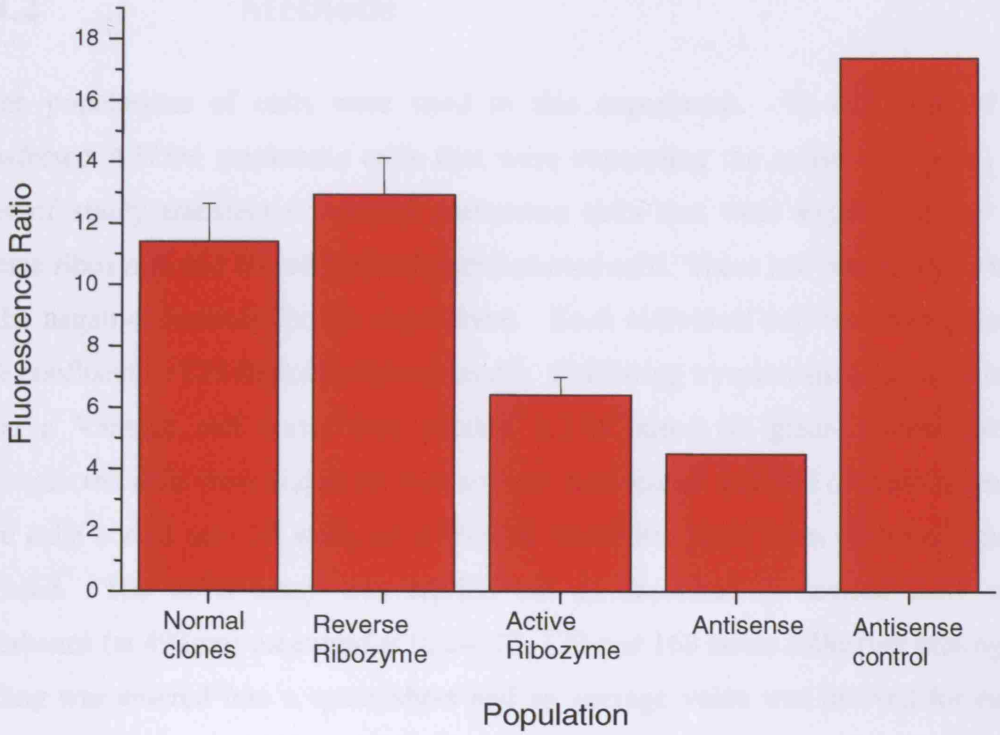

Figure 5.4 The expression of c-myc in clones derived from stable transfections and antisense treated A375M melanoma cells. The bars represent the mean value with the S.E.M.

5.4.1 Investigation of growth using the MTS growth assay in ribozyme transfected A375M cell lines.

Antisense oligonucleotides targeting *c-myc* have been shown to down regulate *c-myc* protein expression and produce a reduction in the growth of A375M melanoma cells. A375M cells lines that are stably transfected with the pREV plasmid expressing the *c-myc* ribozyme have been shown to both express the plasmid to high levels and also significantly reduce the c-myc protein expression in cells. The next stage of the investigation of the ribozyme was to assess the effect of the ribozyme on growth.

5.4.2 Methods

Three populations of cells were used in this experiment. 10 cell lines of stably transfected A375M melanoma cells that were expressing the active ribozyme, 10 cell lines of stably transfected A375M melanoma cells that were expressing the control reverse ribozyme and 10 cell lines of untransfected cells. These last two groups would act as the negative controls for the experiment. Each individual cell line was grown until 50% confluent in T25 flasks in normal media. Following tryspinization, cells were sorted using a Vantage cell sorter (see section 2.2.8) based on green fluorescence. The untransfected cells were sorted on forward and side scatter and 500 of these normal cells were each sorted into 10 wells of a 96-well microtitre plate from each cell line to be assessed. The MTS assay was carried out as described in section 2.5.7 and the absorbance (at 492nm) measured at 0, 24, 72, 120 and 168 hours following plating. Each reading was entered into a spreadsheet and an average value was derived for each cell line at each time point. The ten cell lines that made up either the ribozyme, reverse or untransfected cells were then averaged to produce a measure of each group at each time point. If any wells became infected with bacteria they were removed from all calculations. Data were collected on a Windows Excel spreadsheet package.

5.4.3 Results

The variability shown by each of the 10 clones in each experimental group can be seen in Figure 5.5. For each group the spread of individual data points are shown as boxes that demonstrate both the standard deviation and the standard error of the mean for each group. There is a significant down regulation of growth in the *c-myc* ribozyme transfected group compared to both the reverse and untreated controls compared using Anova test of variance ($p<0.0001$, F-ratio 12.62). When the active ribozyme is compared to the reverse clone using a t-test there is significant down regulation of growth ($t=-4.871$, $p<0.0001$). Also when the active ribozyme is compared to the normal group, again a significant down regulation is seen ($t=-4.123$, $p<0.003$). The average absorbance at 168

hours for the ribozyme group is 1.85 compared to 1.97 and 2.12 for the reverse and untreated groups.

The average absorbance values are shown graphically in Figure 5.6. Each test group has been plotted as an average of all ten clones with the error bars representing the standard error of the mean. All groups start from the same value for absorbance at 0 hours. The gradient of the curve indicates the growth and it can be seen that the normal cells grow most rapidly. The ribozyme transfected group grew at the slowest rate compared to the other two groups. The reverse ribozyme groups have an intermediate growth rate. All three curves have the most rapid growth initially which then slows as the experiment proceeds and confluence is reached.

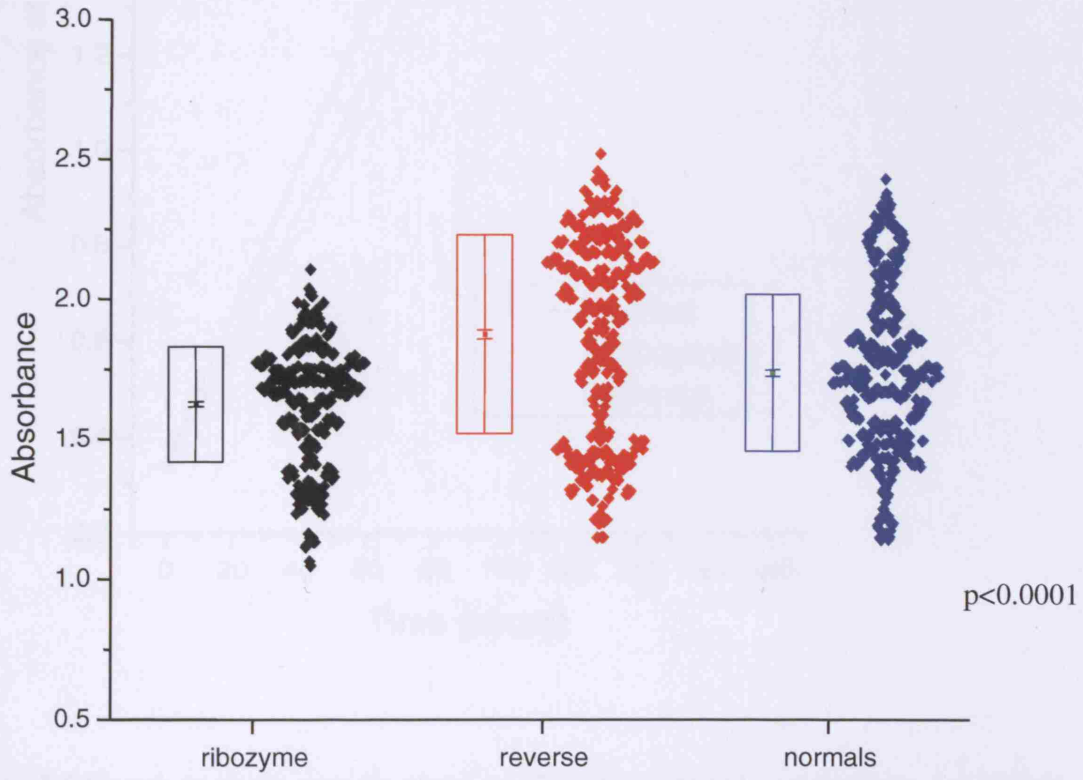

Figure 5.5 Graph to show absorbance of cloned populations of A375M melanoma cells at 168 hours. The bars are standard error of the mean and the boxes are standard error of the mean. The error bars are standard error of the mean.

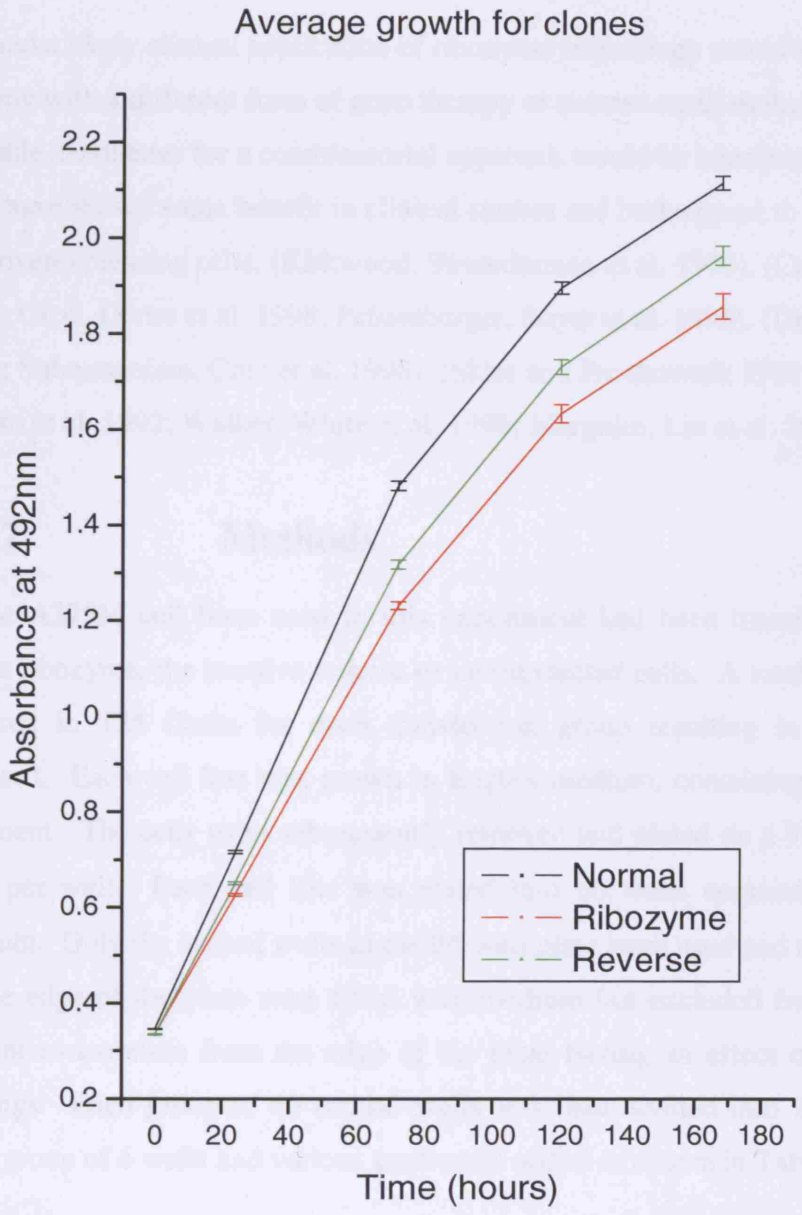

Figure 5.6 Graph to show growth curve produced by cloned populations of A375M melanoma cells studied in an MTS assay.

5.5.1 Investigation of the effect on growth of a *c-myc* ribozyme in combination with interferon and cis-platin in A375M melanoma cells.

The most likely clinical application of ribozyme technology would be as a combination therapy with a different form of gene therapy or current small molecule drug therapy. Suitable candidates for a combinatorial approach would be interferon and cis-platinum as both have shown some benefit in clinical studies and both appear to less effective in *c-myc* overexpressing cells. (Kirkwood, Strawderman et al. 1996). (Creagan, Dalton et al. 1995; Grob, Dreno et al. 1998; Pehamberger, Soyer et al. 1998). (Dron, Modjtahedi et al. 1986; Subramaniam, Cruz et al. 1998). (Sklar and Prochownik 1991; Kashani-Sabet, Funato et al. 1992; Walker, White et al. 1996; Margolin, Liu et al. 1998).

5.5.2 Methods

Stable A375M cell lines used in this experiment had been transfected with either the active ribozyme, the inactive reverse or untransfected cells. A total of 10 cell lines were cultured in T25 flasks for each transfection group resulting in 30 cell lines being assessed. Each cell line was grown in Eagle's medium, containing no G418, until 50% confluent. The cells were subsequently removed and plated on a 96-well plate with 500 cells per well. Each cell line was plated into 60 wells containing 200µl of Eagle's medium. Only the central wells in the 96-well plate were used and the 36 wells that were on the edge of the plate were filled with medium but excluded from the experiment to prevent evaporation from the edge of the plate having an effect on the optical density readings. Each group of 60 central wells was then divided into 10 groups of 6 wells. Each group of 6 wells had various treatments added as shown in Table 5.1.

Group	Treatment
1	Untreated
2	Untreated
3	Antisense ODN's
4	Scrambled Antisense ODN's
5	Interferon
6	Interferon + Antisense ODN's
7	Interferon + Scrambled Antisense ODN's
8	Cis-platinum
9	Cis-platinum + Antisense ODN's
10	Cis-platinum + Scrambled Antisense ODN's

Table 5.1 Treatment of cells in 96-well plates during MTS assay.

Antisense was diluted to a final concentration of 5nm per µl. Interferon was diluted to 1000 IU/ml and cis-platinum to 57µg/ml, the estimated normal physiological tissue concentrations.

MTS was then added to each well as described in section 2.5.7 and optical density readings were obtained using a plate reader (at 492nm) at 0, 24, 72, 120 and 168 hours following addition of MTS to the medium. Optical density readings were entered in to a spreadsheet and mean values calculated for the 6 wells used for each clone individually and for each of the transfection groups.

5.5.3 Results

5.5.3.1 Growth of untreated clonogenic A375M melanoma cell lines.

Before any additional treatment, the ribozyme, reverse and untreated clones were assessed for growth in an MTS assay for 168 hours. Fig. 5.7 shows the results for the three sets of untreated clones and confirms that the ribozyme is effective in down regulating growth independently of other treatments.

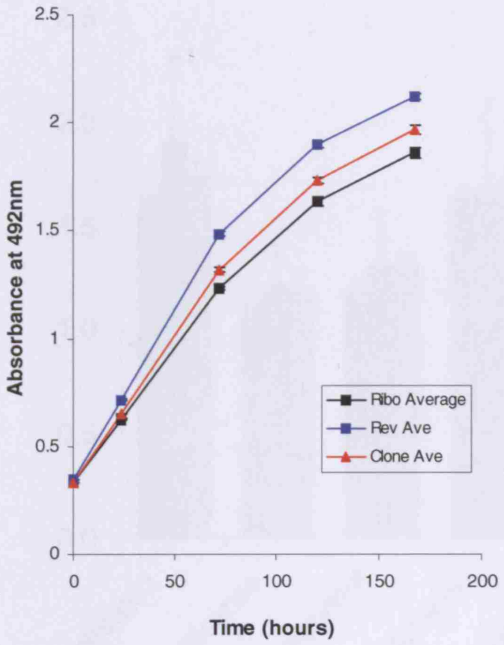

Figure 5.7 Growth of untreated clones

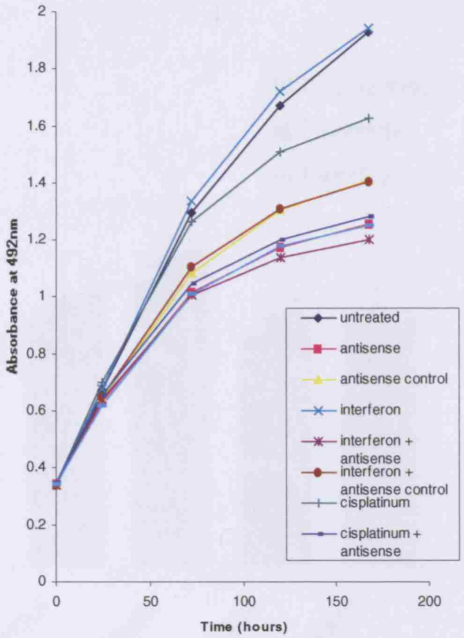

Figure 5.8 Growth of clones untransfected clones

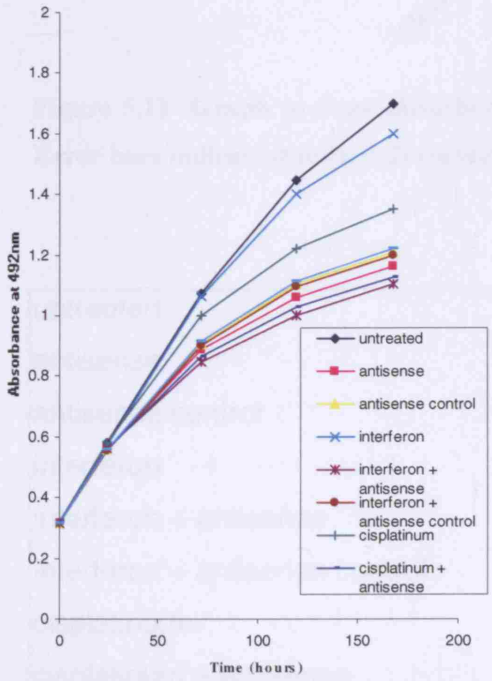

Figure 5.9 Growth of ribozyme transfected clones

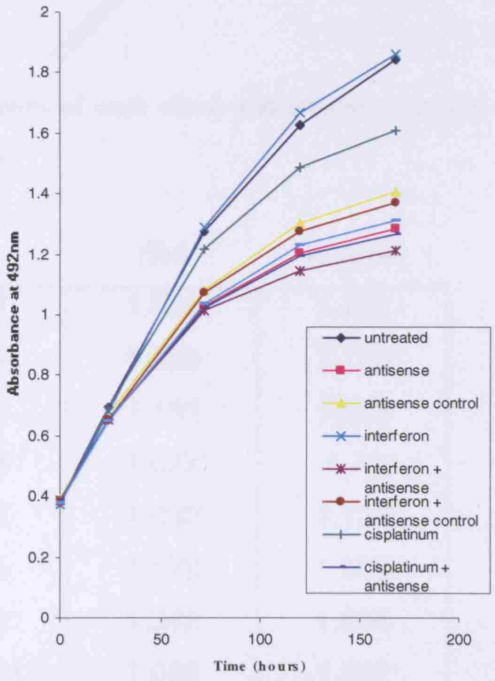

Figure 5.10 Growth of reverse transfected clones

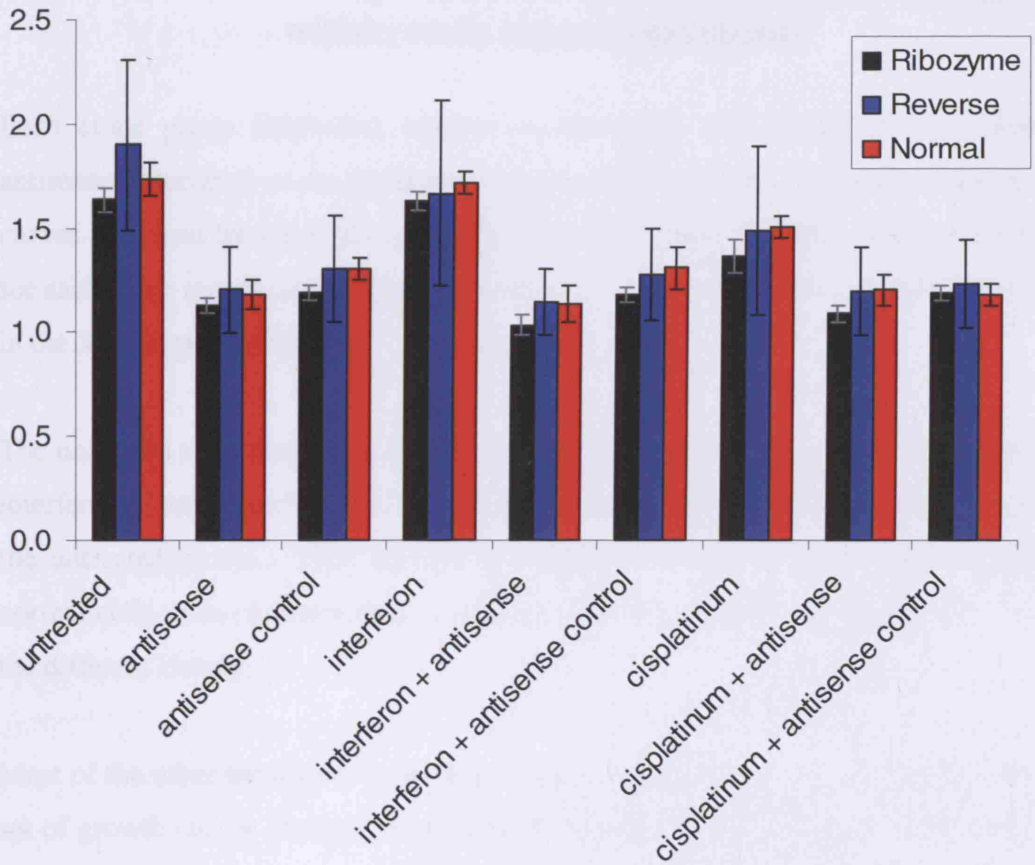

Figure 5.11 Graph to show absorbance at 120 hours of each clone and treatment group. Error bars indicate standard deviation of the mean.

	rev	ribo	normal
untreated	1.897	1.634	1.732
antisense	1.202	1.126	1.176
antisense control	1.303	1.189	1.303
interferon	1.664	1.627	1.72
interferon + antisense	1.145	1.032	1.136
interferon + antisense control	1.275	1.178	1.309
cisplatinum	1.488	1.362	1.506
cisplatinum + antisense	1.196	1.088	1.202
cisplatinum + antisense control	1.232	1.185	1.177

Table 5.2 Absorbance at 120 hours for different treatment groups.

5.5.3.2 Comparison of the different treatment groups within each clone population.

Each clone group (untreated, reverse or ribozyme) was subjected to treatment with antisense, interferon or cis-platinum or appropriate controls. For each clone the growth curves produced by the MTS assay are shown in figures 5.8-5.10. The curves produced for each clone are all similar suggesting that the added treatments all have a similar effect in the 3 clone populations.

The untreated clones have the highest growth rates as would be expected. However, the interferon alone treated groups have growth rates that are very similar or even greater to the untreated clones. This suggests that interferon alone had no effect on growth of normal cells. Cis-platinum alone produced a modest decrease in growth rate in each of the different clones.

Most of the other treatments involving antisense or antisense controls produced a similar set of growth curves showing inhibition of growth. Active antisense produced a greater reduction in growth than its control but the results were similar. Interestingly, antisense in combination with cis-platinum produced little additive effect, however, the antisense in combination with interferon produced the lowest growth in all three clone groups inspite of the little effect of interferon alone.

Quantitative data was obtained by analysing the absorbance values at 120 hours. The data obtained is represented in Figure 5.11 and Table 5.2. Each bar represents an absorbance for a particular clone group and treatment and the error bars indicate the corresponding standard deviation for each of the groups.

The untreated control groups for the three clone groups all demonstrated the greatest increase in absorbance and therefore the fastest growth when compared to the clones that received any treatment in the MTS assay. The ribozyme transfected group had an

absorbance of 1.634 at 120 hours compared to 1.897 in the reverse ribozyme group, and 1.732 in the non transfected group.

5.5.3.3 Antisense treatment

Antisense directed against *c-myc* has previously been shown to have a significant reduction in growth of A375M melanoma cells in vitro. As expected, the antisense reduced growth in all three clones. Again the ribozyme group had the lowest growth having an absorbance 1.126 compared to 1.202 for the reverse and 1.176 for the non-transfected group. The control for the antisense group, the non-sense treated clones demonstrated a reduction in growth that was intermediate between the untreated clone and the antisense treated. This suggests the non-sense was indeed having some effect but not to the same degree as the active antisense. The clones treated with antisense had a reduction in growth compared to the untreated clones. The percentage reduction was 31% for the ribozyme group, 37% in the reverse group and 32% in the untransfected group. If the ribozyme was actually reducing the amount of *c-myc* mRNA within cells then one would expect that the antisense would have the smallest effect on these cells as there would be less *c-myc* mRNA available.

5.5.3.4 Interferon

Interferon was used either alone or in combination with either antisense or the nonsense control. Interestingly, when interferon was used alone it appeared to have very little effect on the growth of cells. There was no significant difference between untreated clones or those treated with interferon. However the ribozyme clones again had the lowest growth of all the 3 clone groups but this did not appear significantly less than the untreated ribozyme clones. This may well suggest that there is no additive effect between the ribozyme and the interferon. When interferon was used in combination with antisense oligonucleotides there was a significant reduction in growth compared to the interferon treatment alone. Indeed this combination of treatments produced the slowest growth of all the treatment groups and the reduction was greater than either of the two

used alone. The ribozyme clone treated with both interferon and antisense had an absorbance of 1.032 compared to 1.126 with antisense alone and 1.627 with interferon alone. Each of the other two clone groups also demonstrated a similar trend. The reduction in absorbance by interferon and antisense compared to interferon alone is 37% in the ribozyme-expressing clones compared to 31% and 34% reductions in the reverse and normal clones respectively.

5.5.3.5 Cis-platinum

The clones treated with cis-platinum all demonstrated a reduction in growth when compared to their corresponding untreated controls. The addition of cis-platinum reduced the absorbance at 120 hours to 1.362 for the ribozyme clones and 1.488 and 1.506 for the reverse and untransfected clones. This was a greater reduction than interferon alone. The use of cis-platinum in combination with antisense resulted in a further reduction in growth of the clones. Growth was reduced in all 3 clone groups by exactly the same amount, 20%. The reduction in growth produced by cis-platinum, when used in combination with antisense, was not as great as that achieved with interferon in combination with antisense.

5.6 Discussion

Corrective gene therapy targeting *c-myc* must have an anti-proliferative effect on cells if it is to be useful in clinical practice. Previous work with antisense has demonstrated that a reduction in *c-myc* expression correlates with a reduction in cell growth both *in-vitro* and in an *in-vivo* mouse model (Chana, 2002). Transient transfection with ribozymes has not demonstrated a reduction in *c-myc* expression. A stable transfection strategy was then pursued in an attempt to investigate a ribozyme targeting *c-myc* and the results have been presented in this chapter. It has been shown that pREV can effectively be used to transfect cells and then develop stable transfections by selecting cells using G418 in the growth medium, confirmed by GFP expression within cells. These stably transfected cells have then been shown to have a reduced level of *c-myc* expression when compared

to non-transfected clones and also those expressing a non-functioning ribozyme. However, these reductions were not as much as naked antisense oligonucleotides. This may be for several reasons. Firstly the ribozyme may not be expressed in large quantities within cells and, despite its catalytic functions, may not be able to inactivate the same quantity of *c-myc* mRNA. Secondly, the ribozyme may not be acting in a catalytic manner and so will be used up rapidly and may not be destroying as much *c-myc* mRNA as expected. However, stable transfection with a ribozyme targeting *c-myc* can reduce c-myc protein expression when measured using immunostaining and flow cytometry.

The ribozyme can reduce growth of A375M melanoma cells when grown in a MTS growth assay. This experiment reveals that A375M melanoma cell lines that under go stable transfection with a ribozyme specifically targeting *c-myc* can reduce growth in an *in vitro* model. The MTS assay is a simple system of colorimetric change produced by metabolism of cells and is a sensitive growth assay. However, it is very difficult to predict the growth reduction that ribozyme therapy would achieve *in vivo* and ultimately in patient care. The reduction in growth that has been produced should be investigated further to assess what place ribozyme treatment will have in the clinical scenario.

Ribozymes are likely to be ultimately used in combination with other treatment modalities such as chemotherapy or biological treatments. The experiments described in this chapter suggest there is a complex relationship between *c-myc* reduction and interferon and cis-platinum. There is an additive effect demonstrated between *c-myc* antisense and interferon. If corrective gene therapy could be combined with interferon treatment it might have a significant role to play in clinical practice.

Further directions for investigation of the actions of the ribozyme on melanoma cells could be considered. In-vitro testing of the ribozyme using a target sequence of mRNA produced by reverse transcription could be attempted. The efficiency of the ribozyme could be assessed by analysis of the breakdown products and new ribozymes targeting different areas of the *c-myc* gene could quickly be investigated. The addition of a tyrosinase switch to the pREV plasmid could be considered to improve the selectivity of

the ribozyme thereby limiting expression to melanin producing cells. This would reduce side effects of any therapy, as the active treatment would only be produced in specific cells. This series of experiments have shown the potential of *c-myc* targeted corrective gene therapy when used in combination with interferon and further investigation of this relationship could be profitable.

Chapter 6

Investigation of oncogene expression in cutaneous melanoma utilizing a tissue micro-array.

6.1.1 Introduction

Cancer development and progression involves many genes that control cell proliferation, differentiation and death. The multi-step process leading to cancer involves losses, rearrangements and amplifications of chromosomal regions and genes. These modifications in gene structure lead to disruption of key signal pathways followed by the development of the malignant phenotype. New techniques, such as cDNA micro-arrays, have led to the analysis of thousands of genes in cancer. However these new and expensive modalities for gene investigation are probably still far from entering routine clinical practice where the traditional formalin-fixed paraffin sections still dominate. Simultaneous analysis of expression changes in multiple genes is needed to increase understanding of the genetic changes in different stages of cancer. Potential diagnostic and prognostic markers also need to be compatible with the current system of histological evaluation. Recently, a technique to allow high-throughput molecular analysis of tumours has been developed (Kononen, Bubendorf et al. 1998). A system based on the construction of an array of up to 1000 cylindrical tissue biopsies was described as a method for parallel *in situ* detection of markers. Cylindrical tissue samples, 0.6mm in diameter, were taken from tissue samples of 1290 breast carcinomas and then assembled in a new paraffin block. FISH analysis of gene amplification was then performed for visualization and detection of genetic rearrangements in individual cells. Tissue array

technology therefore allows rapid and controlled analysis of hundreds of paraffin specimens in an efficient and simple way. Procurement, fixation and storage are simple and consumption of precious tumour specimens is minimized.

6.1.2 *C-myc* is a key gene regulator

The *c-myc* proto-oncogene is one of the key regulators of mammalian cell proliferation, differentiation and apoptosis. It is found to be over-expressed in several tumour types and indeed is prognostic in many (Field, Spandidos et al. 1989). The *c-myc* gene is normally transcribed in a highly proliferation-dependent manner. However, independent and unregulated expression of *c-myc* can occur in tumour cells as a consequence of mutations of the gene itself or in signalling pathways that regulate *c-myc* expression. The c-myc protein binds to and transactivates genes via E boxes with a partner protein, max. However it is thought that this transactivation is modulated by interactions with other genes such as p107 (Gu, Bhatia et al. 1994) or Bin 1 (Sakamuro, Elliott et al. 1996). Myc has been discovered to be associated with the protein, p107, which physically associates with myc and represses transcriptional activation. These gene modulations still require further investigation to elicit the exact mechanisms involved. Another up-stream regulator is the cyclin D1/cdk4 kinase complexe. This complex can induce a rapid upregulation of *c-myc* expression, which in turn results in a slower induction of cyclin D1/cdk4 kinase complexes in a form of positive feed back (Afar, McLaughlin et al. 1995). However the *c-myc* effect on cyclin D1/cdk2 kinase complexes is subtle and probably insignificant compared to other regulators of this cyclin. Repression of p107 by cyclin D1/cdk2 kinase complexes in turn relieves the negative effects of p107 on *c-myc*. Cyclin D1 also acts upstream of another transcription factor, E2F, that has similar biological properties to *c-myc* and both induces cell cycle entry and apoptosis when over expressed. It has been suggested that this factor can also activate *c-myc* expression (Yu, Jing et al. 1998).

The regulatory effects of *c-myc* are mediated through a variety of genes that control multiple cellular pathways such as the cell cycle, apoptosis, DNA dynamics and macromolecular synthesis. Direct target genes are those that undergo changes in

expression due to direct interaction of the c-myc molecule with their gene regulatory elements (Dang 1999). The time course of induction of these target genes should be intimately related to changes in *c-myc* expression. These target genes provide a link between *c-myc* dysregulation and the progression of the cell to neoplastic transformation or apoptosis. There is a range of *c-myc* targets listed in Table 6.1. It is thought that the *c-myc* related phenotypes are mediated through specific subsets of target genes and not solely by single target genes. Investigation of gene activation has used different approaches. Firstly identifying genes whose expression is altered following forced over-expression of *c-myc*. Secondly, searching for genes that contain myc/max binding regions within their regulatory elements. Utilizing these methods, a series of down-stream target genes have been identified.

6.1.3 *C-myc* gene interactions

Myc has been shown to be an upstream regulator to cyclin-dependent kinases including cdc25A. Galaktionov demonstrated that cdc25A plays a key role in mediating the effect of *c-myc* on the cell cycle (Galaktionov, Chen et al. 1996). By encoding for a crucial G1-specific protein phosphatase that is required for initiation of the cell cycle and progression through G1, cdc25A allows progress into the cycle. It was shown that induction of cdc25A mRNA was as a direct result of *c-myc* action on the cdc25A gene via stimulation via an E-box region on intron 1 of the cdc25A DNA.

Sequence analysis also revealed three potential myc-max binding sites in the human gene. The evidence strongly suggests that cdc25A is both a direct transcriptional target of *c-myc* and also a mitogenic effector. Cellular apoptosis is also triggered by *c-myc* and cdc25A is thought to have an important role in this pathway. Galaktionov et al demonstrated that cdc25A induces apoptosis in an identical fashion as *c-myc* in serum-deprived fibroblasts and also that *c-myc* was unable effectively to produce apoptosis when cdc25A expression was blocked with antisense oligonucleotides (Galaktionov, Chen et al. 1996). It seems that the *c-myc* down-stream pathways of cell proliferation and cell death bifurcate through cdc25A (Zornig and Evan 1996).

Cellular function	*c-myc* target genes
Cell cycle	cyclin A
	cyclin E
	p27
	cdc25A
	gadd45
Apoptosis	p53
	ARF
DNA metabolism	DHFR
	cad
	TK
DNA dynamics	RCC1
	Telomerase
Macromolecular synthesis	ECA39
	elf2alpha
	eIF4E
	MrDB

Table 6.1 Gene targets of *c-myc*.

Another down-stream kinase induced by *c-myc* expression is cyclin E/cdk2 kinase. Activation of *c-myc* has been shown to invoke rapid induction of cyclin E/cdk2 kinase activity (Steiner, Philipp et al. 1995). It is thought unlikely that this increase in cyclin E/cdk2 kinase activity was produced by changes in gene expression as it preceded the increase in cyclin E protein. Cdc25A did not seem to play a role in the change in activity, however, cdc25A does remove two inhibitory proteins from Cdk2. Cyclin E/cdk2 kinase was discovered to contain the inhibitor protein, p27, before activation by *c-myc* but following activation of cyclin E/cdk2 kinase the p27 was degraded. The inhibition of p27 by *c-myc* is thought to be mediated by degradation in addition to other unknown mechanisms. Ectopic p27 expression inhibits cyclin E/cdk2 kinase activity and expression of cyclin A but this is reversed by *c-myc* expression *in-vitro*. Certainly, *c-myc*

degradation of p27 prevents inhibition of cyclin E/cdk2 kinase activity and can allow entry into the cell cycle. Indeed, over-activity of cyclin E is linked to the passage of the cell through the restriction point and thus committing the cells to another round of replication. Therefore in *c-myc* over-expressing cells there is immediate re-entry into another round of proliferation immediately following exit from mitosis and may explain why *c-myc* transformed cells can proliferate in the absence of growth factors.

Apoptosis is a key event in the genesis of the malignant phenotype. Apoptosis-protection genes such as bcl-2, play a key role in the development of cancer by preventing cell death by a variety of agents and mechanisms. Paradoxically, deregulation of proliferation through activated oncogenes, such as *c-myc* is also a stimulus for apoptosis. However, co-operation between *c-myc* and overexpression of bcl-2 suppresses the induction of apoptosis. This interaction allows myc to continue to drive the cell cycle whilst preventing the cell death that over expression of myc would normally produce, thus breaking the connection between the cell cycle and cell death. By this mechanism bcl-2 plays a crucial role in tumour development by prolonging the survival of cells to form populations of aberrant clones.

The role of the tumour suppressor gene, p53, is to prevent accumulation of errors in DNA damaged cells. In the presence of mutated or silenced, p53, cells fail to enter apoptotic pathways following DNA damage, leading to accumulation of further mutations and resistance to anti-neoplastic therapy. Down-regulation of bcl-2 results from p53 acting as a transcriptional silencer. However when bcl-2 and *c-myc* are overexpressed, the reciprocal antagonism between p53 and bcl-2 is lost and p53-mediated growth arrest and apoptosis are blocked. The cooperation between *c-myc* and bcl-2 results in the loss of a crucial tumour suppressor and speeds the progression to a more malignant phenotype.

A tissue micro-array (TMA) would be a useful method for screening the expression of different genes related to *c-myc* in multiple melanoma specimens. To this end, suitable genes were selected for analysis in the TMA to assess for prognostic significance based on the scheme outlined in Figure 6.1.

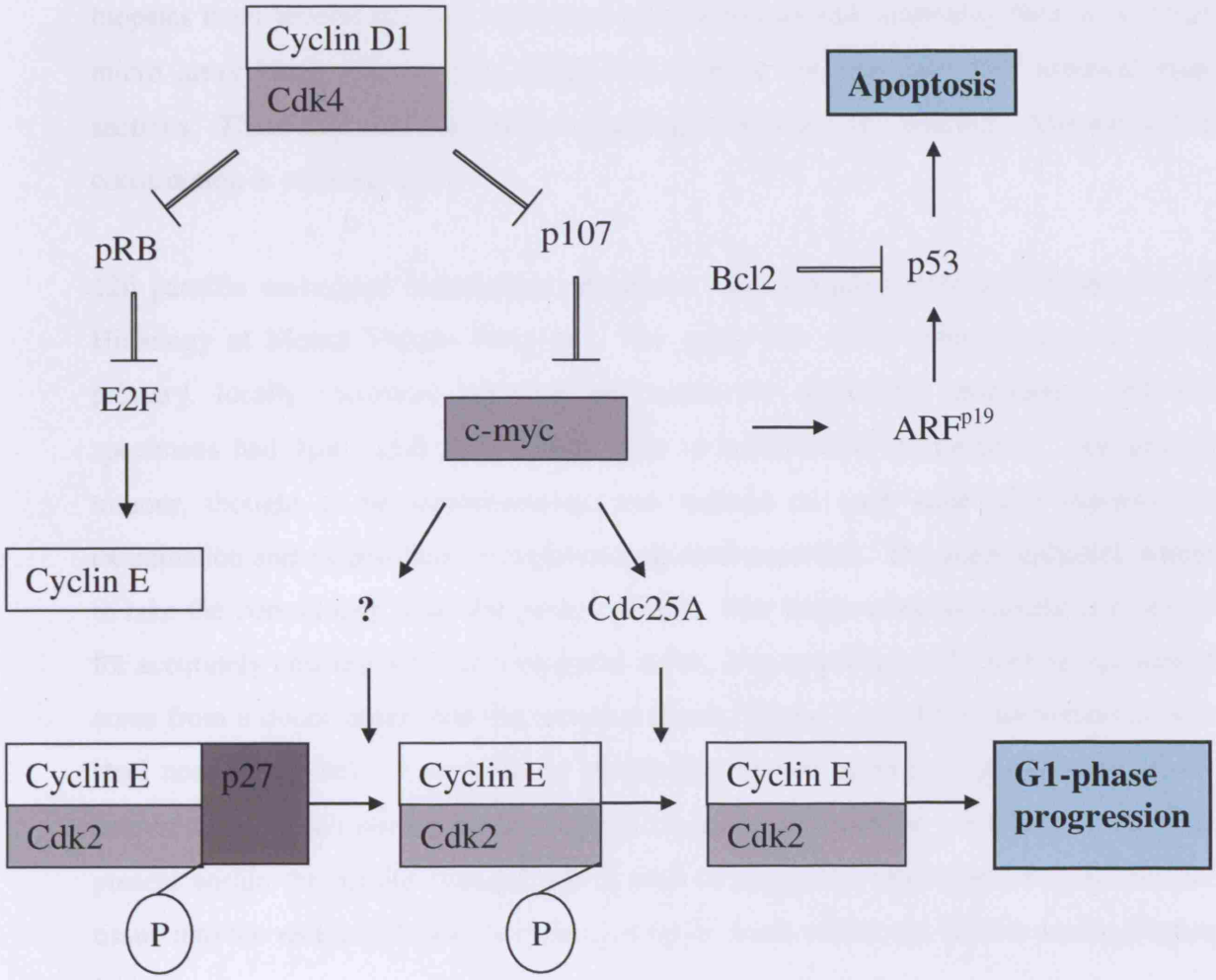

Figure 6.1 Summary of c-myc related pathways. Arrows indicate stimulation of proteins or processes. Blocked arrows demonstrate a suppression of the target protein.

6.2.1 Construction of the tissue array.

The tissue micro array is a tool for high throughput molecular analysis of hundreds of tissue specimens in a single experiment. It is constructed by obtaining cylindrical biopsies from several hundred individual tumour tissues and combining them in a single micro array block (Figure 6.2) which can then be cut into over 200 identical 4μm sections. These then undergo immunohistological staining and analysis. The method of construction is outlined below.

126 paraffin embedded histological specimens were obtained from the Department of Histology at Mount Vernon Hospital. The array was made from a series of naevi, primary, locally recurrent, regional and metastatic melanoma specimens. All the specimens had 4μm H&E slides made prior to construction of the array. An area of tumour, thought to be representative, was marked on each slide after microscopic examination and a consultant histopathologist confirmed this. The guide indicated where to take the core biopsy from the paraffin block. The tissue-array instrument is a device for accurately creating holes in a recipient block, then acquiring and inserting cylindrical cores from a donor block into the recipient block (Figure 6.2). Two thin-walled hollow steel needles are held in position by guides and ensure accurate x-y alignment to the nearest 1μm. Each needle has a different central core diameter. A thin wire stylet is present within the needle cylinder and is used to empty the tube contents or to transfer tissue into the recipient block by moving it up or down within the hollow needle (Figure 6.3).

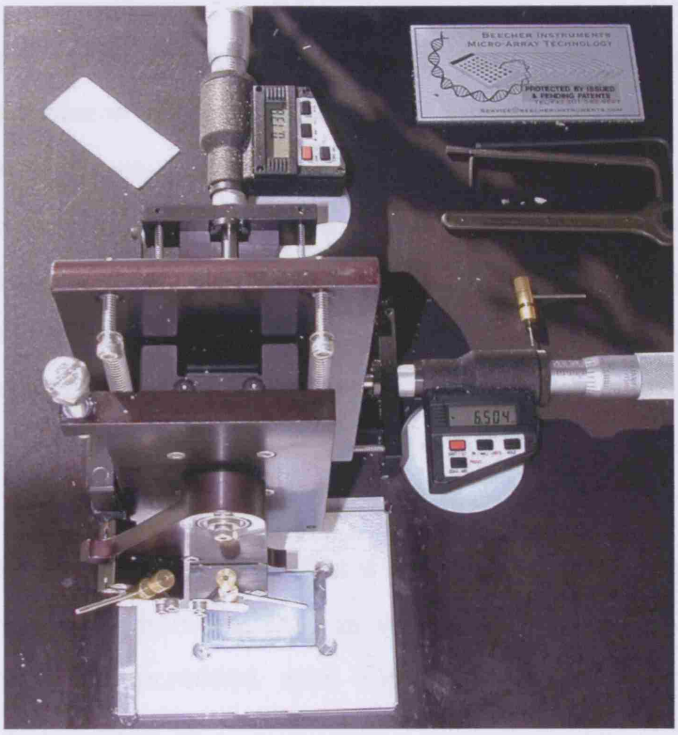

Figure 6.2 Photograph of the tissue micro array. The two micrometers can be seen above and to the right side of the instrument. The block is seen at the bottom of the photograph.

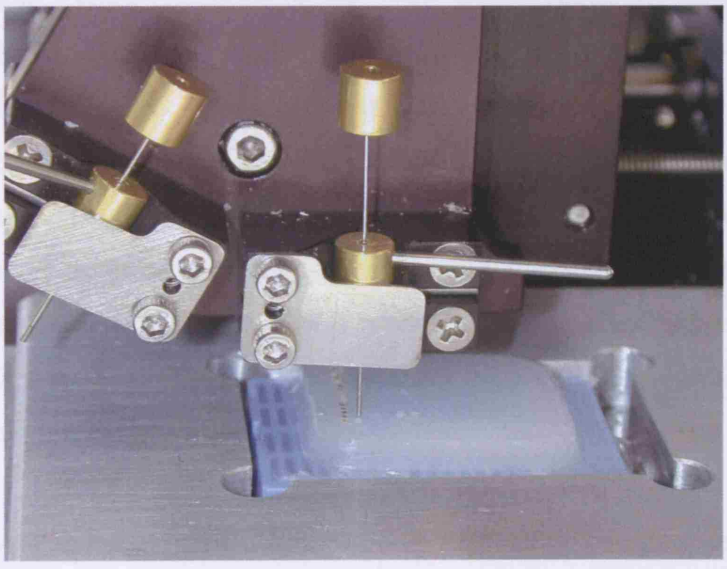

Figure 6.3 Photograph of tissue micro array needles. The thin (600μm) needle can be seen having just made a hole in the recipient block. The stylet has been raised to allow a core of paraffin to be removed. The needle-mount would then be rotated anti-clockwise and the thick (800μm) needle can then remove a core from a specimen.

The process began by preparing a hole in the recipient block using the thinner needle (600μm internal diameter) in a predetermined x-y position that would receive the specimen core. A representative sample core of tumour was then extracted by the thicker needle (800μm diameter) from the known area of tumour donor block. The cylindrical core of tumour was then pushed gently downwards out of the needle using the stylet until it fitted snugly into the previously prepared recipient hole. The core was slightly wider than the recipient hole ensuring that there was good contact and that the core was unlikely to fall out.

Following insertion of the core, the needles were moved an exact x-y distance (1000μm) to the next coordinate by micrometers. In this way, a large grid was accurately and rapidly constructed and permitted easy identification of each specimen core by coordinates (Figure 6.6 and 6.7)

Between two and four specimen cores were used per specimen depending on the amount of tissue available. High concordance has been shown between 3 sample cores (Hoos 2001) and therefore, wherever possible, at least 3 were used. A total of 464 cores were inserted in a 16 by 29 grid. A gap of 1mm was left between cores. Once all the cores were inserted, the paraffin block was gently heated to 40^0C until the specimen cores had bonded with the surrounding paraffin. A glass slide was then pressed down on top of the block to push cores down to correct depth and ensure the block was flat so cutting could take place. The position of each core was recorded onto an Excel work sheet at the time of insertion using numeric notation so that each core could be identified later during microscopic examination.

3μm sections were then cut using a conventional microtome and mounted on glass slides. No covering tape was used. H&E staining was performed on the first slide and examination by a consultant histopathologist confirmed the presence of tumour within each core. If there was no tumour present in the core then it was ignored in subsequent analysis. As three cores were used for each specimen there was a high chance that one of the representative cores would contain tumour.

Figure 6.4 The author constructing the micro array block

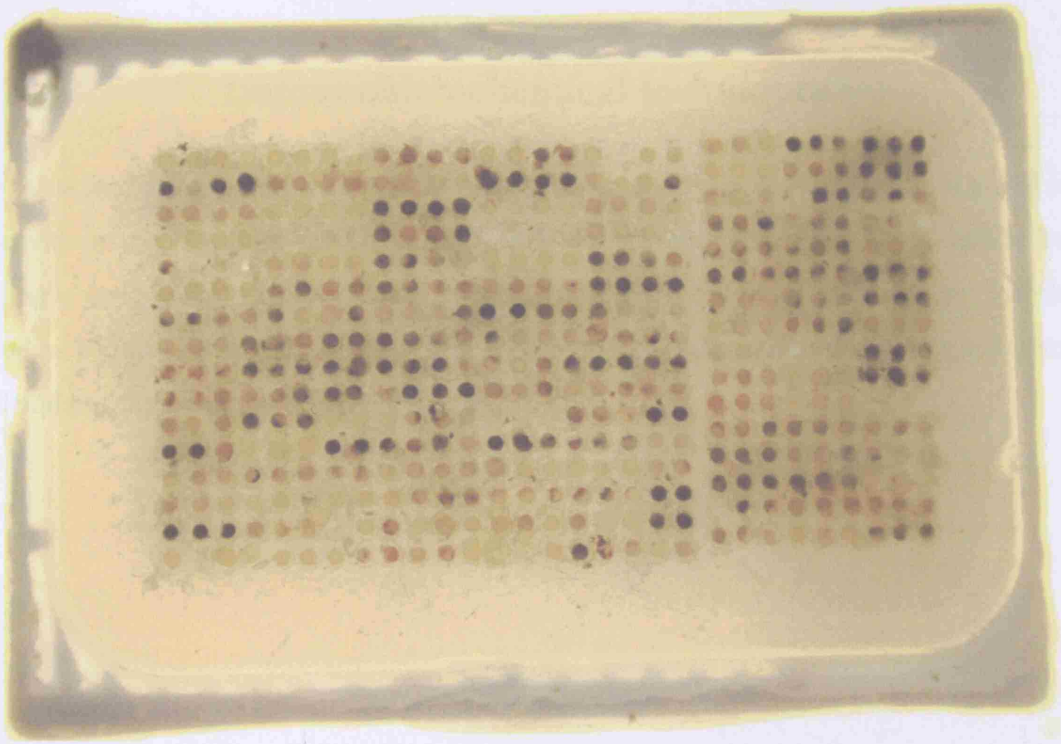

Figure 6.5 The photograph shows the construction of the final array block.

Further sections were then cut from the block and each one stained for an individual protein using immunohistochemistry. A range of proteins closely related to *c-myc* was assessed. Following staining, each section was examined under a light microscope. Firstly, each of the cores had the number of positively staining cells estimated as a percentage of total cells in the core. Secondly, the intensity of staining was estimated representing low or high intensity of staining of cells. Three of the oncogenes (bcl-2, cdc25A and cyclin A) had intensity scored for low, medium and high intensity of staining.

The score was recorded in an Excel spreadsheet for further analysis. Each of the three cores from each specimen was scored and then the average was calculated. The data was then analysed using JMP statistical software investigating the correlation between the different histological stages and gene expression.

The construction of the tissue array can been seen in Figure 6.4 and the final array paraffin block can be seen in Figure 6.5. The cut and mounted sections are shown in Figure 6.6 and 6.7.

6.2.2 Immunohistochemical techniques

Once the tissue array block had been made then immunohistochemical analysis could be performed on the sections taken from it. Staining was performed using antibodies targeting a variety of antigens closely related to *c-myc* and tumour progression. All the antibodies used were indicated for use in formalin-fixed, paraffin embedded specimens. The details of the antibodies are in Table 6.2 below.

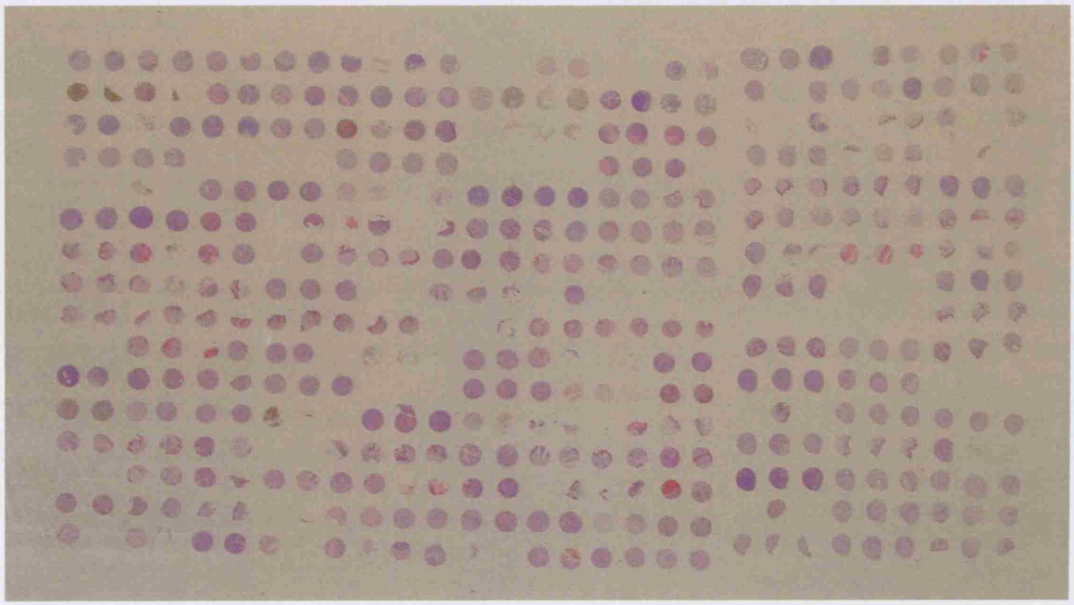

Figure 6.6 Photograph of a single slide of the micro array. Note some of the core specimens are missing.

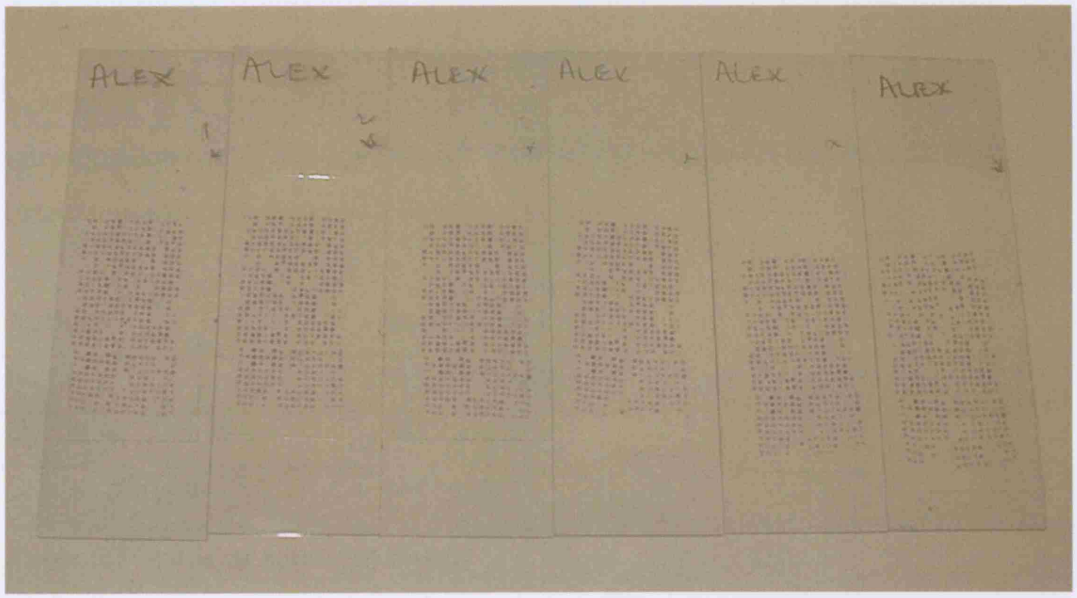

Figure 6.7 Photograph of 6 identical consecutive slides taken from the tissue array block.

Target Antigen	Manufacturer	Dilution used in (tris buffer saline)	Positive control	Area of cell stained
Cdc25A	Neomarkers	1:150	Tonsil	Nuclear
p27	Neomarkers	1:100	Tonsil	Nuclear
c-myc	Novacastra	1:50	Breast Carcinoma	Nuclear
Cyclin D1	Novacastra	1:100	Lymphoma	Nuclear
Cyclin A	Novacastra	1:100	Tonsil	Nuclear
Cyclin E	Novacastra	1:100	Placenta	Nuclear
p53	Dako	1:300	Breast Carcinoma	Nuclear
Bcl-2	Dako	1:300	Tonsil	Cytoplasmic

Table 6.2 Antibody staining information.

The histological preparation of the array slides was routine, using standard protocols as described below.

1 Heat mediated antigen retrieval was used for the array slides consisting of incubation in a microwave whilst bathed in 10mM citric acid. This step improves immunoreactivity of the specimen. Each antigen requires slightly different lengths of incubation and time to stand following microwave heating.

Antigen	Time in microwave	Time standing
Bcl-2	2x5 minutes	20 minutes
Cyclin A, D, E, p53	3x4 minutes	20 minutes
C-myc, p27, cdk25A	4x4 minutes	20 minutes

Table 6.3 Antigen retrieval times.

2 Following antigen retrieval the slides were washed in running tap water and transferred to the Dako Autostainer. The Autostainer performed a programmed sequence of staining:

3 5 minutes incubation in endogenous peroxidase block.

4 1 hour primary antibody incubation diluted to the above concentrations (see Table 6.2) in antibody dilutent (Dako). A negative control was created for each antigen using isotypic IgG on a separate control slide to ensure staining was genuine.

5 30 minutes incubation with a biotinylated link antibody, ChemMate secondary reagent (Dako)

6 30 minutes incubation with a streptavidin labelled with horseradish peroxidase, ChemMate tertiary reagent (Dako)

7 5 minutes incubation with Diaminobenzidine (DAB)

8 Slides were then removed from the Autostainer and counter stained with Mayers Haematoxylin (VWR International) for between 10 and 30 seconds followed by thorough washing in running tap water.

9 The slides were then dehydrated through graded alcohols followed by clearing in xylene.

10 Sections were then mounted in DPX (VWR International)

The protocol resulted in a positive brown stain on a blue background.

6.2.3 Clinical and Pathological data

The aim was to investigate the role of protein markers in melanoma by simultaneous analysis of multiple histological specimens. 126 historical specimens from melanomas diagnosed between 1990 and 1993 were collected from the department of histology at Mount Vernon Hospital to be prepared for the tissue array. For each sample the case notes were obtained and examined, collecting information regarding the clinical and pathological details of each patient. If no clinical information could be found the

histological specimens were not used in the array. Each set of case notes was examined for the following information outlined in Table 6.4.

Patients are routinely followed up in the clinic at least yearly for the first 10 years following the diagnosis of melanoma. The patients who had a benign naevus removed were only seen for one post-operative visit and therefore no survival data is available. It is presumed that they all survived.

Data gathered for each patient	Data gathered for each Tumour
Name	Date of Diagnosis
Hospital Number	Breslow thickness of the tumour
Date of birth	Histology Number
Age	Tumour stage – primary, secondary,
Sex	node, met, naevus
When the patient was last seen at clinic	Site
Date of death if appropriate	Growth pattern
	Clarke's level of invasion
	Presence of ulceration
	Mitotic Index
	Vascular invasion
	Lymphoid reaction
	Percentage c-myc positivity
	Date of recurrence/s

Table 6.4 Clinico-pathological data retrieval.

6.2.4 Statistical methods

Storage and analysis of data was performed on an IBM compatible personal computer. Initially, data were stored in an Excel spreadsheet package. Further statistical analysis was performed using JMP statistical software (JMP v4, SAS Institute). Statistics used for

examining correlation was the Spearman rank correlation coefficient as the data was expected to by non-parametric.

For each of the 126 specimens on the array block, 2, 3 or 4 cores had been taken from the original histological specimen. The number of cores used was determined by the size of the original lesion and also by how much tissue was left to remove. Small naevi usually only had enough for two cores where large metastatic deposits of melanoma provided plenty of tissue and 4 cores were taken to improve the representation of the tumour.

Every core in the array was visualised using a light microscope and scored in a semi-quantitative way for both intensity of staining or percentage positivity of cells. The array slides were examined and scored by the same investigator throughout the analysis. Each core was scored for the intensity of staining of the positive cells. Each group of cores for a given specimen had the average intensity calculated and also the maximum intensity of each group was also recorded out of the 2, 3 or 4 cores for each specimen.

Each of the specimen cores had the total number of cells counted in addition to the number of cells staining positive for each marker. Each group of specimens from one tumour had the average percentage of positive cells calculated to give an average positivity for each specimen and also a maximum positivity representing the tumour. So for intensity of staining and positivity of cells there was a mean figure calculated in addition to the maximum value. For further analysis of data these figures had to be converted into ordinal numbers and so each group was divided into two or three levels depending on the spread of the data. Positivity was divided around a figure of 50% into either high or low positivity. Intensity of staining was divided into three groups for cdc25A, bcl-2 and cyclin A, two groups for the other markers. This would allow the data to be reduced and aid simple analysis. Parametric and non-parametric analysis of the data was undertaken to estimate the correlation between the different oncogene levels and the clinicopathological parameters. Survival curves were also plotted for the different oncogenes and stage of disease. Significant correlations were considered if the p value was <0.05.

The tissue-array produces a large amount of data and the following section presents the most relevant and important findings.

6.3 Results

6.3.1 Clinicopathological data.

A total of 126 specimens were used in the array with a total of 464 cores. There were 22 benign naevi, 58 primary melanomas, 21 local skin recurrences, 23 nodal metastasis and 2 distant metastatic specimens. The mean age was 60 years with a range of 25 to 93 years. There were 93 female and 33 male patients included in the study population. 45 patients died during the follow up period that lasted for an average 64 months and up to a maximum of 144 months. The mean Breslow thickness was 2.29mm with a range from 0 to 8.5mm for the primary melanomas.

6.3.2 Protein correlations.

The ordinal maximum and average staining intensities were analysed using the using Pearson Chi-squared. The results can be seen in Tables 6.5 and 6.6. The results in bold are statistically significant correlations. The results indicate multiple strong correlations between various proteins. There are strong correlations between *c-myc* and cyclin A and E and bcl-2. There is no significant correlation between cdc25A and cyclin E.

The percentage positivity figures were analysed using Spearman's rank correlation. The results can be seen in Tables 6.7 and 6.8. The significant positive correlations are in bold. There are multiple correlations between several of the different proteins. There appears to be a strong link between bcl-2 positivity and cyclin D1, p27, c-myc and the cyclins A and E. p27 and p53 seem to be strongly correlated with each other and cyclin D1. Cyclin E and cyclin A are highly similar in expression levels. It is interesting to note the similarity of the two sets of correlations produced between the maximum positivity value and also the average positivity value. All the correlations reported were

noted to be positive. C-myc is related to cyclin E and there appears to be a strong relationship with bcl-2. However there was not any significant association with the positivity of other proteins. bcl-2 and myc are known to antagonise each other's growth inhibitory effects (Strasser, O'Connor et al. 1996) and synergise in cell transformation. This close relationship may be important in the formation and progression of melanoma by blocking apoptosis and altering signalling pathways.

	cyclin D1	p53	p27	c-myc	cyclin E	cyclin A	bcl-2
cdc25A	0.6175	**0.0009**	0.596	0.2135	0.6634	0.1651	**0.0145**
bcl-2	0.4331	0.1311	**0.0001**	**0.0154**	**0.0017**	0.9378	
cyclin A	**0.045**	**0.0174**	0.0781	**0.0023**	**0.0015**		
cyclin E	0.1209	**0.0013**	**0.0005**	**<0.0001**			
c-myc	0.9038	0.1084	0.0919				
p27	0.8494	0.2821					
p53	**0.0406**						

Table 6.5 The p-value for the significance of correlations between the average intensity of staining of each molecular marker. Significant values are shown in bold.

	cyclin D1	p53	p27	c-myc	cyclin E	cyclin A	bcl-2
cdc25A	0.2863	0.1022	**0.0393**	0.3089	0.3938	0.6492	**0.012**
bcl-2	0.0539	0.5989	**0.0052**	**0.0161**	**0.0062**	0.5435	
cyclin A	0.354	0.0547	0.2052	**0.0014**	**0.022**		
cyclin E	**<0.0001**	**0.0024**	0.1991	**0.0003**			
c-myc	**0.0024**	0.2252	0.7171				
p27	0.297	0.7035					
p53	0.0723						

Table 6.6 The p-value for the significance of correlations between the maximum intensity of staining of each molecular marker. Significant values are shown in bold.

	cyclin D1	p53	p27	c-myc	cyclin E	cyclin A	bcl-2
cdc25A positivity max	0.5509	0.4824	**0.0775**	-0.2225	-0.8335	-0.4289	0.7996
bcl-2 positivity max	**0.0074**	0.282	**0.0955**	**0.000002**	**0.0167**	**0.0031**	
cyclin A positivity max	**0.0001**	**0.0017**	0.2249	**0.0009**	**<0.0001**		
cyclin E positivity max	0.0759	**0.00004**	0.0704	0.3607			
c-myc positivity max	0.0593	0.4928	-0.9594				
p27 positivity max	**0.0002**	**0.0098**					
p53 positivity max	**0.0016**						

Table 6.7 The p-value for the Spearman's rank correlation of the maximum percentage positivity for each molecular marker. Significant values are shown in bold.

	cyclin D1	p53	p27	c-myc	cyclin E	cyclin A	bcl-2
cdc25A positivity av	0.0941	0.6467	0.1328	-0.5331	-0.4337	-0.1404	0.1897
bcl-2 positivity av	**0.0181**	**0.0819**	**0.0129**	**0.00006**	**0.0422**	**0.0138**	
cyclin A positivity ave	**0.0069**	**0.0015**	0.3432	**0.0062**	**<0.0001**		
cyclin E positivity ave	0.2096	**0.0001**	0.1718	0.3870			
C-myc positivity ave	0.2228	0.6566	0.8158				
p27 positivity ave	**0.0006**	**0.0084**					
p53 positivity ave	**0.0024**						

Table 6.8 The p-value for the Spearman's rank correlation of the average percentage positivity for each molecular marker. Significant values are shown in bold.

6.3.5 Correlation with disease progression

Malignant transformation is a process in which several key genes become abnormally expressed as the cell mutates from normal cellular behaviour to one of uncontrolled growth and replication. Many genes have been implicated in this process and demonstrated to be important in both the genesis and progression of neoplastic disease. Progression markers change in expression as the disease progresses through the different stages of neoplastic development. The tissue array is an ideal tool for looking at changes in protein expression as melanoma reaches distinct biological stages. By dividing up the melanoma specimens into naevi, primary melanomas, local recurrence and distant recurrence it was possible to determine any differences in protein expression. Further analysis was also undertaken with the stage grouped into either primary or secondary disease.

The results can be seen in Figures 6.8 to 6.15 below.

Each of the markers studied was analysed for the percentage of positive cells at each stage of tumour progression. The results can be seen in the graphs below and represent the average percentage of cells at each stage expressing each protein. As the tumour stage advances there is an increase in the number of cells expressing the cyclins A, E, D1 and also c-myc. There is a fall in the expression of p27 and cdc25A with increasing tumour stage and it is also seen with p53 and bcl-2. This observation confirms that as the melanoma progresses it continues to lose cell cycle coordination as more cyclins are expressed that drive the cell cycle and the genes that regulate entry into the cycle are lost. The data would be consistent with an increase in cell proliferation seen in the advanced stages of disease.

There are two patterns of expression in the tumour that can be seen in the percentage positivity of cells. Several of the cyclins have low positivity in benign naevi but then increase significantly in the neoplastic stages of disease. This pattern can be seen for cyclin A, E and D1. The second pattern is a gradual and progressive change in the

number of cells expressing proteins as the tumour progresses. Both c-myc and p27 demonstrate this pattern of expression. c-myc increases in positivity as melanoma progresses with naevi having the lowest expression and recurrent disease the highest number of positive cells. The regulatory gene, p27, has the opposite pattern. This would be consistent with the loss of cell cycle regulation, as the biological stage of the tumour becomes more aggressive. These two patterns of gene expression may be able to help the clinician. Firstly, the cyclin expression levels may help diagnosis in difficult histological specimens. Low cyclin positivity would indicate a benign lesion and a high percentage of cells expressing the protein would tend towards a more sinister lesion. Both p27 and c-myc change in positivity as the disease progresses, albeit in opposite directions. The positivity of cells for these two proteins may indicate a prognostic significance and this will be investigated later in the chapter.

bcl-2, p53 and cdc25A reveal trends that are difficult to interpret but show a trend of lower positivity corresponding to advancing tumour stage. Primary melanoma however, appears to break the trend in each case. The ordinal assessment for intensity of staining and positivity are shown in Figures 6.16 and 6.17.

Figur 6.16 represents the percentage of tumours that have either lower than 50% of cells being positive (red bar) or greater than 50% positivity on the (blue bar). Changes in positivity of the markers can be seen across the tumour stages.

Figure 6.17 has a y axis of percentage of tumours falling into each category of either low or high intensity of staining. The x axis groups each tumour stage. The lower red bars represent the number of tumours with low intensity of staining and the upper blue bars represents the percentage of tumours with high intensity of staining. Green represents high staining of those tumours divided into low, medium or high staining.

The progression seen in average positivity by c-myc in Figure 6.10 is not repeated in the ordinal positivity in Figure 6.16. This is due to the second graph being ordinal data divided either side of the 50% level in positivity.

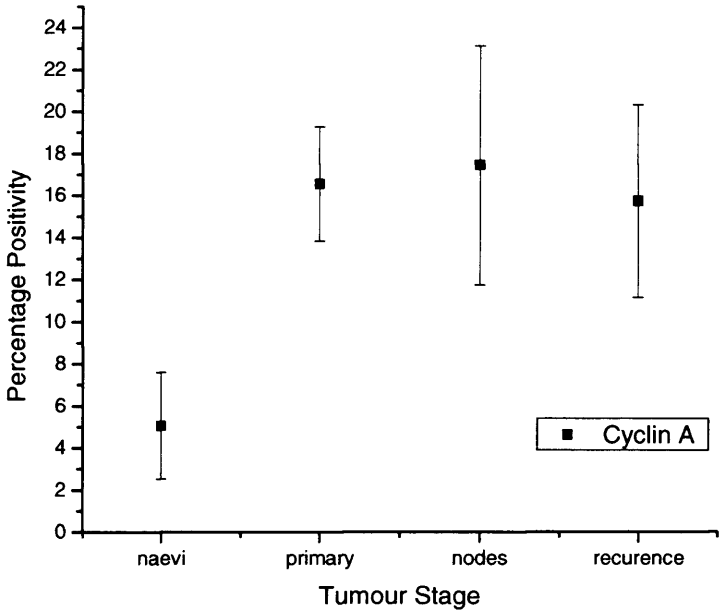

Figure 6.8 Graph to show the average number of cells positively expressing cyclin A for each tumour stage. Error bars represent standard error of the mean.

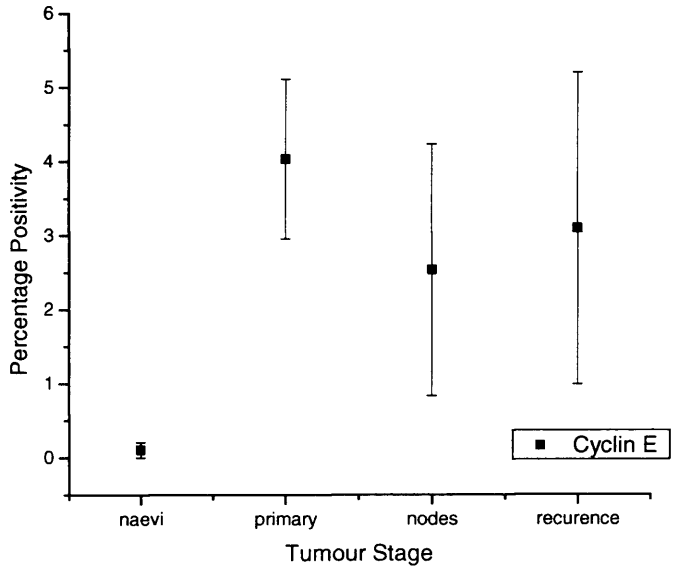

Figure 6.9 Graph to show the average number of cells positively expressing cyclin E for each tumour stage. Error bars represent standard error of the mean.

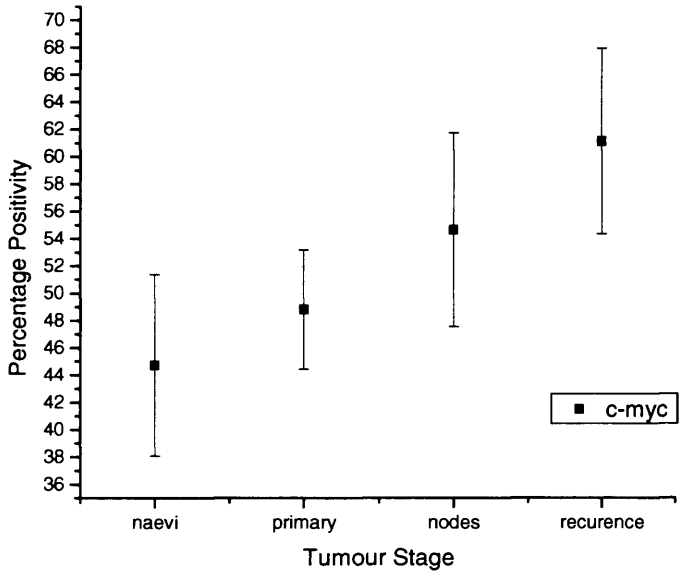

Figure 6.10 Graph to show the average number of cells positively expressing c-myc for each tumour stage. Error bars represent standard error of the mean.

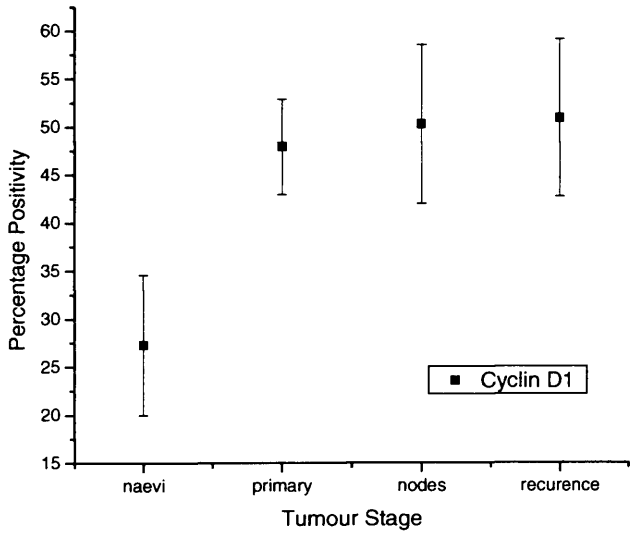

Figure 6.11 Graph to show the average number of cells positively expressing cyclin D1 for each tumour stage. Error bars represent standard error of the mean.

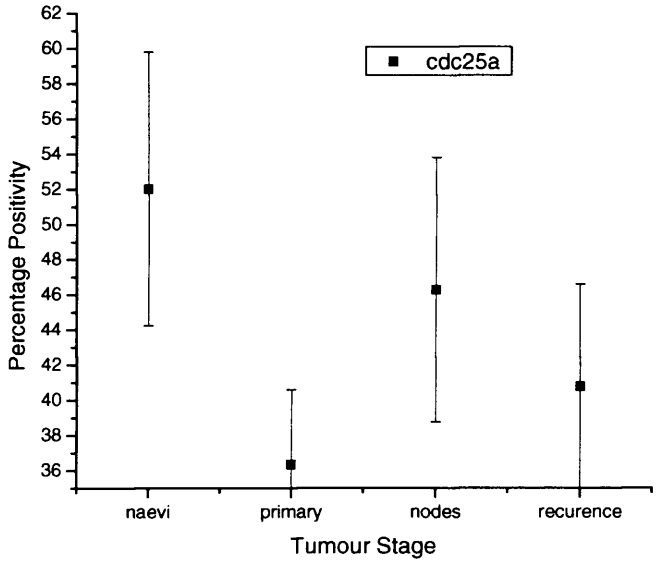

Figure 6.12 Graph to show the average number of cells positively expressing cdc25a for each tumour stage. Error bars represent standard error of the mean.

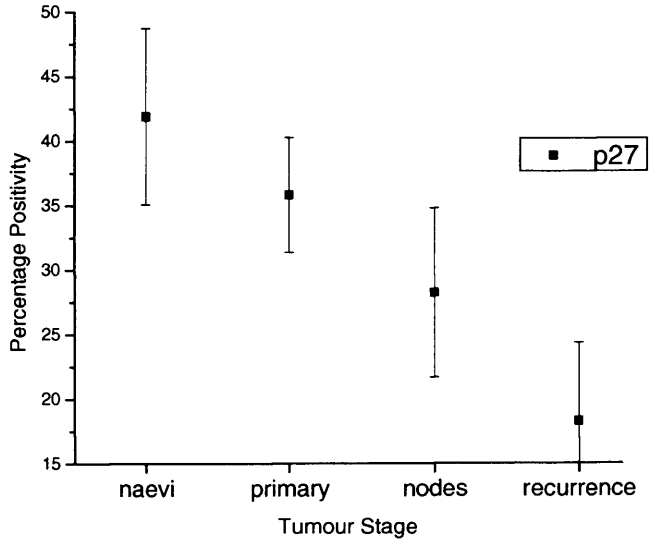

Figure 6.13 Graph to show the average number of cells positively expressing p27 for each tumour stage. Error bars represent standard error of the mean.

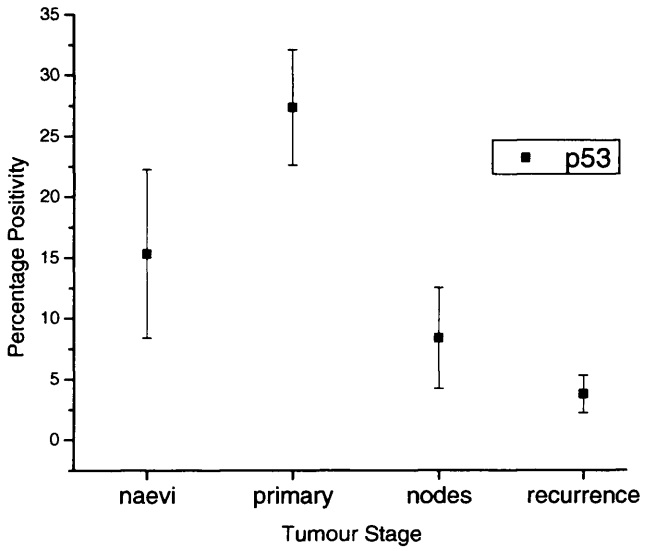

Figure 6.14 Graph to show the average number of cells positively expressing p53 for each tumour stage. Error bars represent standard error of the mean.

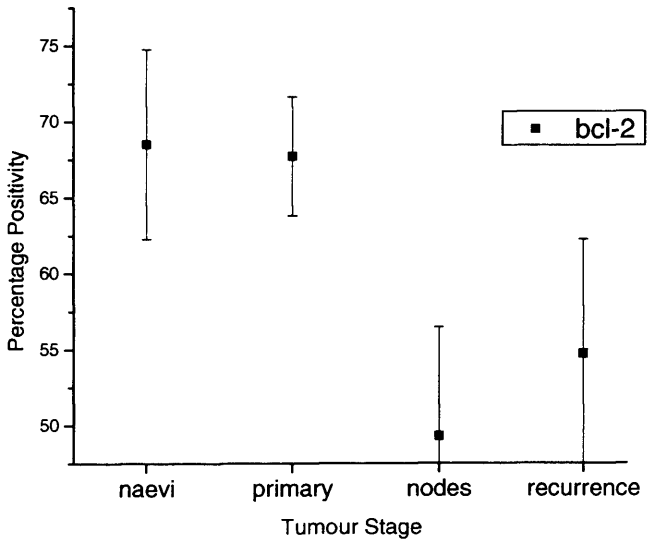

Figure 6.15 Graph to show the average number of cells positively expressing bcl-2 for each tumour stage. Error bars represent standard error of the mean.

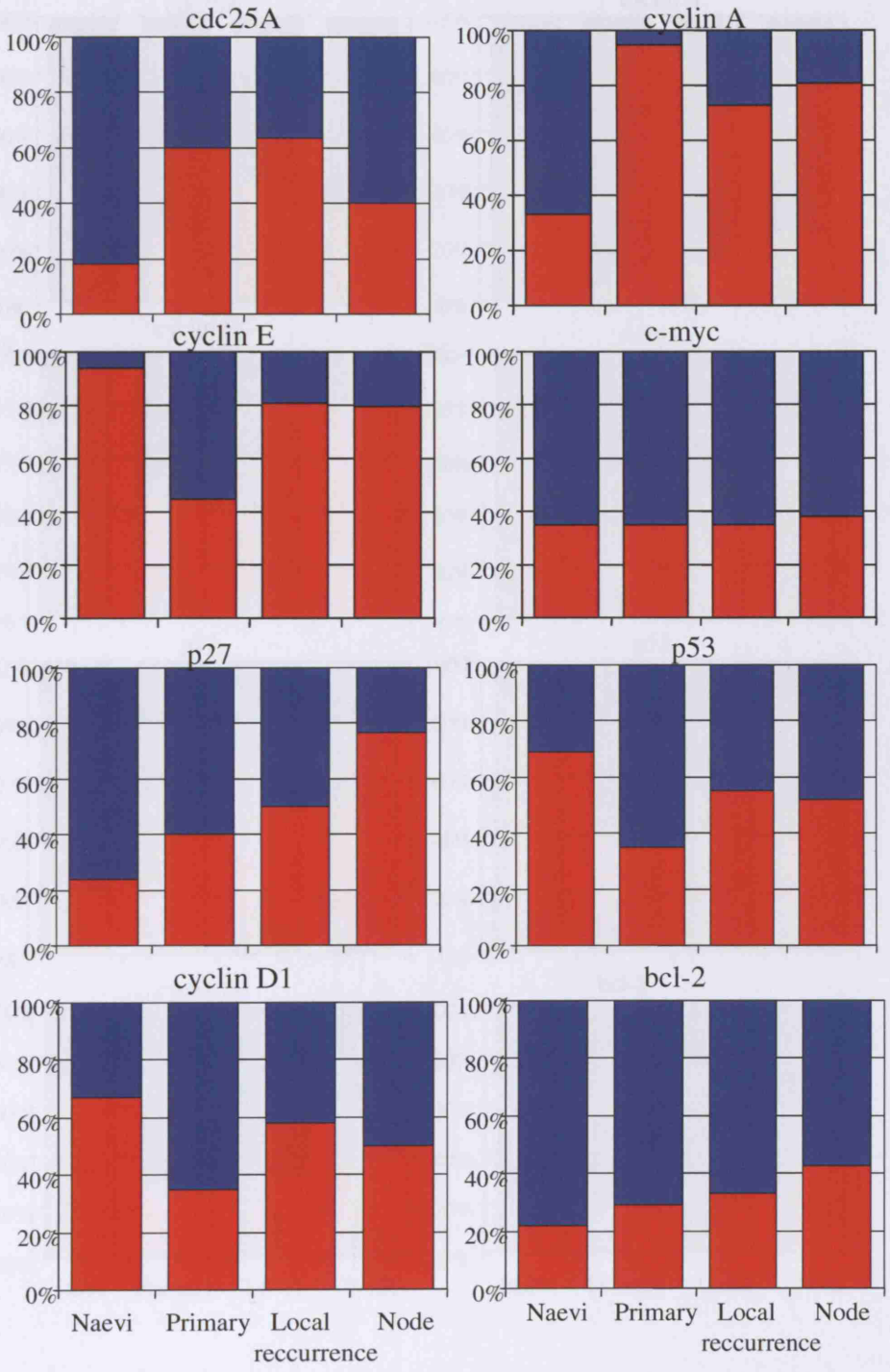

Figure 6.16 Graphs to show the proportions of positive and negative tumours for expression of each marker. The red bars represent the percentage of tumours that were negative for each marker the blue those that were positive.

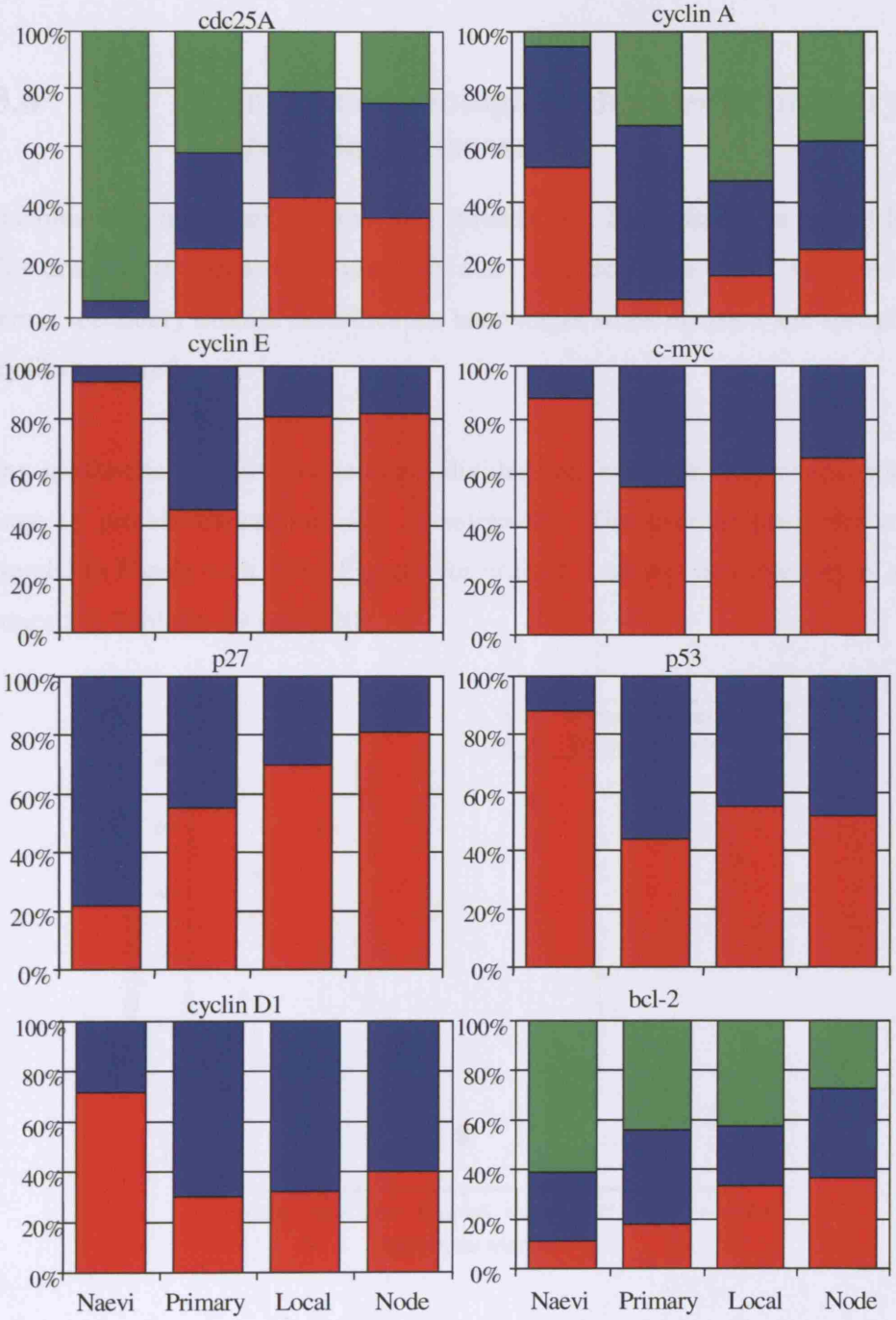

Figure 6.17 Graphs show the proportions of specimens demonstrating high or low intensity of staining for each tumour stage. The red bars represent low intensity of staining and the blue bars high. Green bars represent high levels when tumours were scored into three groups ie low, medium or high.

6.3.6 Immunohistological changes in primary and secondary disease.

Melanoma is a malignant tumour and spreads into local tissues or to the local lymph nodes draining the area of tumour. Primary disease is the initial localized melanoma whereas secondary disease describes the later stages when invasion and spread around the body has occurred.

Using specimens from the tissue array, divided into either primary or secondary disease, change in protein expression was investigated. The average positivity readings are presented in Figure 6.18. The Figures for ordinal positivity and intensity of staining are produced in Tables 6.19 and 6.20.

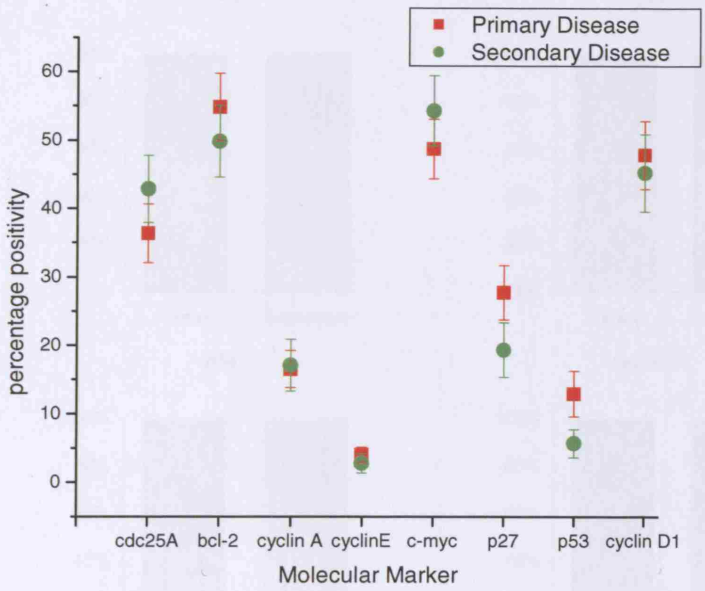

Figure 6.18 Graph to show the percentage of positive cells for each marker in primary and secondary disease. The error bars represent the standard error of the mean.

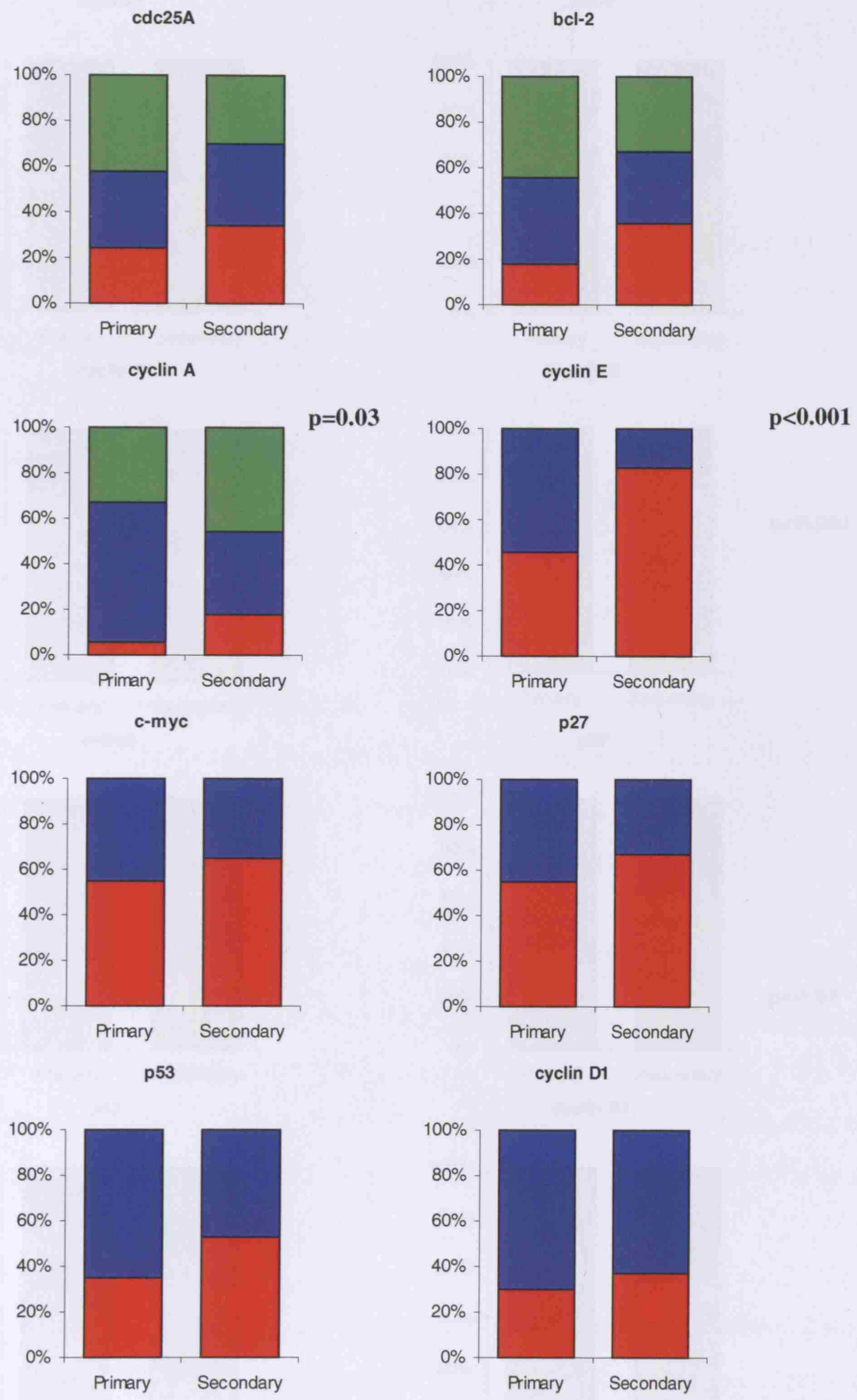

Figure 6.19 Graphs show the proportions of specimens demonstrating high or low intensity of staining for each tumour stage. The red bars represent low intensity of staining and the blue bars high. Green bars represent high levels when tumours were scored into three groups ie low, medium or high.

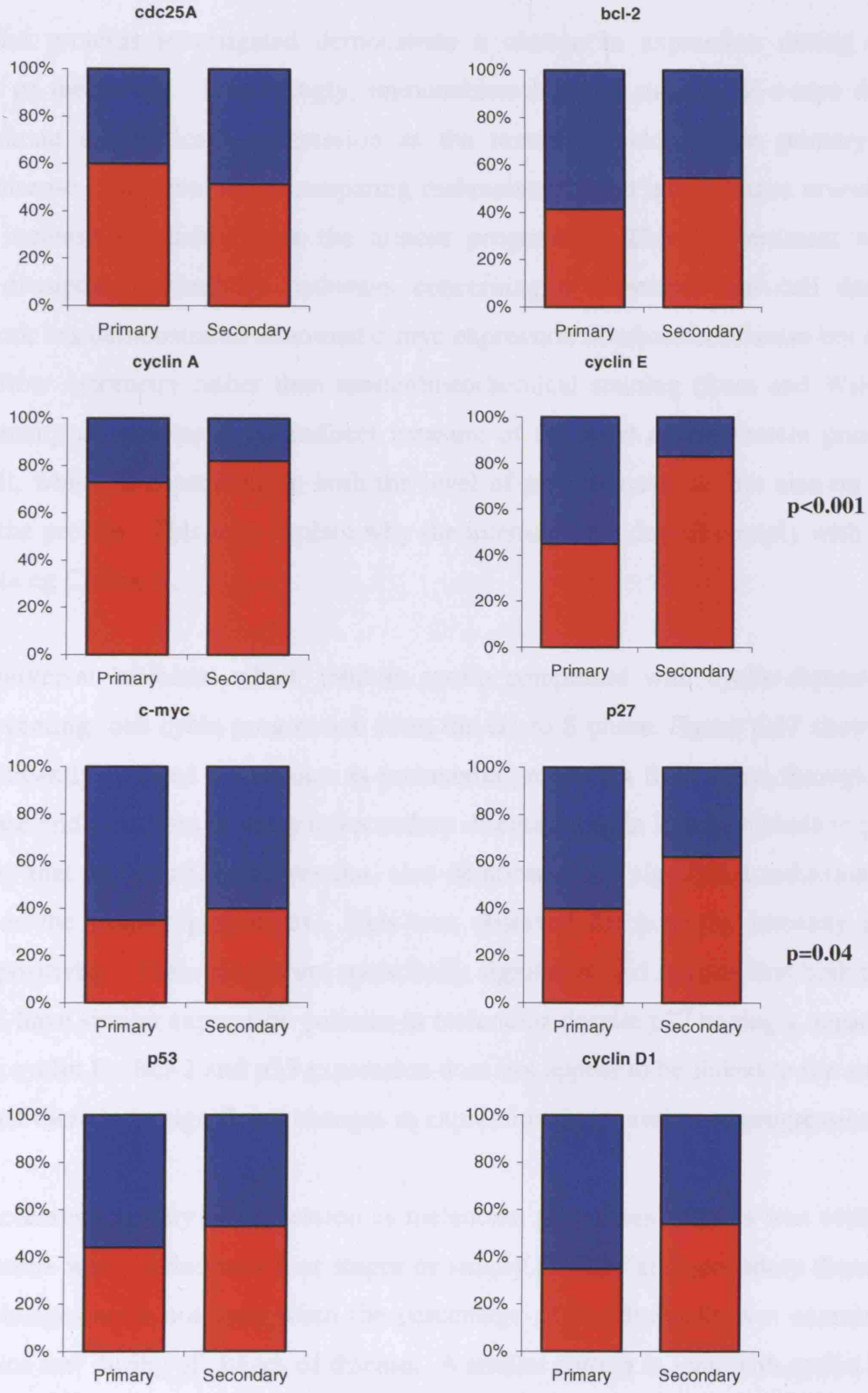

Figure 6.20 Graphs to show the proportions of positive and negative tumours for expression of each marker in primary and secondary disease. The red bars represent the percentage of tumours that were negative for each marker the blue those that were positive.

Many of the proteins investigated demonstrate a change in expression during the progression of melanoma. Interestingly, immunohistochemical staining of c-myc does not demonstrate a significant progression as the tumour develops from primary to secondary disease. However, data comparing melanoma divided into 4 stages reveals a significant increase in positivity as the tumour progresses. This is consistent with increasing disruption to cellular pathways concerning proliferation and cell death. Previous work has demonstrated abnormal c-myc expression in advanced disease but this was using flow cytometry rather than immunhistochemical staining (Ross and Wilson 1998). Intensity of staining is an indirect measure of the level of the protein present within a cell, which is dependent on both the level of protein synthesis but also on the half life of the protein. This may explain why the intensity data doesn't comply with the postivity data eg Cyclin A.

p27 is a 'universal inhibitor' which inhibits cyclin complexes with cyclin-dependent kinases, preventing cell cycle progression from the G1 to S-phase. Figure 6.17 shows a highly significantly reduced expression as melanoma progresses from naevi through to distant disease and also from primary to secondary disease. Cyclin E, which binds to p27 in a pathway that leads to G1 progression, also demonstrates a significant reduction in expression as the tumour progresses. This was observed for both the intensity and percentage positivity. These results are statistically significant and suggest that both p27 and cyclin E have similar expression patterns in melanoma despite p27 having a negative feedback on cyclin E. Bcl-2 and p53 expression does not appear to be linked to the stage of disease and there is no significant changes in expression that correlate to progression.

Cyclin A increases intensity of expression as melanoma progresses and this was evident when melanoma was divided into four stages or simply primary and secondary disease. The same changes were not seen when the percentage of positive cells was examined which remains low during all stages of disease. A similar pattern is seen with cyclin D1 expression where intensity appears to be more significant than the percentage of cells that are expressing the gene.

Proliferation and cell death need to be balanced and controlled in normal tissue and this is achieved through integration of signalling pathways that regulate these processes. Abnormalities within these two systems can lead to a synergistic effect on cell transformation to the malignant phenotype. Increased cell cycling because of c-myc expression combined with reduced apoptosis, due to bcl-2 deregulation, have been shown to cooperate in tumourigenesis in mammary glands (Jager, Herzer et al. 1997). Links between cell division and apoptosis pathways exist with cell cycle regulators playing critical roles in apoptosis and some members of the bcl-2 family affecting entry into the cell cycle (King and Cidlowski 1998). However, in this study there was no significant progression in either c-myc or bcl-2 expression with disease stage except for the average positivity values. The average number of cells expressing both markers increased significantly with disease stage suggesting greater deregulation of cell cycle and apoptosis. *c-myc* and other transcriptional regulators are not essential for cell death but trigger apoptosis via the p53 pathway. Conversely, DNA damage causes p53 inhibition of cyclin dependent kinases via induction of p21 leading to cell cycle arrest. bcl-2 and its homologues inhibit apoptosis but surprisingly their overexpression delays entry into the cell cycle and promotes exit from the cycle (Mazel, Burtrum et al. 1996). The lower proliferative capacity of lymphomas that have high levels of bcl-2 indicate that this effect can be physiologically relevant (Winter, Andersen et al. 1998). The positivity of tumours for p53 fell with disease stage, allowing apoptotic pathways to fail and therefore reducing cell death but also stopping any block on entry into the cell cycle. Many links have been discovered between cell death and the cell cycle and may help to explain why bcl-2 and *c-myc* in combination promote tumourigenesis. Both oncogenes antagonise each other's growth inhibitory effects and so act in a synergistic manner.

p53 is known as the 'guardian of the genome' because it prevents accumulation of errors in DNA by guiding damaged cells to apoptosis. When this function is lost, neoplastic cells fail to enter apoptosis following DNA damage leading to both resistance to antineoplastic therapy and the further accumulation of DNA mutations. These effects are important in radioresistance of tumours. p53 plays a role both at the G1/S and the G2/M checkpoint indicating a function in control of the cell cycle.

Over-expression of *c-myc* has an inhibitory effect on p53 and cyclin D1 yet has a positive effect on cyclin A and E. It therefore overrides the negative effect of p53 on the cell cycle and produces a strong mitogenic effect, paradoxically leading to cell death. However, this can be counteracted by the concomitant overexpression of the apoptosis protection gene, bcl-2. This complex relationship between p53, bcl-2 and c-myc manifests in control of both the cell cycle and apoptotic pathways. The tissue array data reveals that p53 expression falls with disease progression, therefore allowing further DNA mutation and deregulation of central cellular pathways. Normally p53 expression is associated with a poor prognosis in many tumours but melanoma seems have the opposite effect mainly through modified function of wtp53 tumour suppressor gene. Interestingly bcl-2 expression also falls with advancement of disease but is highly expressed in primary melanoma but is reduced at later stages of the disease. It's anti-apoptotic effects may be needed at an early stage in tumourigensis but as increasing DNA mutation is produced this may become less critical.

6.3.7 Survival Analysis

One of the aims of the tissue array was to use high throughput analysis to investigate the role of molecular markers in predicting survival. Prognostic indicators are important for both treatment selection and informing the patient as to the likely outcome of disease. They are also logical targets for gene therapy as they are thought to often play a critical role in tumour progression. Each of the proteins investigated using the tissue array was correlated with survival of the patient. The time to death from the first diagnosis of the disease was correlated with both oncogene positivity and intensity of expression scores. Each specimen was divided into high or low scoring groups for each oncogene tested and Kaplan-Meier survival curves were constructed using JMP statistical software. The statistical significance for each gene was then calculated. Survival curves were plotted for each gene and examples can be seen in Figure 6.21 and 6.22.

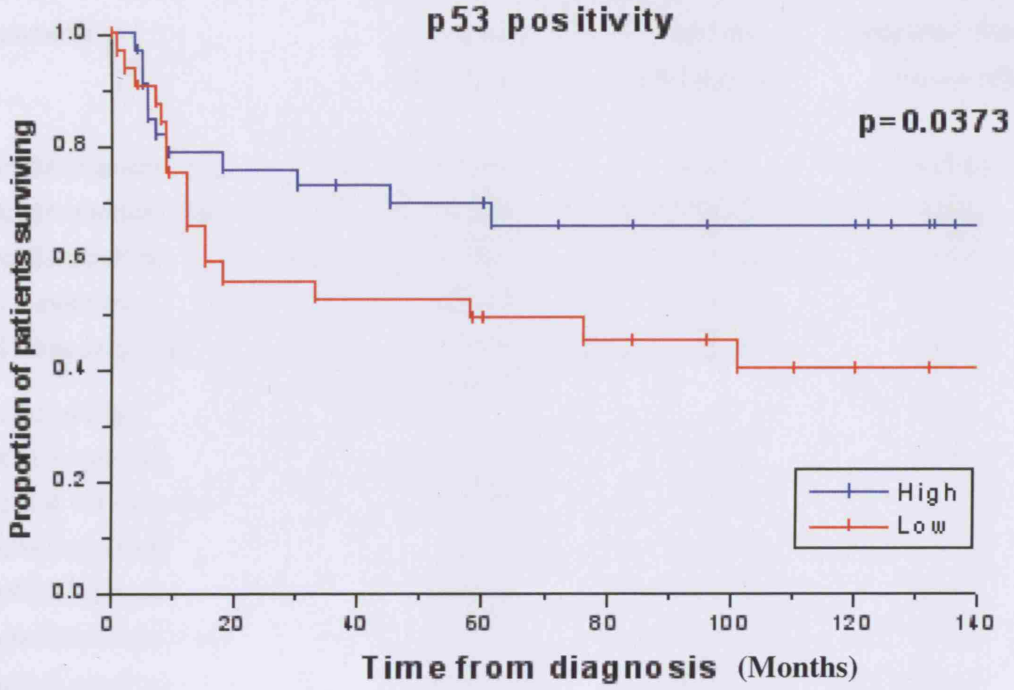

Figure 6.21 Survival of patients grouped for p53 oncogene positivity

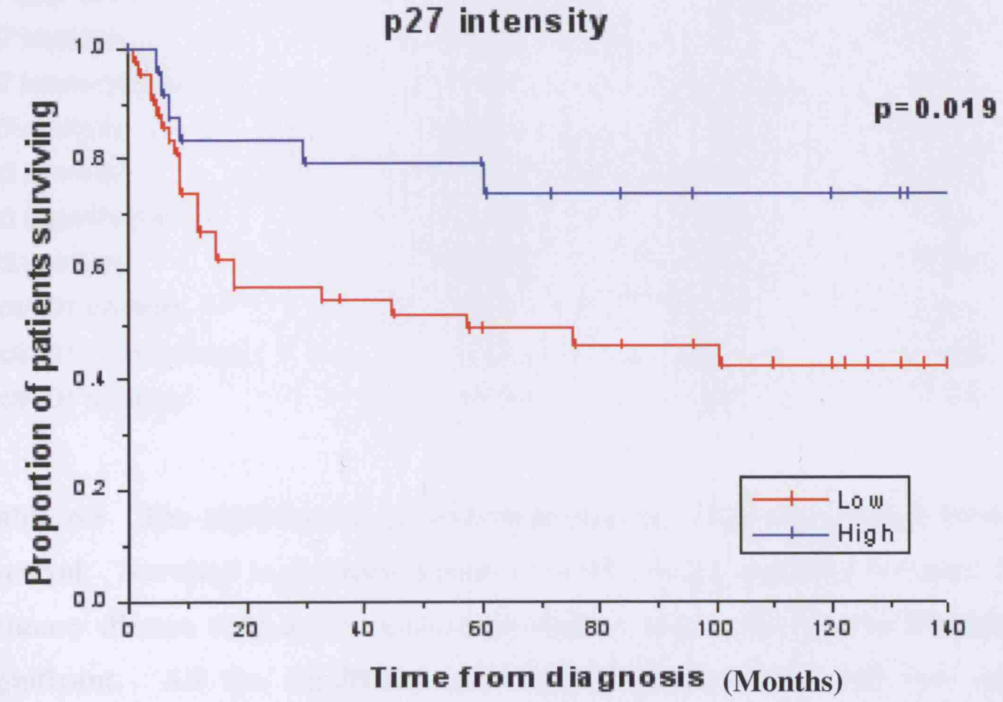

Figure 6.22 Survival of patients grouped for p27 oncogene staining intensity.

Parameter	Overall survival for all groups (Ki squared)	Survival for primary disease (Ki squared)	Survival for metastatic disease (Ki squared)
cdc25A intensity	0.5567	0.542	0.8248
cdc25A intensity max	0.463	0.0973	0.206
cdc25A positivty	0.3101	0.4241	0.8665
bcl 2 intensity	0.3116	0.4529	0.8873
bcl 2 intensity max	0.124	0.1815	0.6889
bcl 2 positivity	0.7325	0.497	0.995
cyclin A intensity	0.084	0.8483	0.6953
cyclin A intensity max	**0.0167**	0.7923	0.5
cyclin A positivity	0.537	0.2087	0.4179
cyclin E intensity	**0.0329**	0.6413	0.6601
cyclin E intensity max	0.0595	0.0747	0.5686
cyclin E positivity	**0.0318**	0.6413	0.6601
c-myc intensity	0.4779	0.8266	0.8436
c-myc intensity max	0.6295	0.8399	0.5493
c-myc positivity	0.5604	0.7752	0.531
p27 intensity	**0.019**	0.3169	0.0937
p27 intensity max	0.0919	0.2283	0.2098
p27 positivity	0.3961	0.8396	0.91
p53 intensity	0.1325	0.4322	0.2323
p53 intensity max	0.3174	0.7241	0.4875
p53 positivity	**0.0373**	0.4876	0.2873
cyclin D1 intensity	0.4672	0.3544	0.7542
cyclin D1 intensity max	0.104	0.2819	0.7804
cyclin D1 positivity	0.4619	0.941	0.5102

Table 6.9 The significance of molecular marker expression when compared to survival. Survival is grouped either with all groups together (column 2) or for primary disease only or for metastatic disease only. The figures highlighted are significant. All the significant associations demonstrated that low expression correlated with a worse prognosis. Both intensity and positivity values are average values for each specimen converted to ordinal values.

The survival analysis reveals that the majority of the proteins tested have little prognostic significance. However cyclin A and E are both significant as are p27 and p53 when overall survival is examined. Interestingly, for each of the significant markers, low expression is associated with a worse survival. Intuitively, high oncogene expression would be expected to drive the cell into G1 and increase the aggressive nature of melanoma and therefore reduce survival. That low expression in these particular oncogenes is associated with a reduced patient survival is an interesting finding. Previous work has shown high cyclin E expression to be associated with high p27 in primary invasive melanomas and be linked to a worse prognosis (Bales, Dietrich et al. 1999) but this is the opposite of the correlation presented in this thesis that low cyclin E corresponds to a worse prognosis. However, immunohistochemical studies of p27 expression have shown an inverse correlation with Breslow thickness in melanoma with high expression being associated with early stages of disease but p27 had no effect on prognosis (Florenes, Maelandsmo et al. 1998). Cyclin D1 has not been shown to demonstrate significant prognostic value for either disease free or overall survival unlike cyclin D3 which was prognostic for superficial melanomas (Florenes, Faye et al. 2000). The published evidence on the role of cyclin A in melanoma is inconclusive. Correlations with Breslow thickness and survival in invasive melanomas have been reported by Tran and corroborated in later studies by Florenes in superfical spreading, but not nodular, melanomas (Tran, Ross et al. 1998; Florenes, Maelandsmo et al. 2001). The data from the tissue array appears to support an important role for cyclin A but a low expression is correlated with worse prognosis. High nuclear p53 expression has been associated with disease progression using immunhistochemistry in a small study (Loggini, Rinaldi et al. 2001) but the tissue array demonstrated a significant relationship between low expression and a worse prognosis. Correlations with survival from the tissue array are for all histological tumour types grouped as one. There were only a total of 58 primary tumours included in the array and this doesn't provide sufficient numbers to allow further subdivisions of the histological subtypes.

When the melanomas were treated as either primary disease or metastatic disease alone then none of the genes tested had any significant prognostic value. To be useful as prognostic indicators, oncogenes need to be significant predictors of outcome, early in the disease process, ie primary disease. Management of the patient can be altered and survival improved either by more aggressive surgery, adjuvant chemotherapy or potentially targeting known oncogenes using gene therapy strategies.

6.4 Combining molecular markers

The tissue array provides the ideal setting to study combinations of molecular markers that may delineate a biological phenotype or define an improved prognostic index. In this section, a series of phenotypes and prognostic groups were investigated by combining the markers on the basis of biological insight or individual prognostic significance. Caution must be applied to the interpretation of the data, as clinical outcome was available for only 75 primary and metastatic tumours and within these patients not all markers were successfully scored due to missing or inadequate cores. Dividing these patients into smaller subgroups will reduce the statistical power and reliability of the analysis. However, the analysis was undertaken to show the potential of the tissue array and to guide future development of an improved melanoma tissue array.

The interplay between p53 and bcl-2 has been the subject of study in several different groups of tumours. In this group of patients, 28 had a high bcl-2 and p53 positivity score. Within this subgroup, each of the other molecular markers was studied for correlation with clinical outcome. Only p27 positivity ($p=0.041$) and intensity ($p=0.077$) showed any influence on clinical outcome where, again, high expression was associated with better outcome. Notably, c-myc lacked any influence in this phenotype. A second phenotype was defined, which consisted of high bcl-2 expression and low p53 positivity and consisted of 23 patients. Again, none of the markers, with the exception of p27, provided any clinical significance in this phenotype. Although the data for p27 did not quite reach statistical significance, it suggests that this protein has prognostic significance irrespective of p53 and bcl-2 status.

As c-myc is an important regulator of p27 and an inverse relationship was observed with progressing tumour stage (see Fig 6.10 & 6.13), the patients were subdivided according to these two markers. The best prognostic group was presumed to be the high p27/low c-myc tumours and the worst was the low p27/high c-myc expressors. Univariate analysis failed to reveal any significance of subgroups based on expression of these two proteins.

An alternative strategy was explored in which individual markers that showed some clinical significance but may not be directly related biologically were combined. Of these, the combination of both a high p27 and p53 expression was found to confer further prognostic power. Twenty of 66 patients presented these characteristics and their 5-year survival rate was 80.0% compared to 51.5% in the other tumours (p=0.0133). The relationship held for both primary (86.7 vs 65.5%) and secondary disease (60.0 vs 31.6%), but these did not reach statistical significance. This may be due to small sample size or it might not have significance. Other analyses were performed but none succeeded in providing prognostic information.

Chapter 7

An investigation of c-myc oncoprotein expression in cutaneous melanoma.

7.1 Introduction

Malignant melanoma is a heterogenous disease with large variability in clinical outcome, which provides the clinician with a difficult dilemma in evaluating the prognosis for individual patients. A number of clinicopathological parameters have been evaluated in primary melanoma as prognostic markers (Balch, Soong et al. 2001). The thickness of the primary tumour remains the most important prognostic determinant. However, there is a significant number of tumours whose behaviour is different from that expected from the Breslow thickness measure. Some thin lesions metastasize and some thick lesions don't. There is an ongoing search for markers that can predict those patients who have a greater likelihood to develop metastasis so existing or experimental treatments can be given to those who would benefit most. Greater understanding of tumour biology will help to establish new prognostic markers that allow increasingly accurate and individual predictions of tumour progression. Elucidating gene involvement in tumour behaviour can lead to the discovery of novel markers. One of the earliest events in melanoma progression involves the dysregulation of cell cycle control and apoptosis leading to a net increase in melanocytes (Albino 1997). Previous work based at Mount Vernon Hospital has demonstrated *c-myc* to be an important prognostic marker in melanoma based on retrospective studies of histological specimens (Grover, Grobbelaar et al. 1997; Grover, Ross et al. 1997; Chana, Grover et al. 1998; Grover, Chana et al. 1999; Chana, Grover et al. 2001). Breslow thickness has remained the most accurate prognostic marker for

management of primary disease, but it may fail to predict outcome in a significant proportion of patients such as tumours of between 0.75 - 2.5mm in thickness (Slingluff, Vollmer et al. 1988). Since previous experiments undertaken on a series of primary melanomas have suggested that *c-myc* expression is a more accurate prognostic marker than Breslow thickness, the aim of this chapter was to investigate the prognostic value of *c-myc* expression in a rigorous and prospective manner.

Many genes are regulated by *c-myc* either as a transactivator or as a repressor. Over expression of *c-myc* is associated with a poor survival in hepatocellular and colorectal carcinomas (Abou-Elella, Gramlich et al. 1996; Bhatavdekar, Patel et al. 1997). Flow cytometric analysis of c-myc demonstrated that high expression of c-myc predicted poor outcome in both primary and metastatic disease and was also able to discriminate prognosis in thick (>3mm) melanomas.

A study was designed to evaluate the role of c-myc expression in primary melanoma in a prospective trial.

7.2 Methods

A prospective trial was initiated in 1996 to assess the c-myc expression of melanomas using flow cytometric analysis of each tumour. All new melanomas diagnosed at Mount Vernon Hospital were included from 1996 to 1998 following histological confirmation of disease. Four-micron H & E sections of all tumours studied in this project were examined by a single consultant histopathologist. Histological data was then gathered from the formal histology report in the patient's notes and the following points were recorded for primary melanomas:

Conformation of diagnosis
Maximal tumour thickness (Breslow)
Clinical subtype of tumour
    Superficial spreading melanoma (SSM)

Nodular melanoma (NM)

Lentigo maligna melanoma (LMM)

Acral lentiginous melanoma (ALM)

Subungual melanoma (SUM)

Clark's level of invasion

Presence of ulceration

Comments on mitotic figures

Presence of lymphocytic infiltrate

Evidence of regression

Presence of vascular and/or lymphatic invasion

Completeness of excision

Each patient was followed clinically as an outpatient according to the protocol at Mount Vernon Hospital. This involves initial 3-month appointments that then reduced to 6-monthly and finally yearly appointments for a total of 10 years. Follow-up data was taken directly from the clinical notes or from GP records. The patients were assessed during April 2002. In order to evaluate the clinical significance of oncoprotein expression, the following clinical information was sought from each patient's records:

Age

Sex

Date of primary diagnosis

Site of primary tumour

Head and Neck

Limbs

Trunk

Histological parameters of secondary lesion

Nodal positivity

Extracapsular spread

Site of first recurrence

Wound/local (i.e. <3cm from original lesion)

Regional nodes

Distant metastases

Disease free interval

Length of follow up

Overall survival

Once the primary melanoma specimens were obtained, thick sections (35μm) of melanoma specimens were cut from paraffin blocks and rehydrated using a modified technique described by Hedley (Hedley, Friedlander et al. 1983). The specimens were enucleated and stained for c-myc oncoprotein as described in section 2.2.9-10 and analysed by flow cytometry. Data were evaluated on at least 10,000 events (nuclei) for each sample with oncoprotein level measured by calculation of percentage positivity compared to the control.

7.3 Results

7.3.1 Clinical and Histopathological Data

A total of 117 melanomas were included in the study. The sex distribution was 60 females and 57 males. The average age was 60.5 years (range 22-97 years). The average follow up was 45 months that includes either the time to death or until the patients were last confirmed alive. 23% of cases were ulcerated compared to 77% of tumour that had no ulceration. There were 17 tumours on the head and neck region, 36 on the trunk, 10 on the upper limb and 46 on the lower limb. The average Breslow depth was 2.49mm.

7.3.2 Overall Survival

28% of patients had died and 72% of the cohort were still alive in April 2002. The overall survival is shown in Figure 7.1.

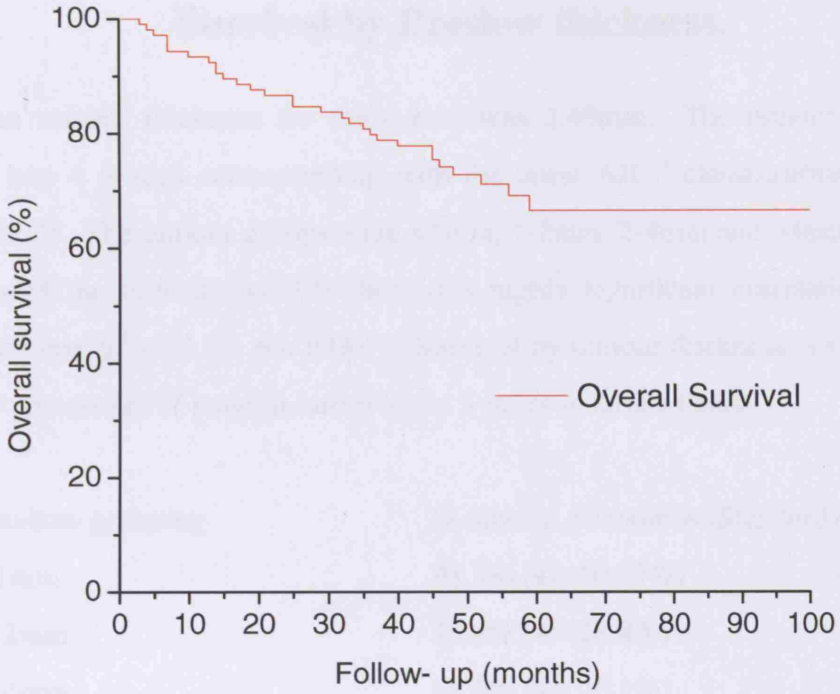

Figure 7.1 Overall Survival

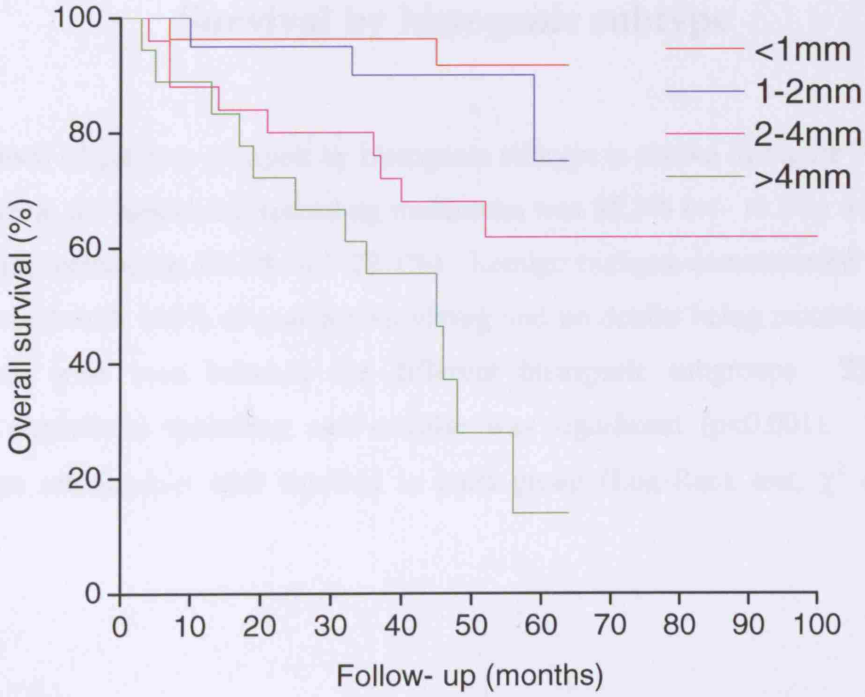

Figure 7.2 Survival by Breslow thickness

7.3.4 Survival by Breslow thickness.

The mean tumour thickness for the cohort was 2.49mm. The tumour thickness was grouped into 4 groups corresponding with the latest AJCC classification of melanoma (Balch 2002). The tumour groups were <1mm, 1-2mm, 2-4mm and >4mm. The Breslow thickness of the tumour (n=117) showed a highly significant correlation to survival. (Log-Rank test, $\chi^2 = 25.39$, $p < 0.001$). Survival by tumour thickness is shown in Figure 7.2. The percentage of patients surviving at 5 years is shown below.

Breslow grouping	% alive at 60 months (Standard error)
<1mm	91.7% (+/- 10.97%)
1-2mm	75.0% (+/- 28.8%)
2-4mm	61.0% (+/- 20.1%)
>4mm	13.8% (+/- 23.5%)

Table 7.1 Table to show survival by Breslow thickness.

7.3.5 Survival by histogenic subtype

The survival of patients grouped by histogenic subtype is shown in Figure 7.3. The five-year survival for superficial spreading melanoma was 85.3% (+/- 13.5%) with the Figure for nodular melanomas 29.6% (+/- 27.4%). Lentigo maligna demonstrated the best five-year survival with 100% of patients surviving and no deaths being recorded. Statistical differences were seen between the different histogenic subgroups. The difference between superficial spreading and nodular was significant ($p<0.001$). There was a significant relationship with survival in each group (Log-Rank test, $\chi^2 = 12.59$, $p < 0.001$).

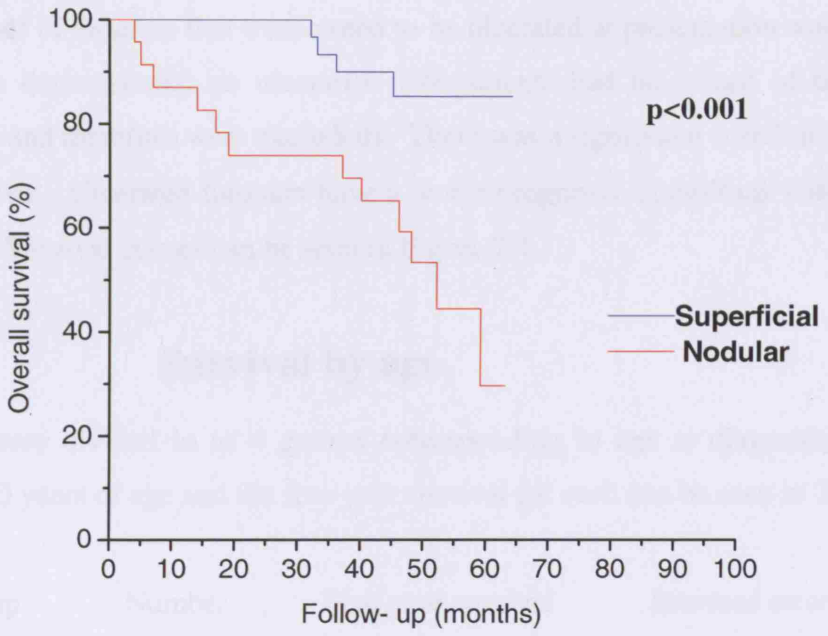

Figure 7.3 Survival by melanoma sub-type.

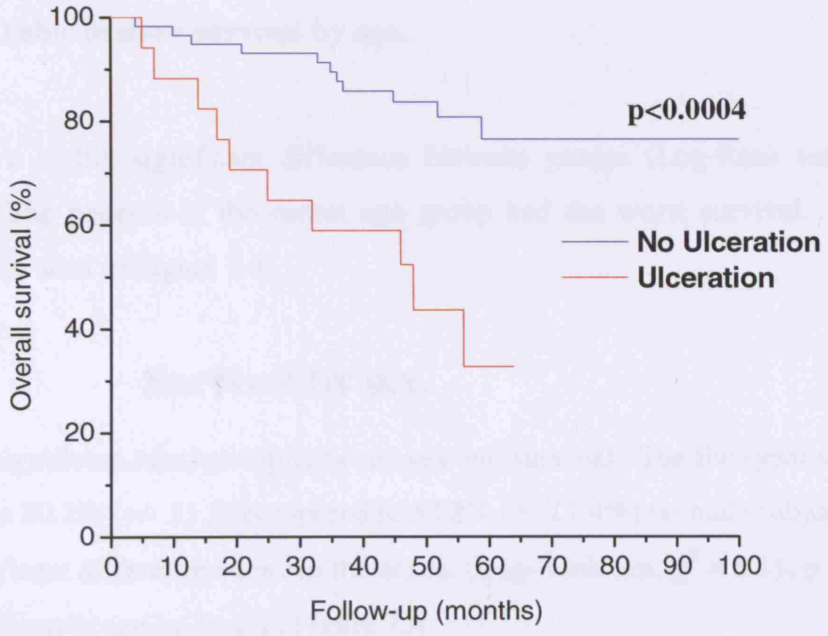

Figure 7.4 Survival and ulceration

7.3.6 Survival by tumour ulceration.

The number of tumours that were noted to be ulcerated at presentation was 17, compared to 59 that demonstrated no ulceration (39 patients had no record of the presence of ulceration and therefore were excluded). There was a significant correlation of ulceration with survival. Ulcerated tumours have a worse prognosis. (Log-Rank test, $\chi^2 = 12.51$, $p < 0.001$). Survival curves can be seen in Figure 7.4.

7.3.7 Survival by age.

Patients were divided in to 4 groups corresponding to age at diagnosis. Each group covered 20 years of age and the five-year survival for each can be seen in Table 7.2

.

Age group	Number	Five-year survival	Standard error
21-40 years	18	76.3%	+/-20.3%
41-60 years	24	83.1%	+/-15.1%
61-80 years	36	69.3%	+/- 20.1%
81-100 years	14	26.8%	+/- 24.1%

Table 7.2 Table to show survival by age.

There was a highly significant difference between groups (Log-Rank test, $\chi^2 = 16.3$, $p=0.001$). The patients in the oldest age group had the worst survival. The survival curves can be seen in Figure 7.5.

7.3.8 Survival by sex.

There is a significant relationship between sex and survival. The five-year survival for females was 80.2% (+/- 11.2) compared to 52.8% (+/-17.4%) on male subjects. There was a significant difference between the sexes. (Log-Rank test, $\chi^2 = 6.11$, $p < 0.013$). The survival curve can be seen in Figure 7.6.

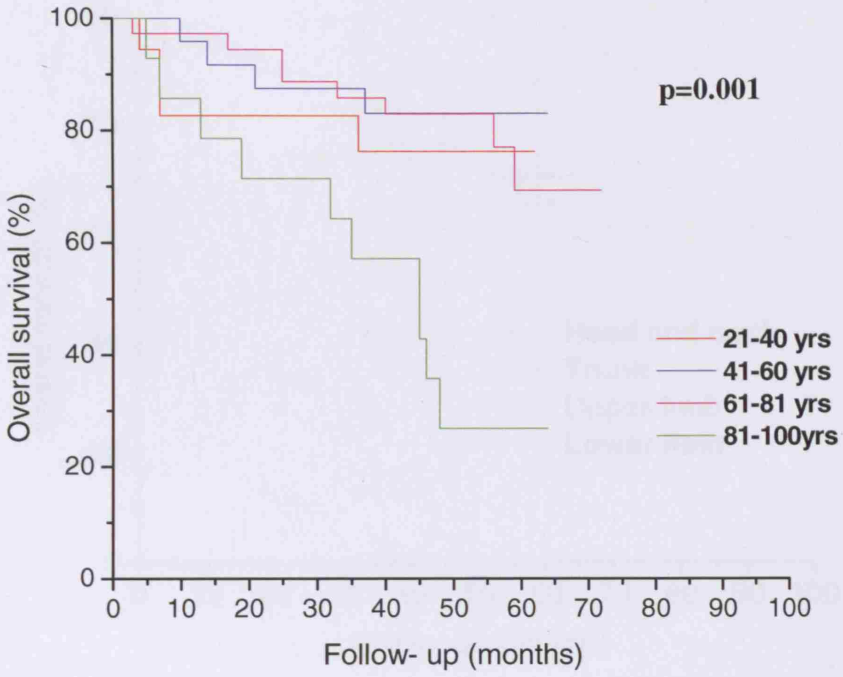

Figure 7.5 Survival and age.

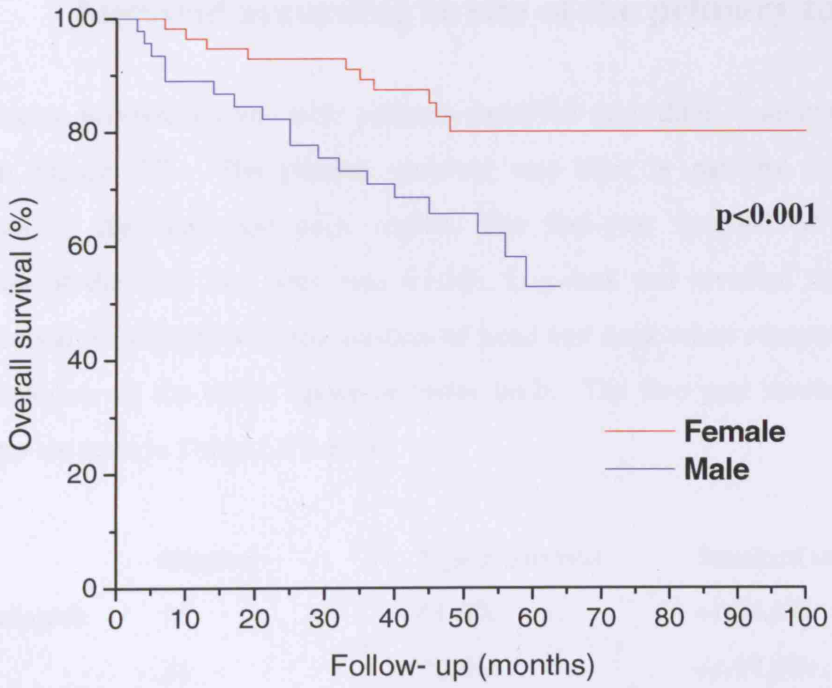

Figure 7.6 Survival and sex.

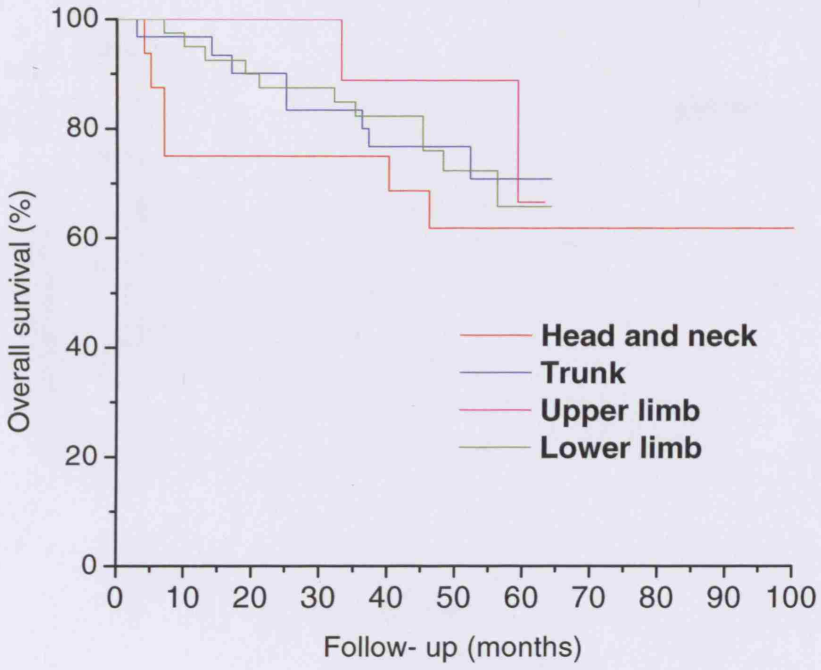

Figure 7.7 Survival by site of primary tumour

7.3.9 Survival according to site of the primary tumour.

Kaplan-Meier survival curves with patients stratified according to anatomical site are shown in Figure 7.7. The poorest survival was seen in patients presenting with melanomas of the head and neck region. The five-year survival of patients with melanomas of the head and neck was 61.5%. Log-rank test revealed no significantly worse survival of patients with melanomas of head and neck when compared to patients with melanomas on the trunk, upper or lower limb. The five-year survival figures for each group are seen in Table 7.3 below.

Site	Number	5 year survival	Standard error
Head and neck	16	61.8%	+/-24.1%
Trunk	31	70.8%	+/-17.8%
Upper Limb	9	66.6%	+/-40.7%
Lower Limb	40	65.8%	+/-18.2%

Table 7.3 5 year survival for anatomical site of the primary tumour.

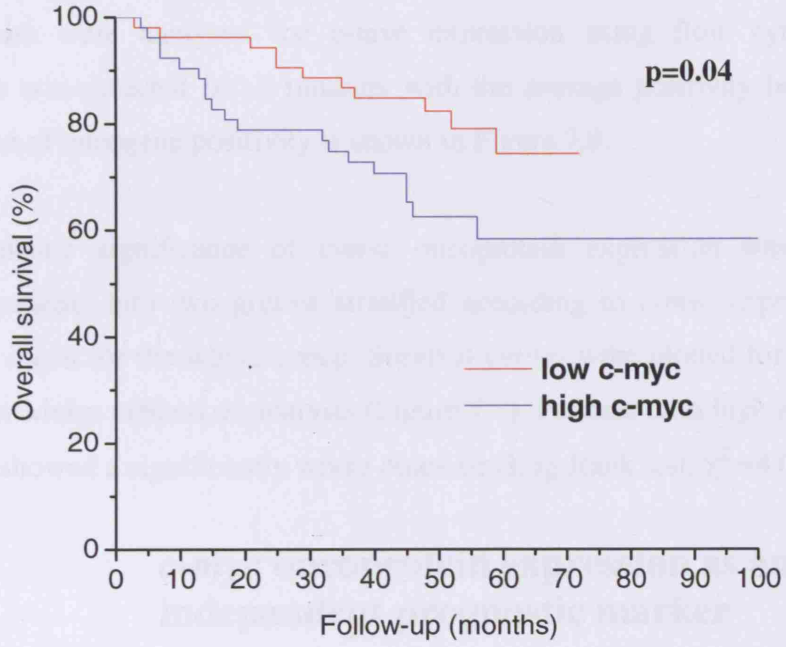

Figure 7.8 Survival by c-myc oncogene expression.

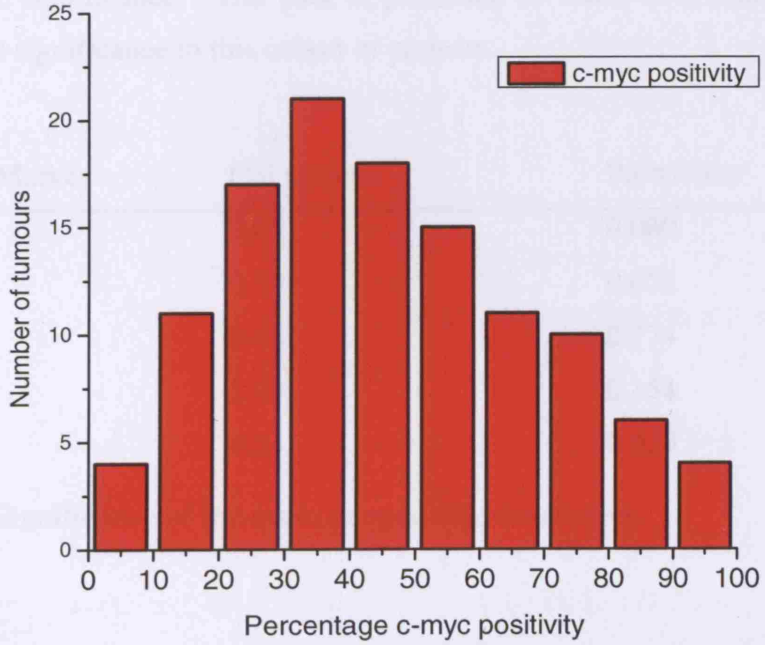

Figure 7.9 Distribution of c-myc positivity.

7.3.10 Survival according to c-myc expression.

All tumours were analysed for c-myc expression using flow cytometry. C-myc expression was detected in all tumours with the average positivity being 41.7%. The distribution of oncogene positivity is shown in Figure 7.9.

The prognostic significance of *c-myc* oncoprotein expression was investigated by dividing patients into two groups stratified according to *c-myc* expression above and below the mean for the whole group. Survival curves were plotted for each group using the Kaplan-Meier method of analysis (Figure 7.8). Patients with high *c-myc* oncoprotein positivity showed a significantly worse outcome (Log-Rank test, $\chi^2 = 4.09$, $p < 0.043$).

7.3.11 *c-myc* oncoprotein expression as an independent prognostic marker

Each of the main prognostic parameters (Breslow, age, sex, ulceation, histological subtype and *c-myc*) were entered into a Cox Proportional Hazards model to assess their independent significance. The data is presented in Table 7.4. Only *c-myc* retained independent significance in this cohort of patients.

Prognostic Marker	Chi squared	Probability
Breslow	3.05	0.080
Sex	0.19	0.655
Age	0.08	0.774
Ulceration	2.03	0.154
c-myc	4.24	0.039

Table 7.4 Significance of the main prognostic parameters.

7.3.12 *c-myc* correlation to other prognostic markers.

The level of *c-myc* expression in each histological subtype demonstrated superficial spreading had a mean of 50.4% compared to nodular with 41.1%. There was not a significant difference between the two groups.

The age group 20-40 had the lowest *c-myc* expression value of 40.7% compared to the oldest, which had a mean of 50.6% positivity. However there was no significant difference in *c-myc* expression of tumours correlating to age of the patients.

Breslow thickness, sex or ulceration were not significantly correlated to *c-myc* expression as can be seen in Table 7.5.

Prognostic Marker	Significance
Breslow	NS
Sex	NS
Age	NS
Ulceration	NS
Histological sub type	NS

Table 7.5 Significance of correlation between each prognostic marker and *c-myc*.

7.3.13 c-myc positivity and prognosis according to tumour thickness.

The vertical depth of invasion was investigated to ascertain if *c-myc* expression could discriminate prognosis within each of the major subgroups of Breslow thickness. There were 31 melanomas of less than 1mm, 19 between 1 and 2mm, 24 between 2 to 4mm and 19 greater than 4mm in vertical depth. No groups showed that *c-myc* had a significant impact on prognosis. However when dividing the total number of melanomas into 4 groups there are relatively small numbers in this cohort and the sample size may not be

large enough to detect any differences at this level. The probability for each group can be seen in Table 7.6.

Vertical invasion	Chi squared	Probability
<1mm	0.0632	0.8016
1-2mm	0.0309	0.8605
2-4mm	0.3958	0.5293
>4mm	0.6033	0.4373

Table 7.6 Significance of *c-myc* on prognosis for groups according to Breslow thickness.

7.4 Discussion

A large number of prognostic indicators have been described in melanoma. The largest study to date analysed factors in 17,600 patients over a ten-year period (Balch, Soong et al. 2001). In that study, multivariate analysis of clinico-pathological prognostic indices was performed and found that the two most powerful independent prognostic markers were tumour thickness and the presence of ulceration. Other statistically significant factors were patient age, site of primary melanoma, level of invasion and sex. These powerful predictive markers are used in the routine clinical management of patients with primary melanoma. Breslow thickness is the gold standard prognostic indicator in melanoma and this is again demonstrated in this investigation.

Tumour thickness has remained the major prognostic marker in primary melanoma governing surgical excision margins and the selection of patients for adjuvant therapy. However, Breslow thickness has been found to fail to predict the clinical outcome of patients with 0.75 - 2.5 mm thickness tumours (Slingluff, Vollmer et al. 1988; Blessing, McLaren et al. 1990). It has been suggested that these inaccuracies may arise either due to difficulties in measuring the true maximum vertical depth, or because thickness may not determine the metastatic potential and ultimately the outcome between different

histological subtypes of tumour or anatomical sites. This problem underscores the need to search for and identify other markers that can predict the outcome for given patients, especially those who have an intermediate thickness tumour and who would otherwise receive conservative treatment.

The selection of patients for adjuvant therapy, or novel gene therapy techniques, should be based on identifying those patients at high risk. Since the established prognostic markers discussed above have limitations, the identification of more accurate biological markers may prove more effective in predicting outcome and stratifying patients for treatment selection. Measurement of *c-myc* oncoprotein positivity by a previous RAFT research fellow was found to be the most accurate independent prognostic factor and even more accurate than Breslow thickness. This initial study was restricted to two series of primary melanoma patients. The first examined a series of primary melanomas of between 0.75 - 2.5 mm thickness of predominantly superficial spreading melanoma from trunk and extremity sites (Grover, Pacifico et al. 2003). The second series examined acral lentiginous melanomas of all thicknesses from plantar and subungual sites (Chana, Grover et al. 2000). In both these series *c-myc* oncoprotein estimation was found to be the most accurate independent prognostic marker on multivariate analysis. Further work measured *c-myc* oncoprotein in a more heterogeneous group of head and neck melanoma (Chana, Grover et al. 2001). Univariate analysis revealed a significant association between high *c-myc* oncoprotein positivity and poorer outcome. This was confirmed on multivariate analysis where *c-myc* expression maintained an independent association with outcome.

The aim of this chapter was to investigate the prognostic significance in a prospective trial of melanoma patients to study whether *c-myc* positivity measured by flow cytometry is a useful and practical marker in melanoma. This study demonstrates a median *c-myc* positivity of 41% that is comparable to that seen in head and neck melanomas (39%) (Chana 1998) but lower than that of Grover in 1996 (Grover, Ross et al. 1996). High *c-myc* positivity was significantly associated with a worse prognosis using univariate analysis. Previous studies have shown a stronger independent prognostic value for *c-myc*

that has not been repeated in this investigation. However the data presented suggests a strong role for *c-myc* in the pathogenesis of cutaneous melanoma. Importantly *c-myc* positivity was the strongest independent factor in predicting survival and the only parameter to reach significance by multivariate analysis.

The strength of this study is that it is performed in a consecutive series of patients followed up in a longitudinal prospective study that has enough patients to achieve statistically relevant outcomes. *c-myc* is not the strongest predictor of survival taken alone in univariate analysis, Breslow thickness had the highest p-value, but only *c-myc* was significant in multivariate analysis. Prognostic markers need to guide treatment and influence patient management if they are to be of anymore than academic interest. *c-myc* positivity can contribute to other prognostic markers that are routinely used in clinical practice and should be considered for all patients at the time of primary diagnosis. The availability of flow cytometric facilities in most hospitals is low and this factor alone may limit the clinical relevance of *c-myc* positivity in melanoma. Oncongene expression in melanoma can play a role in the clinical management by highlighting the risk of death in patient groups and it is hoped that combining work with the tissue micro-array described in chapter 6, new genes with prognostic importance can be identified. It is then for medicine to incorporate this information into the care of patients with melanoma.

Chapter 8

General Discussion:

The prognostic and therapeutic significance of the *c-myc* proto-oncongene.

8.1 The role of *c-myc* in melanoma.

The aim of this thesis was to investigate the role of the *c-myc* in the development and progression of melanoma. Gene therapy strategies were investigated using a ribozyme targeting *c-myc* in order to modulate gene expression in melanoma cells.

Previous work in this project has demonstrated that *c-myc* expression is correlated with a poorer prognosis in melanoma using retrospective immunological examination of historical specimens (Chana 1998). The work presented in this thesis utilized a prospective approach to examine *c-myc* expression using flow cytometry at the time of excision of the primary melanoma lesion. The aim was to investigate whether *c-myc* is a helpful prognostic marker that could aid clinicians in the management of cutaneous melanoma.

Outcome in melanoma is only improved by early surgical intervention and there is a significant lack of therapeutic options for patients following surgery. No medical treatment has consistently been demonstrated to improve outcome and increase survival. A potential new approach is gene therapy and manipulation in gene expression can lead to modulation of tumour behaviour (Pehamberger, Soyer et al. 1998). Antisense targeting of *c-myc* has been shown to reduce both *c-myc* expression and melanoma cell growth in *in-vitro* and *in-vivo* models (Chana 1998). However antisense technology is expensive and relatively inefficient and this has lead to the development of novel gene

therapy strategies. The process of designing, constructing and testing of a ribozyme targeting *c-myc* has been described in this thesis.

There should be a continuous search for new prognostic markers and potential gene therapy targets that may help to improve management and therapy for melanoma. A tissue micro-array is a powerful new tool in the hunt for genes associated with both progression of disease and prognostic relevance. This thesis presents the method for construction and analysis of a tissue micro-array for cutaneous melanoma.

8.2 The prognostic significance of *c-myc* in cutaneous melanoma.

A prospective investigation of 117 melanomas was undertaken. Clinico-pathological details were recorded at the time of initial diagnosis and *c-myc* expression was analysed using immunostaining and flow cytometric analysis. The average follow up was 45 months with a similar number of males and females. Kaplan-Meier analysis of the data revealed that high *c-myc* expression was significantly associated with a worse prognosis ($p<0.043$) (Figure 8.1). Multivariate analysis demonstrated that high *c-myc* expression was also an independent prognostic marker measured against other commonly used parameters: Breslow thickness, age, sex, ulceration and histological sub-type.

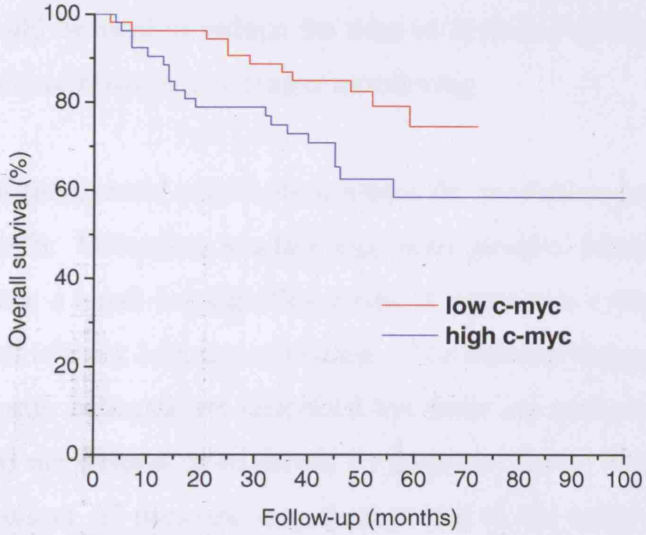

Figure 8.1 Survival by *c-myc* oncogene positivity

The analysis of *c-myc* expression in cutaneous melanoma presented in Chapter 7 continues to support the hypothesis that *c-myc* plays a significant and prognostic role in the pathogenesis of melanoma. No previous work has been performed in a prospective study and the work shows that *c-myc* plays an important role in the. Further analysis of the data, dividing tumours into either histological sub types or thickness groups, failed to reveal any further significance, primarily due to an insufficient sample size. Ideally a larger cohort of patients would have been recruited into this study and followed up for a longer period of time. A prognostic marker must reveal information about the biological behaviour of the tumour that can be used to determine the management of given patients to improve the outcome. Realistic options may be aggressive surgical clearance, closer follow-up of patients who are at a high risk of recurrence, or the use of adjuvant chemotherapy. However surgical margins appear to have little effect on the survival but do affect the local recurrence rate in melanoma (Bishop, Corrie et al. 2002). This investigation did not examine the role of *c-myc* expression and the local recurrence rate so further work would be needed to establish if *c-myc* would be able to guide the size of excision margins.

Clinical follow up of patients with melanoma is designed to provide an early detection system for recurrent disease. Further resection of metastatic tumour from either lymph nodes or skin may not change the overall prognosis for the patient but improves their quality of life and reduces the tumour load. In known high-risk groups closer follow up than normal could be used to reduce the time to detection of recurrent disease, either as more frequent clinic visits or as a longer monitoring.

It is the area of therapeutic intervention where the predictive power of *c-myc* may have the greatest benefit. Melanoma is a heterogeneous group of tumours in terms of outcome. Thin lesions have a small but significant risk of metastasis compared to thicker lesions. However, not all of thick lesions metastasise. The Breslow depth of a tumour is probably the best prognostic indicator yet described but there are small and significant groups of tumours that do not behave as expected by Breslow alone. Genes that can predict the biological behaviour of tumours may further add to the prognostic value of Breslow

depth and be able to tease out the tumours that will have a worse prognosis than Breslow predicts ie thin but aggressive tumours. Accurate targeting of this group of patients that have the most to gain from adjuvant treatment at the time of diagnosis will eliminate unnecessary treatment. The aim of adjuvant therapy is to destroy the small, clinically undetectable, deposits of melanoma that are present in the patients and will develop into further disease. *c-myc* can play a role in the identification of these patients and guide their treatment to be more aggressive. A low *c-myc* expression will concurrently allow patients to abstain from aggressive adjuvant therapy, as they will be unlikely to gain any benefit.

However there remains a significant problem that remains to be resolved. There is currently no effective adjuvant therapy that has consistently been shown to prolong survival. Identification of patients at a high risk of recurrent disease is rendered of little practical benefit if no additional therapeutic intervention is available to treat these high-risk patients. Interferon was the first treatment to demonstrate an improvement in patient survival in sub-groups of melanoma patients (Kirkwood, Strawderman et al. 1996) but this has not been confirmed in later trials (Pehamberger, Soyer et al. 1998; Cascinelli, Belli et al. 2001; Kirkwood, Ibrahim et al. 2001). Currently, use of interferon remains controversial and while it is accepted that it may increase relapse-free survival, produces no significant increase in overall survival (Eggermont 2001). Immunotherapy, BCG, chemotherapy and radiotherapy have demonstrated no significant improvement in outcome and are not routinely used for melanoma therapy. The search for novel treatment strategies has turned to the potential of gene therapy in an attempt to improve the outcome in cutaneous melanoma.

8.3 Ribozyme modulation of *c-myc* expression *in-vitro.*

Gene therapy involves transfection of cells with nucleic acids that modulate cell function for therapeutic gain. Antisense oligonucleotides modify gene expression at the translation stage and have been used in various tumours. Antisense targeting of *c-myc* has been shown to reduce *c-myc* expression both *in-vitro* and *in-vivo* (Chana 1998).

However, antisense is relatively inefficient, short lasting and therefore expensive to use but has been shown to improve sensitivity to chemotherapy in melanoma patients and reduce gene expression in clinical trials (Jansen, Wacheck et al. 2000). Recent advances in molecular biology highlighted catalytic RNA molecules called ribozymes, as highly efficient and specific tools for gene therapy. These short RNA chains form a simple 3D structure that confers the ability to cleave GUC sequences of RNA chains that are flanked by specific target sequences. Whilst still at an early stage of development, ribozymes have the potential to be both more efficient and produce longer lasting down regulation of gene function than antisense oligonucleotides. Ribozymes have the potential to be key tools in corrective gene therapy either alone or used in combination with other existing treatment options such as chemo or immunotherapy.

The work in chapters 3, 4 and 5 describes the design and testing of a ribozyme targeting *c-myc*. A hammerhead ribozyme was designed targeting the translation-initiation codon of exon 2 based on a GUC triplet sequence. Transfection of a pREV plasmid encoding the ribozyme cassette was performed in A375M melanoma cells *in-vitro* to allow assessment of the ribozyme. Both transient and stable transfection strategies were pursued and compared against antisense controls. Ribozyme treatment in stable clones produced a significant down regulation in *c-myc* expression compared to controls ($p<0.001$) and this corresponded to a reduced growth rate of cells ($p<0.001$). These results confirm the potential for ribozymes as a gene therapy tool and corroborate previous work by Cheng using an anti-myc ribozme in hepatoma cell lines (Cheng, Luo et al. 2000). Ribozymes designed to target many oncogenes have been described including ras, c-fos, bcl-2 amongst others (Kashani-Sabet, Funato et al. 1992; Feng, Cabrera et al. 1995; Ohta, Kijima et al. 1996) mainly in *in-vitro* models. However clinical trials have recently started using ribozymes targeting VEGF receptors demonstrating the transition from the laboratory to the clinical setting (Sandberg, Parker et al. 2000).

It is unlikely that the use of ribozymes will prove effective in cancer for use as single agents since by targeting one gene alone they may only work on a 'one-hit' basis.

However, due to its prognostic influence, targeting *c-myc* may prove useful. The pleiotropic effects of *c-myc* overexpression on proliferation, HLA expression and chemoresistance gives rise to the potential for exploiting a multi-targeted approach. Together with advances with delivery systems it is proposed that in future a combination of a biological approach using *c-myc* antisense, together with current cytotoxic agents such as cisplatinum or interferon may yield an effective therapy. Previous work at RAFT has demonstrated an additive effect between interferon and antisense oligonucleotides targeting *c-myc* and this provides the most promising route for investigation.

Despite the promising approach of gene therapy with high specificity and efficacy in laboratory systems there remain large obstacles to be overcome before it enters routine clinical practice. Gene delivery is a major stumbling block in the advancement of ribozymes. Whilst advancement of delivery techniques was outside the aims of this thesis, practical use of antisense or ribozymes will be limited until this problem is overcome. The ideal delivery vehicle should be safe for the patient and environment, protect the gene therapy from immune attack and deliver the therapy in appropriate levels to achieve therapeutic effect over a sufficient period. To this end, retroviruses, adenoviruses and liposomes have all been used in clinical trials with varying success. None have proved ideal and new approaches currently being investigated include bacteria, adeno-associated and lentiviruses, cationic polymer-DNA complexes and electroporation. Intra-tumoral injection has had limited effect and would be of no use in the adjuvant setting. Delivery remains a crucial obstacle for gene therapy and the world awaits a perfect delivery system.

In order to engineer targeted cancer related expression of therapy, transcriptional regulation specific to certain tissues has been investigated. Stimuli such as radiation, (Marples, Greco et al. 2002) hypoxia (Nettelbeck, Jerome et al. 2000) or DNA regulatory sequences from cancer selective genes such as α-feto protein (hepatoma), c-erbB2 and DF3/MUC1 (breast) or prostate specific antigen, can be used to activate localised gene therapy. Melanoma has promised tyrosinase activated gene therapy (Brown and Kirkwood 2001) that could be specific for melanocytes thus reducing side effects and a

tyrosinase switch would be easy to construct and implement into plasmid delivered therapy.

Human gene therapy is a complex process involving multiple steps (organ delivery, tissue targeting, cellular trafficking, safety of vector and gene product, regulation of gene expression and duration, effects of the therapeutic protein) many of which are not completely understood. Evidence shows that *c-myc* plays a key role in the development and pathophysiology of melanoma and so stands out as a suitable gene for therapeutic intervention.

8.4 Melanoma tissue micro-array technology for screening of prognostic markers.

Formalin-fixed paraffin blocks are the routine method for mounting and storing histological specimens. They provide a huge resource for investigating progression and prognostic markers in melanoma. Mount Vernon Hospital has specimens dating back for over 30 years, many blocks with corresponding clinical records and follow-up. Indeed it has been estimated that paraffin sections retain their antigenicity for up to 60 years allowing vast numbers of historical blocks to be analysed (Camp, Charette et al. 2000). New technology, first described in 1998, allows high throughput molecular analysis of tumour specimens (Kononen, Bubendorf et al. 1998). To facilitate rapid screening for molecular alterations in melanoma a tissue micro-array was created and described in chapter 6. Large numbers of representative tumour cores were inserted into a single array block that could then be screened using routine immunohistochemical staining. 126 tumours were included in the array representing all the stages of the disease. Each melanoma had corresponding clinical data and follow up data, allowing prognostic markers to be screened, in addition to progression markers.

Data analysis demonstrated a rise in cyclin A, E and D1 correlating with disease progression. The regulatory gene, p27 had the opposite correlation and decreased with progression as would be expected. The number of cells positive for *c-myc* protein also increased with advancing stage of melanoma. Survival analysis for each of the 8

molecular markers revealed that high p53 positivity and high p27 intensity were significantly associated with a better survival. The other markers were not signficantly related to survival. The oncogene at the centre of this thesis, *c-myc* was not associated with prognosis in this study, which doesn't agree with the flow-cytometric analysis of *c-myc*. There has been a concern with the immunohistochemical staining of *c-myc*. Previous work performed in this project has used flow-cytometric analysis of *c-myc* expression (Grover, Ross et al. 1997; Grover, Chana et al. 1999; Chana, Grover et al. 2001; Chana, Grover et al. 2002). Antibody staining for *c-myc*, using immunohistochemistry stains, identifies mainly cytoplasmic protein. However, *c-myc* protein is a nuclear transcription factor and this is only seen using flow-cytometry to measure nucleic protein. It appears that flow cytometry and immunhistochemical staining are looking at different parameters of *c-myc*.

Tissue array technology allows increased capacity on a single block with minimal damage to the original specimens, accurate positioning of specimens on the block and the potential for automated construction and analysis using digital image analysis. Once an array block is made then hundreds of proteins can rapidly be screened for prognostic significance with the potential to re-use the original paraffin block if needed due to the small size of cores used. It has been estimated that 10,000 analyses could be made from a tumour having a diameter of 10mm (Schraml, Kononen et al. 1999). The tissue array described in this thesis produced large amounts of information rapidly and easily. However there were several problems. Firstly, thin melanomas do not contain large amounts of tissue and the depth of each core was not maximal into the array block. With each section taken from the array block then some of the thinner specimens would be used up most quickly. This was not a problem with thicker nodular primaries or metastatic lesions where the size of the lesion is much greater. Construction of an array containing superficial spreading tumours would not result in so many analyses as more bulky tumours. The array block in this thesis contained 126 tumour specimens with three cores per tumour. Despite this, some analyses were of low significance due to relatively low numbers of tumours especially when dividing melanoma into groups eg superficial spreading and nodular or by Breslow depth. The array constructed was a preliminary

block to assess the merits of the technique. Further blocks should have greater numbers of tumours to allow freedom to analyse expression in subgroups of tumours more accurately. Limitations are also placed on the array by the number of immunhistochemical antibodies that can be appropriately used. Many markers have no current antibodies that have high specificity and sensitivity in histological analyses. This is highlighted by the results we obtained with the *c-myc* antibody stain.

Problems of numbers can be overcome simply by using larger blocks with increased numbers of tumours contained in each array. One advantage of the tissue-array technique is that there is capacity for large numbers of patients. Fluorescence *in-situ* hybridisation techniques can be used to investigate a wider range of targets to be assessed including DNA, RNA and proteins (Schraml, Kononen et al. 1999). This approach would overcome some of the limitations of traditional antibody staining.

Mount Vernon Hospital has a huge archive of histological specimens and the tissue-array has proved to be a simple and powerful tool for extracting information on melanoma. The search to identify new prognostic and progression markers has much to gain from array technology. Indeed important new biological markers could translate to novel gene therapy targets for ribozymes.

8.5 Future Research

The findings presented in this thesis confirm the important role that *c-myc* plays in the development and progression of melanoma. It provides a solid base for future research investigating the therapeutic potential of gene therapy targeting *c-myc* and also encourages the search for new prognostic markers.

The prospective trial of *c-myc* has shown that it is a significant prognostic marker and should be added to the armamentarium of the clinician in deciding therapy. Flow-cytometric assessment of *c-myc* expression can divide melanomas into high and low risk

of death. The next step should be using that information to determine therapy for the patient. Conceivably a trial could be arranged to investigate treating high-risk patients with adjuvant interferon at the time of diagnosis. Destruction of occult micrometastasis in high-risk patients at an early stage should increase survival in that group. The low expressing melanoma group may also benefit but the number of patients that potentially may respond is less. Adjuvant therapy with interferon may be improved with a combinatorial approach utilising corrective gene therapy targeting *c-myc*. Additive benefits between interferon and *c-myc* antisense have been demonstrated *in-vitro* and repeated again in this thesis (Chapter 5). Interferon produces up regulation of p27/WAF with reduced *c-myc* expression leading to G1/S phase delay. Corrective gene therapy targeting *c-myc* would lead to increased down regulation of *c-myc* via a different mechanism with the potential to increase growth arrest.

Previous trials have used antisense oligonucleotides targeting bcl-2 in combination with dacarbazine for advanced melanoma. In a small trial consisting of 16 patients, patients with high bcl-2 expressing tumours were given intravenous or subcutaneous antisense in conjunction with standard dose dacarbazine. The regimen was well tolerated and six patients showed an anti-tumour response (Jansen, Wacheck et al. 2000). This approach could be utilized with interferon and *c-myc* gene therapy. Antisense has been used in several clinical trials and its pharmaceutical properties are known. The wealth of evidence on the important role of *c-myc* in melanoma should be pursued into a meaningful clinical option.

Novel gene therapy strategies continue to be described and improved. Small interfering RNAs are double stranded RNA molecules that are only activated once inside cells. An RNAse enzyme present within cells, Dicer, cleaves the RNA and releases the single stranded RNA, which then interferes with RNA translation to prevent gene expression. Originally discovered in plants, this approach appears to have a 'bystander effect' with cell to cell spreading of the 'gene silencing' effect being described (Shuey, McCallus et al. 2002). More work needs to be performed, but these molecules open a new area of

research into gene therapy. However the same problems with gene delivery exist and must be overcome before gene therapy becomes a routine treatment in clinical practice.

Prognostic markers will be needed in a heterogeneous disease such as melanoma to tailor treatment to individual patients. Oncogene expression could be used to guide or even be the specific target of therapy. Greater knowledge and understanding of the biology of melanoma gained through tissue array technology will promote novel treatment strategies. The oncogene *c-myc* is a suitable candidate for further research to use as both a prognostic marker and therapeutic target in cutaneous melanoma.

References.

Abou-Elella, A., T. Gramlich, et al. (1996). "c-myc amplification in hepatocellular carcinoma predicts unfavorable prognosis." Mod Pathol **9**(2): 95-8.

Adema, G. J., A. J. de Boer, et al. (1994). "Molecular characterization of the melanocyte lineage-specific antigen gp100." J Biol Chem **269**(31): 20126-33.

Afar, D. E., J. McLaughlin, et al. (1995). "Signaling by ABL oncogenes through cyclin D1." Proc Natl Acad Sci U S A **92**(21): 9540-4.

Ahmann, D. L., E. T. Creagan, et al. (1989). "Complete responses and long-term survivals after systemic chemotherapy for patients with advanced malignant melanoma." Cancer **63**(2): 224-7.

Albino, A. (1997). Molecular Biololgy of Cutaneous Malignant Melanoma. Principles and Practice of Oncology, New York Lippencott-Raven: p1935.

Allen, A. C. and S. Spitz (1953). "Malignant melanoma; a clinicopathological analysis of the criteria for diagnosis and prognosis." Cancer **6**(1): 1-45.

Amarzguioui, M. and H. Prydz (1998). "Hammerhead ribozyme design and application." Cell Mol Life Sci **54**(11): 1175-202.

Amati, B., T. D. Littlewood, et al. (1993). "The c-Myc protein induces cell cycle progression and apoptosis through dimerization with Max." Embo J **12**(13): 5083-7.

American Cancer Society. (2001). Cancer Facts and Figures 2001: http://www.cancer.org/eprise/main/docroot/STT/content/STT_1x_2001_Facts_and_Figures.pdf.

Andersson, A. P., K. K. Dahlstrom, et al. (1996). "Prognosis of thin cutaneous head and neck melanoma (<1mm)." Eur J Surg Oncol **22**(1): 55-7.

Atkins, M. B. (1997). "The treatment of metastatic melanoma with chemotherapy and biologics." Curr Opin Oncol **9**(2): 205-13.

Austin, P. F., C. W. Cruse, et al. (1994). "Age as a prognostic factor in the malignant melanoma population." Ann Surg Oncol **1**(6): 487-94.

Autier, P., J. F. Dore, et al. (1995). "Melanoma and use of sunscreens: an Eortc case-control study in Germany, Belgium and France. The EORTC Melanoma Cooperative Group." Int J Cancer **61**(6): 749-55.

Balch, C. M., A. C. Buzaid, et al. (2001). "Final version of the American Joint Committee on Cancer staging system for cutaneous melanoma." J Clin Oncol **19**(16): 3635-48.

Balch, C. M., T. M. Murad, et al. (1978). "A multifactorial analysis of melanoma: prognostic histopathological features comparing Clark's and Breslow's staging methods." Ann Surg **188**(6): 732-42.

Balch, C. M., S. J. Soong, et al. (1996). "Efficacy of an elective regional lymph node dissection of 1 to 4 mm thick melanomas for patients 60 years of age and younger." Ann Surg **224**(3): 255-63; discussion 263-6.

Balch, C. M., S. J. Soong, et al. (2001). "Prognostic factors analysis of 17,600 melanoma patients: validation of the American Joint Committee on Cancer melanoma staging system." J Clin Oncol **19**(16): 3622-34.

Balch, C. M., S. J. Soong, et al. (1992). An analysis of prognostic factors in 8500 patients with cutaneous melanoma. Cutaneous Melanoma. C. M. Balch. Philidelphia, Lippincott Co: 165-187.

Balch, C. M., M. M. Urist, et al. (1993). "Efficacy of 2-cm surgical margins for intermediate-thickness melanomas (1 to 4 mm). Results of a multi-institutional randomized surgical trial." Ann Surg **218**(3): 262-7; discussion 267-9.

Bales, E. S., C. Dietrich, et al. (1999). "High levels of expression of p27KIP1 and cyclin E in invasive primary malignant melanomas." J Invest Dermatol **113**(6): 1039-46.

Barth, A., L. A. Wanek, et al. (1995). "Prognostic factors in 1,521 melanoma patients with distant metastases." J Am Coll Surg **181**(3): 193-201.

Bauer, G., P. Valdez, et al. (1997). "Inhibition of human immunodeficiency virus-1 (HIV-1) replication after transduction of granulocyte colony-stimulating factor-mobilized CD34+ cells from HIV-1-infected donors using retroviral vectors containing anti-HIV-1 genes." Blood **89**(7): 2259-67.

Bhatavdekar, J. M., D. D. Patel, et al. (1997). "Coexpression of Bcl-2, c-Myc, and p53 oncoproteins as prognostic discriminants in patients with colorectal carcinoma." Dis Colon Rectum **40**(7): 785-90.

Bishop, J. A., P. G. Corrie, et al. (2002). "UK guidelines for the management of cutaneous melanoma." Br J Plast Surg **55**(1): 46-54.

Bleehen, N. M., E. S. Newlands, et al. (1995). "Cancer Research Campaign phase II trial of temozolomide in metastatic melanoma." J Clin Oncol **13**(4): 910-3.

Blessing, K., K. M. McLaren, et al. (1990). "Thin malignant melanomas (less than 1.5 mm) with metastasis: a histological study and survival analysis." Histopathology **17**(5): 389-95.

Borst, M. P., V. V. Baker, et al. (1990). "Oncogene alterations in endometrial carcinoma." Gynecol Oncol **38**(3): 364-6.

Bramlage, B., E. Luzi, et al. (1998). "Designing ribozymes for the inhibition of gene expression." Trends Biotechnol **16**(10): 434-8.

Breslow, A. (1970). "Thickness, cross-sectional areas and depth of invasion in the prognosis of cutaneous melanoma." Ann Surg **172**(5): 902-8.

Breslow, A. and S. D. Macht (1977). "Optimal size of resection margin for thin cutaneous melanoma." Surg Gynecol Obstet **145**(5): 691-2.

Bubendorf, L., J. Kononen, et al. (1999). "Survey of gene amplifications during prostate cancer progression by high-throughout fluorescence in situ hybridization on tissue microarrays." Cancer Res **59**(4): 803-6.

Buer, J., M. Probst, et al. (1997). "Elevated serum levels of S100 and survival in metastatic malignant melanoma." Br J Cancer **75**(9): 1373-6.

Burns, B. F. (1989). "Molecular genetic markers in lymphoproliferative disorders." Clin Biochem **22**(1): 33-9.

Burton, R. C., M. S. Coates, et al. (1993). "An analysis of a melanoma epidemic." Int J Cancer **55**(5): 765-70.

Buttner, P., C. Garbe, et al. (1995). "Primary cutaneous melanoma. Optimized cutoff points of tumor thickness and importance of Clark's level for prognostic classification." Cancer **75**(10): 2499-2506.

Camp, R. L., L. A. Charette, et al. (2000). "Validation of tissue microarray technology in breast carcinoma." Lab Invest **80**(12): 1943-9.

Cancer Research Campaign (1997). Cancer Statistics, Cancer Research Campaign.

Cao, X., C. Chen, et al. (1996). "Enhanced efficacy of combination of IL-2 gene and IL-6 gene-transfected tumor cells in the treatment of established metastatic tumors." Gene Ther **3**(5): 421-6.

Cascinelli, N. and F. Belli (1993). "The case for minimal margins and delayed regional node dissection for high-risk cutaneous melanoma." Curr Opin Gen Surg: 310-5.

Cascinelli, N., F. Belli, et al. (2001). "Effect of long-term adjuvant therapy with interferon alpha-2a in patients with regional node metastases from cutaneous melanoma: a randomised trial." Lancet **358**(9285): 866-9.

Cascinelli, N., F. Belli, et al. (2000). "Sentinel lymph node biopsy in cutaneous melanoma: the WHO Melanoma Program experience." Ann Surg Oncol **7**(6): 469-74.

Cascinelli, N., R. Bufalino, et al. (1994). "Results of adjuvant interferon study in WHO melanoma programme." Lancet **343**(8902): 913-4.

Cech, T. R., A. J. Zaug, et al. (1981). "In vitro splicing of the ribosomal RNA precursor of Tetrahymena: involvement of a guanosine nucleotide in the excision of the intervening sequence." Cell **27**(3 Pt 2): 487-96.

Cerni, C., K. Bousset, et al. (1995). "Differential effects by Mad and Max on transformation by cellular and viral oncoproteins." Oncogene **11**(3): 587-96.

Chalfie, M., Y. Tu, et al. (1994). "Green fluorescent protein as a marker for gene expression." Science **263**(5148): 802-5.

Chana, J. (1998). The prognostic and therapeutic significance of c-myc expression in melanoma. University College London.

Chana, J. S., R. Grover, et al. (2002). "The c-myc oncogene: use of a biological prognostic marker as a potential target for gene therapy in melanoma." Br J Plast Surg **55**: 623-627.

Chana, J. S., R. Grover, et al. (1998). "The clinical significance of c-myc oncogene expression in melanomas of the scalp." Br J Plast Surg **51**(3): 191-4.

Chana, J. S., R. Grover, et al. (2000). "An analysis of p16 tumour suppressor gene expression in acral lentiginous melanoma." Br J Plast Surg **53**(1): 46-50.

Chana, J. S., R. Grover, et al. (2001). "The prognostic importance of c-myc oncogene expression in head and neck melanoma." Ann Plast Surg **47**(2): 172-7.

Cheng, J., J. Luo, et al. (2000). "Inhibition of cell proliferation in HCC-9204 hepatoma cells by a c-myc specific ribozyme." Cancer Gene Ther **7**(3): 407-12.

Citro, G., I. D'Agnano, et al. (1998). "c-myc antisense oligodeoxynucleotides enhance the efficacy of cisplatin in melanoma chemotherapy in vitro and in nude mice." Cancer Res **58**(2): 283-9.

Clark, W. H., Jr., D. E. Elder, et al. (1989). "Model predicting survival in stage I melanoma based on tumor progression." J Natl Cancer Inst **81**(24): 1893-904.

Clark, W. H., Jr., L. From, et al. (1969). "The histogenesis and biologic behavior of primary human malignant melanomas of the skin." Cancer Res **29**(3): 705-27.

Coats, J. (1885). "On a case of multiple melanotic sarcoma." Glasgow Med J(24): 92.

Cochran, A. J., D. R. Wen, et al. (1992). "Management of the regional lymph nodes in patients with cutaneous malignant melanoma." World J Surg **16**(2): 214-21.

Cole, C. A., P. D. Forbes, et al. (1986). "An action spectrum for UV photocarcinogenesis." Photochem Photobiol **43**(3): 275-84.

Collis, S. J., A. Tighe, et al. (2001). "Ribozyme minigene-mediated RAD51 down-regulation increases radiosensitivity of human prostate cancer cells." Nucleic Acids Res **29**(7): 1534-8.

Cooke, K. R., D. C. Skegg, et al. (1984). "Socio-economic status, indoor and outdoor work, and malignant melanoma." Int J Cancer **34**(1): 57-62.

Coulie, P. G., V. Brichard, et al. (1994). "A new gene coding for a differentiation antigen recognized by autologous cytolytic T lymphocytes on HLA-A2 melanomas." J Exp Med **180**(1): 35-42.

Creagan, E. T., R. J. Dalton, et al. (1995). "Randomized, surgical adjuvant clinical trial of recombinant interferon alfa-2a in selected patients with malignant melanoma." J Clin Oncol **13**(11): 2776-83.

Dang, C. V. (1999). "c-Myc target genes involved in cell growth, apoptosis, and metabolism." Mol Cell Biol **19**(1): 1-11.

Day, C. L., Jr., M. C. Mihm, Jr., et al. (1982). "Cutaneous malignant melanoma: prognostic guidelines for physicians and patients." CA Cancer J Clin **32**(2): 113-22.

Day, C. L., Jr., A. J. Sober, et al. (1981). "A prognostic model for clinical stage I melanoma of the lower extremity. Location on foot as independent risk factor for recurrent disease." Surgery **89**(5): 599-603.

Day, C. L., Jr., A. J. Sober, et al. (1981). "A prognostic model for clinical stage I melanoma of the upper extremity. The importance of anatomic subsites in predicting recurrent disease." Ann Surg **193**(4): 436-40.

de Smet, M. D., C. J. Meenken, et al. (1999). "Fomivirsen - a phosphorothioate oligonucleotide for the treatment of CMV retinitis." Ocul Immunol Inflamm **7**(3-4): 189-98.

Del Prete, S. A., L. H. Maurer, et al. (1984). "Combination chemotherapy with cisplatin, carmustine, dacarbazine, and tamoxifen in metastatic melanoma." Cancer Treat Rep **68**(11): 1403-5.

Demierre, M. F. and H. K. Koh (1997). "Adjuvant therapy for cutaneous malignant melanoma." J Am Acad Dermatol **36**(5 Pt 1): 747-64.

Desjardins, J. P., B. S. Sproat, et al. (1996). "Pharmacokinetics of a synthetic, chemically modified hammerhead ribozyme against the rat cytochrome P-450 3A2 mRNA after single intravenous injections." J Pharmacol Exp Ther **278**(3): 1419-27.

Dietrich, A., E. Tanczos, et al. (1997). "High CD44 surface expression on primary tumours of malignant melanoma correlates with increased metastatic risk and reduced survival." Eur J Cancer **33**(6): 926-30.

Dolnikov, A., A. King, et al. (1996). "Ribozyme-mediated suppression of v-myc expression abrogates apoptosis in transformed monocytes." Cancer Gene Ther **3**(5): 289-95.

Dron, M., N. Modjtahedi, et al. (1986). "Interferon modulation of c-myc expression in cloned Daudi cells: relationship to the phenotype of interferon resistance." Mol Cell Biol **6**(5): 1374-8.

ECACC (2001). European Collection of Cell Cultures. http://www.ecacc.org/.

Eggermont, A. M. (2001). "The role interferon-alpha in malignant melanoma remains to be defined." Eur J Cancer **37**(17): 2147-2153.

Elwood, J. M. and J. Jopson (1997). "Melanoma and sun exposure: an overview of published studies." Int J Cancer **73**(2): 198-203.

Evan, G. and T. Littlewood (1998). "A matter of life and cell death." Science **281**(5381): 1317-22.

Evan, G. I., G. K. Lewis, et al. (1985). "Isolation of monoclonal antibodies specific for human c-myc proto- oncogene product." Mol Cell Biol **5**(12): 3610-6.

Evan, G. I., A. H. Wyllie, et al. (1992). "Induction of apoptosis in fibroblasts by c-myc protein." Cell **69**(1): 119-28.

Evans, R. D., A. W. Kopf, et al. (1988). "Risk factors for the development of malignant melanoma--I: Review of case-control studies." J Dermatol Surg Oncol **14**(4): 393-408.

Falkson, C. I., J. Ibrahim, et al. (1996). "A randomized phase III trial of dacarbazine (DTIC) versus DTIC + interferon alfa-2b (IFN) versus DTIC + tamoxifen (TMX) versus DTIC + IFN + TMX in metastatic malignant melanoma: An ECOG trial." Proc Am Soc Clin Oncol **15**: A1350.

Fedor, M. J. and O. C. Uhlenbeck (1990). "Substrate sequence effects on "hammerhead" RNA catalytic efficiency." Proc Natl Acad Sci U S A **87**(5): 1668-72.

Feng, M., G. Cabrera, et al. (1995). "Neoplastic reversion accomplished by high efficiency adenoviral- mediated delivery of an anti-ras ribozyme." Cancer Res **55**(10): 2024-8.

Field, J. K. and D. A. Spandidos (1990). "The role of ras and myc oncogenes in human solid tumours and their relevance in diagnosis and prognosis (review)." Anticancer Res **10**(1): 1-22.

Field, J. K., D. A. Spandidos, et al. (1989). "Elevated expression of the c-myc oncoprotein correlates with poor prognosis in head and neck squamous cell carcinoma." Oncogene **4**(12): 1463-8.

Florenes, V. A., R. S. Faye, et al. (2000). "Levels of cyclin D1 and D3 in malignant melanoma: deregulated cyclin D3 expression is associated with poor clinical outcome in superficial melanoma." Clin Cancer Res **6**(9): 3614-20.

Florenes, V. A., G. M. Maelandsmo, et al. (2001). "Cyclin A expression in superficial spreading malignant melanomas correlates with clinical outcome." J Pathol **195**(5): 530-6.

Florenes, V. A., G. M. Maelandsmo, et al. (1998). "Protein expression of the cell-cycle inhibitor p27Kip1 in malignant melanoma: inverse correlation with disease-free survival." Am J Pathol **153**(1): 305-12.

Forster, A. C. and R. H. Symons (1987). "Self-cleavage of plus and minus RNAs of a virusoid and a structural model for the active sites." Cell **49**(2): 211-20.

Fuhrmann, G., G. Rosenberger, et al. (1999). "The MYC dualism in growth and death." Mutat Res **437**(3): 205-17.

Fussenegger, M. and J. E. Bailey (1998). "Molecular regulation of cell-cycle progression and apoptosis in mammalian cells: implications for biotechnology." Biotechnol Prog **14**(6): 807-33.

Galaktionov, K., X. Chen, et al. (1996). "Cdc25 cell-cycle phosphatase as a target of c-myc." Nature **382**(6591): 511-7.

Garbe, C., P. Buttner, et al. (1995). "Primary cutaneous melanoma. Prognostic classification of anatomic location." Cancer **75**(10): 2492-8.

Garte, S. J. (1993). "The c-myc oncogene in tumor progression." Crit Rev Oncog **4**(4): 435-49.

Gelsleichter, L., A. M. Gown, et al. (1995). "p53 and mdm-2 expression in malignant melanoma: an immunocytochemical study of expression of p53, mdm-2, and markers of cell proliferation in primary versus metastatic tumors." Mod Pathol **8**(5): 530-5.

Gene Therapy Advisory Group (1997). Third Annual Report January 1996 - December 1996.

Gershenwald, J. E., W. Thompson, et al. (1999). "Multi-institutional melanoma lymphatic mapping experience: the prognostic value of sentinel lymph node status in 612 stage I or II melanoma patients." J Clin Oncol **17**(3): 976-83.

Giard, D. J., S. A. Aaronson, et al. (1973). "In vitro cultivation of human tumors: establishment of cell lines derived from a series of solid tumors." J Natl Cancer Inst **51**(5): 1417-23.

Gibson, S. A., C. Pellenz, et al. (2000). "Induction of apoptosis in oral cancer cells by an anti-bcl-2 ribozyme delivered by an adenovirus vector." Clin Cancer Res **6**(1): 213-22.

Goodchild, J. and V. Kohli (1991). "Ribozymes that cleave an RNA sequence from human immunodeficiency virus: the effect of flanking sequence on rate." Arch Biochem Biophys **284**(2): 386-91.

Green, R. J. and L. M. Schuchter (1998). "Systemic treatment of metastatic melanoma with chemotherapy." Hematol Oncol Clin North Am **12**(4): 863-75, viii.

Gregory, M. A. and S. R. Hann (2000). "c-Myc proteolysis by the ubiquitin-proteasome pathway: stabilization of c-Myc in Burkitt's lymphoma cells." Mol Cell Biol **20**(7): 2423-35.

Grob, J. J., B. Dreno, et al. (1998). "Randomised trial of interferon alpha-2a as adjuvant therapy in resected primary melanoma thicker than 1.5 mm without clinically detectable node metastases. French Cooperative Group on Melanoma." Lancet **351**(9120): 1905-10.

Grover, R., J. Chana, et al. (1999). "Measurement of c-myc oncogene expression provides an accurate prognostic marker for acral lentiginous melanoma." Br J Plast Surg **52**(2): 122-6.

Grover, R., A. O. Grobbelaar, et al. (1997). "The clinical significance of oncogene expression in subungual melanoma." Br J Plast Surg **50**(1): 15-9.

Grover, R., M. D. Pacifico, et al. (2003). "Use of oncogene expression as an independent prognostic marker for primary melanoma." Ann Plast Surg **50**(2): 183-7.

Grover, R., D. A. Ross, et al. (1996). "C-myc oncogene expression in human melanoma and its relationship with tumour antigenicity." Eur J Surg Oncol **22**(4): 342-6.

Grover, R., D. A. Ross, et al. (1997). "Measurement of c-myc oncoprotein provides an independent prognostic marker for regional metastatic melanoma." Br J Plast Surg **50**(7): 478-82.

Grover, R. and G. D. Wilson (1996). "Bcl-2 expression in malignant melanoma and its prognostic significance." Eur J Surg Oncol **22**(4): 347-9.

Gu, W., K. Bhatia, et al. (1994). "Binding and suppression of the Myc transcriptional activation domain by p107." Science **264**(5156): 251-4.

Guerrier-Takada, C., K. Gardiner, et al. (1983). "The RNA moiety of ribonuclease P is the catalytic subunit of the enzyme." Cell **35**(3 Pt 2): 849-57.

Halpern, A. C. and J. F. Altman (1999). "Genetic predisposition to skin cancer." Curr Opin Oncol **11**(2): 132-8.

Halpern, A. C. and L. M. Schuchter (1997). "Prognostic models in melanoma." Semin Oncol **24**(1 Suppl 4): S2-7.

Hampel, A. (1998). "The hairpin ribozyme: discovery, two-dimensional model, and development for gene therapy." Prog Nucleic Acid Res Mol Biol **58**: 1-39.

Hampel, A. and R. Tritz (1989). "RNA catalytic properties of the minimum (-)sTRSV sequence." Biochemistry **28**(12): 4929-33.

Handley, W. S. (1907). "The pathology of melanotic growths in relation to their operative treatment." Lancet: i: 927, 996.

Hann, S. R. and R. N. Eisenman (1984). "Proteins encoded by the human c-myc oncogene: differential expression in neoplastic cells." Mol Cell Biol **4**(11): 2486-97.

Haseloff, J. and W. L. Gerlach (1988). "Simple RNA enzymes with new and highly specific endoribonuclease activities." Nature **334**(6183): 585-91.

Hauschild, A., G. Engel, et al. (1999). "Predictive value of serum S100B for monitoring patients with metastatic melanoma during chemotherapy and/or immunotherapy." Br J Dermatol **140**(6): 1065-71.

Hauschild, A., J. Michaelsen, et al. (1999). "Prognostic significance of serum S100B detection compared with routine blood parameters in advanced metastatic melanoma patients." Melanoma Res **9**(2): 155-61.

Hedley, D. W., M. L. Friedlander, et al. (1983). "Method for analysis of cellular DNA content of paraffin-embedded pathological material using flow cytometry." J Histochem Cytochem **31**(11): 1333-5.

Heerdt, B. G., S. Molinas, et al. (1991). "Aggressive subtypes of human colorectal tumors frequently exhibit amplification of the c-myc gene." Oncogene **6**(1): 125-9.

Hendry, P. and M. McCall (1996). "Unexpected anisotropy in substrate cleavage rates by asymmetric hammerhead ribozymes." Nucleic Acids Res **24**(14): 2679-84.

Hermeking, H. and D. Eick (1994). "Mediation of c-Myc-induced apoptosis by p53." Science **265**(5181): 2091-3.

Herschlag, D. (1991). "Implications of ribozyme kinetics for targeting the cleavage of specific RNA molecules in vivo: more isn't always better." Proc Natl Acad Sci U S A **88**(16): 6921-5.

Hieken, T. J., M. Farolan, et al. (1996). "Beta3 integrin expression in melanoma predicts subsequent metastasis." J Surg Res **63**(1): 169-73.

Holly, E. A., D. A. Aston, et al. (1995). "Cutaneous melanoma in women. II. Phenotypic characteristics and other host-related factors." Am J Epidemiol **141**(10): 934-42.

Homann, M., S. Tzortzakaki, et al. (1993). "Incorporation of the catalytic domain of a hammerhead ribozyme into antisense RNA enhances its inhibitory effect on the replication of human immunodeficiency virus type 1." Nucleic Acids Res **21**(12): 2809-14.

Hoos, A. U., M. Stojadinovic, A. Mastorides, S. Dudas, M. Leung D. Kuo, D. Brennan, M. Lewis, J. Cordon-Cardo, C. (2001). "Validation of Tissue Microarrays for Immunohistochemical Profiling of Cancer Specimens Using the Example of Human Fibroblastic Tumours." American Journal of Pathology **158**(4): 1245-1251.

Hurlin, P. J., C. Queva, et al. (1995). "Mad3 and Mad4: novel Max-interacting transcriptional repressors that suppress c-myc dependent transformation and are expressed during neural and epidermal differentiation." Embo J **14**(22): 5646-59.

Irie, A., B. Anderegg, et al. (1999). "Therapeutic efficacy of an adenovirus-mediated anti-H-ras ribozyme in experimental bladder cancer." Antisense Nucleic Acid Drug Dev **9**(4): 341-9.

Jack, A. S., I. B. Kerr, et al. (1986). "The distribution of the c-myc oncogene product in malignant lymphomas and various normal tissues as demonstrated by immunocytochemistry." Br J Cancer **53**(6): 713-9.

Jackel, A., M. Deichmann, et al. (1999). "[S-100 beta protein in serum, a tumor marker in malignant melanoma-- current state of knowledge and clinical experience]." Hautarzt **50**(4): 250-6.

Jager, R., U. Herzer, et al. (1997). "Overexpression of Bcl-2 inhibits alveolar cell apoptosis during involution and accelerates c-myc-induced tumorigenesis of the mammary gland in transgenic mice." Oncogene **15**(15): 1787-95.

Jansen, B., V. Wacheck, et al. (2000). "Chemosensitisation of malignant melanoma by BCL2 antisense therapy." Lancet **356**(9243): 1728-33.

Jarvis, T. C., F. E. Wincott, et al. (1996). "Optimizing the cell efficacy of synthetic ribozymes. Site selection and chemical modifications of ribozymes targeting the proto-oncogene c-myb." J Biol Chem **271**(46): 29107-12.

Johnson, P. W., S. A. Burchill, et al. (1995). "The molecular detection of circulating tumour cells." Br J Cancer **72**(2): 268-76.

Kamarashev, J., S. Ferrone, et al. (2001). "TAP1 down-regulation in primary melanoma lesions: an independent marker of poor prognosis." Int J Cancer **95**(1): 23-8.

Karakousis, C. P., C. M. Balch, et al. (1996). "Local recurrence in malignant melanoma: long-term results of the multiinstitutional randomized surgical trial." Ann Surg Oncol **3**(5): 446-52.

Kashani-Sabet, M., T. Funato, et al. (1992). "Reversal of the malignant phenotype by an anti-ras ribozyme." Antisense Res Dev **2**(1): 3-15.

Kato, G. J., W. M. Lee, et al. (1992). "Max: functional domains and interaction with c-Myc." Genes Dev **6**(1): 81-92.

Kawakami, Y., S. Eliyahu, et al. (1994). "Cloning of the gene coding for a shared human melanoma antigen recognized by autologous T cells infiltrating into tumor." Proc Natl Acad Sci U S A **91**(9): 3515-9.

Ketcham, A. S., F. L. Moffat, et al. (1992). Classification and Staging. Cutaneous Melanoma. C. M. Balch. Philidelphia, Lippincott**:** 213-220.

King, K. L. and J. A. Cidlowski (1998). "Cell cycle regulation and apoptosis." Annu Rev Physiol **60**: 601-17.

King, M., D. Spooner, et al. (2001). "Spontaneous regression of metastatic malignant melanoma of the parotid gland and neck lymph nodes: a case report and a review of the literature." Clin Oncol (R Coll Radiol) **13**(6): 466-9.

Kirkwood, J. M., J. G. Ibrahim, et al. (2000). "High- and low-dose interferon alfa-2b in high-risk melanoma: first analysis of intergroup trial E1690/S9111/C9190." J Clin Oncol **18**(12): 2444-58.

Kirkwood, J. M., J. G. Ibrahim, et al. (2001). "High-dose interferon alfa-2b significantly prolongs relapse-free and overall survival compared with the GM2-KLH/QS-21 vaccine in patients with resected stage IIB-III melanoma: results of intergroup trial E1694/S9512/C509801." J Clin Oncol **19**(9): 2370-80.

Kirkwood, J. M., M. H. Strawderman, et al. (1996). "Interferon alfa-2b adjuvant therapy of high-risk resected cutaneous melanoma: the Eastern Cooperative Oncology Group Trial EST 1684." J Clin Oncol **14**(1): 7-17.

Koh, H. K. (1991). "Cutaneous melanoma." N Engl J Med **325**(3): 171-82.

Kononen, J., L. Bubendorf, et al. (1998). "Tissue microarrays for high-throughput molecular profiling of tumor specimens." Nat Med **4**(7): 844-7.

Kraemer, K. H., M. M. Lee, et al. (1987). "Xeroderma pigmentosum. Cutaneous, ocular, and neurologic abnormalities in 830 published cases." Arch Dermatol **123**(2): 241-50.

Kruger, K., P. J. Grabowski, et al. (1982). "Self-splicing RNA: autoexcision and autocyclization of the ribosomal RNA intervening sequence of Tetrahymena." Cell **31**(1): 147-57.

Land, H., A. C. Chen, et al. (1986). "Behavior of myc and ras oncogenes in transformation of rat embryo fibroblasts." Mol Cell Biol **6**(6): 1917-25.

Land, H., L. F. Parada, et al. (1983). "Tumorigenic conversion of primary embryo fibroblasts requires at least two cooperating oncogenes." Nature **304**(5927): 596-602.

Leavitt, M. C., M. Yu, et al. (1994). "Transfer of an anti-HIV-1 ribozyme gene into primary human lymphocytes." Hum Gene Ther **5**(9): 1115-20.

Lee, J. A. and D. Strickland (1980). "Malignant melanoma: social status and outdoor work." Br J Cancer **41**(5): 757-63.

Lee, S. M., D. C. Betticher, et al. (1995). "Melanoma: chemotherapy." Br Med Bull **51**(3): 609-30.

Legha, S. S. (1997). "Durable complete responses in metastatic melanoma treated with interleukin-2 in combination with interferon alpha and chemotherapy." Semin Oncol **24**(1 Suppl 4): S39-43.

Legha, S. S., S. Ring, et al. (1989). "A prospective evaluation of a triple-drug regimen containing cisplatin, vinblastine, and dacarbazine (CVD) for metastatic melanoma." Cancer **64**(10): 2024-9.

Leonetti, C., I. D'Agnano, et al. (1996). "Antitumor effect of c-myc antisense phosphorothioate oligodeoxynucleotides on human melanoma cells in vitro and and in mice." J Natl Cancer Inst **88**(7): 419-29.

Lincoln, S. T. and K. D. Bauer (1989). "Limitations in the measurement of c-myc oncoprotein and other nuclear antigens by flow cytometry." Cytometry **10**(4): 456-62.

Liu, J., R. Voutilainen, et al. (1997). "Expression patterns of the c-myc gene in adrenocortical tumors and pheochromocytomas." J Endocrinol **152**(2): 175-81.

Loggini, B., I. Rinaldi, et al. (2001). "Immunohistochemical study of 49 cutaneous melanomas: p53, PCNA, Bcl-2 expression and multidrug resistance." Tumori **87**(3): 179-86.

MacKie, R., J. A. Hunter, et al. (1992). "Cutaneous malignant melanoma, Scotland, 1979-89. The Scottish Melanoma Group." Lancet **339**(8799): 971-5.

MacKie, R. M., D. Hole, et al. (1997). "Cutaneous malignant melanoma in Scotland: incidence, survival, and mortality, 1979-94. The Scottish Melanoma Group." Bmj **315**(7116): 1117-21.

MacLennan, R., A. C. Green, et al. (1992). "Increasing incidence of cutaneous melanoma in Queensland, Australia." J Natl Cancer Inst **84**(18): 1427-32.

Margolin, K. A., P. Y. Liu, et al. (1998). "Phase II study of carmustine, dacarbazine, cisplatin, and tamoxifen in advanced melanoma: a Southwest Oncology Group study." J Clin Oncol **16**(2): 664-9.

Marhin, W. W., Y. J. Hei, et al. (1996). "Loss of Rb and Myc activation co-operate to suppress cyclin D1 and contribute to transformation." Oncogene **12**(1): 43-52.

Marincola, F. M., Y. M. Hijazi, et al. (1996). "Analysis of expression of the melanoma-associated antigens MART-1 and gp100 in metastatic melanoma cell lines and in in situ lesions." J Immunother Emphasis Tumor Immunol **19**(3): 192-205.

Marples, B., O. Greco, et al. (2002). "Molecular approaches to chemo-radiotherapy." Eur J Cancer **38**(2): 231-9.

Mazel, S., D. Burtrum, et al. (1996). "Regulation of cell division cycle progression by bcl-2 expression: a potential mechanism for inhibition of programmed cell death." J Exp Med **183**(5): 2219-26.

McCarthy, W. H., Shaw, H M (1998). "The surgical treatment of primary melanoma." Hematology/Oncology Clinics of North America **12**(4): 797-805.

McClay, E. F., M. J. Mastrangelo, et al. (1987). "Combination chemotherapy and hormonal therapy in the treatment of malignant melanoma." Cancer Treat Rep **71**(5): 465-9.

McKay, D. B. (1996). "Structure and function of the hammerhead ribozyme: an unfinished story." Rna **2**(5): 395-403.

Meichle, A., A. Philipp, et al. (1992). "The functions of Myc proteins." Biochim Biophys Acta **1114**(2-3): 129-46.

Minks, M., A. Di Vinci, et al. (1992). "Interleukin-3 dependent c-myc protein expression during the cell cycle of murine mast cells." Cancer Lett **62**(3): 243-9.

Morton, D., F. R. Eilber, et al. (1970). "Immunological factors which influence response to immunotherapy in malignant melanoma." Surgery **68**(1): 158-63; discussion 163-4.

Morton, D. L., R. A. Malmgren, et al. (1968). "Demonstration of antibodies against human malignant melanoma by immunofluorescence." Surgery **64**(1): 233-40.

Morton, D. L., D. R. Wen, et al. (1992). "Technical details of intraoperative lymphatic mapping for early stage melanoma." Arch Surg **127**(4): 392-9.

Mugrauer, G., F. W. Alt, et al. (1988). "N-myc proto-oncogene expression during organogenesis in the developing mouse as revealed by in situ hybridization." J Cell Biol **107**(4): 1325-35.

Mugrauer, G. and P. Ekblom (1991). "Contrasting expression patterns of three members of the myc family of protooncogenes in the developing and adult mouse kidney." J Cell Biol **112**(1): 13-25.

Natali, P. G., C. V. Hamby, et al. (1997). "Clinical significance of alpha(v)beta3 integrin and intercellular adhesion molecule-1 expression in cutaneous malignant melanoma lesions." Cancer Res **57**(8): 1554-60.

Noguchi, M., S. Hirohashi, et al. (1990). "Heterogenous amplification of myc family oncogenes in small cell lung carcinoma." Cancer **66**(10): 2053-8.

Norris, W. (1820). "Case of fungoid Disease." Edinburgh Medical and Surgical Journal **16**: 562.

Norris, W. (1857). Eight Cases of Melanosis with Pathological and Therapeutic Remarks on that Disease, London, Longman, Brown, Green, Longman and Roberts.

Ohta, Y., H. Kijima, et al. (1996). "Tissue-specific expression of an anti-ras ribozyme inhibits proliferation of human malignant melanoma cells." Nucleic Acids Res **24**(5): 938-42.

Packham, G. and J. L. Cleveland (1994). "Ornithine decarboxylase is a mediator of c-Myc-induced apoptosis." Mol Cell Biol **14**(9): 5741-7.

Paterson, B. M., B. E. Roberts, et al. (1977). "Structural gene identification and mapping by DNA-mRNA hybrid-arrested cell-free translation." Proc Natl Acad Sci U S A **74**(10): 4370-4.

Pavelic, Z. P., P. Steele, et al. (1991). "Evaluation of c-myc proto-oncogene in primary human breast carcinomas." Anticancer Res **11**(4): 1421-7.

Pehamberger, H., H. P. Soyer, et al. (1998). "Adjuvant interferon alfa-2a treatment in resected primary stage II cutaneous melanoma. Austrian Malignant Melanoma Cooperative Group." J Clin Oncol **16**(4): 1425-9.

Penn, L. J., M. W. Brooks, et al. (1990). "Negative autoregulation of c-myc transcription." Embo J **9**(4): 1113-21.

Perriman, R., A. Delves, et al. (1992). "Extended target-site specificity for a hammerhead ribozyme." Gene **113**(2): 157-63.

Peterson (1962). "Regional Lymph-nodes in malignant melanoma." Lancet **1 (452)**: 1412.

Polsky, D. and C. Cordon-Cardo (2003). "Oncogenes in melanoma." Oncogene **22**(20): 3087-91.

Ranzani, G. N., N. S. Pellegata, et al. (1990). "Heterogeneous protooncogene amplification correlates with tumor progression and presence of metastases in gastric cancer patients." Cancer Res **50**(24): 7811-4.

Reed, J. A., F. Loganzo, Jr., et al. (1995). "Loss of expression of the p16/cyclin-dependent kinase inhibitor 2 tumor suppressor gene in melanocytic lesions correlates with invasive stage of tumor progression." Cancer Res **55**(13): 2713-8.

Riou, G. F., J. Bourhis, et al. (1990). "The c-myc proto-oncogene in invasive carcinomas of the uterine cervix: clinical relevance of overexpression in early stages of the cancer." Anticancer Res **10**(5A): 1225-31.

Rodenas, J. M., M. Delgado-Rodriguez, et al. (1996). "Sun exposure, pigmentary traits, and risk of cutaneous malignant melanoma: a case-control study in a Mediterranean population." Cancer Causes Control **7**(2): 275-83.

Ross, D. A. and G. D. Wilson (1998). "Expression of c-myc oncoprotein represents a new prognostic marker in cutaneous melanoma." Br J Surg **85**(1): 46-51.

Ruffner, D. E. and O. C. Uhlenbeck (1990). "Thiophosphate interference experiments locate phosphates important for the hammerhead RNA self-cleavage reaction." Nucleic Acids Res **18**(20): 6025-9.

Sakamuro, D., K. J. Elliott, et al. (1996). "BIN1 is a novel MYC-interacting protein with features of a tumour suppressor." Nat Genet **14**(1): 69-77.

Sallinen, S. L., P. K. Sallinen, et al. (2000). "Identification of differentially expressed genes in human gliomas by DNA microarray and tissue chip techniques." Cancer Res **60**(23): 6617-22.

Sandberg, J. A., K. S. Bouhana, et al. (1999). "Pharmacokinetics of an antiangiogenic ribozyme (ANGIOZYME) in the mouse." Antisense Nucleic Acid Drug Dev **9**(3): 271-7.

Schadendorf, D., J. Heidel, et al. (1995). "Association with clinical outcome of expression of VLA-4 in primary cutaneous malignant melanoma as well as P-selectin and E-selectin on intratumoral vessels." J Natl Cancer Inst **87**(5): 366-71.

Schaider, H., I. Rech-Weichselbraun, et al. (1997). "Circulating adhesion molecules as prognostic factors for cutaneous melanoma." J Am Acad Dermatol **36**(2 Pt 1): 209-13.

Scherr, M., J. J. Rossi, et al. (2000). "RNA accessibility prediction: a theoretical approach is consistent with experimental studies in cell extracts." Nucleic Acids Res **28**(13): 2455-61.

Schraml, P., J. Kononen, et al. (1999). "Tissue microarrays for gene amplification surveys in many different tumor types." Clin Cancer Res **5**(8): 1966-75.

Scott, W. G. and A. Klug (1996). "Ribozymes: structure and mechanism in RNA catalysis." Trends Biochem Sci **21**(6): 220-4.

SEER (2001). "Surveillance, Epidemiology and End Results Program Cancer Statistics Review, 1973-1996." http://seer.cancer.gov/.

Setlow, R. B. and A. D. Woodhead (1994). "Temporal changes in the incidence of malignant melanoma: explanation from action spectra." Mutat Res **307**(1): 365-74.

Shih, I. M., D. Speicher, et al. (1997). "Melanoma cell-cell interactions are mediated through heterophilic Mel- CAM/ligand adhesion." Cancer Res **57**(17): 3835-40.

Shuey, D. J., D. E. McCallus, et al. (2002). "RNAi: gene-silencing in therapeutic intervention." Drug Discov Today **7**(20): 1040-6.

Sikora, K., S. Chan, et al. (1987). "c-myc oncogene expression in colorectal cancer." Cancer **59**(7): 1289-95.

Simons, R. W. and N. Kleckner (1983). "Translational control of IS10 transposition." Cell **34**(2): 683-91.

Sinn, E., W. Muller, et al. (1987). "Coexpression of MMTV/v-Ha-ras and MMTV/c-myc genes in transgenic mice: synergistic action of oncogenes in vivo." Cell **49**(4): 465-75.

Sioud, M. and L. Jespersen (1996). "Enhancement of hammerhead ribozyme catalysis by glyceraldehyde-3- phosphate dehydrogenase." J Mol Biol **257**(4): 775-89.

Sklar, M. D. and E. V. Prochownik (1991). "Modulation of cis-platinum resistance in Friend erythroleukemia cells by c-myc." Cancer Res **51**(8): 2118-23.

Slingluff, C. L., Jr., R. T. Vollmer, et al. (1988). "Lethal "thin" malignant melanoma. Identifying patients at risk." Ann Surg **208**(2): 150-61.

Stein, C. A. (2001). "The experimental use of antisense oligonucleotides: a guide for the perplexed." J Clin Invest **108**(5): 641-4.

Steiner, P., A. Philipp, et al. (1995). "Identification of a Myc-dependent step during the formation of active G1 cyclin-cdk complexes." Embo J **14**(19): 4814-26.

Stewart, T. A., P. K. Pattengale, et al. (1984). "Spontaneous mammary adenocarcinomas in transgenic mice that carry and express MTV/myc fusion genes." Cell **38**(3): 627-37.

Strasser, A., L. O'Connor, et al. (1996). "Lessons from bcl-2 transgenic mice for immunology, cancer biology and cell death research." Behring Inst Mitt(97): 101-17.

Straume, O. and L. A. Akslen (1997). "Alterations and prognostic significance of p16 and p53 protein expression in subgroups of cutaneous melanoma." Int J Cancer **74**(5): 535-9.

Subramaniam, P. S., P. E. Cruz, et al. (1998). "Type I interferon induction of the Cdk-inhibitor p21WAF1 is accompanied by ordered G1 arrest, differentiation and apoptosis of the Daudi B-cell line." Oncogene **16**(14): 1885-90.

Sumner (1953). "Spontaneous regression of melanoma: report of a case." Cancer **6**: 1040-3.

Swerdlow, A. J. and M. A. Weinstock (1998). "Do tanning lamps cause melanoma? An epidemiologic assessment." J Am Acad Dermatol **38**(1): 89-98.

Symons, R. H. (1992). "Small catalytic RNAs." Annu Rev Biochem **61**: 641-71.

Tekur, S. and S. M. Ho (2002). "Ribozyme-mediated downregulation of human metallothionein II(a) induces apoptosis in human prostate and ovarian cancer cell lines." Mol Carcinog **33**(1): 44-55.

Tran, T. A., J. S. Ross, et al. (1998). "Mitotic cyclins and cyclin-dependent kinases in melanocytic lesions." Hum Pathol **29**(10): 1085-90.

Trotter, M. J., L. Tang, et al. (1997). "Overexpression of the cyclin-dependent kinase inhibitor p21(WAF1/CIP1) in human cutaneous malignant melanoma." J Cutan Pathol **24**(5): 265-71.

Tsuchihashi, Z., M. Khosla, et al. (1993). "Protein enhancement of hammerhead ribozyme catalysis." Science **262**(5130): 99-102.

Uhlenbeck, O. C. (1987). "A small catalytic oligoribonucleotide." Nature **328**(6131): 596-600.

Usman, N., L. Beigelman, et al. (1996). "Hammerhead ribozyme engineering." Curr Opin Struct Biol **6**(4): 527-33.

Van Der Esch, E. P., N. Cascinelli, et al. (1981). "Stage I melanoma of the skin: evaluation of prognosis according to histologic characteristics." Cancer **48**(7): 1668-73.

Veronesi, U., J. Adamus, et al. (1982). "A randomized trial of adjuvant chemotherapy and immunotherapy in cutaneous melanoma." N Engl J Med **307**(15): 913-6.

Veronesi, U., J. Adamus, et al. (1977). "Inefficacy of immediate node dissection in stage 1 melanoma of the limbs." N Engl J Med **297**(12): 627-30.

Veronesi, U., J. Adamus, et al. (1982). "Delayed regional lymph node dissection in stage I melanoma of the skin of the lower extremities." Cancer **49**(11): 2420-30.

Veronesi, U. and N. Cascinelli (1991). "Narrow excision (1-cm margin). A safe procedure for thin cutaneous melanoma." Arch Surg **126**(4): 438-41.

Vlaykova, T., T. Muhonen, et al. (1997). "Vascularity and prognosis of metastatic melanoma." Int J Cancer **74**(3): 326-9.

Vogt, T., K. H. Zipperer, et al. (1997). "p53-protein and Ki-67-antigen expression are both reliable biomarkers of prognosis in thick stage I nodular melanomas of the skin." Histopathology **30**(1): 57-63.

Walker, T. L., J. D. White, et al. (1996). "Tumour cells surviving in vivo cisplatin chemotherapy display elevated c-myc expression." Br J Cancer **73**(5): 610-4.

Watson, J. V., J. Stewart, et al. (1986). "The clinical significance of flow cytometric c-myc oncoprotein quantitation in testicular cancer." Br J Cancer **53**(3): 331-7.

Wells, K. E., D. S. Reintgen, et al. (1992). "The current management and prognosis of acral lentiginous melanoma." Ann Plast Surg **28**(1): 100-3.

Westerdahl, J., H. Olsson, et al. (1994). "At what age do sunburn episodes play a crucial role for the development of malignant melanoma." Eur J Cancer **11**(54): 1647-54.

Westerdahl, J., H. Olsson, et al. (1995). "Is the use of sunscreens a risk factor for malignant melanoma?" Melanoma Res **5**(1): 59-65.

Winter, J. N., J. Andersen, et al. (1998). "BCL-2 expression correlates with lower proliferative activity in the intermediate- and high-grade non-Hodgkin's lymphomas: an Eastern Cooperative Oncology Group and Southwest Oncology Group cooperative laboratory study." Blood **91**(4): 1391-8.

Wojtowicz-Praga, S. (1997). "Reversal of tumor-induced immunosuppression: a new approach to cancer therapy." J Immunother **20**(3): 165-77.

Wong, C. K. (1970). "A study of melanocytes in the normal skin surrounding malignant melanomata." Dermatologica **141**(3): 215-25.

Woodruff, J. M. (1976). "Pathology of malignant melanoma - part 1." Clin Bull **6**(1): 15-23.

Xin, Y., A. Grace, et al. (2001). "CD44V6 in gastric carcinoma: a marker of tumor progression." Appl Immunohistochem Mol Morphol **9**(2): 138-42.

Yang, T. T., L. Cheng, et al. (1996). "Optimized codon usage and chromophore mutations provide enhanced sensitivity with the green fluorescent protein." Nucleic Acids Res **24**(22): 4592-3.

Yu, D., T. Jing, et al. (1998). "Overexpression of ErbB2 blocks Taxol-induced apoptosis by upregulation of p21Cip1, which inhibits p34Cdc2 kinase." Mol Cell **2**(5): 581-91.

Zabner, J., L. A. Couture, et al. (1993). "Adenovirus-mediated gene transfer transiently corrects the chloride transport defect in nasal epithelia of patients with cystic fibrosis." Cell **75**(2): 207-16.

Zamecnik, P. C. and M. L. Stephenson (1978). "Inhibition of Rous sarcoma virus replication and cell transformation by a specific oligodeoxynucleotide." Proc Natl Acad Sci U S A **75**(1): 280-4.

Zaug, A. J., M. D. Been, et al. (1986). "The Tetrahymena ribozyme acts like an RNA restriction endonuclease." Nature **324**(6096): 429-33.

Zhang, Y. J., X. P. Wang, et al. (2001). "Suppression of oncogenic viral interferon regulatory factor (vIRF) of Kaposi's sarcoma-associated herpesvirus by ribozyme-mediated cleavage." Cancer Gene Ther **8**(4): 285-93.

Zornig, M. and G. I. Evan (1996). "Cell cycle: on target with Myc." Curr Biol **6**(12): 1553-6.

Zoumadakis, M. and M. Tabler (1995). "Comparative analysis of cleavage rates after systematic permutation of the NUX consensus target motif for hammerhead ribozymes." Nucleic Acids Res **23**(7): 1192-6.

Zuker, M. (1989). "Computer prediction of RNA structure." Methods Enzymol **180**: 262-88.